REPORT UAG-12
PART III

WORLD DATA CENTER A

Upper Atmosphere Geophysics

DATA ON SOLAR-GEOPHYSICAL ACTIVITY ASSOCIATED WITH THE MAJOR GEOMAGNETIC STORM OF MARCH 8, 1970

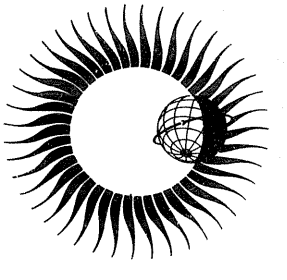

April 1971

WORLD DATA CENTER A

National Academy of Sciences
2101 Constitution Avenue, N. W. Washington, D. C. U.S.A., 20418

World Data Center A consists of the Coordination Office

and nine subcenters:

World Data Center A
Coordination Office
National Academy of Sciences
2101 Constitution Avenue, N.W.
Washington, D. C., U.S.A. 20418
Telephone (202) 961-1478

Solar and Interplanetary Phenomena, Ionospheric Phenomena, Flare-Associated Events, Aurora, Cosmic Rays, Airglow:
World Data Center A:
Upper Atmosphere Geophysics
National Oceanic and Atmospheric Administration
Boulder, Colorado, U.S.A. 80302
Telephone (303) 447-1000 Ext. 3381

Geomagnetism, Seismology and Gravity:
World Data Center A:
Geomagnetism, Seismology and Gravity
Environmental Data Service, NOAA
Rockville, Maryland, U.S.A. 20852
Telephone (301) 496-8160

Glaciology:
World Data Center A:
Glaciology
American Geographical Society
Broadway at 156th Street
New York, New York, U.S.A. 10032
Telephone (212) 234-8100

Longitude and Latitude:
World Data Center A:
Longitude and Latitude
U. S. Naval Observatory
Washington, D. C., U.S.A. 20390
Telephone (202) 698-8422

Meteorology (and Nuclear Radiation):
World Data Center A:
Meteorology
National Climatic Center
Federal Building
Asheville, North Carolina, U.S.A. 28801
Telephone (704) 254-0961

Oceanography:
World Data Center A:
Oceanography
Building 160
Second and N Streets, S.E.
Washington, D. C., U.S.A. 20390
Telephone (202) 698-3753

Rockets and Satellites:
World Data Center A:
Rockets and Satellites
Goddard Space Flight Center
Code 601
Greenbelt, Maryland, U.S.A. 20771
Telephone (301) 982-6695

Tsunami:
World Data Center A:
Tsunami
National Oceanic and Atmospheric Administration
P. O. Box 3887
Honolulu, Hawaii, U.S.A. 96812
Telephone (808) 546-5698

Upper Mantle Project:
World Data Center A:
Upper Mantle Project
Lamont-Doherty Geological Observatory
Palisades, New York, U.S.A. 10964
Telephone (914) 359-2900 Ext. 209

Notes:

(1) World Data Centers conduct international exchange of geophysical observations in accordance with the principles set forth by the International Council of Scientific Unions. WDC-A is established in the United States under the auspices of the National Academy of Sciences.
(2) Communications regarding data interchange matters in general and World Data Center A as a whole should be addressed to: World Data Center A, Coordination Office (see address above).
(3) Inquiries and communications concerning data in specific disciplines should be addressed to the appropriate subcenter listed above.

WORLD DATA CENTER A

Upper Atmosphere Geophysics

REPORT UAG-12 PART III

DATA ON SOLAR-GEOPHYSICAL ACTIVITY ASSOCIATED WITH THE MAJOR GEOMAGNETIC STORM OF MARCH 8, 1970

compiled by

J. Virginia Lincoln and Dale B. Bucknam

WDC-A, Upper Atmosphere Geophysics

Boulder, Colorado

Prepared by Research Laboratories, NOAA, Boulder, Colorado
and published by

U.S. DEPARTMENT OF COMMERCE
NATIONAL OCEANIC AND ATMOSPHERIC ADMINISTRATION

ENVIRONMENTAL DATA SERVICE
Asheville, North Carolina, USA 28801

April 1971

SUBSCRIPTION PRICE: $9.00 a year; $2.50 additional for foreign mailing; single issue price varies.* Order from the Superintendent of Documents, Government Printing Office, specifying the Catalog order number, C52.16/2:12. Checks and money orders should be made payable to the Superintendent of Documents. Remittance and correspondence regarding subscriptions should be sent to the Superintendent of Documents, Government Printing Office, Washington, D. C. 20402.

*Price of this issue $3.00

TABLE OF CONTENTS

TABLE OF CONTENTS

PART III

APPENDIX TO PART III

11. COSMIC RAYS

"Cosmic Ray Intensity Decreases during March 5-8, 1970 and Recurrent Regions"

by

E. Antonucci - G. Cini Castagnoli - M. A. Dodero
Laboratorio di Cosmo-geofisica del C.N.R.
Istituto di Fisica Generale dell'Universita, Torino

Figure 1 shows Alert and Deep River neutron monitor bi-hourly data, Torino meson telescopes (70 meters water equivalent) semidiurnal means and SC in geomagnetic activity during the period 1-15 March 1970, which includes the event under consideration. Moreover we have indicated by rectangles the time intervals during which regions producing flares of importance ≥ 2 during this solar rotation (1868) were at the Central Meridian (CM) of the Sun. The shaded areas give the CMP of the particular zone which has produced the flares East of the CM.

The trend of the intensities registered underground and at sea level at Alert are very similar, due to the fact that at high latitudes the diurnal variations vanish.

Examination of the data demonstrates that intensity decreases of galactic cosmic rays and sc exist during CMP of active regions. We believe that these effects are due to the arrival at Earth of interplanetary streams connected to the active regions on the Sun. The recovery times from the decreases are much shorter underground so that three effects can be distinguished.

The particular strength of the geomagnetic storm of March 8 may be due to the fact that the entrance of McMath region 10614 at CM in the early hours of March 7 was accompanied by intense production of flares (3B,3(2B),2N) between 0131-0333 UT.

The connection between cosmic ray modulation, geomagnetic activity and CMP's of flare-producing regions is clearly evident when the active regions are recurrent. In this particular case we show the history of the longitudes of McMath regions 10614-616 on the diagram of Figure 2, where all regions which have produced flares with importance ≥ 2 are represented starting from the solar rotation 1860. In this figure the latitude and the Carrington longitude of the center of the regions are mapped and the areas are proportional to the number of flares ≥ 2 produced. (The recurrence of the regions is indicated by connecting lines). The sequence of regions which terminates at the 9th rotation with the McMath calcium plage 10616 (in Northern Hemisphere), and the one terminating in McMath 10614 at the fifth rotation (in the Southern Hemisphere) are evident. It will be noticed that the activity produced in the interval of longitudes $L = 60° - 100°$ is 50% of all flares with importance ≥ 2, produced on the Sun during this period. All regions included in these superimposed sequences have produced cosmic ray decreases which are presented in Figure 3, where daily means from Deep River neutron monitor starting from August 1969 are shown together with the number of flares ≥ 2 in the CMP date of the McMath region of their origin.

To every passage of a recurrent region there corresponds a decrease in intensity even though in one case recurrence flares ≥ 2 were not produced (see case of CMP of 10524-22). In 7 cases an SC is present at the same time. Between the decreases produced by the recurrent regions we can find other decreases produced by the passage of some of the other regions drawn in Figure 2. Here we want to draw attention only to the two last solar rotations 1867 - 1868.

Therefore we show in Figure 4 particulars of these two rotations. The absence of intervening regions between 10542/44 and 10567/68 permits recovery terminated only by the decrease due to the latter. This is not so at the recurrence (passage of 10584 and 10614/18) because of the other active regions, 10595 and 10607 formed at intermediate solar longitudes. Thus one of the largest decreases of this period occurs from February 23 through March 17.

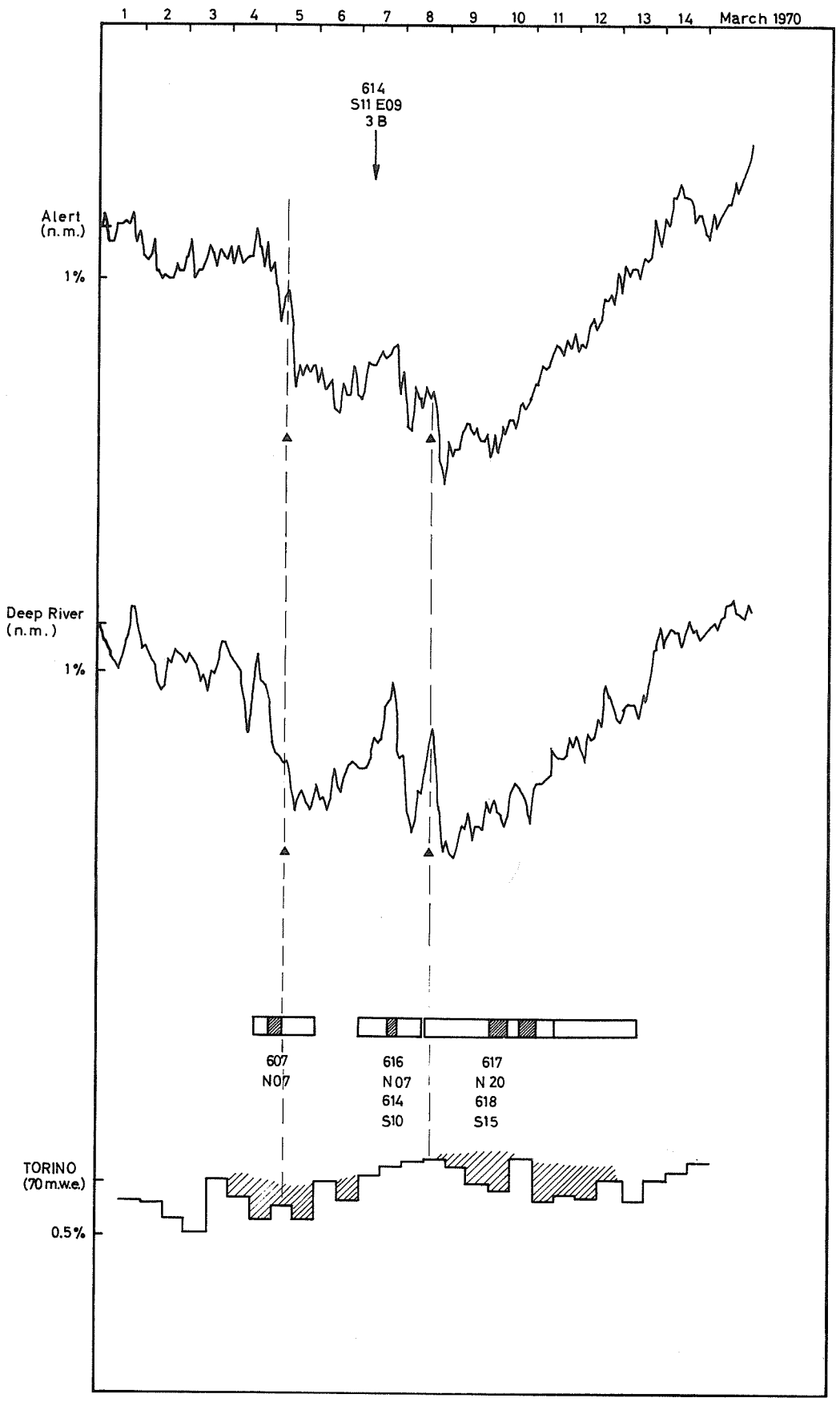

Figure 1. Neutron monitor data from Alert and Deep River and meson telescope data from Torino compared to sc and CMP of active regions March 1-14, 1970.

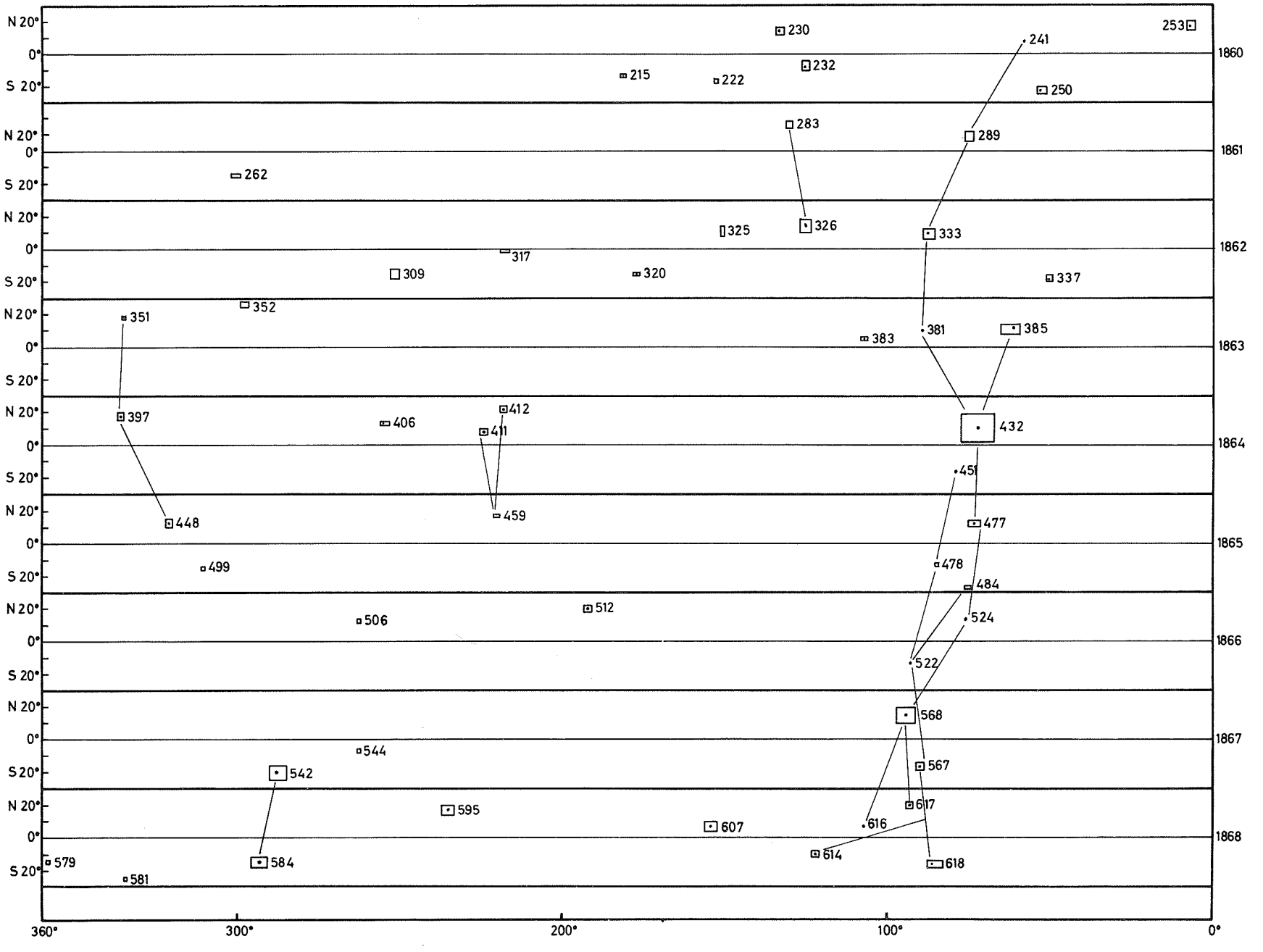

Fig. 2. History of CMP longitudes of McMath regions which produced flares with importance ≥ 2 for solar rotations 1860-1868.

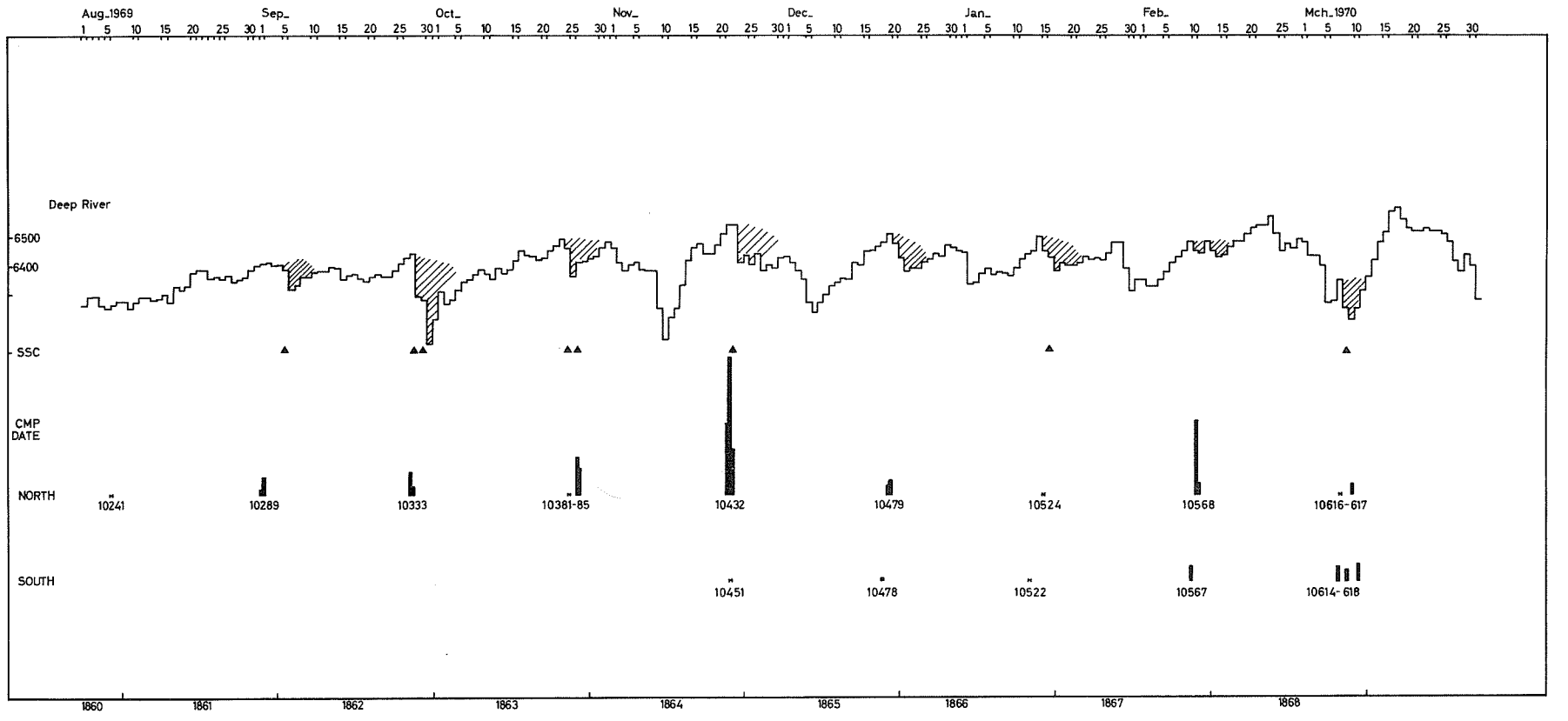

Fig. 3. Deep River cosmic ray decreases, sc and CMP dates of McMath regions indicating number of flares ≥ 2, August 1, 1969 through March 31, 1970.

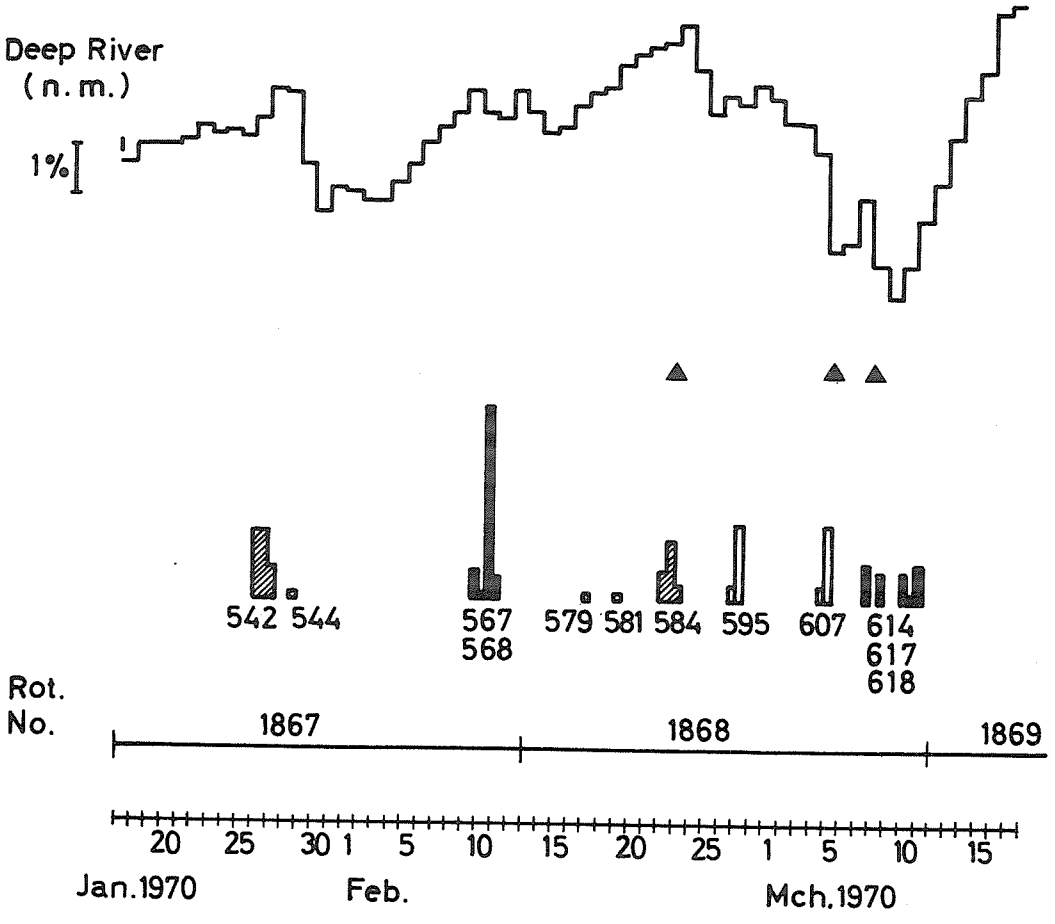

Fig. 4. Detailed comparisons Deep River neutron monitor, sc and CMP of McMath regions, January 15 - March 17, 1970.

"Graphs of Neutron Monitor Observations March 1 - 15, 1970"

by

M. Wada, S. Okutani and Y. Miyazaki
WDC C-2 for Cosmic Rays, Cosmic Ray Laboratory
The Institute of Physical and Chemical Research
Itabashi, Tokyo, Japan

The data presented were submitted to WDC C-2 for Cosmic Rays in keeping with the routine submission of data. The cooperation of all the reporting observatories is hereby gratefully acknowledged.

Graphs present the hourly or bihourly values for the period March 1 - 15, 1970 from 22 stations in cut-off rigidity order as listed in Table 1. The graphs are plotted as a percentage of the average values through the period presented. The average hourly counts are given at the right hand side of the graph represented by the horizontal line. Vertical spacing is 5 percent. The short vertical cuts on each horizontal line indicate the positions of local zero hours calculated from the longitude of the station. They will help readers while inspecting variations of local time component and those of worldwide component.

The points which might be attractive to the readers are as follows:

1. There is significant difference between the variations of Alert and Terre Adelie. It may indicate the north-south asymmetry of primary cosmic ray intensity.

2. From the comparison among variations seen at different longitudes, enhanced diurnal variations are found on March 7 - 8.

3. Short lived anisotropies are seen on March 4 - 5.

4. Semidiurnal variations appear on March 10 and following days. It may be a characteristic point that the semidiurnal variations are seen during the recovering period of the Forbush decrease which started on March 5 or 8.

5. The increases seen at middle latitude stations in the end of March 8 may be an event of the storm time increase which appears at the time of large depression in magnetic Dst component.

6. The increase due to high energy solar cosmic rays are not seen during the period given here.

Table 1

List of Stations

Station Name	Latitude	Longitude	Altitude	Cut-off
Alert	82°30'N	62°20'W	57m	0.00 GV
Terre Adelie	66°40'S	140°01'E	sl	0.01
Inuvik	68°21'N	133°43'W	21	0.18
Goose Bay	53°16'N	60°24'W	46	0.52
Tixie Bay	71°36'N	128°54'E	sl	0.53
Kiruna	67°50'N	20°26'E	400	0.54
Deep River	46°06'N	77°30'W	145	1.02
Calgary	51°05'N	114°08'W	1127	1.09
Sulphur Mt.	51°12'N	115°36'W	2283	1.14
Kerguelen	49°21'S	70°15'E	sl	1.19
Mt. Washington	44°17'N	71°18'W	1909	1.24
Durham	43°06'N	71°00'W	sl	1.41
Chicago	41°50'N	87°40'W	sl	1.72
Kiel	54°20'N	10°08'E	54	2.29
Lindau	51°36'N	10°06'E	140	3.00
Climax	39°22'N	106°11'W	3400	3.03
Halle	51°29'N	11°58'E	100	3.07
Jungfraujoch	46°33'N	7°59'E	3570	4.56
Pic du Midi	42°56'N	0°15'E	2860	5.36
Ushuaia	54°48'S	68°18'W	sl	5.68
Mt. Norikura	36°07'N	137°33'E	2770	11.39
Huancayo	12°02'S	75°20'W	3400	13.49

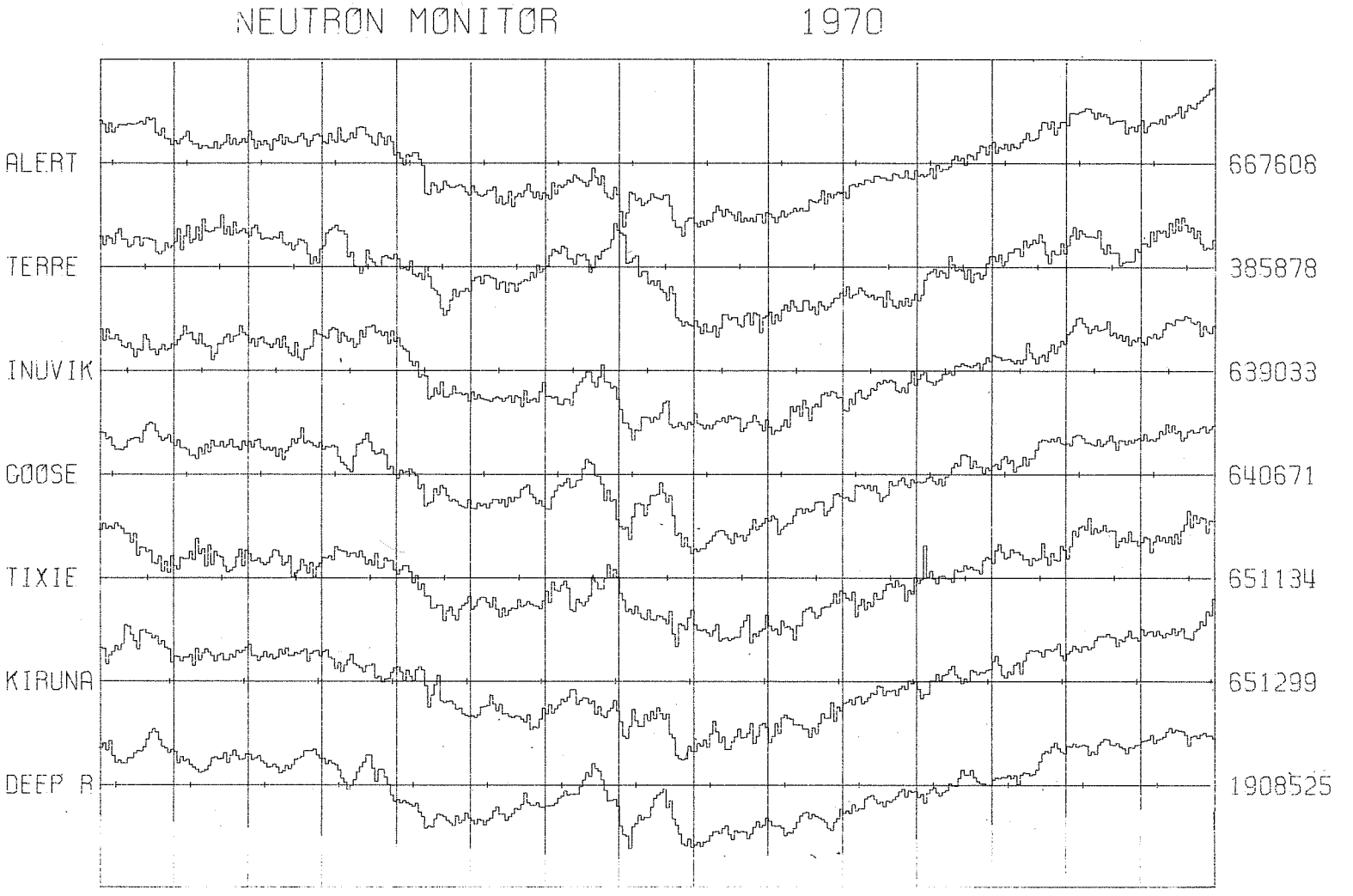
NEUTRON MONITOR 1970
ALERT
TERRE
INUVIK
GOOSE
TIXIE
KIRUNA
DEEP R
667608
385878
639033
640671
651134
651299
1908525

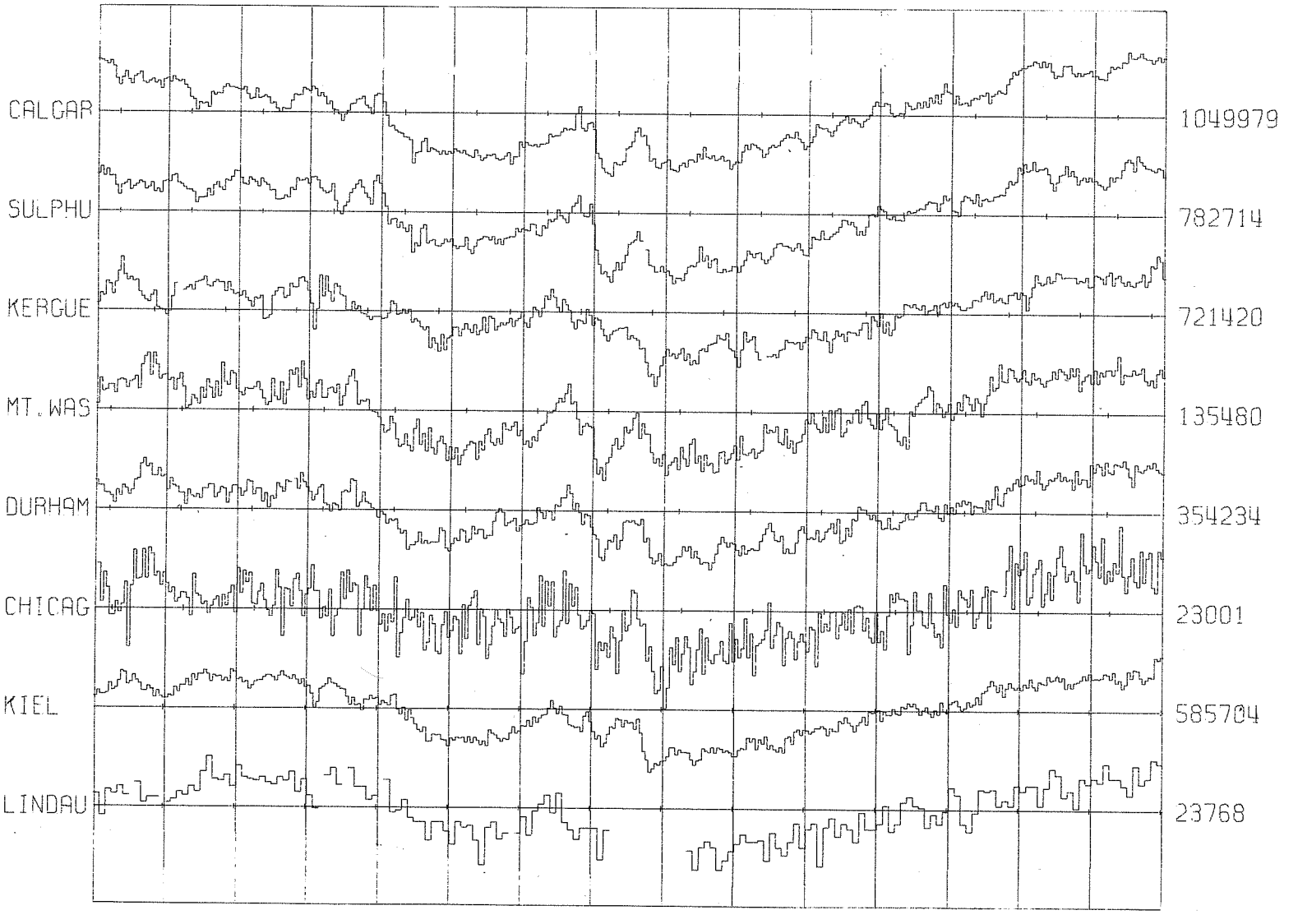
CALGAR
1049979
SULPHU
782714
KERGUE
721420
MT.WAS
135480
DURHAM
354234
CHICAG
23001
KIEL
585704
LINDAU
23768

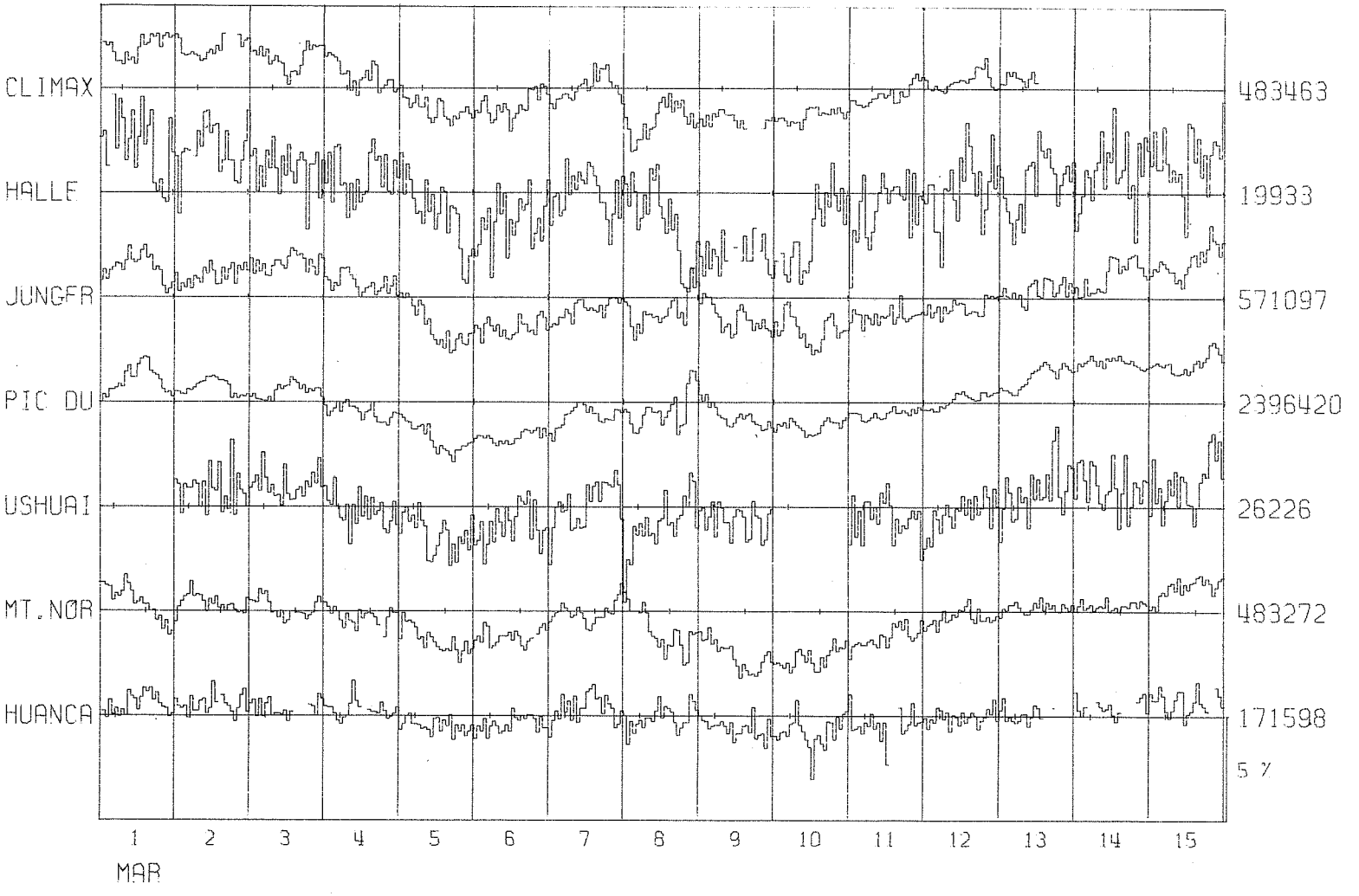
CLIMAX
HALLE
JUNGFR
PIC DU
USHUAI
MT.NOR
HUANCA
483463
19933
571097
2396420
26226
483272
171598
5 γ
1
2
3
4
5
6
7
8
9
10
11
12
13
14
15
MAR

Appendix

[The compiler received cosmic ray information in addition to the data included above.] Table 1 was sent by Professor Oscar Troncoso, Instituto de Geofisica, Ciudad Universitaria, Mexico. It presents the corrected neutron monitor counts for Mexico City.

Table 1

March 1970

Mexico City 19°20'N, 99°11'W, 2274 m. Cutoff Rigidity 9.53
Real Counts 64 Times Tabulated Counts - Neutron Monitor
Corrected to 584.0 mm Hg Coefficient -0.96% mm Hg

Day	01	02	03	04	05	06	07	08	09	10	11	12	Daily
	13	14	15	16	17	18	19	20	21	22	23	24	Average
1	840	847	840	850	849	848	844	855	856	852	850	843	
	850	850	853	840	851	842	844	849	841	835	851	842	846.8
2	847	841	837	830	833	841	839	839	846	844	837	839	
	849	843	846	849	836	846	837	833	848	841	844	847	841.3
3	842	831	830	837	831	840	841	841	841	840	833	846	
	851	850	857	846	853	850	841	829	824	828	826	840	839.5
4	836	842	843	843	846	847	842	832	851	837	836	833	
	832	841	833	829	836	838	838	832	826	826	838	826	836.8
5	841	833	827	829	834	826	828	837	817	833	830	830	
	815	828	826	818	828	821	825	830	830	830	828	816	827.5
6	837	825	828	829	837	824	834	830	829	827	826	843	
	831	827	818	828	825	828	834	832	836	847	839	830	831.0
7	834	825	849	832	834	831	834	842	842	838	833	834	
	845	842	827	844	829	841	827	827	823	830	826	823	833.8
8	811	821	833	831	828	846	825	833	839	832	824	823	
	822	818	823	831	821	826	830	822	838	825	824	822	827.0
9	820	817	820	818	827	824	826	830	825	824	824	832	
	825	819	826	821	828	832	817	827	827	834	834	821	824.9
10	819	822	831	829	824	823	826	824	831	820	0	0	
	0	0	0	0	0	0	0	0	0	0	0	0	0.0
11	0	0	0	0	0	0	0	0	0	0	0	0	
	0	0	0	0	0	0	0	0	0	0	0	0	0.0
12	0	0	0	0	0	0	0	0	0	0	0	0	
	0	841	835	838	838	836	851	836	838	833	831	838	0.0
13	838	837	840	830	837	836	848	842	845	840	833	843	
	829	849	839	846	844	856	858	846	845	833	842	839	841.5
14	847	839	839	847	852	831	847	849	844	850	841	841	
	798	841	843	849	847	843	855	849	846	847	846	846	843.2
15	854	843	852	841	837	853	849	858	845	845	839	848	
	859	844	838	851	853	852	858	852	863	855	846	846	849.2

Table 2 was received from Lomnicky Stit, Czechoslovakia, presenting their corrected neutron monitor counts.

Table 1

March 1970

Lomnicky Stit — Cutoff Rigidity 4.00
Neutron Intensity Monitor — Corrected Values
Scaling Factor 100 — Bar. Coefficient -1.025% mm Hg — Time in GMT

Day	01	02	03	04	05	06	07	08	09	10	11	12
	13	14	15	16	17	18	19	20	21	22	23	24
1	773	778	773	773	781	773	777	774	780	779	775	776
	780	783	788	782	776	775	778	776	772	776	773	779
2	776	773	775	777	776	775	774	774	776	770	768	775
	777	0	766	765+	774	770	768	768	770	765	771	769
3	768	769	766	769	769	766	766	769	770	770	770	770
	771	774	775	772	769	764	770	766	770	769	769	768
4	762	762	765	765	773	766	767	772	766	768	764	759
	758	761	757	759	757	752	756	759	754	767	768	759
5	762	764	754	765	757	754	753	752	755	758	749	754
	743	748	740	740	744	740	740	744	746	751	748	748
6	746	748	745	747	749	740	741	743	744	747	744	753
	747	754	755	751	752	749	747	749	753	753	754	753
7	756	753	754	755	757	763	761	754	757	762	757	755
	754	753	750	751	754	754	750	749	748	751	753	753
8	746	745	740	736	742	750	740	747	747	746	742	749
	748	747	742	745	744	738	735	741	748	754	759	761
9	754	755	756	760	755	753	746	741	744	746	737	749
	744	755	753	750	754	747	749	748	745	745	754	745
10	749	746	751	752	747	751	747	749	751	750	748	747
	743	744	742	750	751	744	746	749	746	755	754	754
11	756	756	755	753	755	752	753	748	755	744	749	744
	752	753	752	745	743	740	738	750	753	749	751	749
12	752	755	755	753	761	755	751	748	756	756	754	758+
	750	751	740	743	752	749	758	751	754	751	757	754

The following figure was received from Dr. U. R. Rao, Physical Research Laboratory, Navrangpura, Ahmedabad 9, India. At Ahmedabad 100% = 4155.5 counts/hour and at Gulmarg 100% = 3558.3 counts/hour.

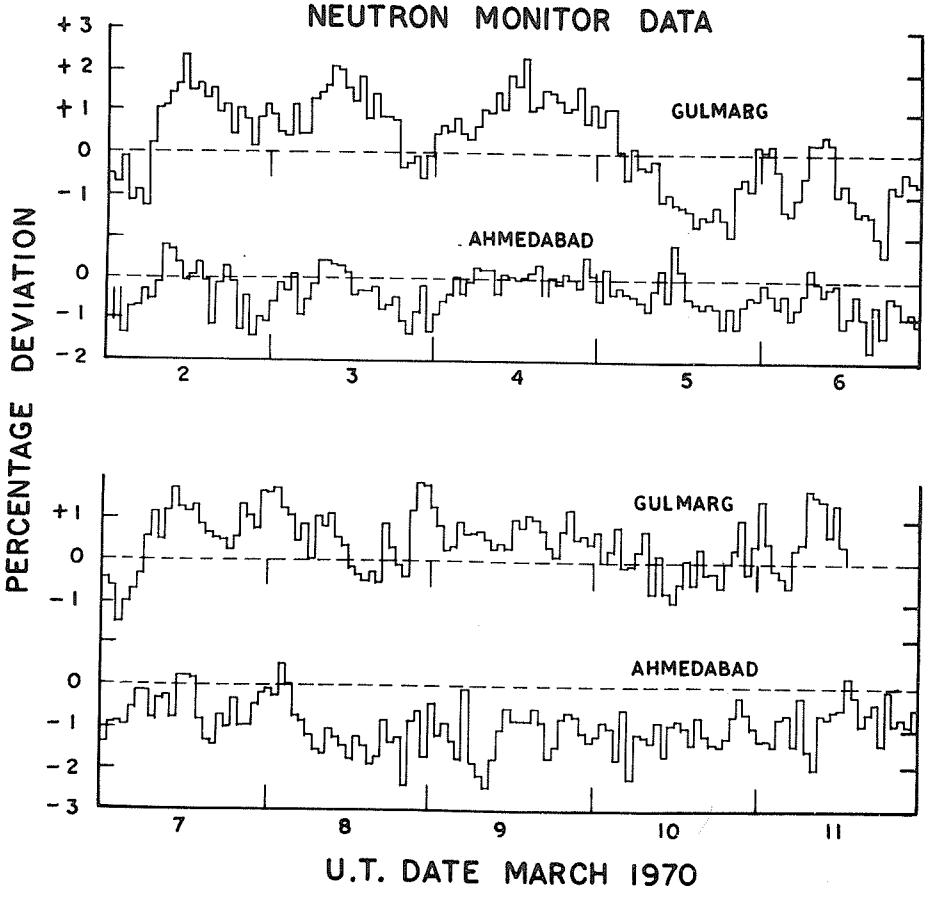

"Auroral-Zone Events of March 1970 on Data of Cola Peninsula Stations"

by

B. E. Brunelli, L. S. Evlashin, S. I. Isaev, L. L. Lazutin, G. A. Loginov, V. K. Roldugin
G. V. Starkov, N. V. Shulgina, G. F. Totunova
Polar Geophysical Institute, Academy of Sciences of USSR

and

E. A. Vasilkova
Observatory of Archangelsk, IZMIRAN, USSR

Description of March 1970 events according to data obtained by the stations mentioned in Table 1 is presented. Cosmic ray variations measured by the neutron monitor and the cubical telescope are given in Figure 1. Figures 2-6 show the time history of the events based on data of ionosonde, riometers, balloons, magnetometers, photometers, all-sky and spectral camera measurements. Figure 7 shows balloon X-ray observations; the balloon launching time, the upper height (in g/cm^2) and the maximum counting rate are presented in Table 2. Figures 8-10 present synoptical charts of the auroras for some moments of March 8, denoted by means of vertical lines in Figure 5.

Table 1

GEOGRAPHIC AND CORRECTED GEOMAGNETIC COORDINATES OF THE STATIONS

	GEOGRAPHIC		GEOMAGNETIC	
	I		II	
	NORTH	EAST	NORTH	EAST
1. Murmansk	68°57'	33°03'	65°06'	115°54'
2. Loparskaya	68°15'	33°05'	64°18'	115°30'
3. Lovozero	67°59'	35°05'	63°42'	116°12'
4. Apatity	67°33'	33°20'	63°18'	114°24'
5. Kem	64°59'	34°47'	60°48'	113°00'
6. Salechard	66°32'	66°32"	61°48'	140°24'
7. Mezen	65°52'	44°13'	61°24'	121°24'
8. Archangelsk	64°35'	40°30'	60°00'	117°30'
9. Pinega	64°42'	43°24'	59°06'	121°00'
10. Sogra	62.6°	46.2°	58.12°	121.12°

Some remarks to the figures: Ionosonde data are given in standard symbols [Piggott and Rawer, 1961]; E_s layers only of type a and r were observed. All riometers operated on frequency 32MHz, antennas being directed toward the Polar Star. Absorption values are given in dB, but the Kem riometer revealed some operation irregularities and the absolute absorption values cited here may be somewhat inaccurate. Even so, the record is presented as the absorption variation but its absolute value is not the matter of interest of this study.

Zenith photometer curves are given in arbitrary units, different for various stations. The field of view is 50° for the photometers in Loparskaya and Karpagory, and 140° for Sogra photometer. Ascaplots [Stoffregen, 1962] are plotted according to the data of the all-sky cameras C-180, shaded areas denote the results obtained by visual observation. The data of spectral cameras C-180-S for a number of lines are given with ordinate approximately corresponding to the logarithm of luminosity. The threshold of photometer is 0.5 kR for 4278Å and 5577Å lines and 0.2 kR for the others.

For the more convenient presentation of the optical observations and the night-time disturbances, the time scales on Figures 2-6 are centered on the Greenwich midnight, which is near to the local one. Synoptical maps of aurora are presented only for March 8. The designations used here are: heavy lines for the auroral arcs, crosses - for diffuse glow, vertical bars - for rays, intermittent heavy line - the boundary of the aurora region (if it is seen in films); dotted lines show the camera field of view. The height of auroras was taken equal to 100km. Geographic (ϕ) and corrected geomagnetic latitudes (Φ') are also given.

Ground-based cosmic ray data show 3 or 4 overlapping Forbush decreases: the first one on March 4, the two next, with low values, on the 7th and the very beginning of the 8th, and the greatest one arises on the second half of March 8. The normal level was recovered on March 12-13.

Geophysical disturbance began at 1615 UT on March 5 as a moderate positive magnetic bay and clear variations in all the other types of data (more weakly on riometer absorption). After 2000 UT a number of superimposed negative bays developed, accompanied by bursts of luminosity and increasing

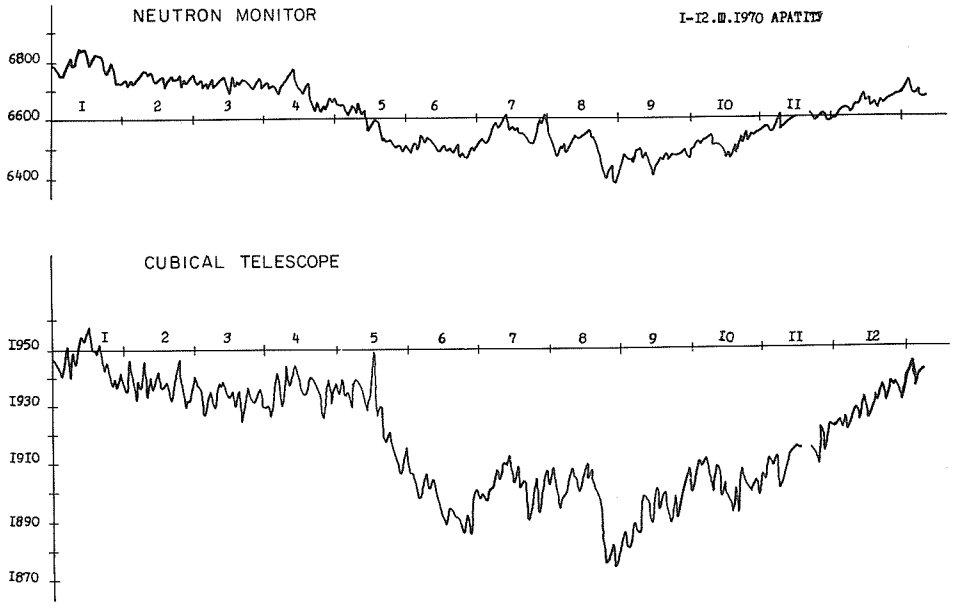

Fig. 1. Cosmic ray data (Apatity). Hourly mean values of counting rate versus days of March.

absorption. Disturbances at 0000 UT on March 6 were accompanied by increasing absorption on the Kem riometer only (with none in Loparskaya) and the decrease of the negative deflection of the H-component. Disturbances of the next night began with very weak positive magnetic disturbance, changing to negative disturbance at approximately 1700 UT. At this local time, as a rule, only positive bays are observed. After 1900 UT began a number of negative magnetic disturbances with time behavior roughly coinciding with the riometer absorption variations. The maximum absorption value was observed near 0000 UT on March 7, the absorption increase began at first at the southeast station. A relatively quiet period was observed near 0800 UT on March 7.

During most of the time of the night on March 7-8, optical observations were not conducted because of the bad weather. All the period was very disturbed with the exception of the interval of 2200-2300 UT near local midnight. This series of disturbances was possibly terminated by this time before a new one began. This new beginning was marked by the negative bay in Lovozero, accompanied by the moderate increase of absorption, still enough to form the ionosonde blackout. It is very unusual that the large number of balloon launches provided during this period reveals no significant X-ray increases, and consequently, large electron fluxes with E >40 kev were not observed in the region of the flight. At 0800 UT on March 8 the new disturbance began superimposing on the previous one.

On the second half of the day of March 8, the disturbances reached a maximum value. The very sharp increase of the riometer absorption (more than 10 dB) coincided with the large fluctuations of magnetic field, however, two neighboring peaks of absorption correspond to fluctuations of the magnetic field with opposite polarity. From 1800 through 2200 UT on March 8 photometers registered three splashes of radiations further discussed in detail. Near midnight of March 8-9 ionospheric activity decreased and reflection was received by the ionosonde. Though activity remained high, aurora was observed south of Murmansk (in Loparskaya the weather was bad, no observations). On the morning of March 9 a new magnetic bay had arisen, followed by an absorption bay. Later the magnetic field became quiet and absorption disappeared. From the balloon flights of this night, only one registered significant X-ray flux at 2300 UT on March 8, the others registered normal or slightly disturbed background levels, though there was a high level of riometer absorption.

On the second half of March 9, two negative bays were registered at 1630 and 2000 UT simultaneously with increasing absorption and in the second case with bright aurora. After 0100 UT on March 10 the disturbance terminated.

Three periods of the night of March 8-9 were chosen for more detailed analysis of disturbance. These periods are marked by vertical lines on Figure 5g and also by arrows on the magnetogram of Figure 10. The first three maps of Figure 8 correspond to the initial phase of the intense negative magnetic disturbance. One can see three arcs of moderate brightness; two of them situated near the southeast boundary of the auroral activity region, which is placed to the south of its usual position. This displacement, as well as bifurcation of the auroral luminosity field may be connected with the action of the ring current [Isaev, et al., 1968]. At 1839 UT the ray arc was broken into separate rays; at 1842 UT the parts of arcs were seen, which then moved to the north leaving behind diffuse

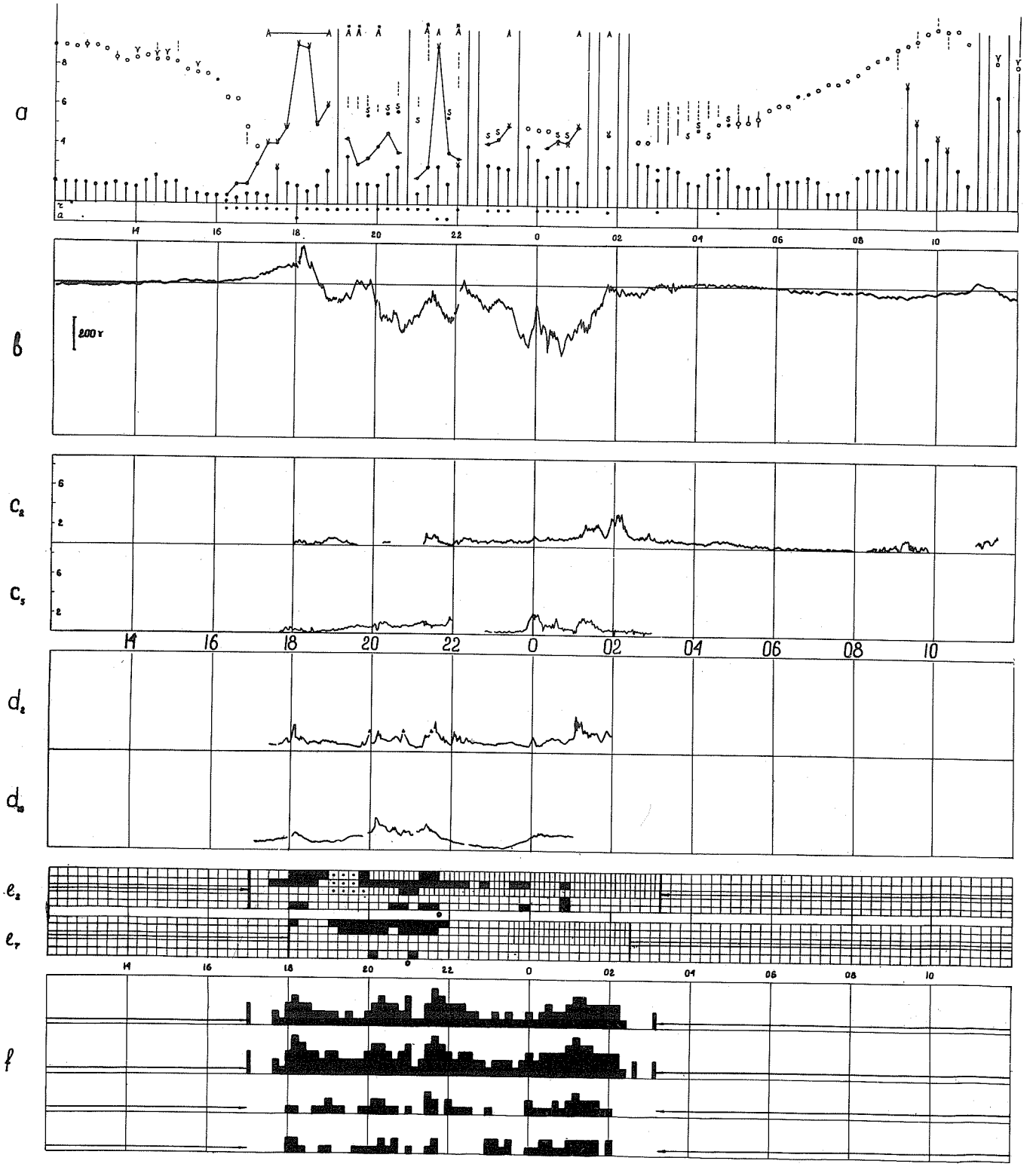

Fig. 2. Development of the disturbance of March 5-6 1970 according to: a) ionosonde data (Murmansk), b) magnetogram (Lovozero), c) riometers, d) photometers, e) ascaplots, indices indicate location of station in accordance with Table 1; f) intensity of 4278Å, 5577Å, 6300Å and $1PGN_2$ emissions. Universal time.

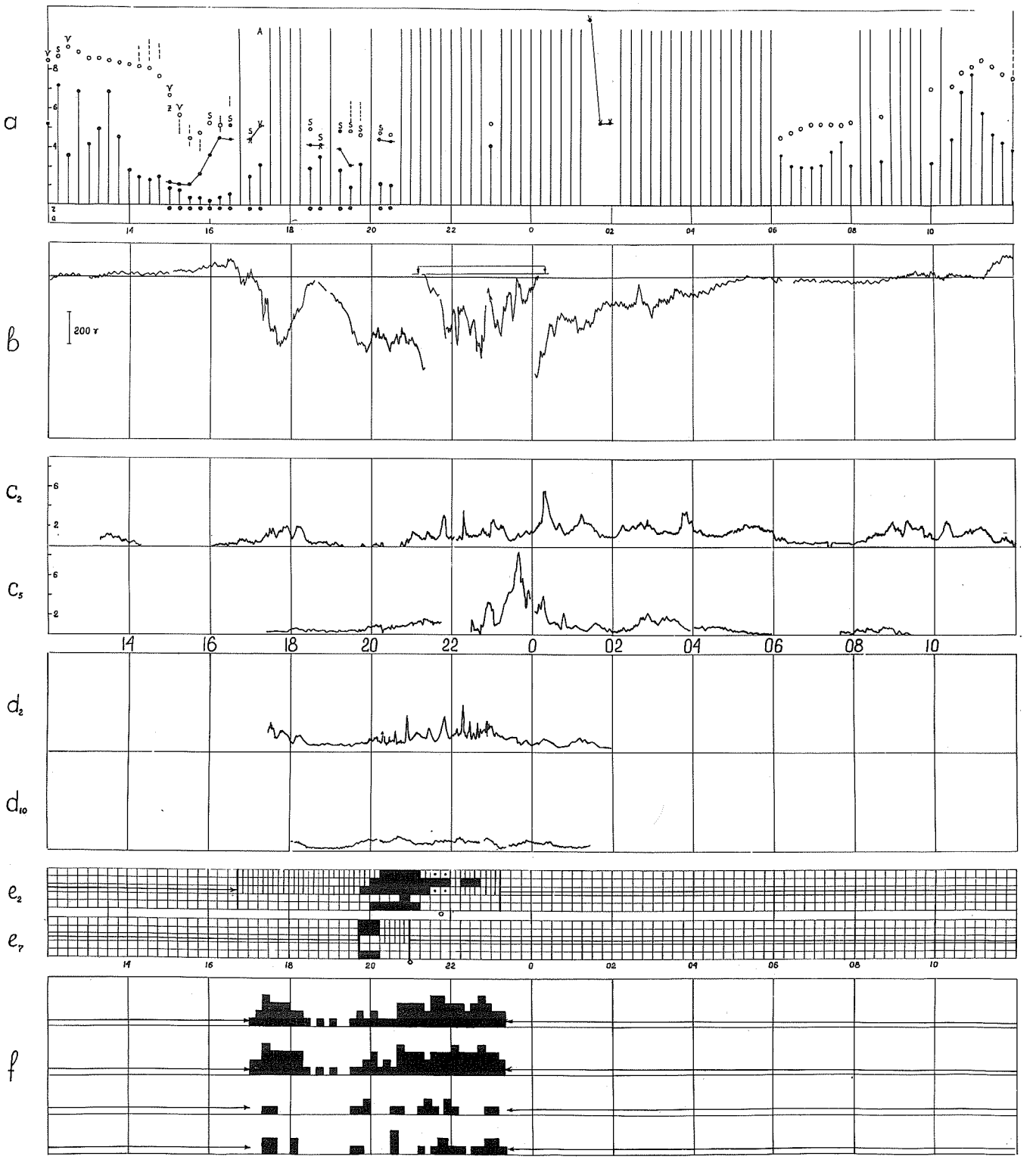

Fig. 3. The disturbances of March 6-7. The designations are similar to Fig. 2.

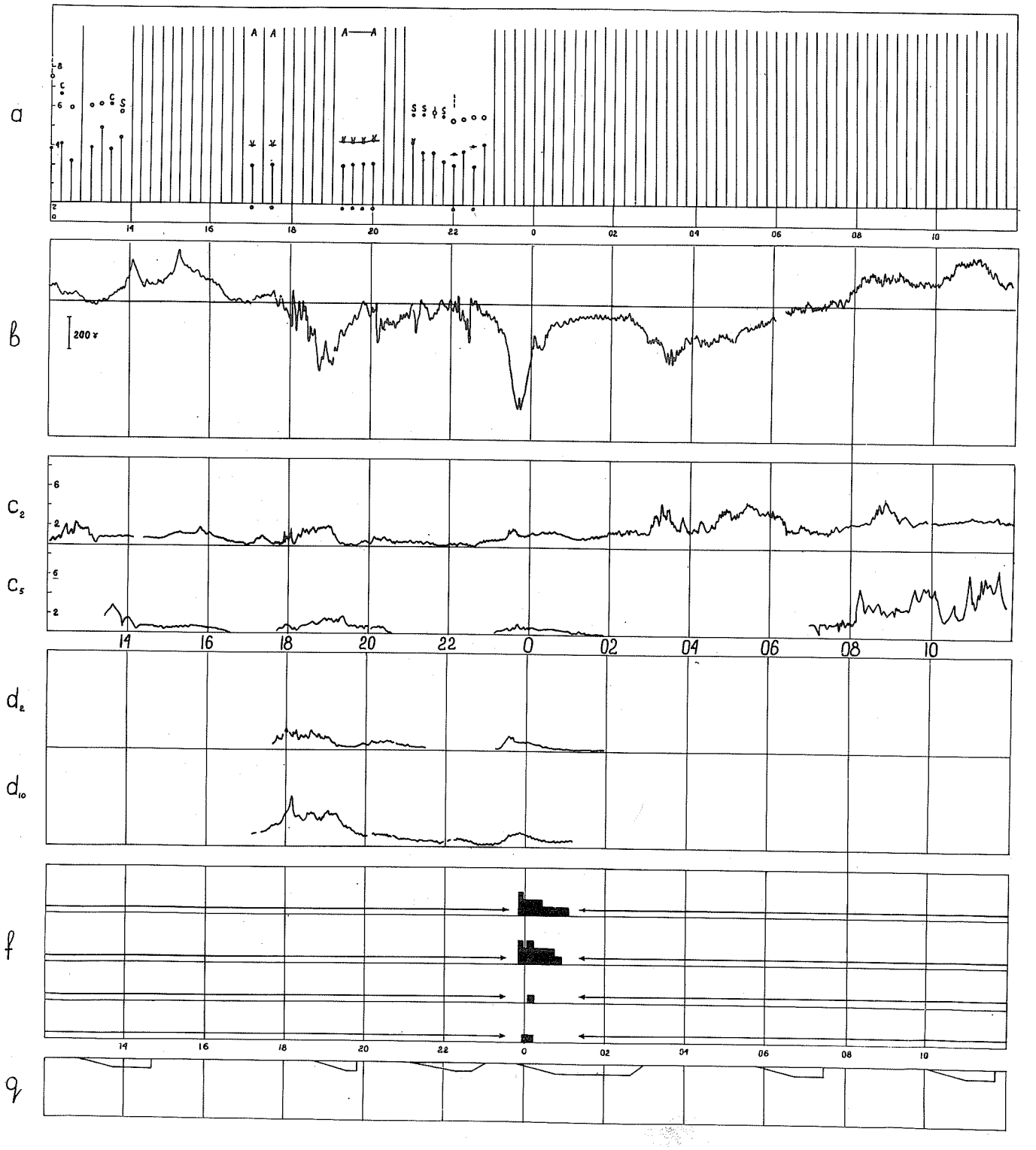

Fig. 4. The disturbances of March 7-8. In line g are indicated the periods of balloon flights. Flat sectors correspond to the flight time at an altitude exceeding the level of 100 g/cm^2. The other designations as in previous Figures.

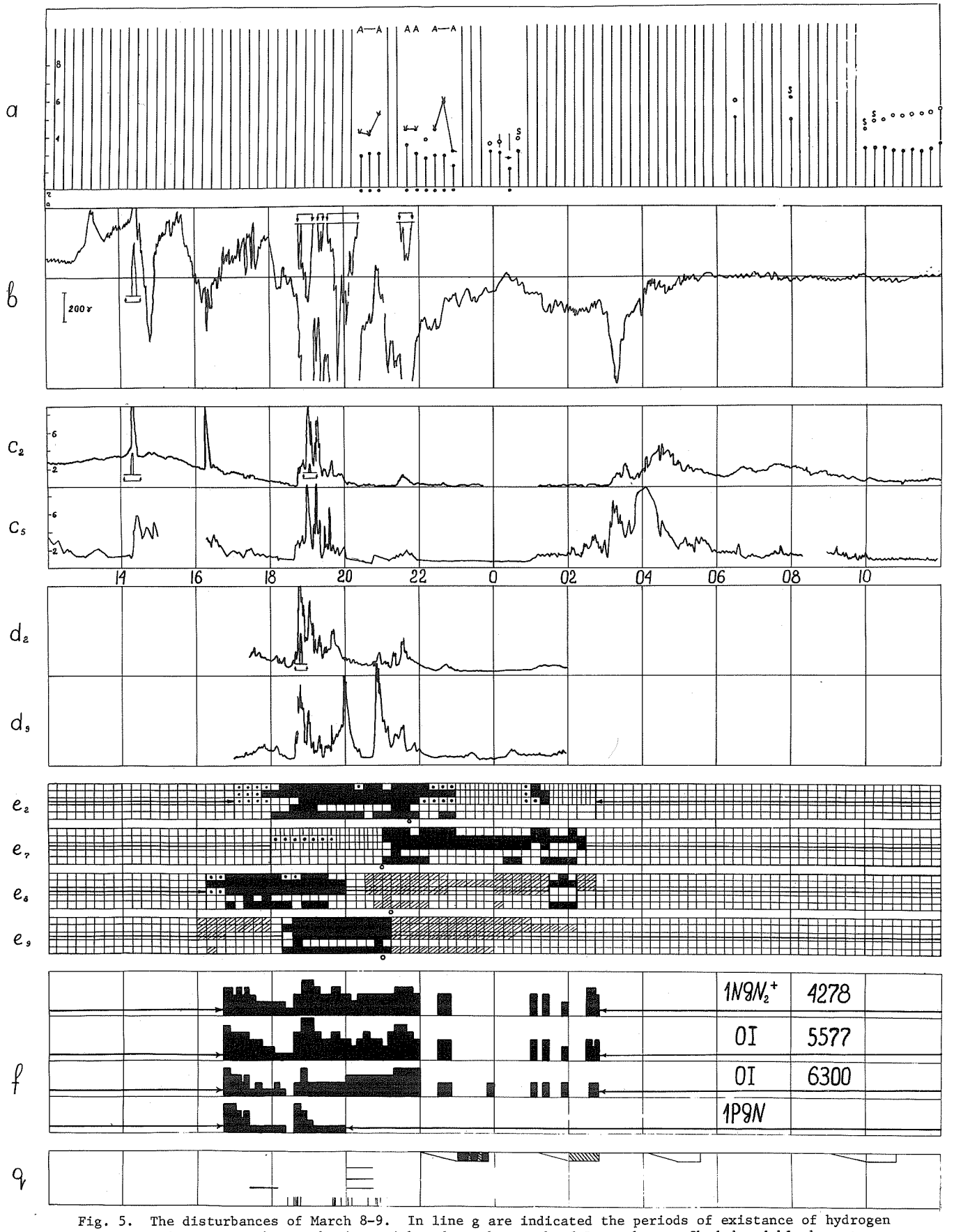

Fig. 5. The disturbances of March 8-9. In line g are indicated the periods of existance of hydrogen existence to the north, in zenith and to the south of Loporskaya. Shaded and black sectors on balloon diagrams indicate times of observation of significant X-ray flux. The other designations as in previous Figures.

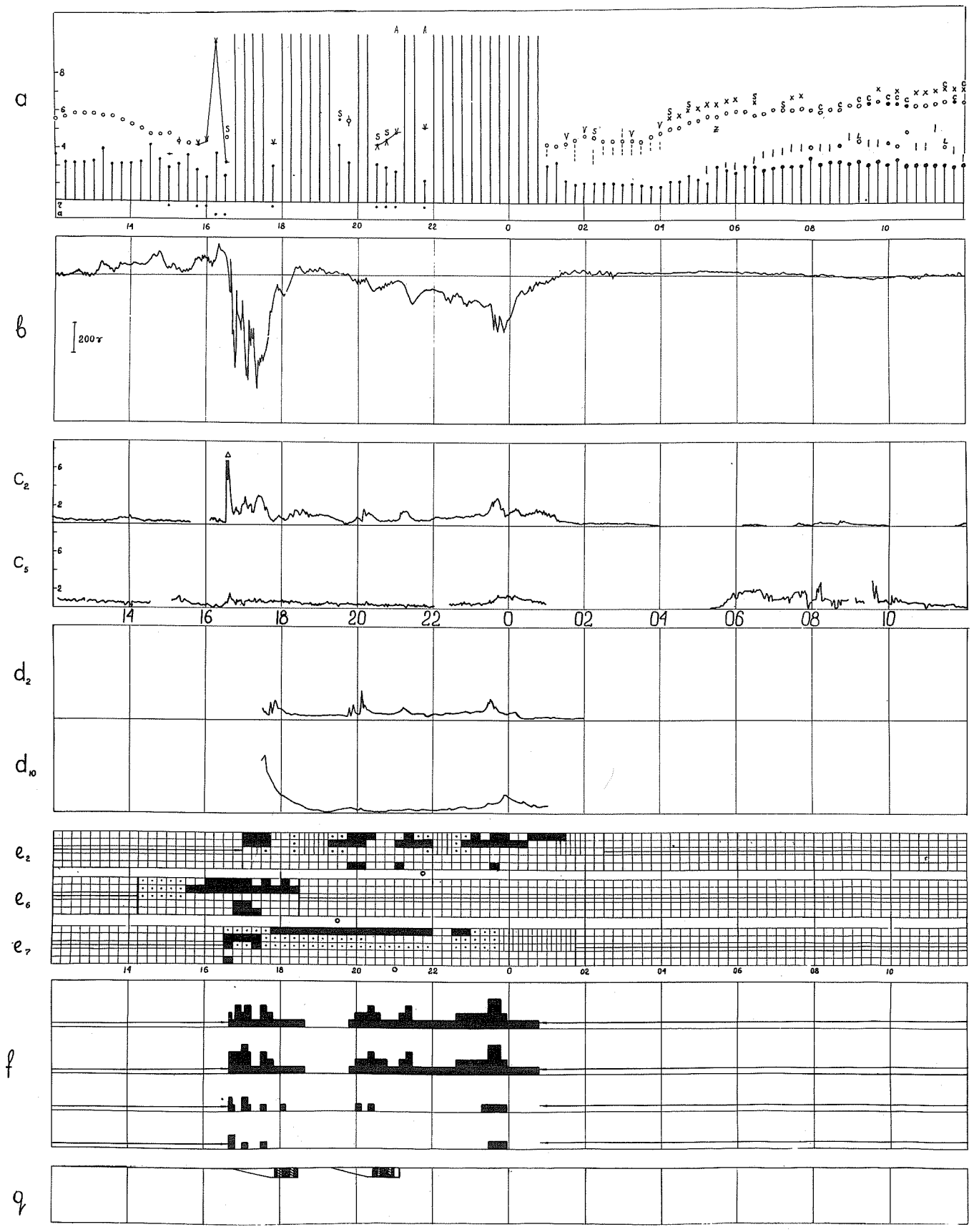

Fig. 6. The disturbances of March 9-10. The designations are as in previous Figs.

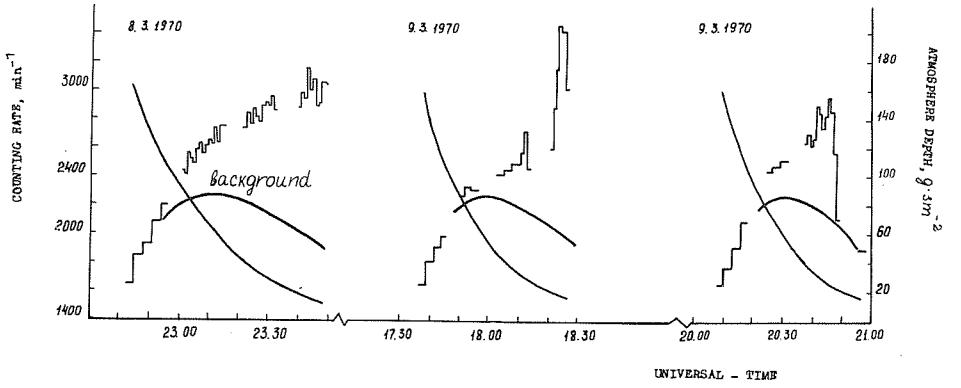

Fig. 7. Balloon-borne X-ray measurements. Counting rate of G-M counters, average level of cosmic ray background and atmosphere depth are shown versus UT.

Table 2

DATA ON BALLOON X-RAY MEASUREMENTS

MARCH 1970	START UT	P_{min_2} g/cm^2	MAX COUNTS PER MIN	TIME UT	REMARKS
7	1256	5.5	2400	1358	Background
7	1845	50	2400	1948	Background
7	2114	70	2300	2232	Background
7	2348	15	2300	0105	Background
8	0549	10	2250	0658	Background
8	1007	14	2250	1112	Background
8	2158	11	3170	2344	Significant Flux
9	0108	12.5	2440	0226	Background
9	0407	14	2250	0518	Background
9	0900	10.5	2200	1008	Background
9	1653	17.5	3460	1825	Significant Flux
9	1924	16	2960	2046	Significant Flux

glows. The space between two regions of auroral luminosity became filled in and simultaneously the westward electrojet developed. Intensity of $1PGN_2$ increased above Loparskaya (Figure 5f).

At 1846 UT in Loparskaya the greatest maximum of luminosity, mostly in $1PGN_2$ emission, took place simultaneously with the maximum of the negative bay; the sharp maximum of absorption appeared with 10-minute delay. All structure in auroral forms disappeared after that and all variations of luminosity became due to the variation of diffuse glow (background luminosity).

During the period of the second auroral substorm (1928-2010 UT), significant intensification of the background luminosity was observed. This intensification was responsible, for example, for the sharp one-minute peak of luminosity at Karpogory at 1838 UT. At 1940 UT the background luminosity increased to the north of Loparskaya, decreasing gradually to the south. Above the station a rayed arc was observed. All this indicates the redistribution of the auroral particle precipitation in space. At 1952 UT short lived separate rays appeared at Karpogory; at 2003 UT (maximum intensity in Karpogory, Figure 5) the rays vanished and only increased background luminosity was observed. At this moment the negative bay at Kem reached its maximum value. The intense westward current in this case was connected with the large rather homogeneous band of ionization about 1000 km width. The equatorial boundary of this band was situated at $\Phi' = 56°$.

It seems that the third substorm, 2045-2200 UT on March 8, was the most interesting. Before its beginning weak rayed arcs were observed near Loparskaya and Karpogory, as well as weak airglow and homogeneous arc at $\Phi' = 56°$. At 2048 UT the sharp increase of auroral intensity began in the region of Karpogory with the maximum at 2051-2052 UT; at this time the polar boundary of luminosity was situated to the south of Loparskaya and the equatorial one was below $\Phi' = 52°$. The glow was diffusive without local forms. Between 2052 and 2215 UT the intensity of luminosity over Karpogory was being decreased almost monotonically; then it became inhomogeneous, with patched structure, changing in different points by different ways. The peak at 2051 UT was the greatest one measured in Karpogory

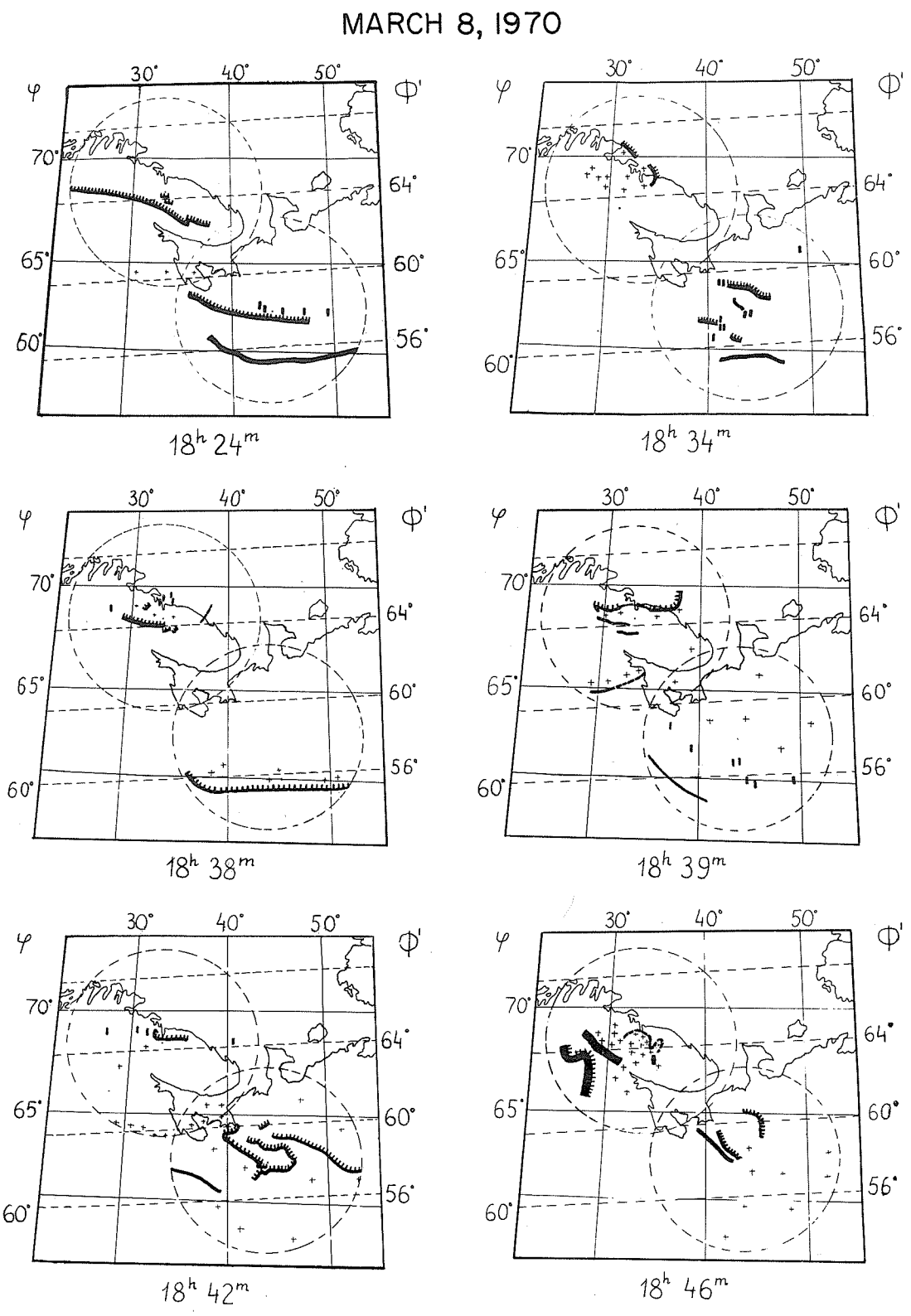

Fig. 8. Maps of aurora for the first active period, according to the all-sky cameras in Loparskaya (northern most) and Karpogory.

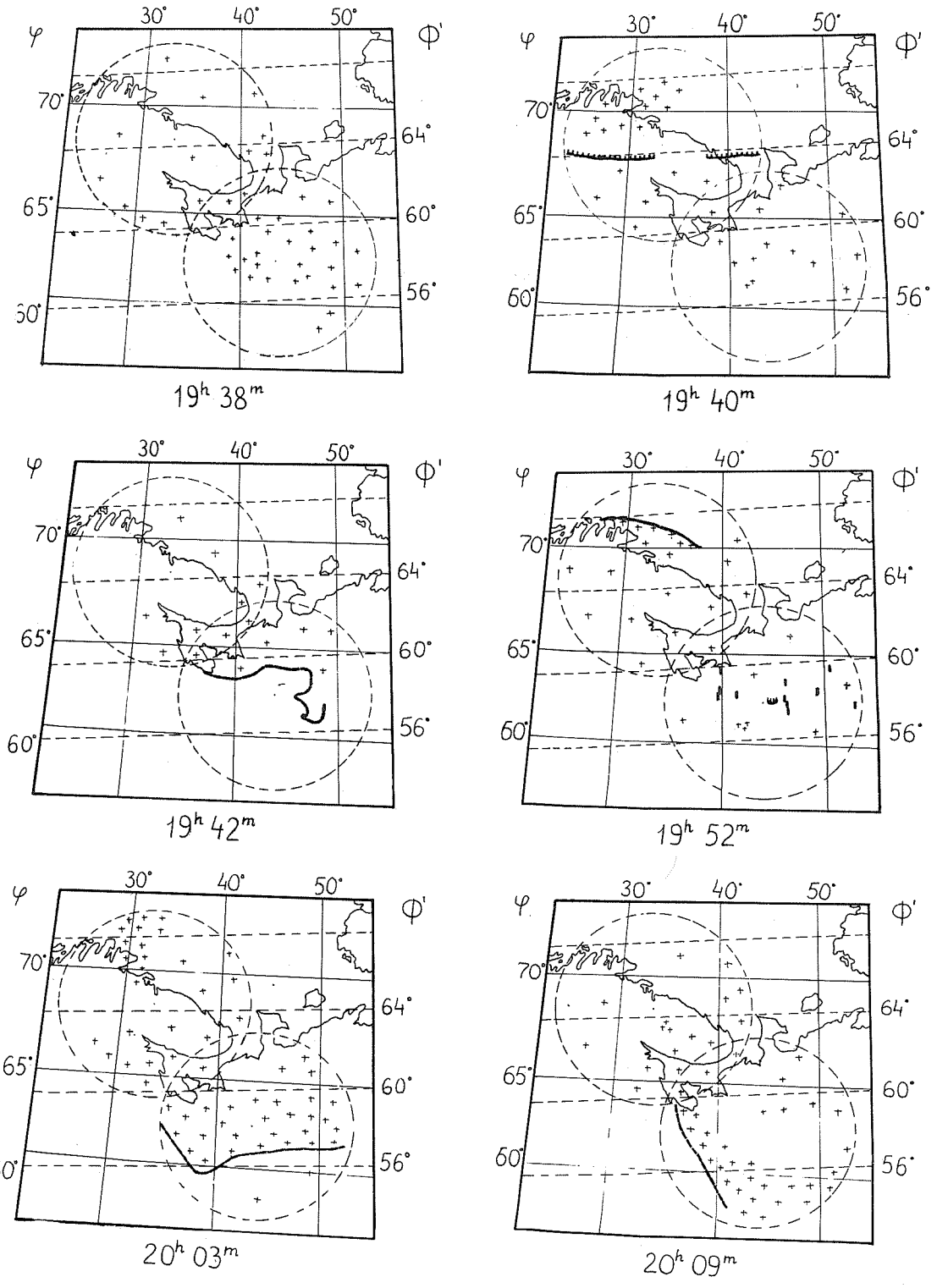

Fig. 9. Maps of aurora for the second active period.

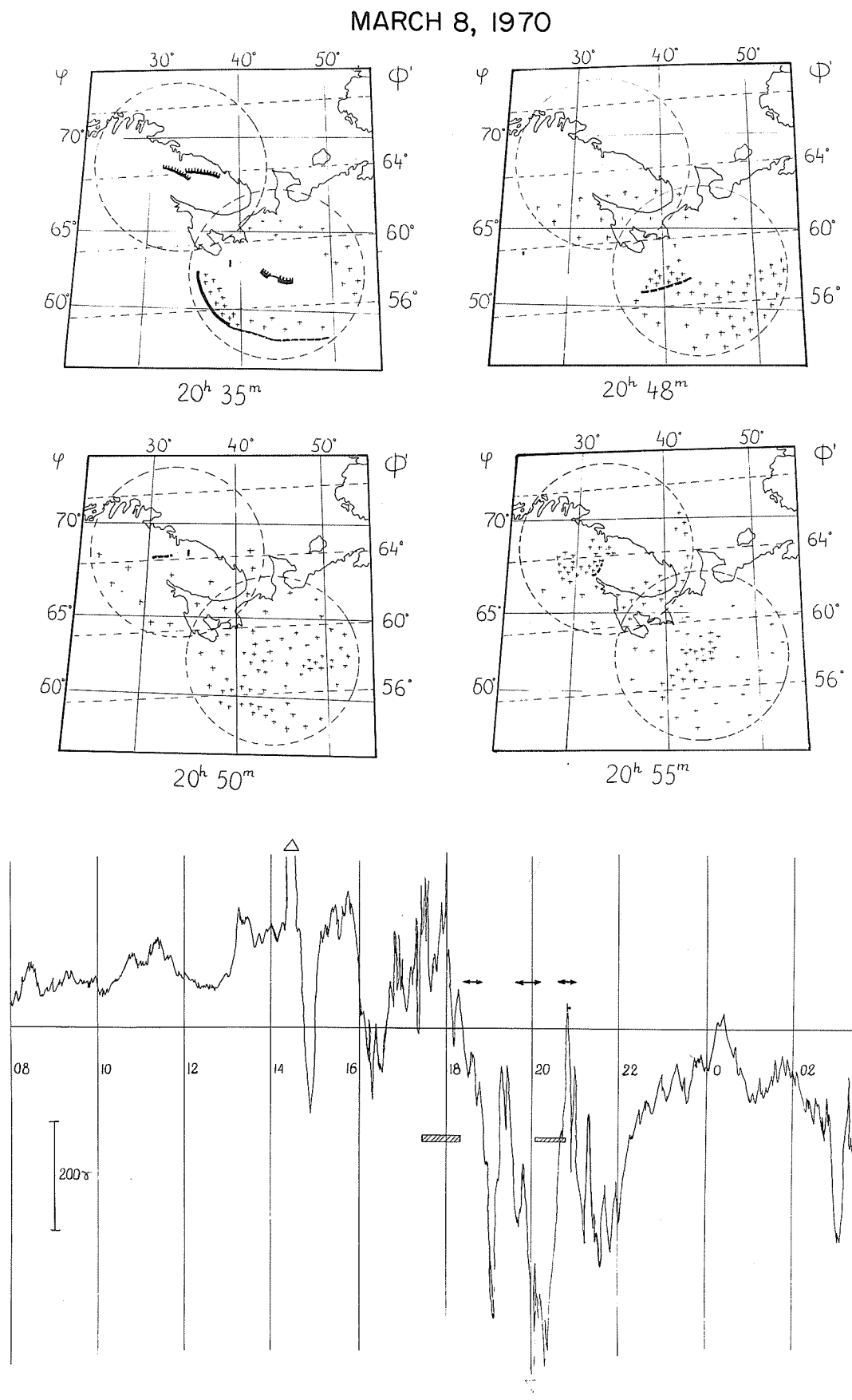

Fig. 10. Maps of aurora for the third active period and magnetogram of Kem station. Active periods and periods of existence of hydrogen emission are shown.

during the observed period, but the luminosity over Loparskaya was practically absent during this substorm. The photometer records at these two stations were quite different - correlation coefficient between them 2044-2113 UT equals +0.15 only.

The sharp increase of the auroral intensity in the region of Karpogory corresponds to the significant change of H-component in Lovozero, but in contradistinction to the previous two cases the magnetic disturbance was positive and in maximum H-component exceeded the undisturbed level. Supposing that the electrojet coincides spatially with the region of luminiscence, and at that time directed westward, the positive sign of the change of the field can be connected with the action of the return currents of the electrojet, then displaced far southward. Due to the anomalous displacement of the auroral oval towards the equator, at this period Lovozero station seems to be inside the polar cap region. A considerable intensification of 6300Å line relative to 5577Å between 2000 and 2200 UT makes this aurora similar to a polar cap one and give additional evidence of such interpretation. [Compiler's note: In a letter Dr. Brunelli stated there is a mistake in Figure 5 for the values of OI 6300 in section f. The correct values are even higher than those plotted in the Figure.]

REFERENCES

ISAEV, S. I., M. I. PUDOVKIN, O. I. SHUMILOV and S. A. ZAYTSEVA	1968	The influence of DR-currents on the development of geomagnetic storms. Proceedings, International Symposium on the Physics of the Magnetosphere, Washington, D. C., September 3-13, 1968.
PIGGOTT, W. R. and K. RAWER	1961	URSI Handbook of Ionogram Interpretation and Reduction, Elsevier Publishing Company, Amsterdam.
STOFFREGEN, W.	1962	IGY Ascaplots. Annals of the International Geophysical Year, XX(1), Pergamon Press.

"The Time Variation of some Solar and Geophysical Events in the Interval about March 6, 1970"

by

L. Krivsky and J. Olmr
Astronomical Institute
Czechoslovakia Academy of Science, Ondrejov

S. Fischer and P. Chaloupka
Institute of Experimental Physics
Slovak Academy of Science, Košice

and

S. Krajcovic and S. Pinter
Geophysical Institute
Slovak Academy of Science, Bratislava

In order to determine the localization of the extraordinary active events on the Sun with the geoactive effects following March 6, 1970 in the context of the previous and following activity and effects, the authors of this paper investigated some solar, interplanetary and geomagnetic characteristics during the period from November 26, 1969 until June 30, 1970.

The radio burst development

From the radio parameters of the solar activity we investigated, first, the slowly varying component (s-component) of the radio emission in middle dm-range, contructed from the Observatories of Ondrejov, Czechoslovakia (56 cm = 536 MHz) and Bedford, Massachusetts, U.S.A. (50 cm = 606 MHz) in order to obtain the maximum possible control of the radio activity during 24 hours. Secondly, there were the radio bursts obtained from both stations. The upper part of Figure 1 shows the daily values of s-component with the bursts superposed so that the lengths of the radio burst lines are proportional to the square root of the radio flux. Particularly great bursts with intensity 200 x $10^{-22}Wm^{-2}Hz^{-1}$ or greater and with duration greater than 15 min. are labeled by full circles at their tops. The graphical presentation suggests that a series of radio bursts always occurs before the Forbush-decrease of cosmic rays. For the purpose of correlation, we have prepared the tables of daily values of simple sums of the bursts Σx_i (without respect to intensity and duration) and using them, we have constructed a curve of a five term weighted moving average according to formula

$$\overline{\Sigma x_i} = \frac{\Sigma x_{i-2} + 2\Sigma x_{i-1} + 3\Sigma x_i + 2\Sigma x_{i+1} + \Sigma x_{i+2}}{9}$$

This defines "burstiness" of the dm-range as shown on the second curve of Figure 1. The count scale is reversed and the time scale is shifted with respect to the other curves.

The s-component shows a quasi-periodic variation which is maintained during some months. Then it is disturbed and a new variation appears. On the s-component curve there are two basic drifts which were found in the separated values from the Ondrejov and Bedford stations. If the s-component was constructed separately from each station, there was identical and quasi-periodical variation on each curve. The total increase is apparent from the beginning of the investigated period, the maximum is in the middle part of February 1970 and then a slow decrease again appears.

With respect to the number of the radio bursts, we can divide the investigated interval into two parts. The first one from November 26, 1969 until the end of February 1970 has little activity, the second part is characterized by high radio burst activity. These two intervals are identical with similar activity as observed on the curves of cosmic rays. The period of the high "burstiness" corresponds to the period of the deep and repeated cosmic ray decreases.

Cosmic ray variation

In order to represent the effect of the activity on the situation in the interplanetary space around the Earth, two stations, namely, Uppsala, Sweden and Kiel, Germany were selected. Only the values of daily averages of the Uppsala station were drawn. The fine structure of the single Forbush-decreases are partially suppressed, but on the other hand, there are impressive series of effects, in particular the deep or long-living effects, Figure 1. All the period can be divided with respect to the different character of activity into two periods. The first, from the beginning of the interval until the end of February 1970, during which there are only unimpressive decreases. The second period is from the beginning of March 1970 until the end of the interval, during which there are very frequent and impressive Forbush decreases. A decreasing drift is evident in the total count.

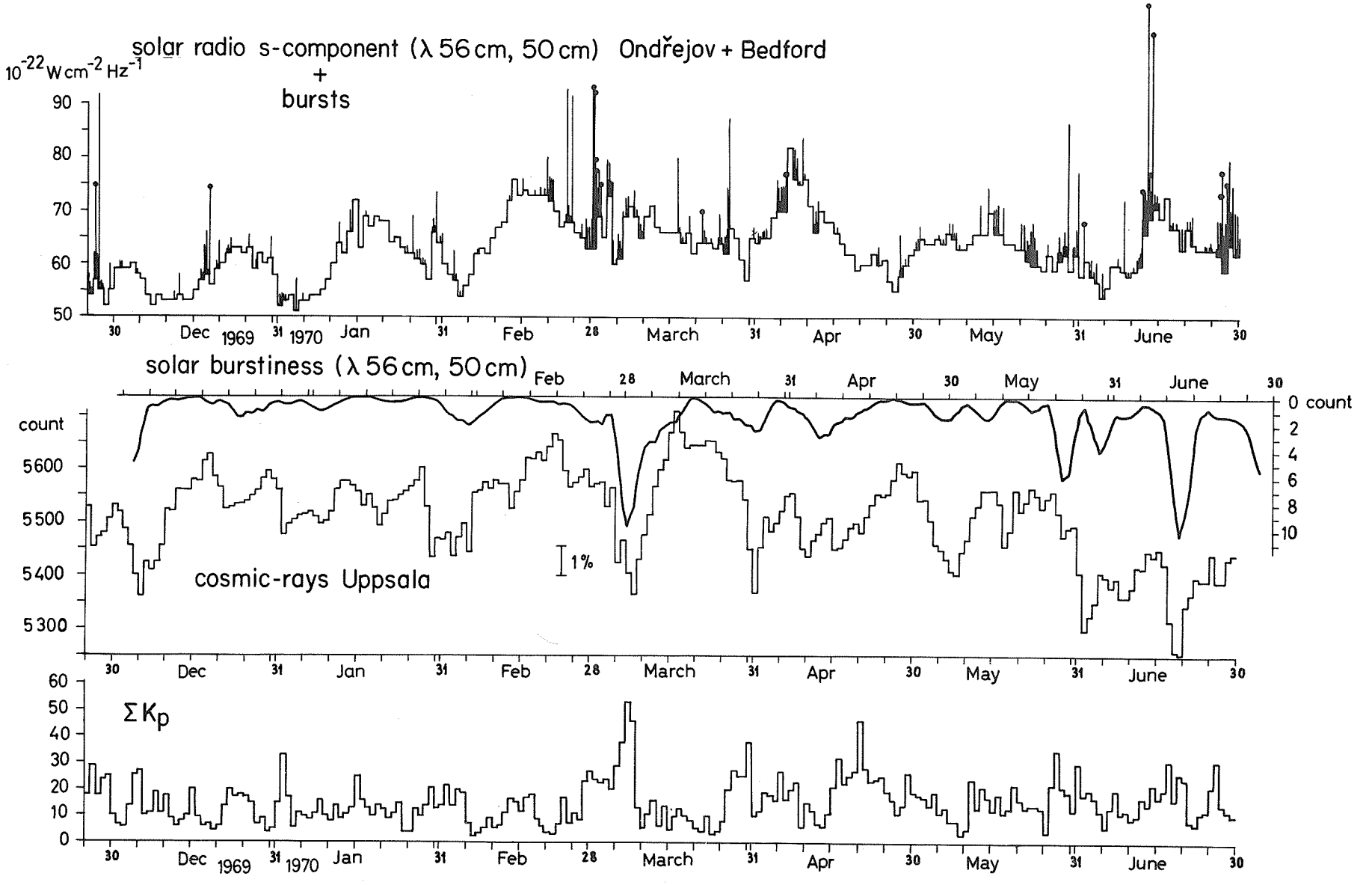

Fig. I. Graph showing the solar radio s-component with superimposed radio bursts, the "burstiness" index (displaced 6.5 days), Cosmic Rays-Upsalla and ΣK_p, for November 26, 1969 to June 30, 1970.

Planetary index ΣK_p variation

On the fourth curve, Figure 1, we show the ΣK_p values. In the whole period besides the normal fluctuations there are three great increases, namely, in March and April 1970. The March increase was the greatest, $\Sigma K_p = 53$. The other increases of ΣK_p to the end of the period are smaller and less important.

The mutual correlation

The radio s-component and burstiness were autocorrelated and correlated with investigated parameters in one day steps, namely, to -48 and to +48 days: s-component vs. burstiness; s-component vs. burstiness (moving average); burstiness (moving average) vs. CR Uppsala; burstiness (moving average) vs. CR Kiel; s-component vs. CR Uppsala; s-component vs. ΣK_p; burstiness vs. ΣK_p; burstiness (moving average) vs. ΣK_p; CR Uppsala vs. ΣK_p; CR Kiel vs. ΣK_p; CR Uppsala vs. CR Kiel.

First of all, we shall describe briefly some results not given on the graph, Figure 2. These, we do not consider to be important.

S-component vs. burstiness (moving average) showed a very weak durable positive correlation. Between the 2nd and the 3rd day there was a weak increase to the value +0.26. Nearly the same result was obtained for the non-reduced values of burstiness. From the graph of Figure 1 it is evident that the time occurrence of the burst series with respect to the fluctuation of the radio s-component is almost accidental. Very often cases occurred when considerable radio burst activity coincided with the minimum of the s-component.

Burstiness (moving average) vs. CR Kiel: after the +1st and the +2nd day the negative correlation increases and reaches -0.30 as the maximum value between the +5th and +7th day.

S-component vs. CR Uppsala: there is very weak correlation and after the -20th day the correlation coefficient increases.

S-component vs. CR Kiel: there is almost significant, very weak positive correlation and after the -20th day the correlation coefficient increases.

S-component vs. ΣK_p: there is a more significant positive correlation of +0.36 about the +16th day.

CR Kiel vs. ΣK_p: a predominantly very weak negative correlation about the zero day is evident; the maximum value of r is -0.32 on the -1st day.

CR Uppsala vs. CR Kiel: the selected station Uppsala was compared and correlated with data of a number of other cosmic ray stations; its daily variation was not different from other stations, i.e. this station is representative. This is documented by the correlation with the Kiel station, characterized by the coefficient +0.74 on the zero day.

The important results

On Figure 2 a choice of all inyestigated correlations is shown. For our purposes and for the review the interval ±20 days was selected.

Burstiness (moving average) vs. CR Uppsala: this result can be considered as the most important and it is shown on Figure 2. One day after the burst an increase of negative correlation coefficient appears and reaches its maximum, -0.4, on +6th day. This negative correlation ends on about the +14th day. The same result was achieved for the CR Kiel station. The correlation coefficient must be considered to be important if we take into account that the correlation coefficient +0.7 was obtained from two cosmic ray stations (i.e. for the values of the same event). On Figure 1 the occurrence of the burstiness (moving average) is shown. It was constructed for the reversed frequency scale and with a phase shift of 6.5 days in order to show the correlation with the CR Uppsala station more distinctly. It is also evident that lesser numbers of solar radio bursts (56 cm, 50 cm) produced the Forbush decreases which were sometimes very small.

Burstiness (moving average) vs. ΣK_p: a more pronounced positive correlation coefficient is obtained for ΣK_p on +4 to +8 days, a maximum +0.4 is reached on day +6. The same result was obtained using the non-reduced values of the burstiness. Thus, it is evident that the phase shift of ΣKp is coincident with the phase shift of the maxima of the Forbush effects, which confirms the known expectation of the common origin and propagation velocity of "agens". From Figure 1 it is evident that the correlation coefficient was influenced mainly by the three greatest increases of ΣK_p during March and April 1970.

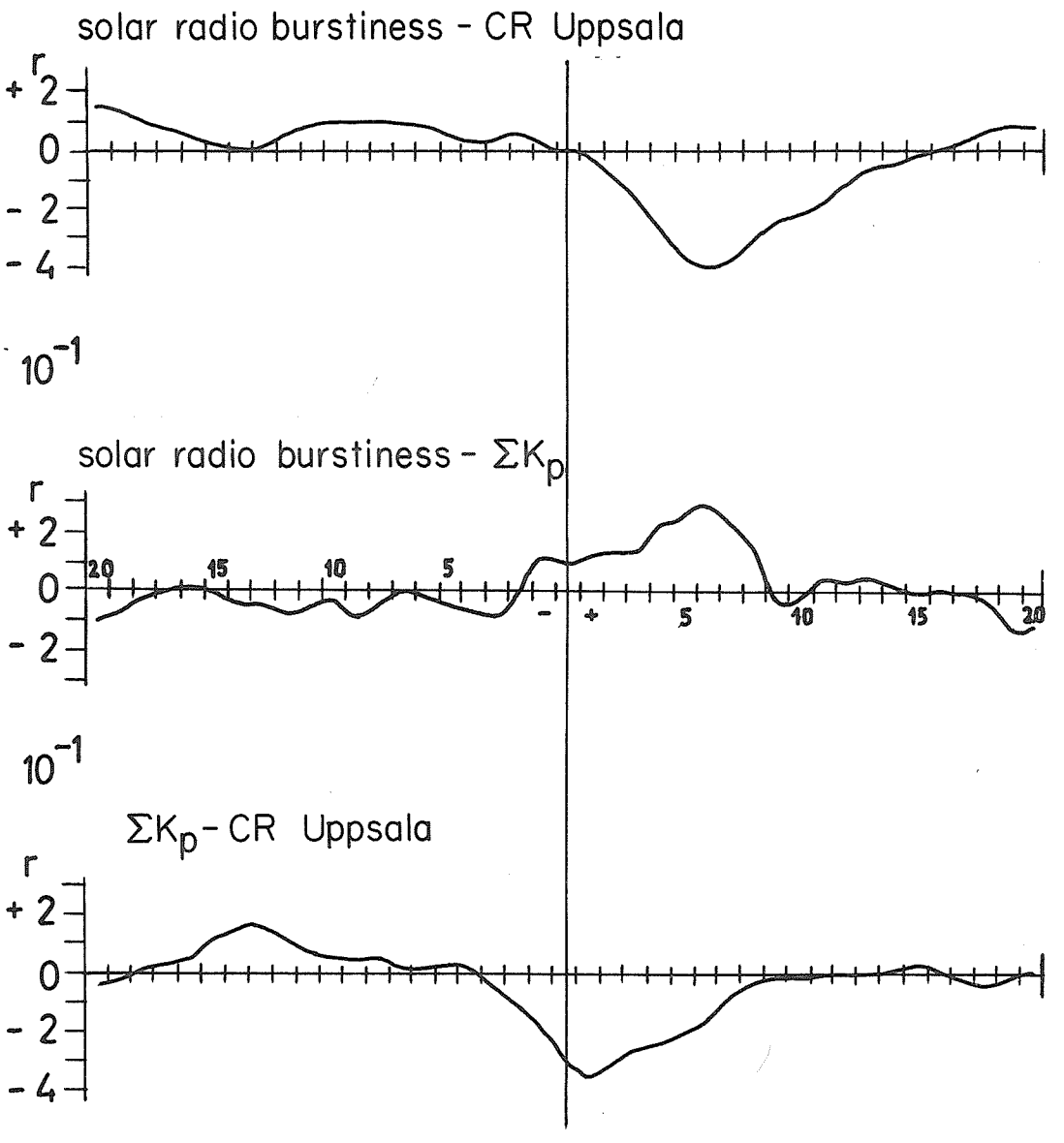

Fig. 2. Correlations between the daily averages of the cosmic ray neutron component at Uppsala, the number of radio bursts (weighted running averages) and the daily sum of the three-hour Kp indices are shown for shifts from -20 to +20 days.

ΣK_p vs. CR Uppsala: see Figure 2. A more pronounced increase of the negative correlation coefficient appears between the days -2 and +6, the maximum of -0.36 was reached on day +1. This result confirms the relationship of the processes producing both events. The same variation of the correlation coefficient was obtained for the correlation ΣK_p vs. CR Kiel. It seems to be real and logical that ΣK_p reaches greatest values predominantly one day before the maximum value of the Forbush decrease; it is produced by the magnetic discontinuities in the interplanetary space interacting with the earth's magnetosphere preceding the center of gravity of the "cloud" shielding the cosmic particles from the universe, i.e. the cosmic ray Forbush decrease.

All the correlations computed with the moving values of the weighted averages of the burstiness, were computed also with the non-reduced values (i.e. with usual daily sums of the radio bursts). In all cases we obtained the same variations but the correlation coefficients were smaller. If we consider that there was no weighting of the radio bursts and that the stations Ondrejov and Bedford cover only about two-thirds of the 24 hour interval, we can expect the moving weighted values of the burstiness to be more representative as we have found. With these latter values we obtained greater correlation coefficients.

Autocorrelations

In order to fix whether the active region on the sun which produced the effects in the period from 6 to 9 March 1970 was active for a long time, we carried out the calculations of the autocorrelation function for all the above mentioned parameters. On the autocorrelation curves we can see the maximum values of the correlation coefficients, namely, for shifts of about 27 days and about 35 days, respectively. From the graph of the s-component variation the 27-day period is evident in the time interval following the beginning of March. This regular variation is then interrupted (see Figure 1). For the other parameters this 27-day variation is evident in the period up to March, but is more complicated. Different from the other parameters, there exists a very pronounced period about 27 days with $r = +0.4$ for the autocorrelation function of the s-component. Thereby the following maxima do not occur. For ΣK_p this periodicity is less evident than for the cosmic ray intensity while for the radio bursts it does not appear at all. The autocorrelation curves will be published in the forthcoming paper.

Discussion

It seems from time variations, autocorrelation and correlation functions for single parameters and their combinations, that a main active region existed on the sun which produced enhanced radio emission at the beginning and at the end of December 1969, January 15 - 20, and February 13 - 20, 1970. Later the influence of this region is superposed on the influence of another evidently increasingly active region, which is most pronounced at the beginning of March. The enhanced radio emission activity from 3 - 5 February 1970 can be the symptom of the above mentioned increasing solar activity in March. The superposition of the effects from both regions in cosmic radiation leads to the higher values of the correlation coefficients with the period of about 36 days for the time interval between decreases of the intensity at the end of January and at the beginning of March and about April 1, and May 8, 1970.

Conclusions

1. The occurrence of the radio bursts series in middle dm-range is not connected at all with the fluctuation of radio s-component. This suggests that the processes on the sun that are the source of s-component, have their own generation mechanism which is not connected to the burstiness or the escape of particles with magnetic discontinuities.

2. The increased number, especially of every series of the radio bursts, connected with a certain configuration of magnetic fields of the active region, characterizes the situation of a given type on the sun which produces such situations in the interplanetary space and around the earth by the transportation of the "agens" causing the Forbush decreases of cosmic radiation which are registered on the earth's surface. In fewer cases there is an increase of geomagnetic planetary indices ΣK_p. It is expected that in the case of the burstiness constructed from additional stations, to cover all 24 hours, the significance of the relation could be still greater. It follows from the comparison of the burstiness curves and CR Uppsala on Figure 1 (with a phase shift 6.5 days) that at the occurrence of increased radio bursts we can forecast future beginning of a Forbush effect by one or two days. The maximum of this effect follows on the average 5-7 days after the radio bursts series.

3. It is most probable that single Forbush decreases of cosmic rays are produced by individual more powerful flares [Gopasyuk and Krivsky, 1967]. It seems that the occurrence of such flares is not accidental but is always connected with such an active region on the sun, where also the other eruptive events are rich in manifestations in the radio emission in dm-range. In other words, the Forbush decrease is produced only by the most powerful flare which originates in the active region producing the radio bursts in the dm-range.

4. It seems that the peaks of enhanced ΣK_p precede by one day the deepest decreases of Forbush effects. The increase of the disturbance of the geomagnetic field is produced probably by a discontinuity of "cloud" and never by its center of gravity; it is in coincidence with up-to-date ideas.

The authors acknowledge the kind cooperation of Dr. T. Kowalski, Geophysical Institute, Warsaw, and J. Ilencik, Institute of Experimental Physics, Košice.

REFERENCES

GOPASYUK, S. and L. KRIVSKY 1967 Bull. Astr. Inst. Czech. 18, 125

"Some Geophysical Characteristics Observed at 120°E for the Period March 6-10, 1970"

by

J. J. Hennessey, S. J. and J. E. Salcedo
Manila Observatory
Manila, Philippines

Introduction

At a time of disturbance in geophysical conditions a composite view of many positive and negative responses taken at one geophysical region can illuminate the operative mechanism of solar events. Likewise ionospheric data and geomagnetic events find a further interpretation in the solar burst data.

I. Radio Solar Burst Data

During the active period 6-8 March 1970 a total of seventeen radio bursts (Fig. 1) were captured at the Manila Observatory (N14.7° E121.1°) and at Sagamore Hill Observatory (N42.6° W70.8°), complementary locations. Three (Nos. 1, 5, 7 not shown in Fig. 1) of the eight bursts at Sagamore Hill were of single frequencies (narrow band) and one (No. 1 not shown in Fig. 1) of the nine recorded bursts at Manila was of single frequency. Of the Manila bursts, five were associated with known optical flares seen at Manila and one other was believed to have originated from region 10595 at a location N09 W90 and so was a behind-the-west-limb event. Three events reported at Sagamore Hill correlated with optical flares.

In the decimeter band Manila event number 3 discussed in a companion paper [Badillo, 1970] and Sagamore Hill events numbers 2 and 6 are the only ones to register in the order of 100 flux units. These latter two bursts have their origin in the eastern hemisphere and are low in intensity. Therefore, they are unlikely sources [Ellison, 1963] of the great magnetic storm of 7-8 March 1970. Manila event number 6 which originated at the favorable location N04 W35 lacks the necessary intensity, duration, and signature for a proton event [Castelli, 1968]. Even considering the garden hose effect it is not likely that these bursts were endowed with the energetic particles responsible for the magnetic storm.

Table 1
Solar Radio Events for March 6-8, 1970

Event No./ Day	UT Time Start	UT Time Max	Dur. Min	Frequencies MHz	Correlations
1 06	0745.9	0746.3	1.6	2695	Optical Flare SN - 0745 U.T. S14 E16 Region 10614
2 06	0851.0	0851.3	0.8	8800, 4995, 2695, 1415, 606	No Flare, no SID's
3 06	0933.2	0933.9	3.5	4995, 2695, 1415	SPA on GBR 16 kHz of 97°; flare believed at N09 W90 BWL Region 10595
4 07	0050.9	0051.0	0.2	2695, 1415, 606	No optical flare.
5 07	0142.2	cf. Fig.3		8800, 4995, 2695, 1415, 606, 245, 24-48 SFIR	Flare 2B; SPA-three paths; SWF-four freq. 18-9.6 MHz; Vertical Incidence Sounding; No SCNA on 18 and 30 MHz.
6 07	0722.0	0722.3	5.0	4995, 2695, 1415, 606, 245, 24-48 SFIR	Flare 1N, 0721 U.T., max at 0724, Loc. N04 W35, Region 10607, No SID's
7 07	0838.5	0839.7	3.0	4995, 2695, 1415, 606	Flare 1B, Loc. S06 E04, Region 10614, No SID's
8 08	0659.1	0700.0	2.9	4995, 2695, 1415, 606	No Flare. SPA on GBR at 16 kHz 18°
9 08	0716.0	0716.6	3.7	8800, 4995, 2695	Flare SF, Loc. N08 W45. Region 10607, No SID's

A summary of some aspects of the Manila bursts is presented in Table 1 above. Events number 2, 4 and 8 were not associated with optical flares. The first two of these showed no SID's, but number 8 had an associated Sudden Phase Anomaly (SPA) on the GBR (London-Manila circuit) with an

advance of 18°. While events 7 and 9 showed up on three discrete frequencies and event 8 on four, each event presented relatively low power flux densities not in excess of 20 flux units. Event number 6 was associated with a 1N flare. Besides the frequencies and flux densities given in Fig. 1, a type V sweep frequency interferometer burst lasted for four minutes. But no SID activity was reported.

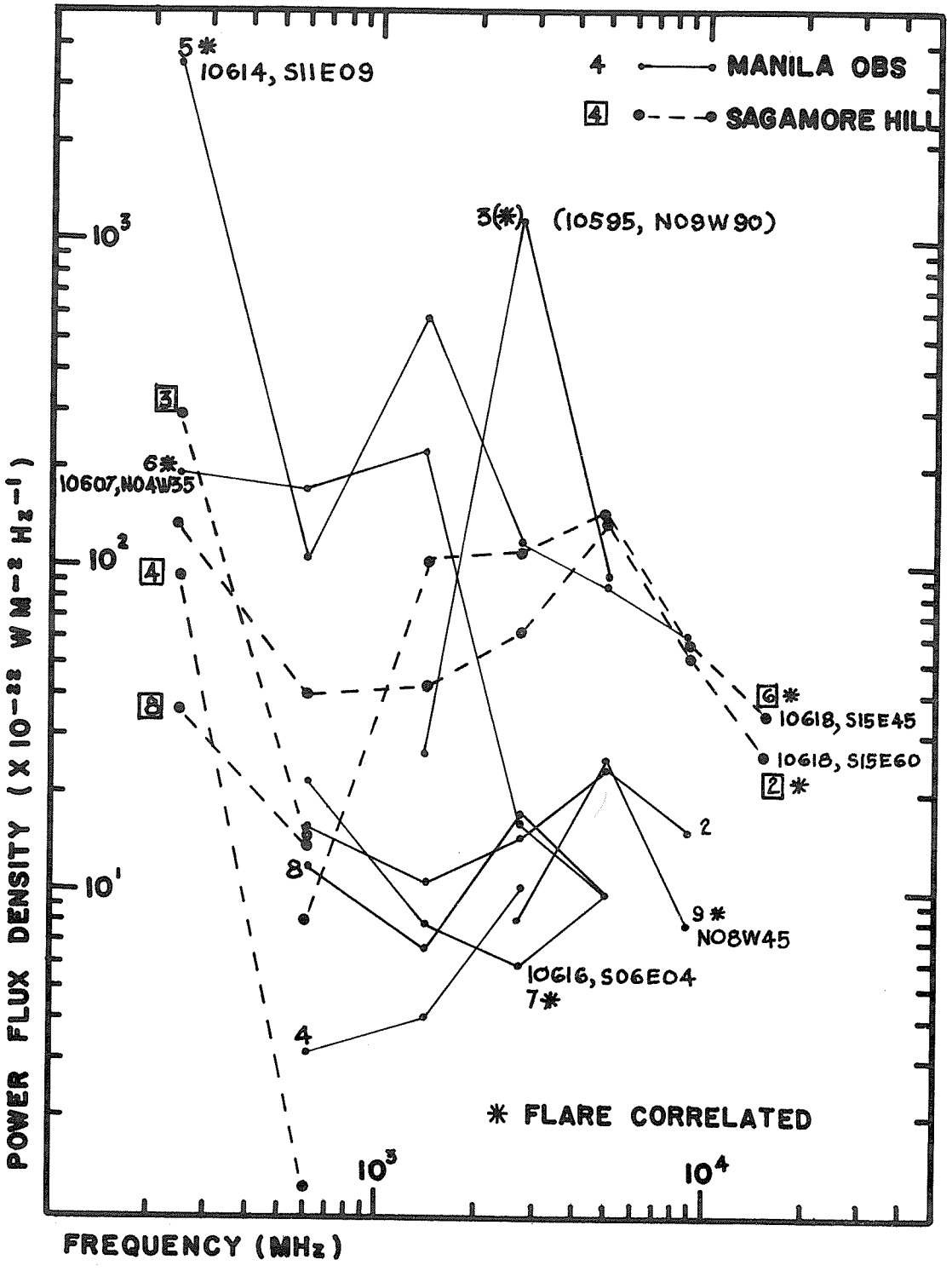

Fig. 1. Peak flux spectra of radio bursts seen at Manila and Sagamore Hill March 6-8, 1970.

Event Number 5 at 07 March 0142 UT

This event deserves more detailed attention for its radio aspects. It is not singularly impressive in intensity compared with others on previous occasions so it fails to reach the category of

great bursts. However, it is the most distinctive burst in this period for its duration and spectral signature [Castelli et al., 1967]. The flux values for this same event recorded at Toyokawa, Japan, at frequencies 9400, 3750, 2000 and 1000 MHz fit in place with the Manila burst spectrum. The optical flare considerations are thoroughly covered in another Manila paper [Miller and Trinidad, 1970]. Fig. 2 presents the burst profiles detected and recorded on the following discrete frequencies 8800, 4995, 2695, 1415, 606 and 245 MHz with their corresponding flux densities. The sweep frequency interferometer (SFIR) presented a brief continuum of radiation from 24 to 48 MHz which lasted for only nine and a half minutes with an intensity of 3.

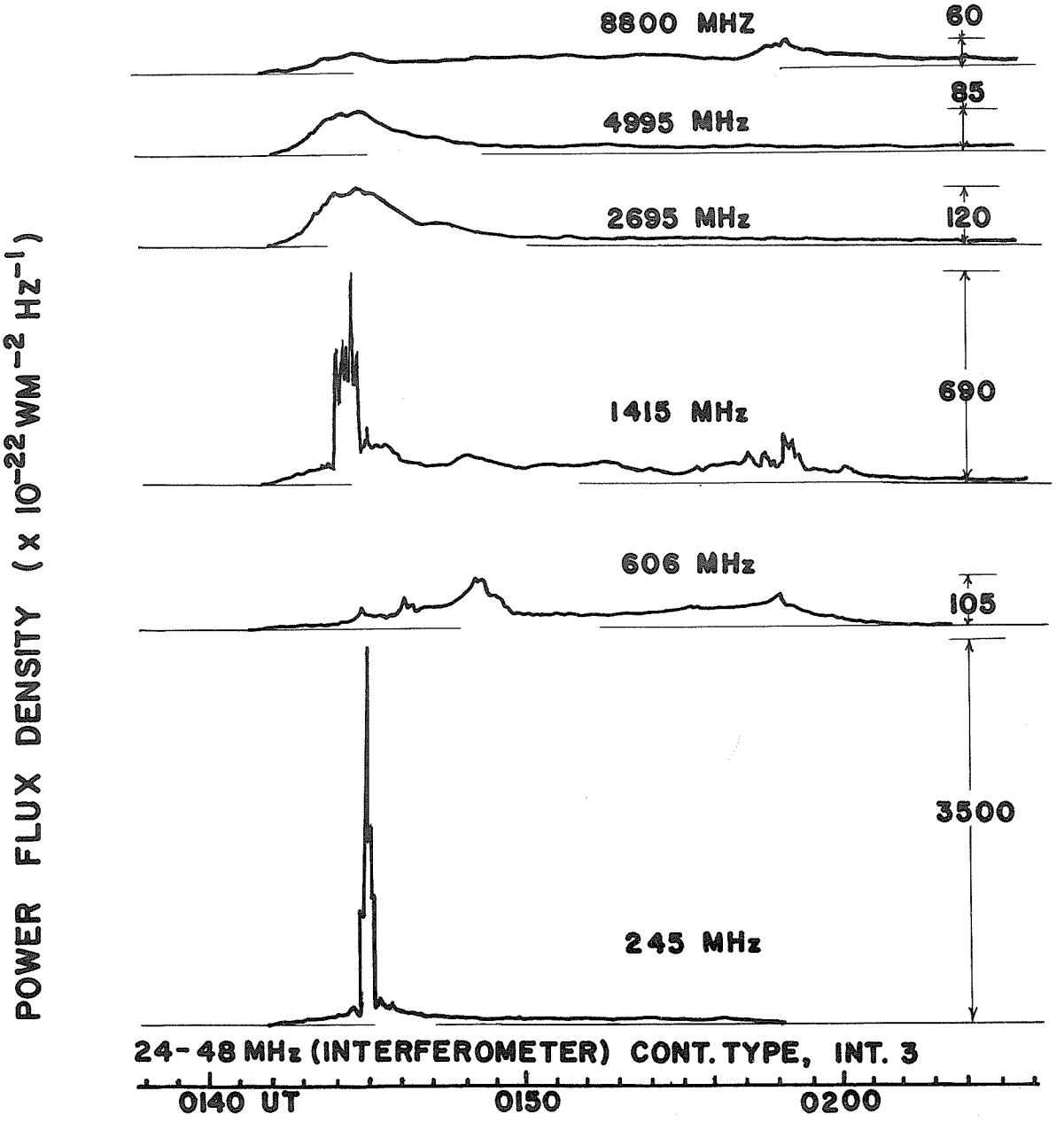

Fig. 2. Complex radio burst of March 7, 1970 observed at Manila Observatory, R.P.

In the discrete frequencies it was the 245 MHz receiver which recorded the highest power flux density through of relatively short duration and slightly later than a sharp peak at 1415 MHz. A secondary maximum about thirteen minutes later appears on three frequencies 8800, 1415 and 606 MHz with the maximum values occurring within a few seconds of one another. The whole radio event lasted for about an hour on the average.

SID effects of Manila Event Number 5

The electromagnetic radiation produced a number of sudden ionospheric disturbances which became apparent in the Manila records. Sudden Phase Anomalies (SPA) appeared on the three paths, (a)

from Rugby, England, GBR at 16 kHz for a 90° phase advance, (b) from NLK, Seattle, Washington at 18.6 kHz likewise for a 90° advance and (c) from NAA, Maine at 17.8 kHz for the largest advance of 122°. Short Wave Fadeouts (SWF) caused the signals on 18, 15, 12 and 9.6 MHz to drop 8, 10, 6 and 4.5 dB, respectively. Conspicuous was the absence of SCNA at either 18 or 30 MHz. Since the Sweep Frequency Interferometer (SFIR) recorded a continuum of radiation, this direct radiation at the two frequencies may have compensated for or neutralized the absorption effects. Heavy ionospheric absorption was evidenced by the rapid and large increase in the f-minimum on the ionograms near 07/0200 UT. Without this absorption the SFIR might have recorded a more lasting background continuum to put it in the class of a type IV, another criterion associated with a proton event [Bell, 1963].

Bifurcation of the F-layer was noticeable with the formation of the F1-layer, an infrequent occurrence during March. An F1.5 layer was indicated but the ionograms were not frequent enough to trace its development. The f-minimum increased rapidly from about 2 MHz just before the flare to 4.6 MHz just after it. Consequently the D-region became heavily ionized and the absorption was enough to prevent the regular E-layer from appearing. Sporadic E either because of the high D-region absorption or because of low ionization density (lower than on other days at this time) failed to appear for about an hour.

II. Geomagnetic Features

For this Observatory's three stations at Davao (N7.088° E125.580°), Manila (N14.633° E121.083°) and Baguio (N16.411° E120.580°) the horizontal components of the magnetic field are shown in Fig. 3. The Davao Station is just south of the dip equator and the other two stations are a little farther north. The horizontal component is, thus, most significant. The period prior to, during and just subsequent to the peak of the great magnetic storm of 08 March 1416 UT is reproduced (Fig. 3). The dotted line on the Manila curve represents the average of the horizontal component for the four days before and the four days after the storm, that is, 03-06 March and 10-13 March 1970.

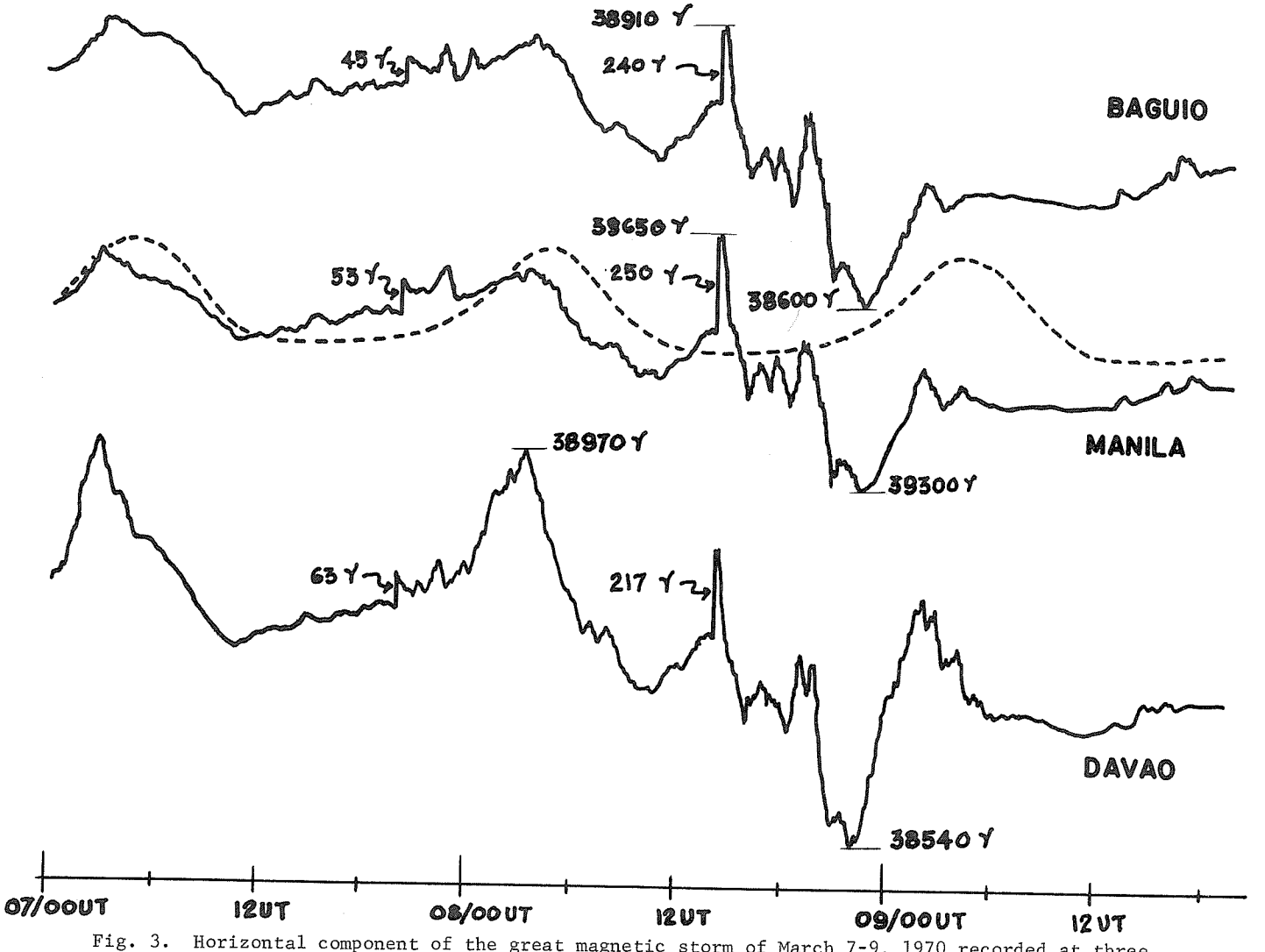

Fig. 3. Horizontal component of the great magnetic storm of March 7-9, 1970 recorded at three Philippine stations.

In the early hours of 07 March the magnetic field showed some disturbance in the clear departure from the diurnal curve. This is probably due to the influence on the ionosphere of the 0142 UT 2B flare located at S11E09 and associated with event number 5.

Two Sudden Commencements (SC) are evident, the first at 2004 UT on the seventh and the second, about four times larger, at 1417 UT on the eighth. This bigger SC coincided with the low energy (5-21 Mev) enhancements of particles (ATS-1) while the first SC may well correlate with the higher energy level 21-70 Mev as the trend showed up before and after ATS-1 was shut down for the eclipse event.

The first SC at 07 March 2004 UT occurred 34 hours and 21 minutes after the radio event number 3 of 06 March 0933 UT. The second SC at 08/1417 appeared 52 hours and 44 minutes after the same radio event. With reference to radio event number 5 at 07/0142 UT the first SC was 18 hours and 22 minutes and the second SC was 36 hours and 35 minutes later. Event number 5 originated at location S11E09 near the center of the sun's disk and so near central meridian passage.

The time of the height of the great magnetic storm agreed with the severe disturbance recorded in the SPA trace of the 16 kHz circuit between Rugby, England and Manila [Miller and Trinidad, 1970].

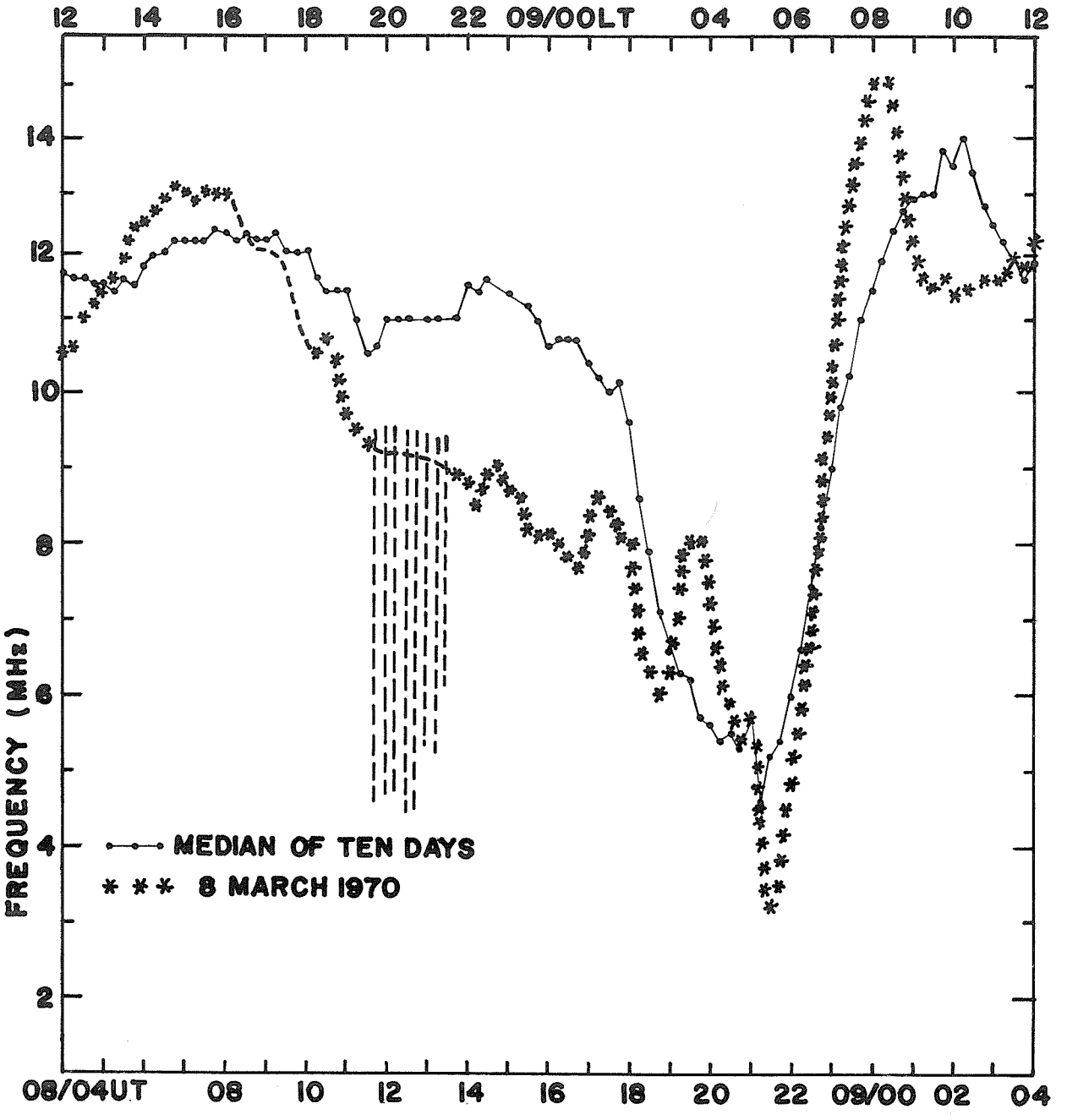

Fig. 4. Manila F2 critical frequencies.

III. The Manila Ionograms for March 8, 1970

The ionospheric storm clearly occurs during the night hours beginning just prior to 1330 UT (2130 local time). At this time solar flux does not directly illuminate the ionosphere at this station (N14.7° E121.1°). All of the indicated changes mentioned below for this storm are made in reference to conditions on five days before and five days after this disturbance (Fig. 4). These are the control days. Even some of these days, the sixth, seventh and ninth are among the magnetically disturbed days of March.

A. Critical Frequencies of the Ionospheric F-region

1. Before the magnetic sudden commencement.

At local noon (0400 UT) the plot of F2-layer critical frequencies (foF2) shows a neat saddle with noon low value at 10.5 MHz and peaks on either side at 13.0 MHz three hours before and three hours after noon.

At 0800 UT the foF2 starts dropping from 13.0 MHz to 9.0 MHz at 1130 UT. This activity reasonably well fits the normal distribution for this month as seen on nearby days. Thereafter spread-F sets in until 1330 UT with the critical frequency during the interval of spread estimated to be somewhat lower than that prior to its start.

2. During the early part of the storm.

Beginning at 1445 UT (the ionosonde records at 15 minute intervals) the critical frequency of the F2-layer, and so also the electron density, shows a general steady drop toward a minimum value which occurred at 2130 UT, the pre-dawn dip [Eccles and King, 1970]. Moreover during this storm period several departures from the usual diurnal curve are noted. The start of the gradual lowering in frequency comes earlier than it does on each of the control days. Instead of a single relatively smooth drop there are three noticeable successive drops each with a subsequent and considerable rise in critical frequency prior to the pre-dawn dip. Significantly the critical frequencies throughout this interval (1445-2130 UT) are lower than the corresponding values of the other days and in general, except for the last rise before the pre-dawn dip, are lower by two or more MHz. The electron density is thus about forty percent below the corresponding median values. Even the minimum value, 3.2 MHz, is lower than that found on any of the control days.

From the minimum, in two hours and a half foF2 goes to 15 MHz at 2400 UT. This is the highest electron density found in the ionosphere during the eleven day period. Further, this peak occurs an hour or more ahead of the peak frequency for each of the five days before and after this stormy day.

An interesting comparison can be made between the geomagnetic excursions and the variations in the foF2 following on the Sudden Commencement of 08/1417 UT. The drops in the magnetic field correspond to F-layer increased ionization densities and vice versa. Evidently the F2-layer current produced a field in opposition to the main magnetic field or there was a common cause.

B. Storm Effects on other F-region Parameters

Other significant changes are noticed in the ionosphere during the storm. The critical heights of the F-region on 8 March for the hours 1700, 1800 and 1900 UT were 285, 290 and 250 kilometers, respectively, corresponding to median values of the control period of 220, 215 and 210 kilometers. For each of these same three hours hpF2 (the virtual height of a frequency equal to 0.834 of the critical frequency) was 390, 400 and 385 kilometers respectively corresponding to control day median values of 285, 265 and 310 kilometers. Consistent with the above height and frequency changes in the F-region at these same hours were the MUF factors, F2(M-3000). The three hourly values were 2.65, 2.70 and 2.65 while the control day medians were 3.35, 3.50 and 3.10. Thus in the storm period the lower critical frequencies and lower MUF factors joined in depressing the maximum usable frequency.

C. E-region Effects

Since the hours showing the greatest F-region disturbance come just after local midnight the normal E-layer and F1-layer parameters do not appear. The sporadic E-layer, however, is subject to changes. The virtual heights, h'Es, for the same three hours (1700-1900 UT), are 149, 133 and 135 kilometers whereas the medians of the reference hours are 101, 101 and 107 kilometers. The type of Es is the same, namely f-type. The frequency foEs at 1700 and 1800 hours fits well the monthly median values but for the next several hours (1900 to 0200 UT) it is remarkably higher than the related monthly median value. foEs is 4.2, 4.4, 5.0, 6.7, 5.8, 6.0, 7.0, 9.2 MHz in comparison with monthly medians respectively of 2.1, 2.3, 3.0, 3.0, 3.2, 3.6, 4.4, 4.3 MHz. Due to noise at the low frequency (f-min) values while possibly higher than usual are not certain.

D. Summary from Ionograms

During this ionospheric nighttime storm, approaching the season of the spring equinox, the following features are apparent. (a) The ionization density in the F-region showed a marked decrease. (b) Virtual heights, parabolic heights and the MUF factors manifest retardation effects in the upper ionosphere. (c) The unusually high values for sporadic E-layer heights suggest that the ionization below the E-region is dense enough to slow down radiation at the low frequency end. (d) After the principal variations in the storm more than the usual amount of ionization condensed in the sporadic E-layer. (e) Due to nighttime activity no definite statements can be made about F1- or regular E-layers.

Conclusion

The wide variety of evidences and correlations among geophysical phenomena tends to place event number 5 as the principal contributor to the great magnetic storm of 07-08 March 1970. In a period of solar activity where several relatively small solar bursts and flares occur one outstanding happening even though on solar evidence not a great event, can be productive of ionospheric effects significant for communications.

Acknowledgement

The authors wish to express their thanks to ESSA (now NOAA), Boulder, Colorado for its support in obtaining the ionospheric data, to NOAA, Rockville, Maryland for the use of magnetic instruments, to AFCRL, Bedford, Massachusetts for significant support of the solar radio program, to Air Weather Service personnel for observations. For ionospheric reduction of ionograms we are grateful to Mr. Florencio Rafael.

REFERENCES

BADILLO, V. L. 1970 Microwave Burst of 6 March 1970 Proton Flare, World Data Center A, Upper Atmosphere Geophysics Report UAG-12, NOAA, Boulder, Colorado, April 1971, p. 85.

BELL, BARBARA 1963 Type IV Solar Radio Bursts, Geomagnetic Storms, and Polar Cap Absorption (PCA) Events, Smithsonian Contribution to Astrophysics, 8, No. 3

CASTELLI, J. P. 1968 Observation and Forecasting of Solar Proton Events, Air Force Surveys in Geophysics, No. 203

CASTELLI, J. P., J. AARONS and G. A. MICHAEL 1967 Flux Density Measurements of Radio Bursts of Proton-Producing Flares and Non-Proton Flares, J. Geophys. Res., 72, 5491-5498.

ECCLES, D. and J. W. KING 1970 Ionospheric Probing Using Vertical Incidence Sounding Techniques, J. Atmos. Terr. Phys., 32, 517-538.

ELLISON, M. A. 1963 Solar Flares and Associated Phenomena, Planetary Space Science, 11, 597-619.

MILLER, R. A. and A. TRINIDAD 1970 Optical Flares and VLF anomalies Related to the Great Magnetic Storm of March 8, 1970, World Data Center A, Upper Atmosphere Geophysics Report UAG-12, NOAA, Boulder, Colorado, April 1971, p. 29.

"March 1970: Solar and Geomagnetic Events"

by

M. C. Ballario
Osservatorio Astrofisico di Arcetri
Florence, Italy

Introduction

The results obtained in examining the correlation between solar and geomagnetic phenomena recorded during the years 1964 [Ballario 1967, 1966a, 1969b], 1968 [Ballario 1970a, 1970b] and in different periods: Retrospective World Intervals for 1965 [Ballario 1966b] and March 1966 [Ballario 1969a], suggested to us the following interpretation [Ballario 1970a]:

Table I

	Solar activity	Geomagn. conditions	Interpretation
I	Very quiet Sun W=0, no flares	Very quiet or slightly disturbed	There are no CMPs of active centers.
II	Very quiet Sun W=0, no flares	Storms and disturbances	There are CMPs of recurrent positive plages rising in the western hemisphere some days after the meridian transit, or of non-identifiable "M solar regions"
III	High or moderate	Very quiet or slightly disturbed	There are only CMPs of recurrent negative plages and/or of non-recurrent plages. Flares may occur.
IV	High or moderate	Storms and disturbances	There are CMPs of recurrent positive plages and/or occurrence of "specific flares"

The discrimination between positive and negative plages is based on the associated spot-group type.

The positive plages are never associated, before the meridian transit, with spot-groups type C or greater but, at the most, with spot-groups type A or B (spots without penumbra).

The negative plages are associated, before the meridian transit and at least for part of their life, with spot-groups type C or greater (spots with penumbra).

From the papers mentioned above, it results that the correlation between CMPs of recurrent positive plages and geomagnetic storms and disturbances is about 78%, while the CMPs of recurrent negative plages, as well as their CMPs in the subsequent rotations, are generally associated with quiet or slightly disturbed geomagnetic conditions.

It is also seen that the CMPs of non-recurrent plages (whatever the associated spot-group type may be) are geomagnetically inactive.

Among the positive plages, the most interesting are those arising in the western hemisphere (labelled pa plages); before and during their meridian transit, these active centers do not show chromospheric-photospheric phenomena and reveal themselves some days after their meridian transit. Since their CMPs are generally correlated with geomagnetic storms or disturbances, we think it possible to identify them with the so-called "M solar regions".

The CMPs of the pa plages (i.e. "M solar regions") are the cause of the storms and disturbances recorded when the Sun is completely quiet (case II, Table I) [Ballario 1967].

Of course an "M solar region" is non-identifiable when, for instance, plages and spots rise after the west limb set of the active center.

While we are able to discriminate between geomagnetically active plages and inactive ones, we cannot, at present, give the characteristics of the geomagnetically active flares (the "specific flares" of Table I, case IV).

It is known that in many cases, importance 2 or 3 flares (even proton flares) are associated with quiet or slightly disturbed geomagnetic conditions, but actually we cannot "a priori" distinguish the geomagnetically active flares from the inactive ones. Only "a posteriori" we may

correlate geomagnetic storms and disturbances with flare occurrences, taking a time-lag of 1 - 2 ½ days.

Of course, when a geomagnetic disturbance is correlated both with the CMP of a positive plage and with the occurrence of a flare, we cannot discriminate between the CMP effect and the flare effect. Only when the storm is not preceded or associated with CMPs of positive plages, may we consider the flare entirely responsible for the storm itself. We call these flares "specific flares".

The aim of this paper is to examine, on the basis of the interpretation given in Table I, the solar and geomagnetic events recorded during the selected interval centered around 6-10 March, 1970 (IUCSTP Symposium of Leningrad, May 1970).

For this purpose we have extended the proposed interval and examined the period February 19 - March 31 which includes two very quiet geomagnetic intervals and two very disturbed ones.

Table II

CMPs of plages recorded during the period Feb. 19 - March 31 and their subdivision into positive and negative plages.

Mc Math Data					Characteristics		REMARKS (from Fraunhofer Institut solar maps)
CMP 1970	Lat.	McMath plage number	Return of region	Age			
Feb.							
19.3	S02	10583	10536	2	recurrent	negative	G groups in the preceding rotation
19.5	S23	10581	New	1	"	"	E groups before the CMP
20.5	S15	10586	10538	4	"	"	H J groups in preceding rotations
21.1	N11	10594	New	1	non-rec.	"	- -
22.6	S15	10584	10542	4	recurrent	"	D groups before the CMP
22.9	N27	10593	New	1	non-rec.	"	- -
23.0	N54	10596	New	1	non-rec.	"	- -
23.0	N23	10597	New	1	recurrent	positive	A group before the CMP, C groups after the CMP
23.3	N14	10591	New	1	non-rec.	negative	- -
23.9	N00	10590	New	1	recurrent	"	C groups before the CMP
23.9	N12	10611	New	1	non-rec.	"	- -
25.2	S07	10588	10544	2	recurrent	"	H D groups before the CMP
25.2	N20	10592	New	1	"	"	D groups before the CMP
25.9	N11	10613	New	1	"	positive	Rising on Feb. 27 in the western hemisphere associated with A,B groups. "M solar region" during the CMP.
26.1	N05	10612	New	1	non-rec.	negative	- -
27.0	N17	10595	10549 10561	2	rec.	"	E groups before the CMP
28.4	S11	10601	New	1	rec.	positive++	Probably recurrent with plage 10552 at 15S, CMP: Feb. 1.8
28.6	N28	10598	New	1	non-rec	negative	- -
March							
1.6	S19	10621	New	1	rec.	positive	Rising on March 7 in the western hemisphere associated with A groups. "M solar region" during the CMP.

Table II (continued)

Mc Math Data					Characteristics		REMARKS (from Fraunhofer Institut solar maps)
CMP 1970	Lat.	McMath plage number	Return of region	Age			
March							
2.3	S13	10602	10566	2	recurrent	negative	C groups in the preceding rotation
2.5	S03	10604	New	1	"	"	C groups before the CMP
3.0	S14	10605	New	1	recurrent	positive[+]	[+]Probably recurrent with plage 10555 at 13S.CMP: Feb. 4.0.
3.8	N09	10606	New	1	recurrent	negative	C group before the CMP
5.1	S29	10609	New	1	non-rec.	"	- -
5.2	N08	10607	10559	2	recurrent	"	D groups before the CMP
5.7	S17	10626	New	1	"	positive	Rising on March 9 in the western hemisphere associated with B groups. "M solar region" during the CMP.
5.8	S13	10608	10560	2	"	negative	C groups in the preceding rotation
6.0	S38	10615	New	1	non-rec.	"	- -
6.3	N26	10610	New	1	non-rec.	"	- -
7.4	S22	10622	New	1	recurrent	positive[++]	[++]Probably recurrent with plage 10658 at 21S, CMP: Apr. 3.5. Plage 10658 is given in the Fraunhofer maps but not in the McMath list in Solar-Geophysical Data.
7.6	S10	10614	10567	4	"	negative	C groups before the CMP
7.9	N07	10616	10568	8	"	"	D groups in the preceding rotation
9.8	N20	10617	10568	2	"	"	H groups before the CMP
9.9	S24	10627	New	1	non-rec.	"	- -
10.3	S15	10618	10571 10567	3,4&5	recurrent	"	E,C groups before the CMP
12.2	N16	10619	10572	5	"	"	J groups before the CMP
13.2	S07	10625	New	1	non-rec.	"	- -
14.5	N20	10623	10587	2	recurrent	"	D groups in the preceding rotation
14.5	S13	10624	10578 10580	3	"	"	D,H groups in the preceding rotation

Table II (continued)

Mc Math Data					Characteristics		REMARKS (from Fraunhofer Institut solar maps)
CMP 1970		McMath plage number	Return of region	Age			
March							
15.4	N38	10636	New	1	non-rec.	negative	- -
15.5	S02	10630	New	1	rec.	"	C groups before the CMP
15.7	N15	10628	New	1	non-rec.	"	- -
16.3	S16	10629	10579	4	rec.	"	D groups in the preceding rotation
17.1	N30	10642	New	1	non-rec.	"	- -
17.9	N21	10631	10599	2	rec.	"	C group before the CMP
18.0	S13	10637	New	1	non-rec.	"	- -
18.7	N17	10638	New	1	rec.	positive	A,B,C groups in the western hemisphere. Exception: correlated with a small Kp fluctuation.
19.2	S27	10632	10581	2	rec.	negative	E groups in the preceding rotation
19.9	N15	10634	New	1	non-rec.	"	- -
21.9	S17	10633	10584	5	rec.	"	J groups before the CMP
23.1	N24	10640	10597	2	rec.	"	D groups in the preceding rotation
24.0	S07	10639	10588 10590	2 & 3	rec.	"	J groups before the CMP
25.4	N16	10641	10592 10613 10595	2 & 3	rec.	"	D groups before the CMP
26.2	S08	10644	New	1	non-rec.	"	- -
26.4	S20	10645	New	1	non-rec.	"	- -
27.1	S10	10646	New	1	rec.	positive	Very small plages before the CMP, C groups rise on March 28 in the western hemisphere. "M solar region" during the CMP.
27.6	N24	10647	New	1	rec.	negative	C group before the CMP
27.6	N07	10650	New	1	non-rec.	"	- -
27.6	S10	10651	New	1	"	"	- -
28.8	N09	10665	New	1	"	"	- -
29.4	S21	10648	10621	2	rec.	positive	No spots. Return of the positive plage 10621
30.2	S03	10649	New	1	rec.	negative	C groups before the CMP
30.5	S11	10659	New	1	non-rec.	"	- -
31.9	N07	10652	10606 10607	2 & 3	rec.	"	D groups before the CMP

The events of February 19 - March 31

Plages

The CMPs of recurrent and non-recurrent plages observed during this period, as given in the McMath calcium plage list [Solar-Geophysical Data, Part I, NOAA Boulder], are presented in Table II.

Their subdivision into negative and positive plages depending on the associated spot-group type, is based on the Fraunhofer Institut solar maps.

We note that from January 1, 1969 a sunspot classification is also published in Solar-Geophysical Data, but often the two classifications differ from each other. Since our previous researches were based on the spot-group types given in the Fraunhofer maps, we continue to use them.

The plage subdivision into recurrent and non-recurrent is also given in the McMath calcium plage list. However, we have to note that, particularly when the active centers show only very small and negligible plages which appear and disappear during their life, some classified non-recurrent plages may be considered as recurrent ones, for instance:

1) Plage 10601 at 11S and heliographic longitude L = 218°, CMP: Feb. 28.4, is probably the second transit of plage 10552 at 15S and L = 209°, CMP: Feb. 1.8. (See Fraunhofer maps of Feb. 1, Feb. 25, Feb. 28).

Plages 10601 and 10552 are positive plages and their CMPs are correlated with recurrent geomagnetic disturbances (see Bartels diagram for 1970).

2) Plage 10605 at 14S and L = 184°, CMP: March 3.0 is probably the third transit of plage 10526 at 14S and L = 171°, CMP: Jan. 8.2 (age 1) and of plage 10555 at 13S and L = 179°, CMP: Feb. 4.0 (age 2). (See Fraunhofer maps of Jan. 9, Jan. 31, Feb. 1-2, March 1-5).

Plages 10605, 10555, 10526 are positive plages and their CMPs are correlated with recurrent geomagnetic disturbances (see Bartels diagram).

3) Plage 10622 at 22S and L = 124°, CMP: March 7.4, is probably the first transit of plage 10658 at L = 129°, CMP: April 3.5. (See Fraunhofer maps of March 7 and April 1).

Plage 10658 appears in the Fraunhofer map of April 1 as a single plage at 17S (perhaps rather 20S), but it is not included in the McMath list published in Solar-Geophysical Data, probably because it has been considered part of plage 10654.

Plages 10622 and 10658 are positive plages and their CMPs are correlated with recurrent geomagnetic disturbances (see Bartels diagram).

Flares

The data referring to importance 2 flares and importance 1 and S proton flares recorded during the period February 19 - March 31, as given in the Quarterly Bulletin on Solar Activity, are presented in Table III and Table IV.

We have also taken into consideration the flare data reported in Solar-Geophysical Data (Remarks in Tables III and IV) since there are some differences between the two classifications of importance. Generally these differences refer to flares with corrected area very near to the upper limit between class 1 and class 2, or to secondary maxima.

The non-proton flares of importance 1 and S have not been taken into account since they are generally geomagnetically inactive [Dodson and Hedeman, 1964].

This inactivity has been confirmed in our previous papers and in the present research. For instance, during the quiet geomagnetic interval 10-25 March, the Quarterly Bulletin reports 21 importance 1 flares and 34 of importance S.

Table III contains the flares which are followed by geomagnetic storms or disturbances (time-lag about 2 days). Many of these disturbances are also preceded by CMPs of positive plages.

Table IV, on the contrary, contains the flares which are followed, for more than 3 days, by quiet or slightly disturbed geomagnetic conditions. Among them there are three importance 2 proton flares.

Table III

List of importance 2 flares and importance 1 and S proton flares followed by geomagnetic storms and disturbances (time-lag about 2 days). The CMPs of positive plages which precede or are associated with some of these disturbances are added.
From Quarterly Bulletin on Solar Activity and Solar-Geophysical Data (S.G.D.).

Date 1970	Max UT	Position	Imp.	App. and Corr. area	Charact.	McMath active region	Remarks	Geomagnetic events (see Fig. 1)
Feb.								
22	0322	28S-05E	1N	280 3.1	EHLRSU	10584	-	sc disturbance on Feb. 24 CMP of pos. plage 10597 on Feb. 23.0
27	2327	07N-69E	2B	260 -	R	10607	Of imp. 1 in S.G.D.	Disturbance on March 2 CMP of pos. plage 10621 on March 1.6
March								
1	0037	13N-27W	1N	190 2.4	EIU	10595	-	
1	1130	13N-31W	2B	420 5.2	HI	10595	-	
1	1201	14N-33W	2N	118 -	IDE	10595	In S.G.D. only	Disturbances on March 3-4
1	2004	15N-37W	2B	460 6.4	HR	10595	-	CMP of pos. plage 10605 on March 3.0
1	2033	07N-43E	2B	430 6.0	HRT	10607	-	
3	2037	15N-65W	2B	340 -	F	10595	Of imp. 1 in S.G.D.	sc disturbance on March 5-6
3	2054	10N-01W	SN	190 1.9	FGHRSU	10606	-	CMP of pos. plage 10626 on March 5.7
5	1450	10S-29E	2F	078 -	FEU	10614	In S.G.D. only	Storm on March 7
5	1623	16S-70E	1B	120 -	FEU	10618	-	CMP of pos. plage 10622 on March 7.4
7	0149	11S-09E	2B	650 6.7	FKLRSU	10614	-	Storm on March 8 No CMPs of positive plages
7	beg. 1050	03N-35W	2N	- -	V	10607	In S.G.D. only	Storm on March 9 No CMPs of positive plages
7	1609	14S-45E	1N	260 -	U	10618	-	

Table III (continued)

Date 1970	Max UT	Position	Imp.	App. and Corr. area	Charact.	McMath active region	Remarks	Geomagnetic events (see Fig. 1)
March								
11	1919	21N-22W	SN	080 1.1	ELU	10617	-	Kp fluctuation on March 13 No CMPs of positive plages
26	2011 2025	05N-66E	2N	500 -	EU	10652	-	Disturbance on March 28-29 CMP of pos. plage 10646 on March 27.1
29	0014 0045	14N-37W	2B	800 10.8	FIKR	10641	-	sc Storm on March 31 No CMPs of positive plages
31	1810	12S-45E	2B	350 5.2	CFIL	10654	-	Disturbance on Apr. 2-3 CMP of pos. plage 10653 on Apr. 2.0

Plages and flares

The data of Tables II, III and IV are shown in Figure 1:

A) CMPs of all recurrent and non-recurrent plages.
B) CMPs of the recurrent positive plages only.
C) Kp geomagnetic index (Bartels diagram).
D) Flares of importance 2 and importance 1 and S proton flares.

Broken lines correlate the CMPs of positive plages and the flare occurrences with the recorded geomagnetic storms and disturbances.

From Figure 1 it results that:

a) During the very quiet geomagnetic interval 19-23 Feb., only CMPs of recurrent negative plages and of non-recurrent ones, are observed (Table II).

The proton flares of importance S and 2, occurring on Feb. 19 and 20, being followed for more than three days by very low Kp index values, have to be considered geomagnetically inactive (Table IV).

b) The subsequent disturbed and very disturbed geomagnetic interval Feb. 24 - March 9 begins with an sc moderate Kp disturbance associated both with the CMP of positive plage 10597 and with the occurrence of a proton flare of importance 1 on Feb. 22.

The CMPs of the "M solar region" 10613 and of the positive plage 10601, appear to be entirely responsible for the disturbances of Feb. 26 and Feb. 28 - March 1, respectively.

The disturbances of March 2, March 3-4, March 5-6, March 7, are related both with the CMPs of the positive plages 10621, 10605, 10626, 10622 respectively and with flare occurrences, thus, at most, they may be considered as due to overlapping effects.

The geomagnetic storm of March 8 appears to be entirely due to the proton flare of importance 2B occurring on March 7, since there are no CMPs of positive plages correlated with the storm itself. The time-lag between the maximum of the flare (March 7.0) and the maximum of the storm (March 8.9) is 1.9 days.

Also, the storm of March 9, not related to CMPs of positive plages, is entirely due to the proton flare of importance 1 occurring on March 7. The time-lag between the maximum of the flare (March 7.7) and the maximum of the storm (March 9.5) is 1.8 days.

Another importance 2 flare reported only in Solar-Geophysical Data and observed by one station (Teheran) occurs on March 7.4. It might be related to one or other storm.

c) A quiet or slightly disturbed geomagnetic interval, March 10-26 follows. CMPs of recurrent negative plages and of non-recurrent ones, are observed. Only one exception is noted: the CMP, on March 18.7, of the pa positive plage 10638 related to a very small Kp fluctuation. But exceptions are foreseeable as described in detail in a previous paper [Ballario 1969a].

Flares of various importance are recorded during this interval but, being followed for more than 3 days by very low Kp values, they have to be considered geomagnetically inactive (Table IV).

Only the importance S proton flare recorded on March 11 may be considered responsible for the modest Kp fluctuation of March 13.

Table IV

List of importance 2 flares and importance 1 and S proton flares followed for more than 3 days by quiet or slightly disturbed geomagnetic conditions. From Quarterly Bulletin on Solar Activity and Solar-Geophysical Data (S.G.D.).

Date 1970	Max. UT	Position	Imp.	App. and corr. area	Charact.	McMath active Region	Remarks	Geomagnetic conditions
Feb.								
19	0937	23S-03E	SN	190 2.0	EHU	10581	-	Very quiet until Feb. 23.7
19	2324	20S-05W	SN	180 1.9	HU	10581	-	" " " " "
20	0947 1008	18S-32E	2B	500 6.0	EHILU	10584	Two distinct maxima of imp 2 in S.G.D.	" " " " "
March								
12	0312	14S-46W	2N	420 5.4	EKLU	10618	-	Small Kp fluctuation on March 15
12	0640 0715	22N-29W	2N	450 6.0	HKL	10617	Of imp. 1 in S.G.D.	" " "
21	0053	19N-66E	2F	350 -	HKLRU	10641	-	Very quiet until March 27.3
22	0023 0035	15N-56E	1N	230 4.5	EHJKLR	10641	Of imp. 2 in S.G.D.	" " " " "
22	2348	16N-29E	2N	420 5.4	EL	10641	Of imp. 1 in S.G.D.	" " " " "
23	0025	15N-32E	2N	420 5.5	E	10641	-	" " " " "
23	0407 0414	14N-42E	SN	090 1.4	ELRU	10641	Of imp. 2 a secondary max. in S.G.D.	" " " " "
24	0806	20N-03W	1N	350 4.1	FHIL	10641	Of imp. 2 in S.G.D.	" " " " "

d) The subsequent disturbed geomagnetic interval, March 27-31, begins with an sc geomagnetic disturbance well correlated with the CMP, on March 27.1, of the "M solar region" 10646 in which C groups appear after the meridian transit (see Fraunhofer maps of March 27 and 28). No flares occur 2 days before this disturbance.

The disturbances around March 29 are preceded both by the CMP of positive plage 10648 and by the occurrence, on March 26, of an importance 2 proton flare.

The sc geomagnetic storm of March 31 appears to be entirely due to the flare of importance 2B occurring on March 29. This flare has a corrected area of 10.8 sq. deg. and its maximum on March 29.0. The time-lag between the maximum of the flare and the maximum of the storm (March 31.3) is 2.3 days.

No CMPs of positive plages precede the storm itself.

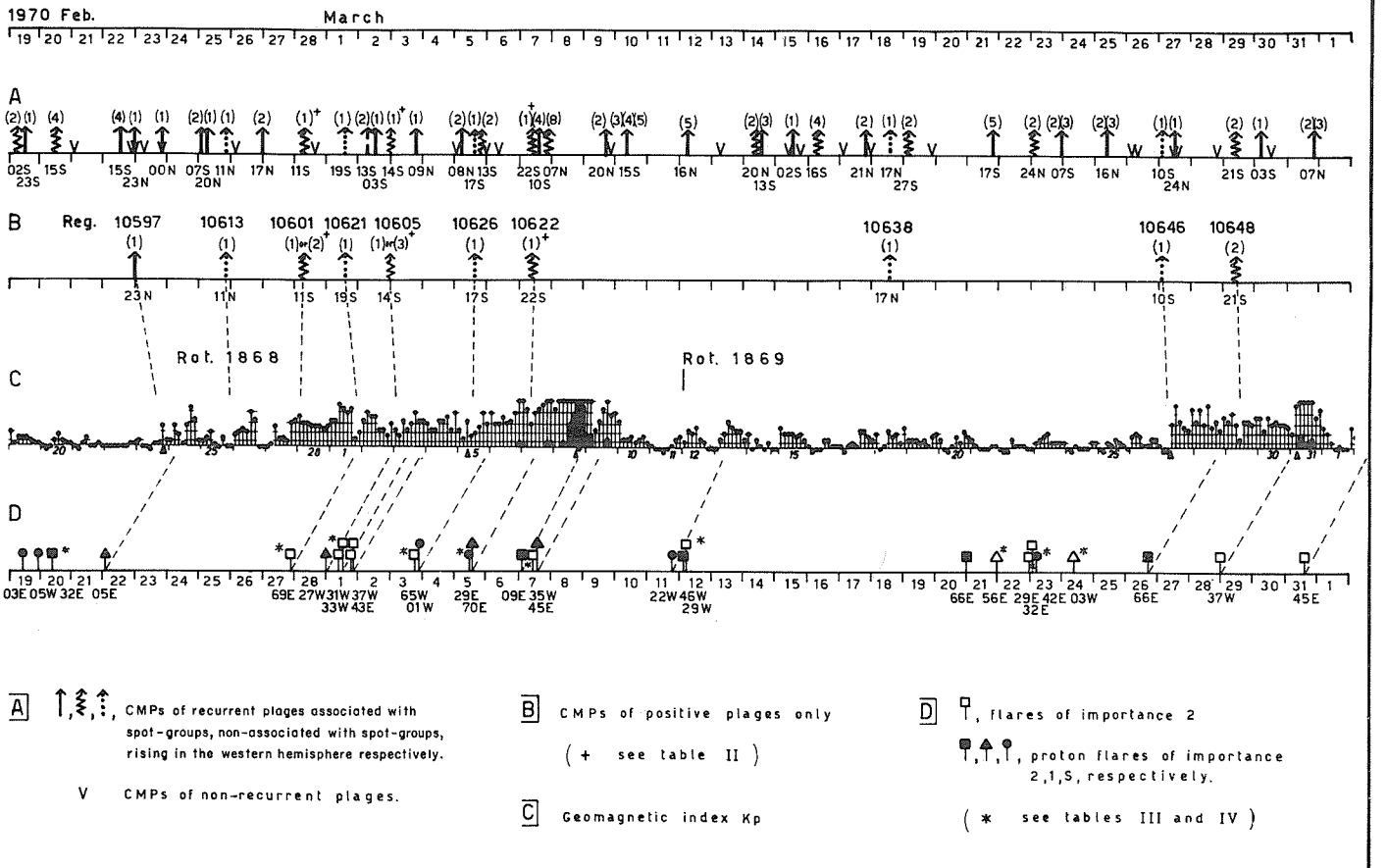

Fig. 1

Conclusion

The behaviour of the Kp geomagnetic index during the period Feb. 19 - March 31 (Figure 1) appears to be in very good agreement with the interpretation (Table I) proposed in a previous paper [Ballario 1970a].

During the very quiet or slightly disturbed geomagnetic intervals Feb. 19-23 and March 10-26 associated with high solar activity (case III of Table I), CMPs of recurrent negative plages and of non-recurrent ones, are prevalently observed (26 in number). Only one CMP of a positive plage is recorded. (Table II).

Flares of various importance are observed, but they have to be considered geomagnetically inactive. The data of these flares are given in Table IV.

During the disturbed or very disturbed geomagnetic intervals: Feb. 24 - March 9 and March 27-31, CMPs of recurrent positive plages and flare occurrences are recorded (case IV, Table I). Some of these disturbances are correlated only with CMPs of positive plages, while others may be related to both the phenomena.

The strong geomagnetic storms of March 8, March 9, March 31 are, on the contrary, entirely due to the occurrence of flares, since no CMPs of positive plages are correlated with the storms themselves.

The data of these flares ("specific flares") are:

March 7: 11S-09E, max. at 0149 UT, imp. 2B proton flare

March 7: 14S-45E, max. at 1609 UT, imp. 1N proton flare

March 29: 14N-37W, max. at 0014 UT, imp. 2B

Also the occurrence of the S proton flare of March 11 (Table III) is probably the cause of the isolated Kp fluctuation recorded on March 13.

The very small number of well identified "specific flares" does not allow establishing of the peculiar characteristics distinguishing these flares from others of the same importance but geomagnetically inactive. Thus, this remains an open question.

We think that the adoption of the "flare profiles" proposed by H. Dodson and R. Hedeman during the XIV IAU General Assembly would be very useful for this purpose.

REFERENCES

BALLARIO, M. C. 1966a — A study of the plages and sunspot-groups observed during the Retrospective World interval for 1964. "IQSY Notes", 17, 2-9.

BALLARIO, M. C. 1966b — The solar and geomagnetic activity observed during the IQSY R.W.I. for 1965. "IQSY Notes", 18, 4-8.

BALLARIO, M. C. 1967 — The quiet Sun Year 1964. Relationship between the CMPs of solar recurrent plages and terrestrial phenomena. "IQSY Notes", 21, 36-48.

BALLARIO, M. C. 1969a — On the special events of March 1966. Ann. Geophys., 25, fasc. 1, 135-146.

BALLARIO, M. C. 1969b — The IQSY 27-day recurrence sequence for 1964. Mem. SAIt., 40, fasc. 3, 271-294.

BALLARIO, M. C. 1970a — Solar and geomagnetic events of the year 1968. Ann. Geophys., 26, 459-473.

BALLARIO, M. C. 1970b — On the solar and geomagnetic events of Oct. - Nov., 1968. World Data Center A-Upper Atmosphere Geophysics Report UAG-8, 231-238.

DODSON, H. W. and E. R. HEDEMAN 1964 — Problems of differentiation of flares with respect to geophysical effects. Planet. Space Sci., 12, 393-418.

13. GEOMAGNETIC DATA

"Geomagnetic Indices"

by

J. Virginia Lincoln
Aeronomy and Space Data Center, Boulder, Colorado

The musical note diagram of Kp reproduced below and the C9 figure diagram show that the March 8, 1970 storm was the greatest of the year. In fact it has the highest Ap value of any storm of this solar cycle to date.

The Kp and Ap for March 6-10, 1970 were as follows:

1970	Kp	Ap	
March 6	4o 3o 3o 4- 2o 3+ 4o 6-	25	D
March 7	5+ 4+ 3o 4o 4+ 5- 6- 6-	42	D
March 8	4+ 5o 6- 5o 7+ 8o 9o 8+	149	D
March 9	6+ 6+ 2+ 3+ 4+ 6o 4- 4o	47	D
March 10	3+ 1+ 1+ 2- 1o 1+ 2- 1o	7	

According to IAGA there was one storm sudden commencement (ssc) between March 6-10, 1970.

March 8, 1417 UT from forty-three stations (ssc: 41 [A: 36; B: 4; C: 1]; si: 2).

There were sudden impulses as follows:

March 7, 2040 UT from twenty-five stations (si: 17 [A: 9; B: 7; C: 1]; ssc: 8).

March 9, 1546 UT from fifteen stations (si: 11 [A: 4; B: 6; C: 1]; ssc: 4).

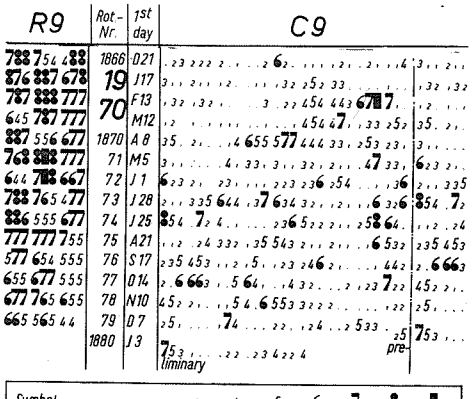

DAILY GEOMAGNETIC CHARACTER FIGURES C9 AND 3-DAY MEAN SUNSPOT NUMBERS R9

For explanation and previous years see J. Bartels, Abhandlungen der Akademie der Wissenschaften zu Göttingen, Beiträge zum I.G.J., Heft 3 (1958) (may be requested from Institut für Geophysik, Postfach 876, 34 Göttingen, Germany).

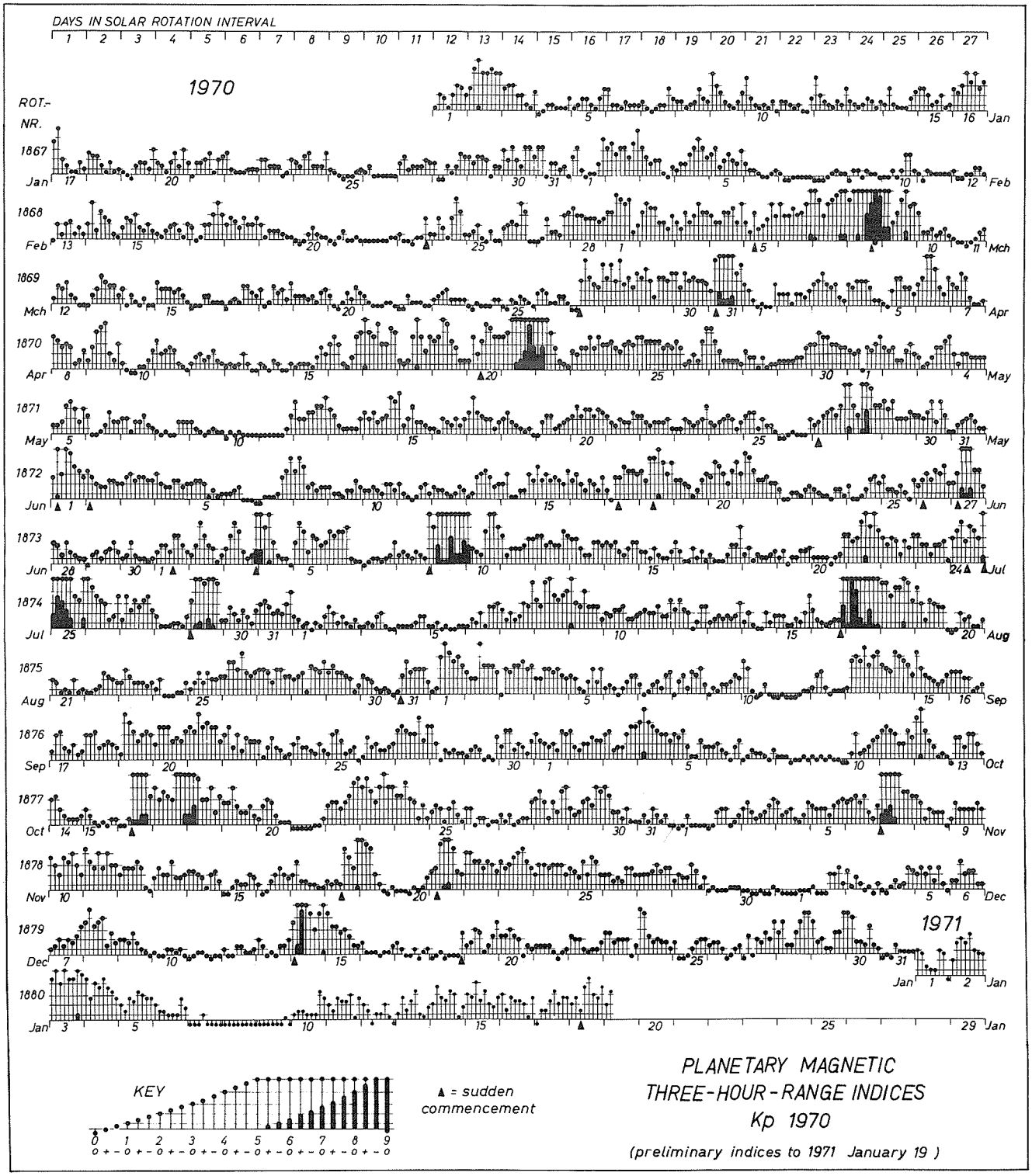
DAYS IN SOLAR ROTATION INTERVAL
1 2 3 4 5 6 7 8 9 10 11 12 13 14 15 16 17 18 19 20 21 22 23 24 25 26 27
1970
ROT.-
NR.
1867 Jan 17 20 25 30 31 1 5 10 12 Feb
1868 Feb 13 15 20 25 28 1 5 10 11 Mch
1869 Mch 12 15 20 25 30 31 1 5 7 Apr
1870 Apr 8 10 15 20 25 30 1 4 May
1871 May 5 10 15 20 25 1 30 31 May
1872 Jun 1 5 10 15 20 25 27 Jun
1873 Jun 28 30 1 5 10 15 20 24 Jul
1874 Jul 25 30 31 1 5 10 15 20 Aug
1875 Aug 21 25 30 31 1 5 10 15 16 Sep
1876 Sep 17 20 25 30 1 5 10 13 Oct
1877 Oct 14 15 20 25 30 31 1 5 9 Nov
1878 Nov 10 15 20 25 30 1 5 6 Dec
1879 Dec 7 10 15 20 25 30 31 Jan
1971
Jan 1 2 Jan
1880 Jan 3 5 10 15 20 25 29 Jan
KEY
0 1 2 3 4 5 6 7 8 9
0 + - 0 + - 0 + - 0 + - 0 + - 0 + - 0 + - 0 + - 0
▲ = sudden commencement
PLANETARY MAGNETIC
THREE-HOUR-RANGE INDICES
Kp 1970
(preliminary indices to 1971 January 19)

"K-Indices March 5-10, 1970"

by

D. van Sabben
International Service of Geomagnetic Indices
Royal Netherlands Meteorological Institute
De Bilt, Netherlands

The geomagnetic K-indices from the individual observatories for March 5-10, 1970 are given below. Please refer to IAGA Bulletin 12v2 or 12w1, page 1-3 for the definitions of the observatory symbols. OT stands for Ottawa, geographic latitude N45°24', geographic longitude E284°27'.

MAR	5		6		7		8		9		10	
BT	4343	2454	5644	5455	5643	8776	6544	9897	6533	6645	6344	3343
CC	4142	1665	5335	5466	5444	7666	6556	9799	5534	7635	5233	1543
TH	3143	4544	4444	4545	5544	5665	5554	9977	5543	4644	5234	3333
DI	3343	3777	6445	4677	6546	8776	7656	9798	6643	6845	5233	2554
TI	3242	4797	6446	6789	5447	9886	5687	9999	5633	8864	4234	3454
PB	2233	2565	3436	4456	3366	5775	4586	8776	4426	6854	3325	3343
TR	4121	2344	4423	3656	5534	4656	5653	8686	4633	3745	5112	2252
GO	2143	3443	4233	4544	4433	4545	5544	8875	4534	4535	4223	3321
MM	4132	2365	0223	2666	7524	5767	5554	8787	5733	4755	5122	2242
KI	4132	2465	6313	3766	7624	5667	5654	8797	5733	4756	3112	1242
SO	4131	1465	6223	2667	7524	5667	5554	8797	5723	4745	5112	1242
WE	1231	1563	3336	3555	4447	7775	4787	8887	5535	7653	2113	1222
CO	2133	1343	3336	3445	4345	6664	3576	9985	5535	6632	2124	2110
RY	5343	3556	5444	4567	6744	5567	6765	9896	7933	4557	7223	2333
DO	3142	2255	5223	2457	6433	5566	5444	7899	7823	4635	4012	2231
YA	4242	1575	4337	4456	4545	5666	5466	7999	5623	8734	5214	1243
NU	3133	2344	3222	2345	5323	4455	4433	6999	7723	5623	3222	2231
LE	3121	1244	4222	1346	6523	4455	4443	6897	7722	3535	4111	1121
MG	2242	1454	3335	3355	3435	4655	4523	6623	4523	6623	3212	1233
LN	3143	3444	3333	3456	5434	5454	4434	7999	6733	4834	3123	2232
LO	3132	2344	3323	2446	5423	4455	5444	7899	7633	4634	4122	2231
SI	1022	1222	2246	1235	4346	6554	2586	9986	5635	6542	3132	1211
SV	3032	1443	3213	1355	4323	4555	3433	6699	4522	4524·	3011	1230
TM	3242	1564	3335	2455	5434	5556	4444	7899	5524	5623	2233	1232
RS	3131	3353	4333	2446	5333	4455	5433	6899	5633	4634	2222	2232
KN	3133	1454	4223	2455	4334	4455	3433	7788	5622	4524	3112	1221
MO	3243	2454	3333	3456	4444	5455	4534	6799	5633	4634	3233	1231
ES	2131	2243	4223	2345	5322	3455	4433	6799	6523	4534	2111	1131
ME	2132	2243	3254	2335	5456	5545	3578	8887	5545	6533	2233	2322
MN	3143	1254	3233	3445	4334	4454	4434	5687	5523	3544	2123	2332
WN	3143	2353	4333	2456	5433	4455	5444	6898	6623	4644	3112	2231
WI	2132	2453	4333	2556	5433	4466	5444	6798	5513	5634	3112	1131
IR	3343	2464	3335	3445	4334	5455	4345	7798	4634	5533	4334	2232
NI	3132	2353	4333	2446	5433	4455	5443	6777	5513	4634	3122	2232
VL	3032	3343	4233	2445	4423	3455	4543	5698	5423	4524	2212	2231
HA	3132	3343	4323	2445	4323	3455	4443	5697	6423	4634	3112	1231
KV	3244	3454	4234	3456	4445	5555	4444	5677	5634	5634	3234	3332
MA	3132	2343	4223	2445	4323	3455	4433	6777	5422	4634	3112	1230
DB	3133	3443	4233	3445	4333	3455	4443	6787	5523	4634	3223	2231
PR	3233	2344	4333	3455	4333	3455	5444	6787	6533	4634	3223	2231
LV	3132	1342	2233	2344	3333	3455	3333	5587	4323	4523	3112	1232
KD	2253	1353	3234	2455	5343	5555	3434	7687	42--	----	--33	0232
VI	1132	1322	3245	2333	5345	5655	3466	8886	4533	5533	2012	1120
NE	2031	1333	3245	2333	6345	3554	3366	8887	5633	4533	2022	1210
FU	2132	2243	3223	2335	4322	3455	3333	5786	4512	3533	3112	1131
CF	3131	2342	4222	2345	4312	3355	4433	5787	5512	3534	2012	1131
UB	3453	2464	3436	3455	5334	5555	5545	8798	5644	6533	5444	1332
JO	2131	2233	5232	2235	5434	3444	3454	7789	6613	3534	3012	1110
SA	2332	1353	3335	3345	4334	5445	3454	7686	4633	5534	3323	1223
TY	2242	2453	4324	3456	5433	4555	5443	6787	5623	5634	3223	2332
OD	2243	3453	3334	2445	4444	4565	3454	6686	5533	5534	3222	2232
KK	2232	1343	2244	2333	3332	4444	3344	655-	-232	4522	2123	1121
GC	2141	1443	4233	3456	4433	4555	5454	6788	5522	4634	3112	1231
MT	1132	1343	2335	2243	3224	4345	3355	7686	3522	4523	2112	1220
OT	1131	2233	6233	2236,	5433	3455	4576	9789	7623	3534	3121	0010
VK	2343	2354	3345	3344	5434	5445	4455	7687	4633	5534	3433	1234
AT	3353	3564	4345	2455	5344	5565	4545	8787	6644	5534	----	----
LG	3131	2543	3323	2445	5443	6797	6523	3566	4513	4625	3012	1231
AQ	3031	2443	4223	3445	4322	4555	4433	5787	5502	4534	3012	1231
TF	2334	2353	3334	4443	3433	3565	3544	6785	5424	4533	3334	3331
TK	0142	2454	3334	3434	4323	5465	4445	7796	5622	5632	2112	1231
IK	2141	2353	4223	2445	4313	4565	3333	6797	5512	4524	3111	1231
CI	3131	23--	----	----	---2	4465	4--3	6787	5---	----	----	----
TL	3131	2333	3223	2334	4321	3455	3433	5686	5312	5324	3111	1231
FR	2132	2233	5234	2235	5334	4455	4455	8799	6622	3544	3021	0111
PE	3031	1243	3221	0345	4112	3456	3132	5686	5301	3434	3001	0031
AK	3332	2233	3334	3443	3455	5454	3456	5788	7777	6665	5665	5555
SM	3223	3333	4333	3334	4424	3444	3443	5676	4323	2424	3223	2232
AE	3132	2433	3222	3345	5432	4565	2442	6677	5422	4424	3122	0221
SF	4223	3444	4333	4356	5433	4566	4543	679-	6522	5545	3113	1232
KA	2132	1343	2335	2243	3223	4345	4344	7686	4422	4523	2122	1220
KS	3142	2353	3324	3535	5423	4676	3544	5899	5522	4625	3122	2241
DS	2142	2334	4344	3344	5334	4566	4455	8786	7623	4534	3122	1220
TU	2142	2323	4245	2333	5334	3555	3455	7786	6623	4533	2021	0211
KY	1132	2353	2335	2243	3223	4345	3344	7686	4522	4523	2122	1220
QU	1242	1453	3344	3333	3343	4455	3554	7696	5522	5533	2233	1232
ML	3332	2453	3233	2345	4334	3565	3435	6786	6323	5534	3222	1233
SZ	3132	2333	4213	3225	5323	4465	4333	6687	6413	3434	3112	2220
LP	3442	2354	3444	2344	3434	5455	4644	7796	5543	4433	3223	1222
HO	1032	1222	2234	1333	2323	3345	3354	6676	5512	3433	2111	1010
TE	3242	3444	4333	3354	5433	3466	3555	6786	5533	4444	3121	1333
AL	1142	2453	3334	3333	3323	4455	3544	7687	4322	4533	2122	2232
SJ	2132	2443	4233	2254	4333	3455	3344	6686	5311	3333	2011	0210
MB	2141	2333	4122	2245	4213	4455	3332	6687	6312	3324	1111	1111
GU	2231	2332	3434	2233	3313	4245	3544	7676	5332	4423	2112	0210
BA	2142	2543	4223	1345	4324	3455	3342	6675	6363	4114	2212	0221
MC	4041	1433	4323	3345	5424	3455	4444	6686	6602	3424	3122	1121
PM	2141	1333	3324	2234	2314	3345	3444	7686	5422	4322	2012	0111
HU	2132	3443	3222	3443	4333	5665	3343	6888	5432	4653	2222	2332
PP	1131	1333	3233	1223	2323	3245	2445	56--	--33	3422	1122	1121
TN	1031	1332	2233	2233	2332	2354	3331	4---	--22	2423	1223	2121
GN	2141	1454	4325	2344	3324	4565	3244	7686	4412	5533	2012	0121
HR	2042	1444	4233	3345	5333	4455	3454	5787	5533	3424	2022	0120
AC	2242	2324	5333	2435	5333	3556	4433	678-	-313	3434	2121	1221
TO	2142	2443	3335	3234	3334	4445	3355	6687	3522	5422	3212	1121
AM	0141	1222	3335	2122	3324	4344	3454	6686	3413	3413	1101	0000
TW	2142	3343	4233	2344	4332	3456	3443	668-	-532	3433	2111	1220
MI	1232	1453	3347	3445	5556	6674	4687	9877	6635	7732	2124	1121
MY	4565	3343	4555	4443	5655	4574	5554	7696	5554	3534	5444	3243
MW	5242	2465	5444	4664	6636	4576	6754	8786	3533	4736	6234	3363
NL	3222	1145	7332	2458	7623	3465	5774	6787	6722	2536	3011	0122
SB	3332	2333	4344	2344	5544	4555	4544	7776	4532	3434	4222	1333
VO	3334	2333	4444	3344	4443	4544	4544	6665	4533	3434	4233	2222

"Provisional Hourly Values of Equatorial Dst March 1970"

by

M. Sugiura and D. J. Poros
Goddard Space Flight Center
Greenbelt, Maryland 20771

Hourly values of Dst given in this report are based on two observatories, Honolulu and San Juan, and are only provisional. They will be replaced later by data based on three observatories. These have been excerpted from the Preprint X-645-70-405 of the Goddard Space Flight Center issued November 1970.

Table 1 presents the daily means of equatorial Dst for January through June 1970. March 9, 1970 is the most disturbed date.

Table 1

Daily Means of Equatorial Dst January - June 1970

	JAN	FEB	MAR	APR	MAY	JUNE
1	13	12	-22	-20	-1	1
2	-14	-2	-13	-4	4	7
3	-14	1	-5	-1	14	3
4	-3	1	-6	11	10	2
5	10	-2	0	19	7	6
6	3	3	-21	-5	3	21
7	8	3	-29	5	19	30
8	12	10	-89	8	20	5
9	10	13	-141	3	12	15
10	13	14	-61	13	14	10
11	15	7	-41	7	25	20
12	14	17	-23	14	11	21
13	14	24	-17	24	-4	15
14	8	4	-10	24	4	16
15	18	4	-8	23	-1	8
16	-18	13	2	-5	7	10
17	-25	11	8	-23	8	24
18	-3	3	1	-3	14	-4
19	11	10	3	-18	21	-4
20	5	12	3	-5	6	-25
21	11	12	3	-66	-3	-27
22	11	16	11	-63	6	12
23	13	26	11	-28	14	18
24	7	24	15	-20	12	31
25	10	15	18	-9	5	13
26	11	-7	16	-11	17	14
27	14	-8	22	-5	13	-5
28	23	-11	-20	0	-36	-10
29	17	0	-21	5	-34	3
30	17	0	-13	-6	-12	11
31	9	0	-16	0	-0	0
MEAN	7	8	-14	-5	6	8

Table 2 gives the hourly values of Dst for March 1970. Figure 1 is a plot of these hourly values of the provisional Dst for January through June 1970.

Table 2

Hourly Values of Dst

MARCH 1970

UNIT=GAMMAS

DAY	1	2	3	4	5	6	7	8	9	10	11	12	13	14	15	16	17	18	19	20	21	22	23	G.M.T. 24
1	-7	-11	-3	-13	-17	-16	-19	-26	-42	-46	-33	-15	-22	-30	-31	-34	-35	-29	-29	-24	-15	-18	-12	-12
2	-22	-30	-32	-30	-30	-39	-33	-28	-30	-22	-21	-16	-12	-7	1	4	4	-1	0	3	8	9	11	5
3	-1	1	-0	-1	0	-4	-5	-9	-10	-8	-4	-5	-6	-5	-4	-2	-4	-10	-11	-9	-11	-14	-5	1
4	3	-2	-7	-4	1	1	-3	-6	-6	-1	-1	-8	-6	-5	-5	-6	-11	-11	-11	-13	-12	-12	-6	-4
5	-9	-10	-4	-2	0	-2	1	-2	3	-1	6	3	4	4	10	19	26	18	-1	-2	-10	-22	-10	-10
6	-24	-31	-13	-11	-8	-9	-9	-16	-19	-22	-9	-10	-12	-13	-13	-10	-12	-20	-19	-23	-36	-47	-57	-51
7	-49	-57	-39	-42	-45	-38	-33	-38	-31	-27	-30	-35	-26	-28	-32	-18	-13	-7	-27	-33	-1	-10	1	-30
8	-37	-35	-34	-35	-52	-70	-79	-73	-63	-61	-49	-41	-52	-52	-41	-41	-52	-25	-76	-152	-210	-265	-281	-266
9	-251	-234	-222	-209	-191	-179	-165	-160	-157	-149	-137	-138	-135	-127	-120	-107	-95	-105	-92	-81	-81	-86	-78	-75
10	-68	-62	-60	-64	-66	-68	-64	-66	-66	-68	-65	-71	-72	-70	-68	-65	-61	-55	-55	-53	-50	-47	-40	-36
11	-38	-40	-38	-39	-38	-40	-40	-44	-48	-50	-48	-55	-54	-55	-53	-48	-46	-43	-41	-37	-29	-25	-21	-24
12	-26	-28	-26	-30	-30	-32	-32	-38	-42	-37	-28	-29	-24	-19	-16	-18	-20	-21	-20	-12	-5	-6	-8	-7
13	-8	-8	-6	-9	-9	-14	-19	-19	-22	-21	-19	-25	-25	-24	-23	-25	-21	-20	-19	-20	-24	-18	-10	-9
14	-11	-16	-13	-12	-10	-13	-10	-13	-18	-18	-16	-18	-19	-17	-14	-10	-7	-6	-8	-4	-1	0	3	4
15	0	-5	-8	-13	-20	-26	-23	-20	-25	-22	-16	-19	-18	-12	-6	0	4	5	2	-0	2	3	9	8
16	8	3	3	-1	-4	-4	-3	-6	-10	-10	-8	-14	-15	-12	-7	-0	5	7	10	16	22	24	28	26
17	22	19	17	13	10	7	8	8	6	8	9	1	-5	-7	-3	3	9	13	12	11	14	13	8	3
18	2	5	5	4	3	2	1	-2	-4	-2	-7	-14	-18	-17	-7	3	2	5	8	10	16	12	5	1
19	1	4	6	5	5	2	1	-3	-6	-5	-4	-10	-6	-1	5	11	11	10	7	12	14	6	5	7
20	9	9	10	7	7	5	5	1	-4	-5	-1	-6	-7	-7	-2	1	6	8	4	2	7	7	5	2
21	0	0	3	-0	2	0	-0	-2	-5	-5	-3	-7	-7	-2	1	7	7	5	1	6	13	14	16	17
22	17	20	20	17	14	12	11	7	2	2	3	-3	-5	-2	5	10	10	11	9	13	19	19	24	23
23	25	23	21	19	17	14	14	8	-1	1	3	-1	-3	-5	-1	5	6	8	8	8	18	22	29	31
24	26	21	21	15	14	11	10	7	3	6	8	5	5	10	15	17	16	15	14	19	27	23	20	22
25	24	24	22	18	18	15	14	11	7	8	12	10	12	14	16	19	21	24	29	22	23	20	22	24
26	25	25	24	19	12	7	8	8	3	5	10	7	6	9	12	13	15	19	21	24	28	27	24	24
27	24	24	25	21	20	16	18	35	42	27	22	33	35	35	33	30	29	29	25	20	12	4	-13	-14
28	-11	-12	-10	-8	-13	-11	-11	-15	-18	-16	-21	-20	-25	-28	-30	-32	-28	-29	-27	-24	-19	-12	-18	-31
29	-29	-20	-26	-30	-31	-31	-30	-22	-25	-26	-25	-29	-29	-24	-19	-13	-15	-21	-20	-21	-9	-6	-0	-5
30	-15	-1	4	-2	-7	-13	-17	-22	-13	-13	-15	-24	-27	-29	-23	-16	-19	-22	-18	-9	-6	-7	5	9
31	8	4	1	-0	-9	5	4	-26	-36	-39	-33	-28	-30	-26	-39	-2	9	4	-16	-30	-30	-19	-26	-38

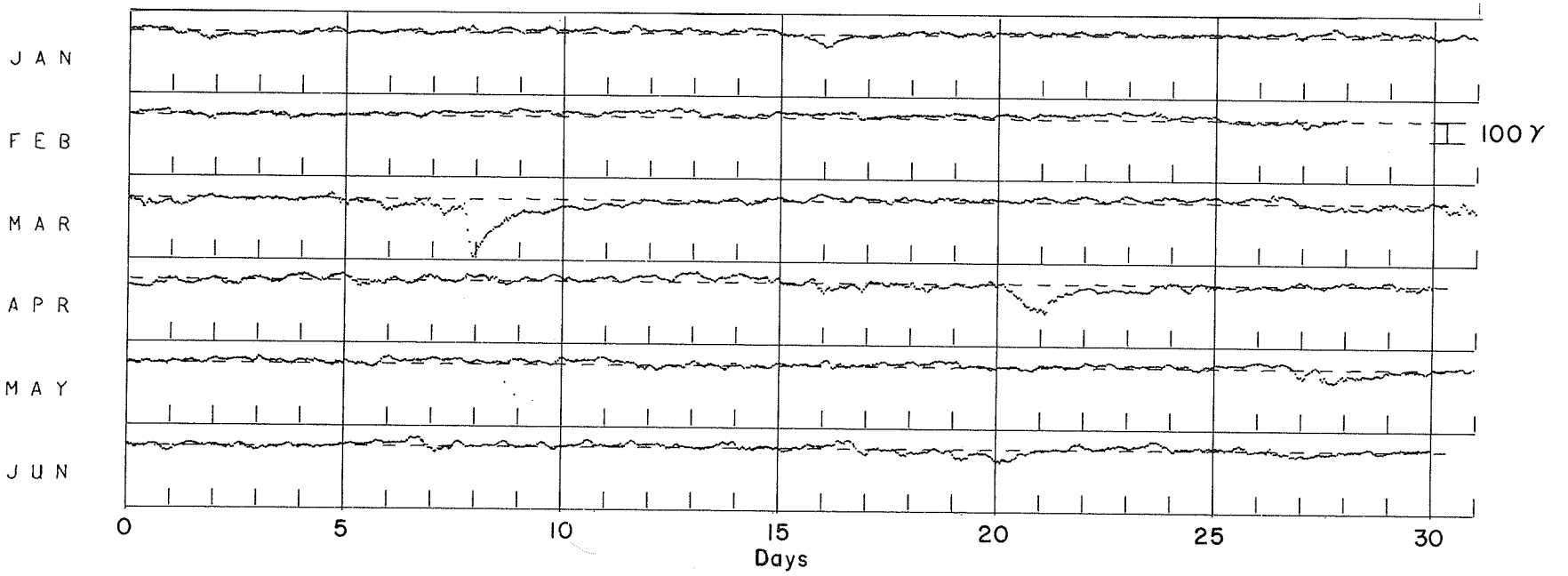

Fig. 1. Hourly values of provisional Dst for January through June 1970.

"Geomagnetic Variations at Ahmedabad, March 5-9, 1970"

by

Dr. T.S.G. Sastry
Physical Research Laboratory
Navrangpura, Ahmedabad 9, India

The table presents the magnetic events as recorded on the proton magnetometer at Ahmedabad (see Figure) from March 5-9, 1970.

Events Recorded on Proton Magnetometer at Ahmedabad
from March 8, 1970 to March 10, 1970

All times are in UT

Date	Type of Event	Start Time	End Time	Peak Time	Duration h.m.	Change in γ	Remarks
Mar. 8	sc (rise	1415	1416	1426	0002	72	Some vigorous pulsations followed as described below.
	(fall	1435	1500		0025	120	
	sc (rise	2003	2006	2006	0003	48	Large fluctuations during the ssc disturbance.
	(fall	2006	2009		0003	24	
	Pulsations	1715	2045	1930	0330		Pulsations are superimposed on the storm that followed sc at 1415. Minimum is 256 gammas below quiet day, reference level at 0400 on March 9, 1970.
Mar.10							Gradual recovery of the storm.

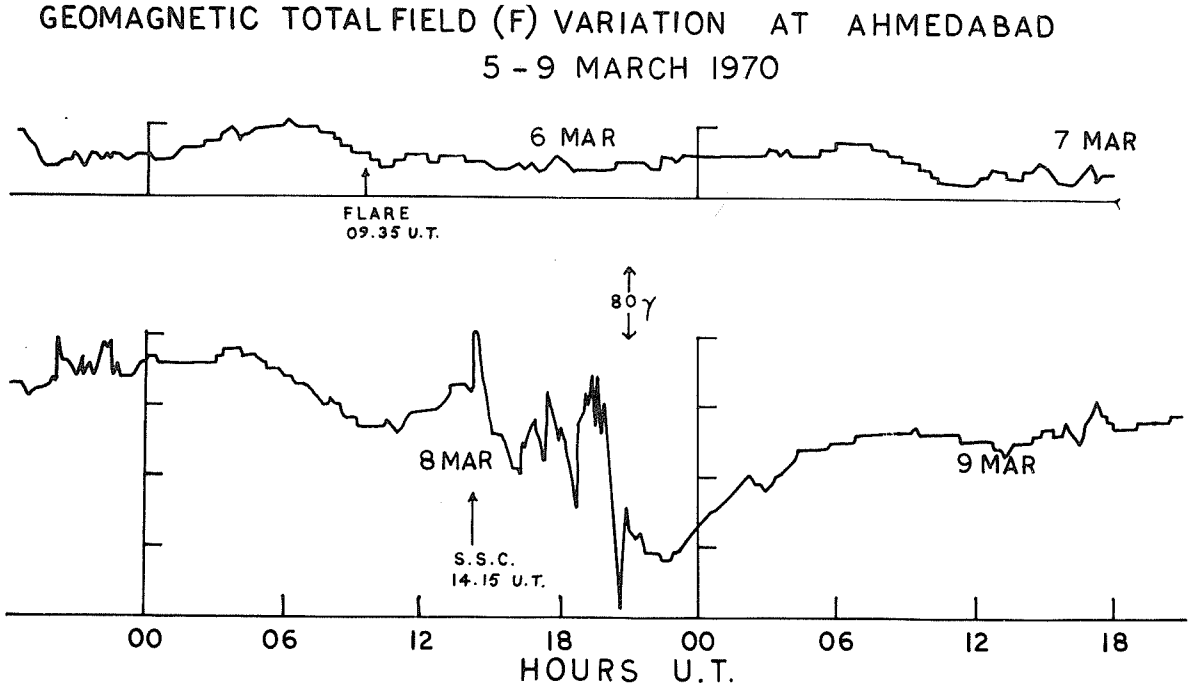

"OGO-6 Magnetometer Data"

by

J. S. Oberfield, R. A. Langel and J. C. Cain
Space Physics Laboratory
Goddard Space Flight Center, Greenbelt, Maryland

General

The March 6-10, 1970 interval included the largest magnetic disturbance that has been recorded by the POGO spacecraft series of magnetometer experiments. During this storm, the OGO-6 orbit had the following approximate configuration:

1. Orbital period - 99.1 min., inclination 82.0°; perigee 395 km; apogee 1039 km
2. Ascending mode - 7.5^h local time 420-450 km altitude
3. Descending mode - 19.5^h local time 1050 km
4. Northern apex of orbit on day side - 570 - 630 km
5. Southern apex of orbit on night side - 820 - 910 km

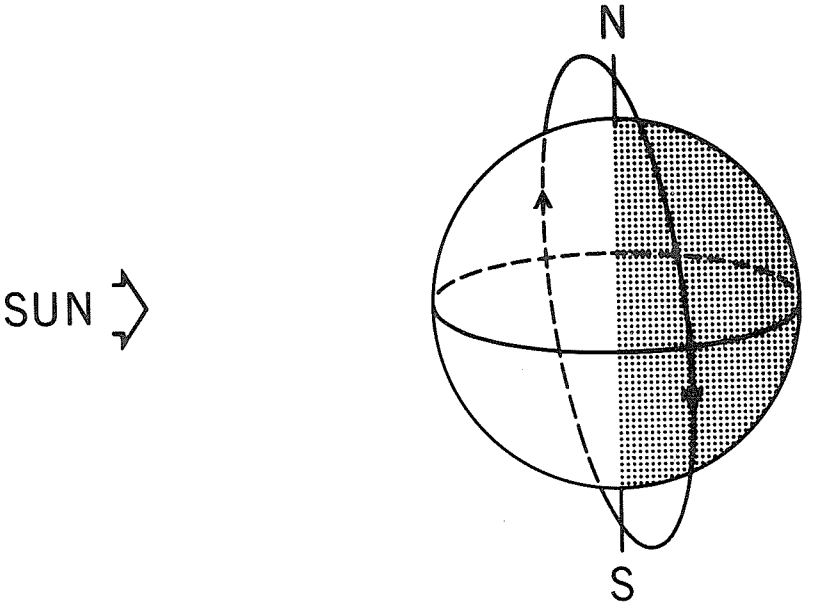

Data

The magnetometer measures (only) the absolute magnitude of the field to an accuracy of $\pm$ 2γ at a sample interval of 0.3 sec. The data acquisition was about 77%. POGO (OGO 2, 4, and 6) data for earlier intervals with Kp $\leq$ 0+ were numerically fit to a spherical harmonic expansion of the internal field potential. The rms deviation of the data over the period October 15, 1965 to August 17, 1969 from this model was 11γ. The data used in analysis are the differences $\Delta F = F_{obs} - F_{calc}$ and thus are less than or equal to the magnitude of the vector field disturbance. This ΔF thus will have random uncertainties of the order of 2σ or 22γ, plus the possibility of systematic average disturbance for the data chosen.

Equatorial

The equatorial disturbance of the field for the orbit in this near twilight local time configuration shows the maximum asymmetry of the external ring current. Values of minimum ΔF were read from

plots of the data corresponding approximately to the position of the dipole equator. These values are given in Table 1 and plotted in Figure 1.

Table 1

March 1970	Descending Local Time is 1935-1945		Ascending Local Time is 0730-0745	
	UT	ΔF	UT	ΔF
6	18.2	-35	19.0	-29
	19.9	-55	20.8	-10
	21.6	-80		
	23.2	-75		
7	9.1	-55	9.8	-6
	10.5	-37		
	14.0	-40	14.7	-44
			16.3	-15
			18.2	-17
	19.0	-80	19.7	-44
	20.7	-25	21.4	-35
	22.7	-13		
	23.8	-65	.7	-25
8	1.7	-40	2.3	-40
	3.1	-45	3.9	-25
	4.8	-100	5.6	-10
	6.4	-125		
			10.6	-35
	11.3	-85	12.5	-65
	13.2	-55	14.1	-50
	15.2	-140	15.7	-40
			17.3	-60
	18.2	-130	18.8	-70
	20.2	-212	20.7	-215
	22.6	-450		
			.0	-220
9	.9	-210	1.7	-140
	2.6	-210	3.4	-150
	4.2	-190	5.0	-150
	6.0	-160	6.7	-115
	9.1	-150	9.9	-117
			11.6	-125
	12.4	-140		
			16.5	-58
	17.4	-100	18.3	-70
	19.0	-90	19.9	-80
	20.7	-95	21.6	-85
	22.4	-95		
10	.1	-90	.9	-60
	1.7	-70	2.5	-42
	3.4	-75	4.2	-60
	5.0	-75	5.8	-38
	6.6	-70	7.5	-35
			9.1	-42
	9.9	-85	10.8	-57
	11.6	-70		
			17.4	-60
	18.2	-65		
	19.8	-60	20.7	-55
	21.5	-65		
	23.2	-65		

Of course further work will be needed to correct these ΔF values to reflect the effect of the external field. A smaller but not negligible fraction of an observed decrease in field is caused by induced currents. These amplify the external effect.

Polar

The maximum dipole latitude of the orbit varied diurnally from 71° to passes directly over the magnetic pole. Thus, although the local times of the equatorial crossings are relatively fixed, the

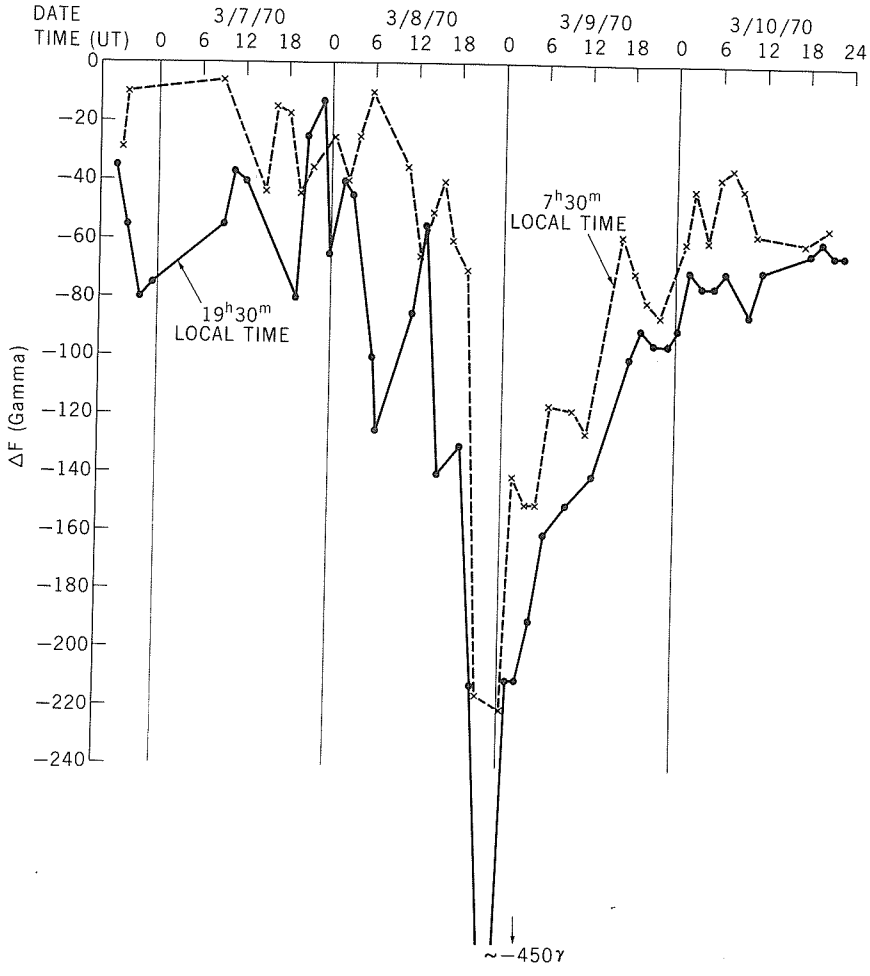

Fig. 1. Equatorial disturbance between March 6 and 10, 1970 as measured by the magnetometer aboard OGO-F. The dashed line is an A.M. plot, the solid line P.M. The points plotted are indicated on the graph. The maximum disturbance, coming at about 23.9 UT on March 8, had a magnitude of about 450 gammas.

orbit scans a range of magnetic local times including the expected "reverse" times when a pass goes between the dipole and geographic poles. In the northern hemisphere the passes over eastern North America thus achieve a near polar penetration traversing the auroral zones at a high angle whereas the passes over Russia cross at more shallow angles and parallel the zone a few degrees to the north. A typical north polar traversal is shown in Figure 2. The heavy line represents the path of the satellite, while the lighter, curved line is a plot of ΔF for that traversal using the satellite trace as a base.

Although Figure 1 may be considered approximately absolute, values over the auroral zone can presently only serve as a relative index since ΔF is dependent on the distance from the auroral currents as well as the geometry of its vector addition to the main field, and the effect of induction.

The data tabulated in Table 2 is for northern passes, and includes a column for the highest magnetic latitude reached. The figures under ΔF refer to the peak value reached; the northern apex column refers to the area within 10° of the highest latitude reached; the ascending-descending columns refer to the peaks outside of this range. All numbers not enclosed by parentheses indicate a definite single peak whereas a parenthesized quantity means that ΔF shows no structure, but rather hovers around the indicated value. The "Day" and "Night" indicator denotes whether the orbit passed on the day or night side of the dipole pole. The satellite ΔF should essentially be a measure of the disturbance in the Z component of the earth's field. A direct comparison between satellite ΔF and surface ΔZ on several occasions when the satellite passed nearly directly over a surface observatory showed satisfactory agreement.

Discussion

During almost the whole March 6-10, 1970 period, the field was lower on the evening side than the morning. Although the data for the early part of March 6 is missing, there is a clearly evident

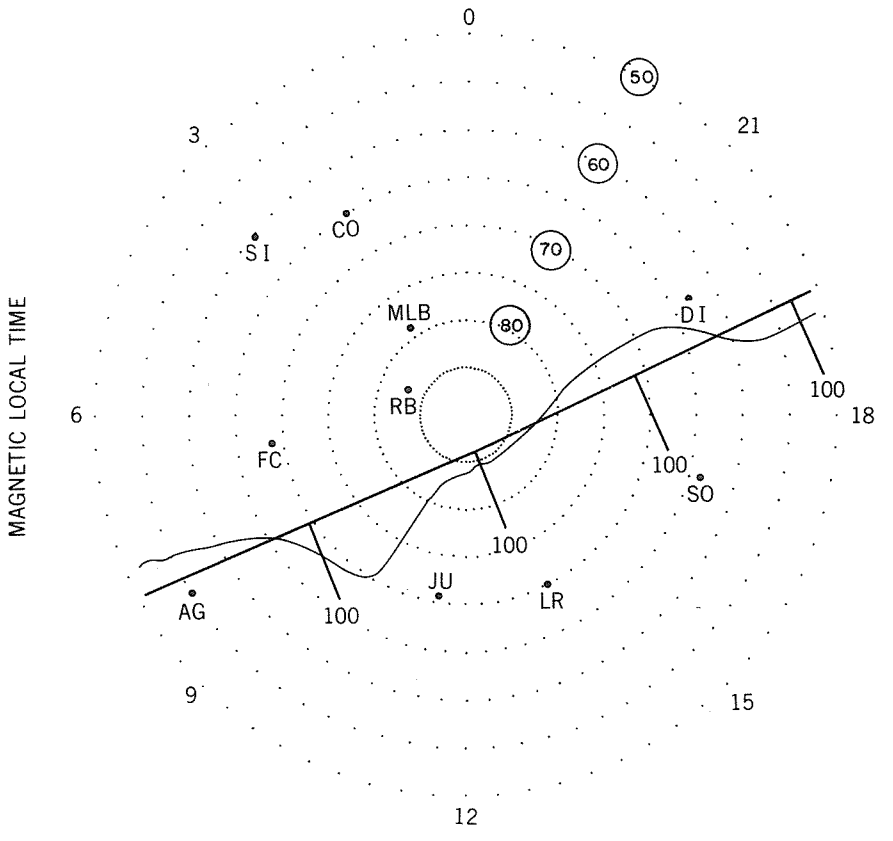

Fig. 2. A representation of the orbit of OGO-6 looking down on the North Pole. The circled numbers are the latitude (magnetic) circles, and the numbers around the perimeter of the plot (3, 6, 9, ...) represent geomagnetic local time. The heavy line is a trace of the satellite path for this particular traversal, while the lighter, curved line is a plot of ΔF. The scale of the ΔF plot is indicated by the lines perpendiculr to the orbit trace, with 100γ being indicated in the positive direction (down). Two letter symbols locate surface magnetic observatories:

Alaska (SI = Sitka, CO = College)
Canada (MLB = Mould Bay, RB = Resolute Bay, FC = Fort Churchill, AG = Agincourt)
Finland (SO = Sodankyla)
Greenland (JU = Julianehaab)
Iceland (LR = Leirvogur)
USSR (DI = Dixon)

partial ring current on the 19h LT side reading a minimum of -80γ on the pass near 2130 UT. As can be seen on Figure 1, the ΔF on the ascending mode maintains a value between -5 and -44γ until the pass near 1210 UT on March 8. During this time - before the large main phase - there are frequent auroral electrojets as seen in Table 2 from the positive and negative excursions. Further work will be needed with the assistance of surface observations to transform such data into information on the strength, location and direction of these electrojets.

Prior to the large main phase decrease of 450γ seen by OGO-6 at its southward traversal of the Atlantic about 2130 UT on March 8, Figure 1 shows that there may have been several injections and recoveries. For example, on March 8 the evening sector clearly drops from -40γ near 0100 to -125γ at 0700 and then rises to -55γ at 1300 before beginning the large main phase at 1500.

Table 2

March 1970 Magnetic Disturbance from OGO-6

March 1970	Time (UT) at northernmost apex	Maximum dipole latitude	Night (N) Day (D) Over Pole (P)	ΔF (gammas) Ascending morning	Northern Apex	Descending evening
6	1750	87	N	-20,+ 100	(20)	75
	1926	87	N	>100	(30)	30
	2105	89	N	-60,+ 200	(50)	(25)
	2245	87	D	-60,+ 125	(20)	20
7	0840	73	D	---	(-20)	-35
	1338	86	D	-50,+ 80	(20)	-40
	1657	87	N	70	---	---
	1838	87	N	-60,+ 250	(100)	-80
	2018	88	N	175	(50)	-35
	2158	89	D	95	---	(20)
8	0117	79	D	45	-60	30
	0257	75	D	40	-55	---
	0434	72	D	60	(-80)	---
	0613	71	D	(10)	(-75)	---
	1107	79	D	55	(-30)	-155
	1247	84	D	105	(±20)	-85
	1426	88	D	250	(±15)	-200
	1748	86	N	>150	(±20)	+50,- 100
	1928	86	N	---	(250)	-100
	2109	90	P	290	(150)	(75)
9	0028	82	D	(25, 190)	(150)	(75)
	0207	77	D	(120)	---	(80)
	0346	73	D	25, 80	---	---
	0523	71	D	(25)	70	---
	0700	71	D	(35)	(50)	(50)
	0840	73	D	---	(45)	(50)
	1018	77	D	(0, 50)	---	---
	1200	82	D	45	(20)	70
	1658	86	N	250	(100)	(150)
	1838	86	N	---	(75)	(50)
	2019	87	N	---	(70)	(35)
	2159	88	D	105	(50)	(50)
10	0118	79	D	(50)	(70)	(50)
	0257	74	D	(60)	(70)	(40)
	0434	72	D	(40)	(50)	---
	0613	71	D	(30)	(30)	---
	0750	73	D	(20)	(25)	(30)
	0929	75.5	D	(±20)	(25)	(40)
	1108	80	D	(30)	(15)	(40)
	1748	86	N	100	(25)	(25)
	1929	87	N	---	(45)	(40)
	2109	90	P	120	(30)	(30)

The last passes through the polar regions where clearly interpretable auroral electrojets can be seen in the data are those near 1750 UT (north) and 1840 UT (south) on March 8. From this orbit until late in the day on March 10, the satellite disturbance in both auroral and polar regions is strictly positive ($\Delta F > 0$). Those peaks which do occur (see Table 2) are usually broad. The ΔF over the northern polar cap during this period attains a value of 250γ at 1928 UT on the 8th; drops to 150γ early on the 9th; drops again to 70γ at 0523 UT on the 9th; and then hovers near 50-75γ until 0600 UT on the 10th. It then declines to 15-30γ, where it stays for the remainder of the 10th. Very similar behavior is evident in the Z components of polar cap observatories. The disturbance in Z at Alert, for example, is greater than or equal to zero from 1900 UT on March 8 to past 0800 UT on March 10. Alert ΔZ peaks at about 185γ at 1950 UT on the 8th; varies between about 80-130γ between 1900 UT on the 8th and 0100 UT on the 9th; goes near zero at 0115 UT on the 9th, then remains near +125γ from 0200 to 0700 UT on the 9th, drops to +50γ at 0830 UT to zero around noon; rises to 50γ at about 1400 UT on the 9th and hovers near 50γ until after 0600 UT on the 10th. ΔZ varies at Resolute Bay in the same manner as at Alert except that its value is generally somewhat larger. One could speculate that the sustained positive ΔZ could be due to the effect of the "ring current" near the poles. However, such an effect would be complicated by the induction in the earth and needs to be modelled carefully. Since the maximum equatorial excursion averaged around the earth (Dst) must occur sometime between 2100 and 2400 UT, it is interesting to note that the peak polar positive value (of +240γ in the south) does not occur until 0300 UT.

On March 10 as the disturbance decayed and became more symmetric at the equator, the polar data remained generally positive with occasional structure characteristic of weak electrojet activity.

In summary this interval includes very complex and potentially useful observations. The summaries given here may be modified somewhat later as further reference models are developed to include data after this time. However the amplitudes of the variations are sufficiently large that such modifications would be only in detail.

"The Geomagnetic Storm of March 8, 1970"

by

K. Kawasaki, S.-I. Akasofu, F. Yasuhara and P. D. Perreault
Geophysical Institute
University of Alaska
College, Alaska 99701

Presented here is an extensive compilation of magnetograms for the 'great' magnetospheric storm of March 8, 1970. The geomagnetic storm which began at 1417 UT March 8, 1970, was one of the most intense to occur since the IGY period (1957/1958). At low latitudes, the brief, maximum main phase depression was of the order of 350 gammas, and at high latitudes the negative bay which began nearly simultaneously to the ssc was of the order of 5000 gammas at College, Alaska.

Reduced H-component magnetograms of the period March 7-9, 1970, are compiled in Figures 1 through 7; they are grouped according to three geomagnetic longitude sectors. The solar quiet day variation, Sq, has been removed from stations lying between 0° to ± 55° in geomagnetic latitudes. The centered geomagnetic dipole and geographic coordinates of the stations are listed in Table 1.

TABLE 1

Station:	Dipole Latitude	Dipole Longitude	Geographic Latitude	Geographic Longitude
Abisko	66.0°	115.0°	68° 21' N	18° 49' E
Alert	85.9°	168.2°	82° 30' N	62° 30' W
Almeria	40.6°	75.3°	36° 51' N	2° 28' W
Baker Lake	73.8°	315.2°	64° 20' N	96° 02' W
Barrow	68.5°	241.1°	71° 18' N	156° 45' W
Boulder	49.0°	316.5°	40° 08' N	105° 14' W
College	64.6°	256.5°	64° 52' N	147° 50' W
Dallas	43.0°	327.7°	32° 59' N	96° 45' W
Dusheti	36.7°	122.1°	42° 05' N	44° 42' E
Fredericksburg	49.6°	349.8°	38° 12' N	77° 22' W
Furstenfeldbruck	48.8°	93.3°	48° 10' N	11° 17' E
Gnangara	-43.2°	185.8°	31° 47' S	115° 57' E
Great Whale River	66.6°	347.4°	55° 16' N	77° 47' W
Guam	4.0°	212.9°	13° 35' N	144° 52' E
Hermanus	-33.3°	80.5°	34° 25' S	19° 14' E
Honolulu	21.1°	266.5°	21° 19' N	158° 00' W
Kakioka	26.0°	206.0°	36° 14' N	140° 11' E
Leirvogur	70.2°	71.0°	64° 11' N	21° 42' W
Lvov	48.0°	105.9°	49° 54' N	23° 45' E
Magadan	50.2°	210.8°	60° 07' N	151° 01' E
M'Bour	21.3°	55.0°	14° 24' N	16° 58' W
Meanook	61.8°	301.0°	54° 37' N	113° 20' W

TABLE 1 (CONTINUED)

Station:	Dipole Latitude	Dipole Longitude	Geographic Latitude	Geographic Longitude
Moca	5.7°	78.6°	3° 21' N	8° 40' E
Mould Bay	79.1°	256.4°	76° 12' N	119° 24' W
Newport	55.1°	300.0°	48° 16' N	117° 07' W
Nurmijarvi	57.9°	112.6°	60° 31' N	24° 39' E
Odessa	43.7°	111.1°	46° 47' N	30° 53' E
Ottawa	57.0°	351.5°	45° 24' N	75° 33' W
Pleshchenitsy	52.1°	111.5°	54° 28' N	27° 48' W
Resolute Bay	83.0°	289.3°	74° 42' N	94° 54' W
Rude-Skov	55.9°	98.5°	55° 51' N	12° 27' E
San Juan	29.6°	3.1°	18° 07' N	66° 09' W
Sitka	60.0°	275.3°	57° 04' N	135° 20' W
St. John's	59.1°	18.9°	47° 36' N	52° 41' W
Sverdlovsk	48.5°	140.7°	56° 44' N	61° 04' E
Tahiti	-15.3°	282.7°	17° 33' S	149° 37' W
Tangerang	-17.6°	175.4°	6° 10' S	106° 38' E
Tashkent	32.3°	144.0°	41° 20' N	69° 37' E
Toolangi	-46.7°	220.8°	37° 32' S	145° 28' E
Tucson	40.4°	312.2°	32° 15' N	110° 50' W
Victoria	54.2°	293.0°	48° 31' N	123° 25' W
Witteveen	54.1°	91.2°	52° 49' N	6° 40' E
Yakutsk	51.0°	193.8°	62° 01' N	129° 43' E
Yuzhno-Sakhalinsk	36.9°	206.7°	46° 57' N	142° 43' E

Although the morphological structure of the ssc, initial phase, and main phase of the storm of March 8-9 are quite complex, some common features within each longitude group or adjacent groups may be noted.

1. In low latitudes there was apparently a substantial asymmetry in the magnitude of the ssc which occurred at 1417 UT, March 8, with a rise time of one to two minutes. In the Western American-Asian sectors, then between 19 and 04 LT (night sector), the amplitude of the ssc was large compared with that in the Eastern American-Western European sectors, then between 06 and 18 LT (day sector), where the ssc was immediately followed by a low latitude negative bay-like depression.

This feature appears to be characteristic of great magnetic storms. In particular, the relatively large, sharp, negative change soon after the ssc at San Juan, for example, is an interesting phenomenon. The magnetic record from Kakioka, Japan, for the Febraury 11, 1958, storm resembled that of the San Juan record of the present storm. The February 11, 1958, storm and some others were discussed by Fukushima [1958]. At the time of the ssc of the February 11, 1958 storm, Kakioka was located in the late morning sector. Another example of a large negative change in low latitudes soon after the ssc occurred during the great storm of July 15, 1959. Akasofu and Chapman [1960] showed that the negative change extended to as low as the magnetic equator in Africa, then located in the

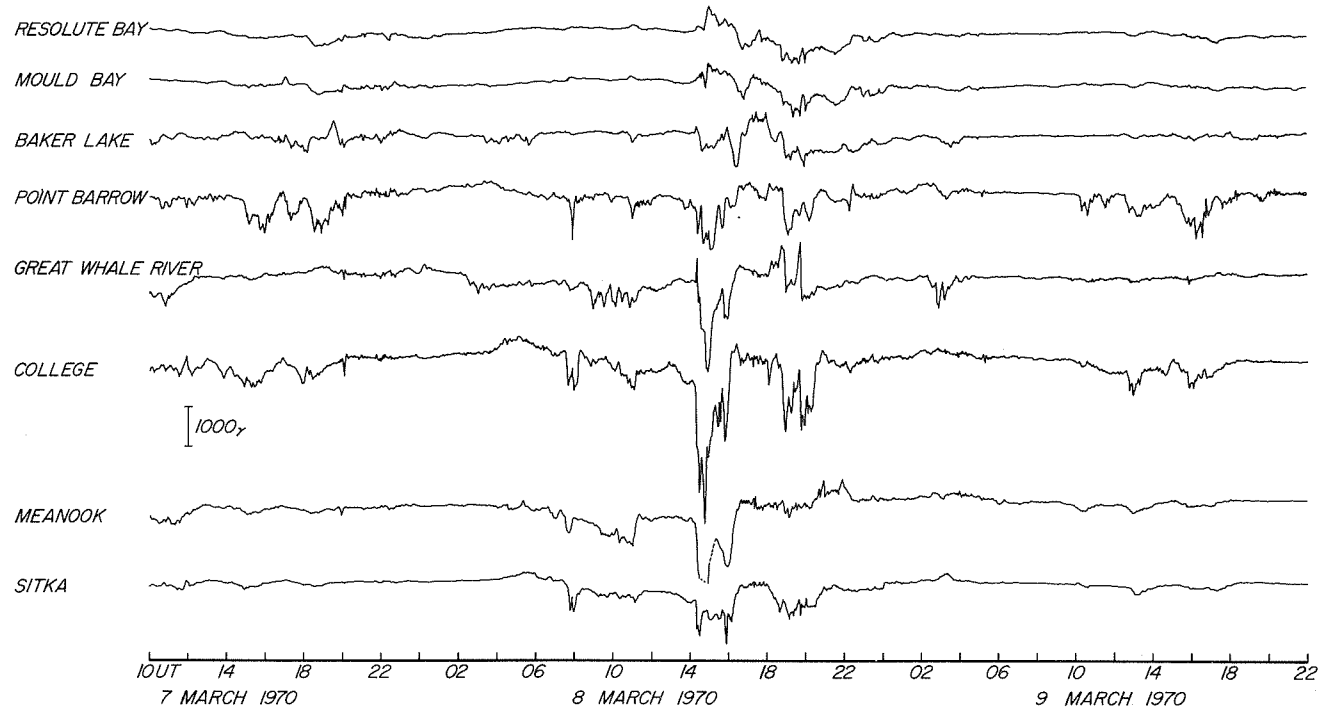

Fig. 1. Magnetograms of auroral and polar cap American sector stations (60^{o}-90^{o}, dp. lat.)

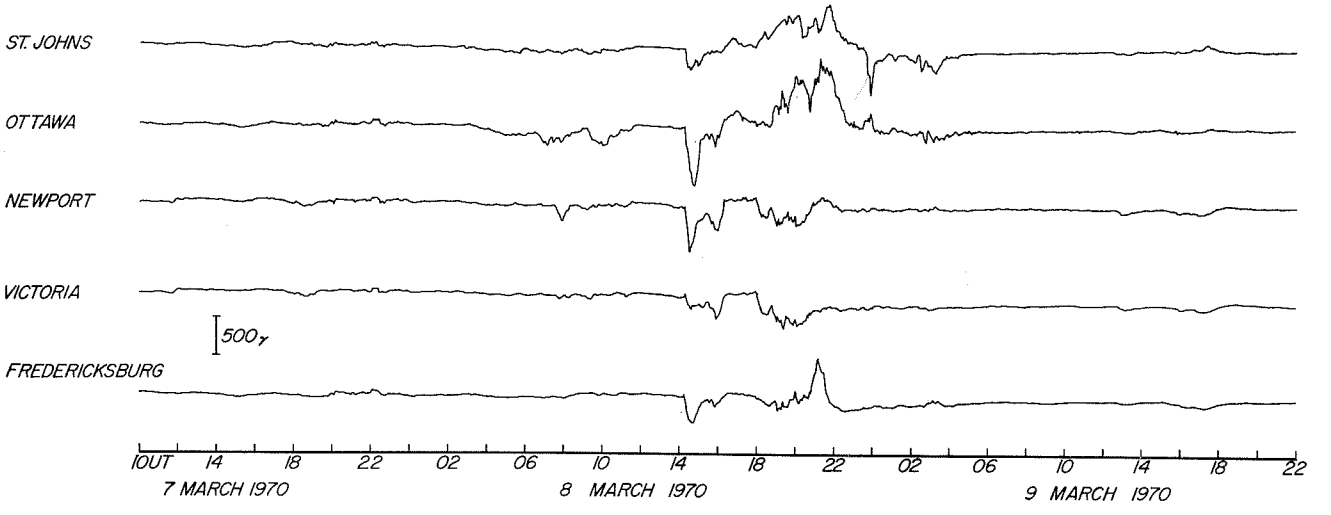

Fig. 2. Magnetograms of sub-auroral American sector stations ($\sim$50 - $\sim 60^{o}$, dp.lat.)

noon sector. Further, the magnitude of the negative change for the July 15, 1959, storm was almost constant in a wide latitudinal range. Unfortunately, the associated substorm was too intense to examine details of the equivalent current system during the ssc and the initial phase.

In the present storm, in the auroral zone negative bays were observed in the sector where the low latitude negative changes were recorded. Therefore, it is reasonable to conclude that the negative change at lower latitudes was not due to the return current from the auroral electrojet. One possibility for the observed low latitude negative change is that the ring current or the tail current was immediately enhanced after the ssc. In the afternoon-midnight sector, however, this effect was masked by the effect of an intense return current from the electrojet.

2. At low latitudes in the Western American-Asian sectors the field remained positive for a time of the order of 30 minutes after the ssc.

3. Simultaneous to within a minute of the beginning of the ssc there occurred an intense negative bay, particularly well-formed at College (then in the early morning sector), where the field decreased some 5000 gammas in half an hour or so. However, the bay was also observed over the whole of the auroral zone. It is quite likely that during such an intense substorm, the electrojet flows all around the auroral oval (although the current intensity may not be uniform), as suggested by Feldstein [1963] and Akasofu, Chapman and Meng [1965].

4. During the somewhat lengthy ($\sim$1 to $\sim$5 hours after the ssc) and complex initial phase there occurred several distinguishable positive and negative si's superposed on generally larger and lengthier positive and negative changes. Throughout the period under study it is seen that positive disturbances of the latter type tend to occur in the midnight-early morning sectors whereas negative ones tend to occur in the noon-early evening sectors.

5. The polar substorm which began about 1930 UT on March 8 was observed over a wide range of longitude in the auroral regions. It is certain that high latitude Siberian stations, not included in Figure 6, would also have recorded this moderately large negative bay, being in the most favorable early morning location. It is thus quite likely that the electrojet flowed all along the oval during the substorm.

6. As noted earlier, the initial phase of the storm was very complex, and it is not possible to determine clearly the onset time of the main phase. However, it appears that the growth of the main phase was first recorded at San Juan at about 1730 UT, so that an intense ring current began to grow in the afternoon sector.

7. The main phase decrease was quite asymmetric even at about the maximum epoch. The largest decrease ($\sim$350 gammas) was observed at Moca, in Africa, then a late evening station.

8. The storm entered its recovery phase at about 22 UT, some 8 hours after ssc; by 02 UT of March 9 the ring current field had very nearly become symmetric. In high latitudes only minor polar substorms were observed during this recovery stage of the geomagnetic storm.

9. An examination of the disturbances which occurred between 20 UT and 23 UT March 7 reveals that these are a series of clearly distinguishable si's; there is an almost exact one-to-one correspondence of changes over the whole of the earth at low latitudes during this period. Little activity was recorded at this time at high latitudes, quite unlike the case for the simultaneous ssc and bay disturbance which occurred at 1417 UT of March 8.

10. The short duration of the storm is another feature of this great magnetic storm. It can be seen that high latitude records became quite normal as early as 24 UT on March 8, about 10 hours after the onset of the storm, although the recovery phase of the main phase was continuing at that time. The duration of the main phase was also relatively short compared with some other intense storms.

Within the interval of 72 to 20 hours preceding the ssc of March 8, there were approximately 19 solar flares of importance 1 or greater. It is probable that the large area, Importance 2+ flare associated with the McMath Plage Region 10614 was responsible for the ssc. This central meridian flare ($\sim$S11 $\sim$E12) began at 0141 UT March 7, which is approximately 36 hours before the time of ssc, well within the distribution of elapsed times between the onset of flares and the observation of ssc's reported by Akasofu and Yoshida [1967]. Further, the large amplitude of the ssc and the amplitude of the Forbush decrease ($\sim$7%), [Solar-Geophysical Data, May, 1970] are also compatible with a flare having a central location [Akasofu and Yoshida, 1967].

Simultaneous ssc's and polar negative bays of the type described in 1, 2 and 3 above have been studied by Schieldge and Siscoe [1970] and Kawasaki, Yasuhara, Akasofu and Meng [1971] who found a high correlation of large amplitude ssc's (about 60 gamma for the March 8 event) with the occurrence of simultaneous negative bays.

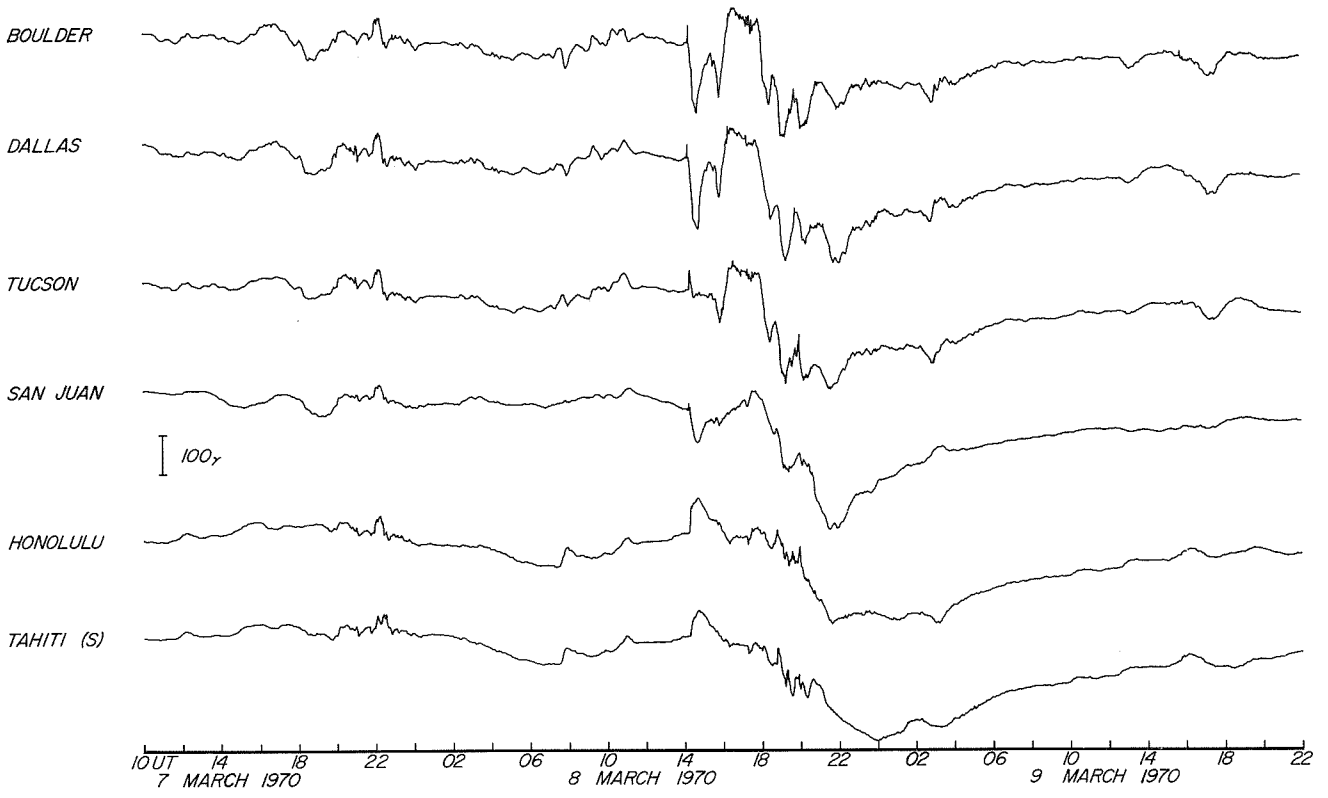

Fig. 3. Magnetograms of low and mid-latitude American sector station (0° - $\sim$+ 50°, dp. lat.). The Southern hemisphere station, Tahiti, is marked (s).

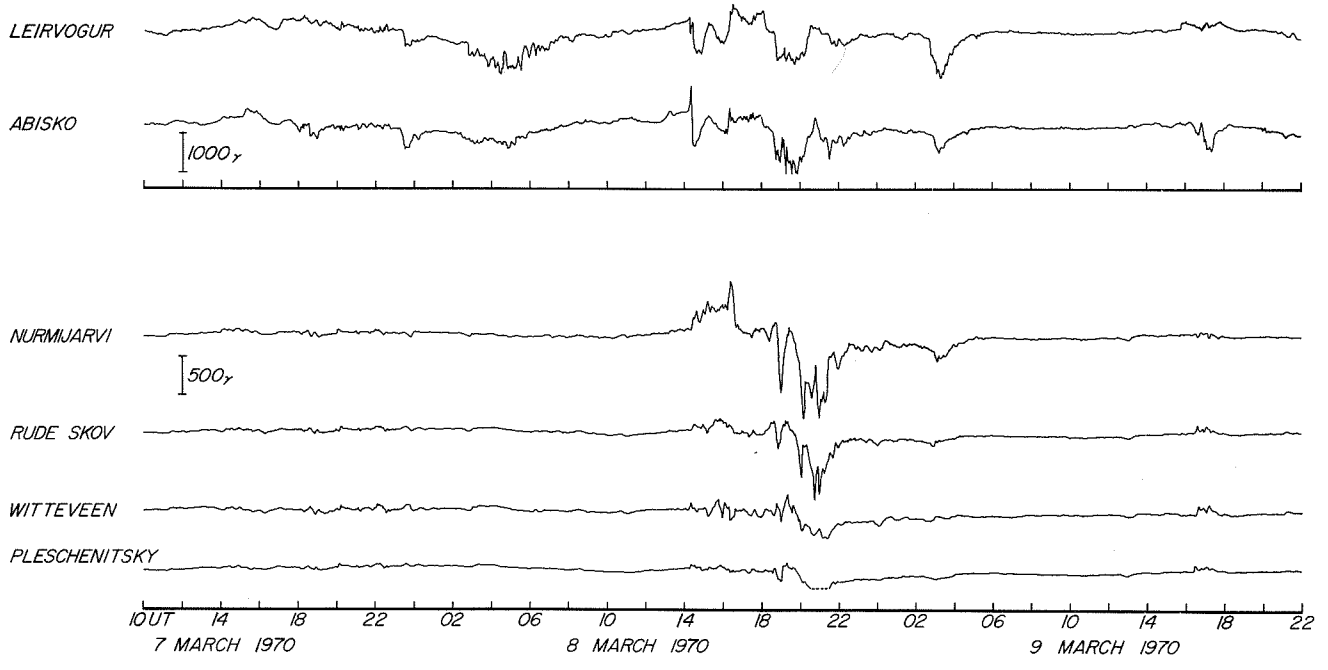

Fig. 4. Magnetograms of auroral and sub-auroral European sector stations ($\sim 50^{\circ}$ - $\sim 70^{\circ}$, dp. lat.)

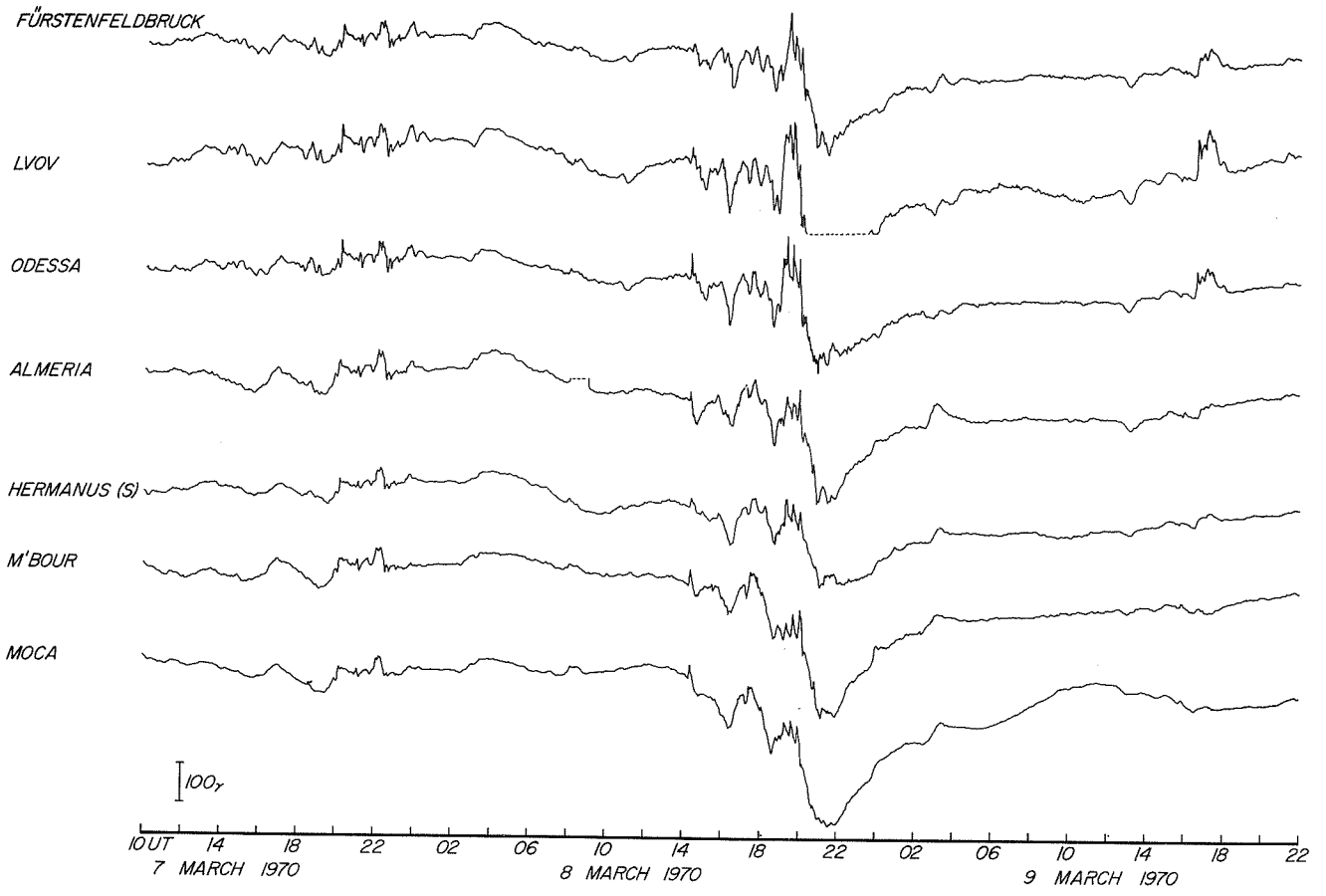

Fig. 5. Magnetograms of low and mid-latitude European sector stations (0° - $\sim 50^{\circ}$ dp. lat.). The Southern hemisphere station Hermanus is marked (s).

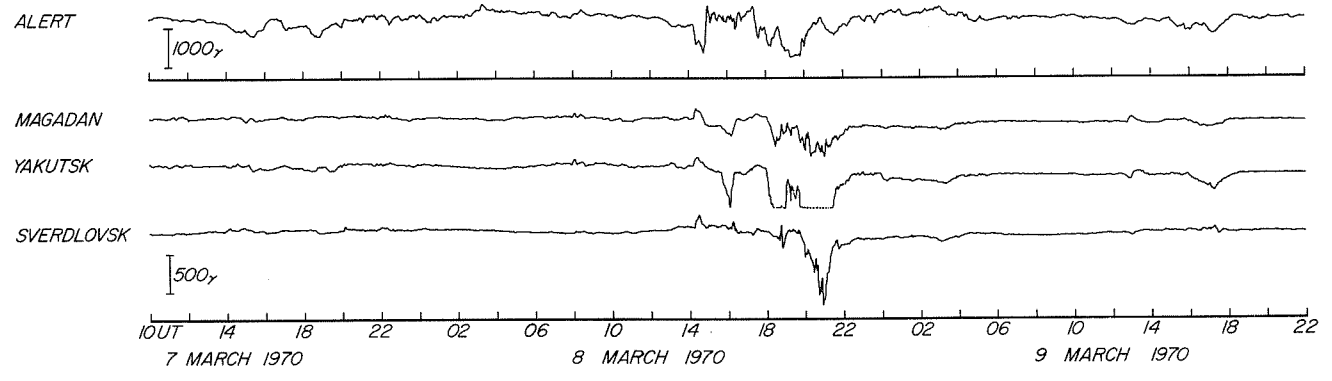

Fig. 6. Magnetograms of polar cap and sub-auroral Asian sector stations ($\sim 50^{\circ}$ - $\sim 90^{\circ}$, dp. lat.)

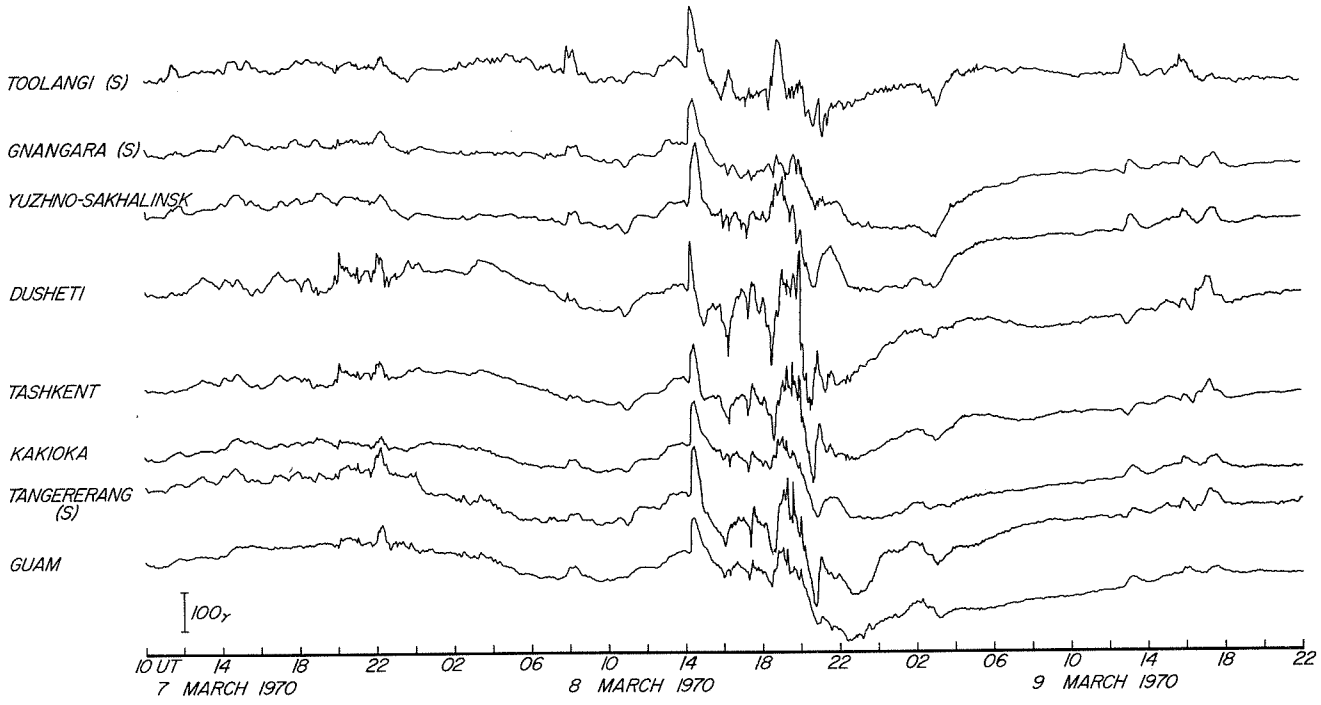

Fig. 7. Magnetograms of low and mid-latitude Asian sector stations (0° - $\sim\pm 50^{\circ}$ dp. lat.). Southern hemisphere stations are marked (s).

Acknowledgements

This work was supported by National Science Foundation Grants GA-1703 and GA-17663. We wish to thank Dr. A. N. Zaitzev, IZMIRAN, Akademgorodok, Moscow, U.S.S.R. and Dr. V. M. Mishin, SibIZMIR, Irkutsk, U.S.S.R. for supplying Russian data and Mr. Wm. Paulishak of WDC-A, Geomagnetism, Rockville, Maryland for expediting other data used in this report.

REFERENCES

AKASOFU, S.-I. and S. CHAPMAN 1960 Some features of the magnetic storms of July 1959, and tentative interpretations, IUGG Monograph, 7, 93-108

AKASOFU, S.-I., S. CHAPMAN and C.-I. MENG 1965 The polar electrojet, J. Atmos. Terr. Phys., 27, 1275-1305

AKASOFU, S.-I. and S. YOSHIDA 1967 The structure of the solar plasma flow generated by solar flares, Planet. Space Sci., 15, 39-47

FELDSTEIN, YA. I. 1963 Some problems concerning the morphology of auroras and magnetic disturbances at high latitudes, Geomag. and Aeronm., 3, 183-192

FUKUSHIMA, N. and S. ABE 1958 The initial phase of the magnetic storm on Feb. 11, 1958, Rept. Ionos. Res. Japan, 12, 44-59

KAWASAKI, K., F. YASUHARA, S.-I. AKASOFU and C.-I. MENG 1971 Storm sudden commencements and polar substorms, (to be submitted for publication)

SCHIELDGE, J. P. and G. L. SISCOE 1970 A correlation of the occurrence of simultaneous sudden magnetospheric compressions and geomagnetic bay onsets with selected geophysical indices, J. Atmos. Terr. Phys., 32, 1819-1830

"Geomagnetic and Cosmic Ray Observations at Hermanus During the Period 5-10 March 1970"

by

A. Elvera Thomas
Magnetic Observatory, Hermanus
Republic of South Africa

Introduction

The magnetic variations at Hermanus (Geographic coordinates: S34°25.2' E19°13.5' or Geomagnetic coordinates: S33.7° E81.7°) and cosmic ray neutron monitor data for periods including the events between 5 and 10 March 1970 are presented graphically.

There is brief description of the magnetic pulsations and other rapid variations recorded by bar fluxmeter, mainly of those which do not show in detail on the normal Askania magnetograms.

The geomagnetic storm or storms as observed at Hermanus

From the Askania magnetograms for the period 1970 March 5 - 10 shown in Figure 1 it may be seen that at least two magnetic storms occur with a possible substorm between them. The principal magnetic storm report for this period shows that:

> A storm began on March 5 at 0805 UT and continued until March 8 with ranges D = 25', H = 132γ and Z = 88γ. There were sc type movements at 07d 20h 04m and 07d 21h 58m UT. Bay type movements continued until the commencement of the following storm at 08d 14h 17m UT. In this storm the ranges were 63' in D, 229γ in H, and 322γ in Z.

The substorm on March 7 lasted about four hours. Its start at 2004 UT is reported as a sudden impulse as it is part of the larger storm which began on March 5, but the start may be considered a sudden commencement of the substorm as the magnetic activity was greater after this time than before.

Some of the bays and the sc and si are indicated in Figure 5.

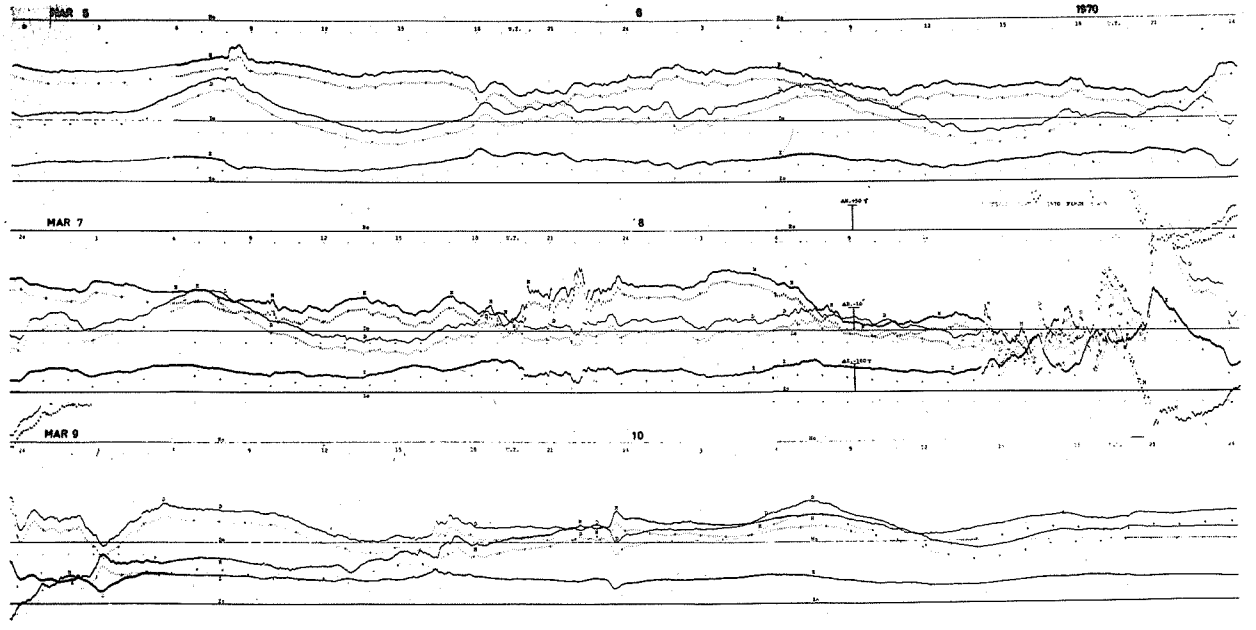

Fig. 1. Geomagnetic storms 1970 March 5 - 10;
Askania magnetograms at 20 mm/hour; Time UT;
Baseline and scaling values for this period:
Horizontal Intensity $H = 12216 + 2.28\ h_{mm}$ (gammas),
Declination $D = -24° 09.0' - 0.543'\ d_{mm}$ (minutes),
Vertical Intensity $Z = -26627 - 4.45\ z_{mm}$ (gammas), where h_{mm}, d_{mm}, z_{mm} are scalings in millimeters from the respective baselines H_O, D_O and Z_O (reckoned positive upwards);
The variation in declination may also be expressed as $-1.9\ d_{mm}$ (gammas).

Pulsations from normal magnetograms (N) and bar fluxmeter records (F)

Bar fluxmeter time-scale value: 6 mm/min
Bar fluxmeter scale value: H = 0.08 γ/mm

Day	Classification	UT Beginning	Ending
5	pc3	0805	1812
5	pi2	2109	2126
6	pi2	0058	0102
6	pc3	0640	1256
6	pi2	2208	2220
6	pi2	2251	2254
6	pi2	2302	2306

pc2: continuous pulsations of period range 5 - 10 s
pc3: continuous pulsations of period range 10 - 45 s
pg : continuous pulsations of period longer than 600 s (only reported if their amplitude is greater than 1 γ)
pi1: individual pulsations of period 1 - 40 s
pi2: individual pulsations of period range 40 - 150 s

Remarkable pulsations

The horizontal intensity record on the fluxmeter is discussed as the declination record was discontinuous when the displacement was too large and/or too rapid.

Time of starting	Mean Period s	Maximum Range γ	Remarks
05d 08h 04.8 ± 0.2m	22.5 ± 0.2	ca 3.6	Very regular set with rapid logarithmic decrement.
07d 20h 03.7 ± 0.2m	300 ± 10 8 ± 2	11 0.1	Very irregular pc2 superimposed
07d 20h 59.0 ± 0.2m	610 ± 10		One "square wave"
07d 21h 58.0 ± 0.2m	390 ± 20 300 ± 20	11+ 8	First movement +
07d 22h 09.8 ± 0.2m	350 ± 20 220 ± 20 270 ± 20	11 6 2.5	First movement +
07d 22h 25m	370 ± 20	14+	First movement -
07d 22h 36.8m		6+	First movement - Very irregular

Pg's have been reported from Furstenfeldbruck from 08d 14h 10m to 08d 23h 00m.

From 08d 17h 14m to 08d 21h .. pulsations of various periods and amplitudes which took them beyond the fluxmeter record were observed at Hermanus and at Hurouque, France the geomagnetic conjugate point.

Magnetic and cosmic ray data 1970 March 7 - 9

The Horizontal, Vertical and Declination elements were traced separately for the period March 7, 18 hours to March 9, 6 hours in Figure 2. The quiet day diurnal variations were calculated as the mean of the values for the international quiet days 21, 22 February and 21, 22 March as these dates were equally spaced before and after the main storm on 8 March and sufficiently far from the storm to be considered "normal". On March 16, the only quiet day nearer the storm, the observed values appeared to be consistently higher by several millimeters than the values on the other four quiet days. March 16 was, therefore, omitted from the calculations.

The quiet day values Qh, Qd and Qz are plotted as curves of dots and dashes.

The maximum value of the Declination is shown as a dotted line as it was deduced from the time marks.

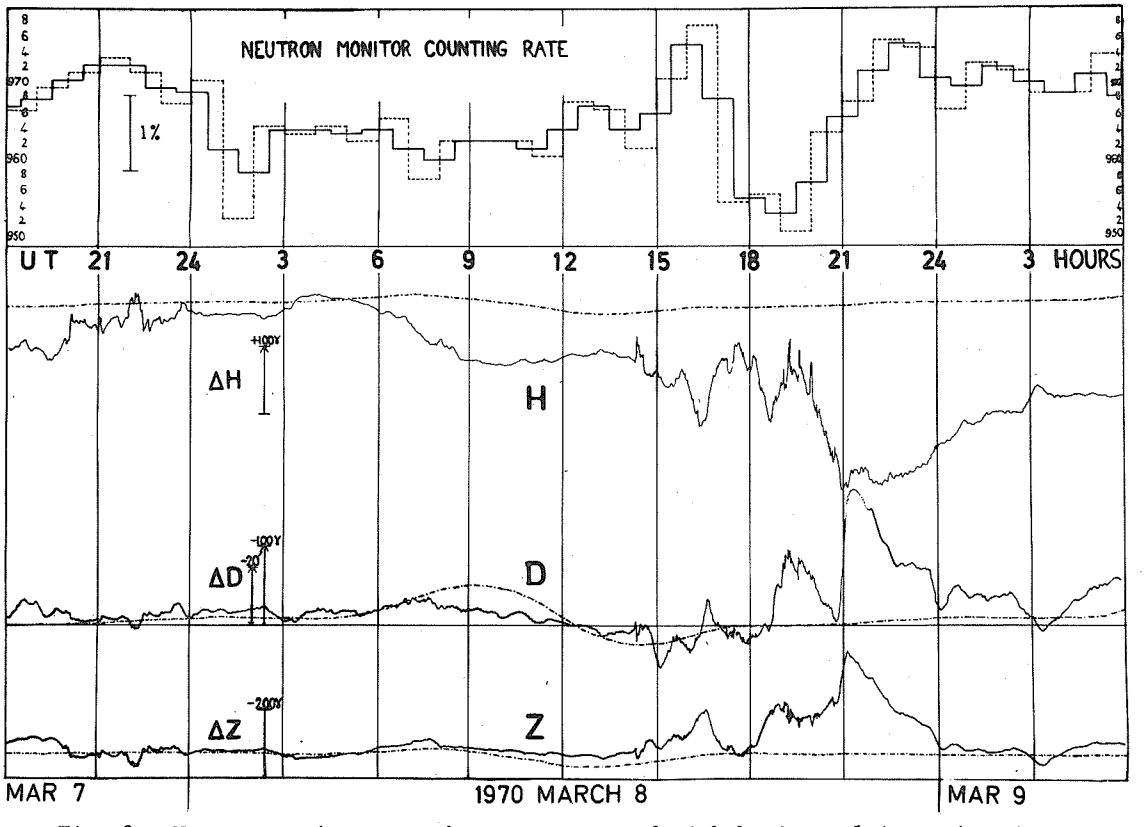

Fig. 2. Neutron monitor counting rate compared with horizontal intensity, H; declination, D; and vertical intensity, Z separately
3-NM-64 hourly counting rate ----
3-NM-64 running mean (two hours) _____
Quiet day curves for H, D, and Z are shown thus ._._.

Above the magnetic elements in Figure 2 the 3-NM-64 Counting Rate at Hermanus is shown. Real Counts = 100 x tabulated counts. In order to diminish the statistical error the mean bihourly values, taken as a running mean were plotted as a solid line. This reduced the apparent variations to an extent not warranted by the reduction in the statistical errors and small, short, real effects may have been masked. The standard deviation is 0.3 per cent.

Decreases in cosmic ray activity occur 3 - 5 hours after the sudden impulses beginning at 07d 20h 05m UT and about 2 hours after the sudden commencement at 08d 14h 17m UT. It is considered that the latter is a 3 per cent Forbush decrease.

It is interesting to note that the times between the sudden increases and decreases of the Horizontal Intensity in Figures 1 and 2 are 35, 28, 26 and 35 minutes beginning at 05d 08h 05m, 07d 20h 04m, 07d 21h 58m and 08d 21h 00m UT, respectively.

Elimination of quiet day variation

In Figure 3 the quiet day values Qh, Qd and Qz as shown by the dotted and dashed curve in Figure 2 were subtracted from the values of the elements H, D and Z at the corresponding hours and a graph from which at least one variable had been eliminated was drawn.

A quasi-periodicity appeared and it was decided to derive the change in element from one hour to the next and plot the resulting values in the method adopted by W. Dieminger et al. [1970] in detecting gravity waves.

Quasi-periodicity

The successive changes in each element were plotted in Figure 4 and a tent-shaped variation appeared to show best in Z and in D, but not very clearly in H.

It was impossible in the limited time to analyze this although ten-minute scalings were made and the method given by J. Bartels [1940, 1951] quoted by Blackman [1958] was attempted. If the period differs too much from a multiple of ten minutes the sets become out of step.

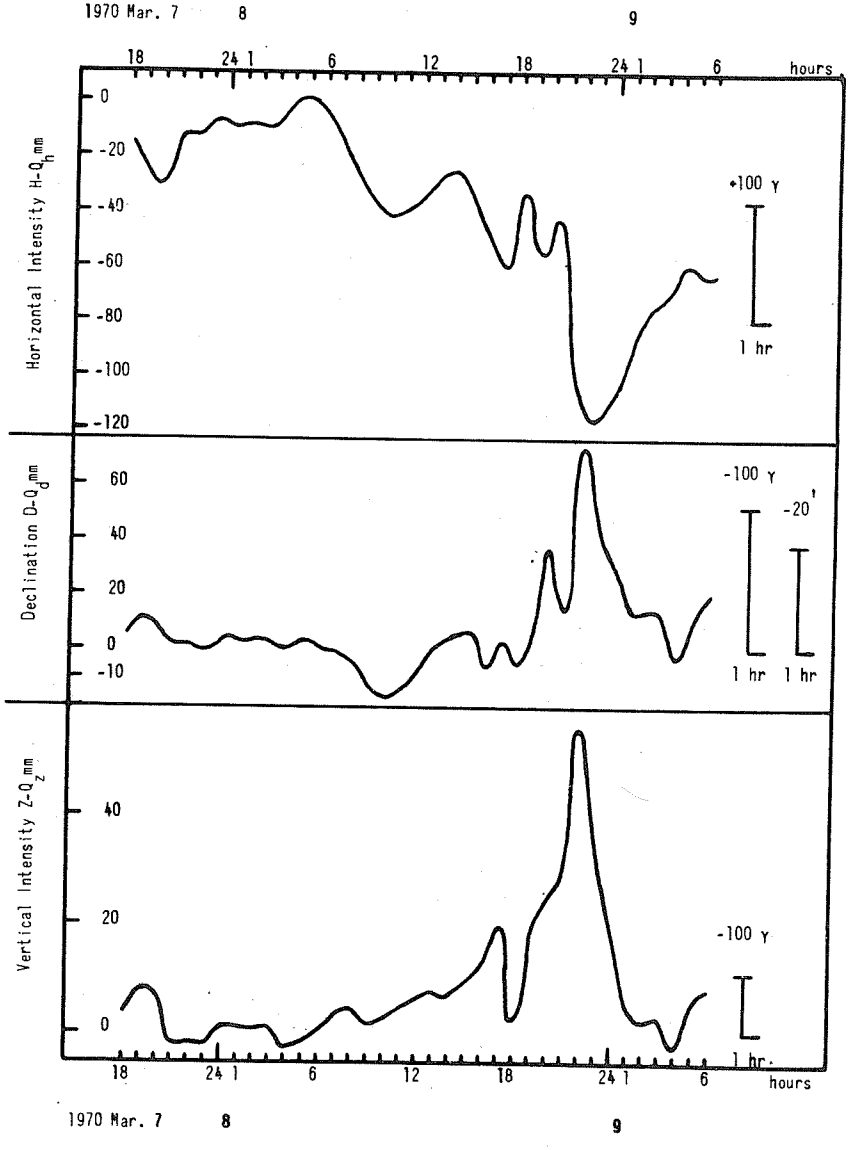

Fig. 3. Storm variations of H, D and Z after eliminating quiet day variations Qh, Qd and Qz.

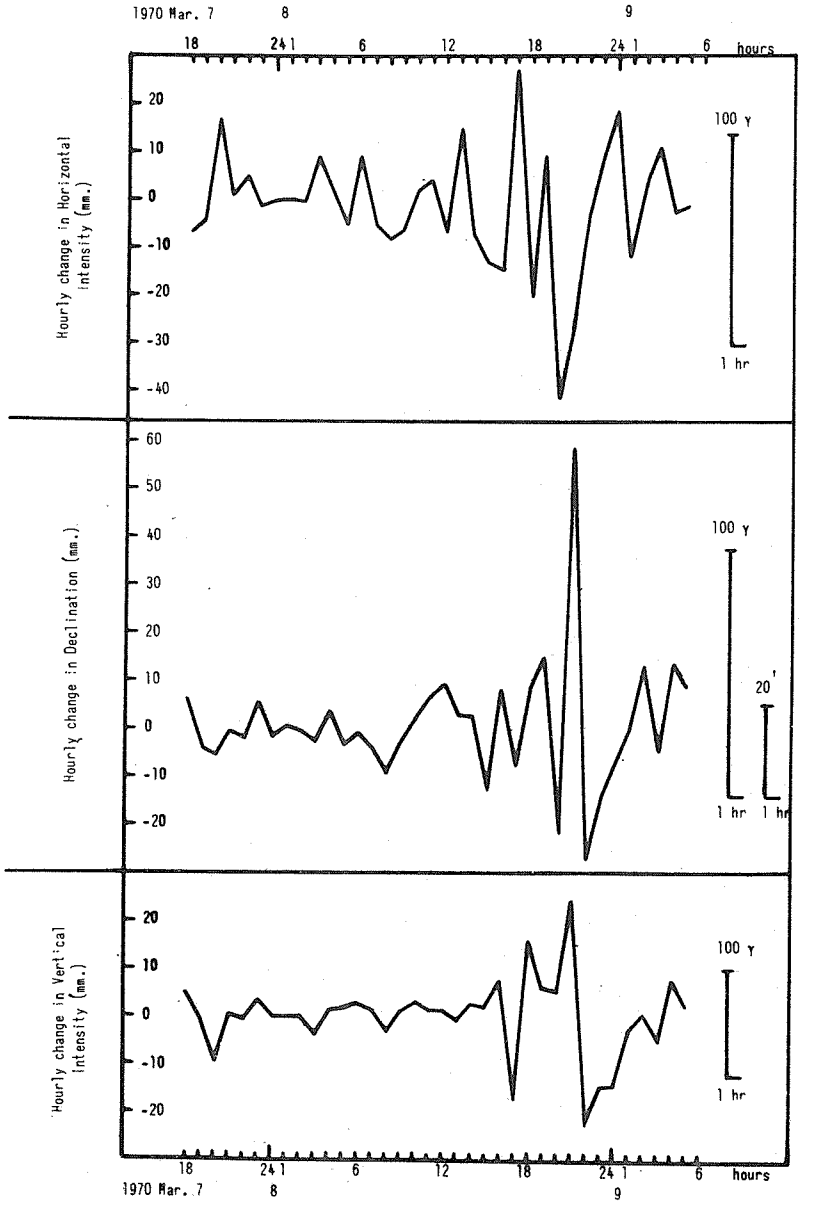

Fig. 4. Difference between successive mean hourly scalings calculated from the values used in Figure 3.

Much interesting work remains to be done on the analysis of the pulsations during magnetic storms, beginning with this event and comparing with others.

Hourly comparison of H-Qh and cosmic ray neutron monitor counting rate

In Figure 5 the hourly means of H-Q_h is shown over the whole period March 5 - 10 and compared with the cosmic ray 3-NM-64 variation.

si, sc and bp and their directions were shown on the same graph. Bays were omitted if their time of starting was vague or if they were without pulsations unless they were of remarkable quality. The list of times and occurrences is given below.

Magnetic Bulletin					Cosmic Ray counting rate + up, - down and time difference
d	UT h	m	Type	Direction same in H,D,Z	
5	08	05	sc	+	+ 2 hrs before - 2 hrs later
5	17	00	bp	-	-
6	23	15	bp	+	+ 1 hr before
7	20	04	si(sc?)	+	+ 2 hrs later - 5 hrs later
7	21	58(a?)	si	+	- 3 hrs later
7	22	25	si	-	- 3 hrs later
8	14	17	sc*	+	+ 2 hrs later - 3 hrs later
	23	48	bp	+	
9	02	45	bp	+	
	15	47	si	+	+ 1 hr before - 1 hr later
9	23	23	bp	+	

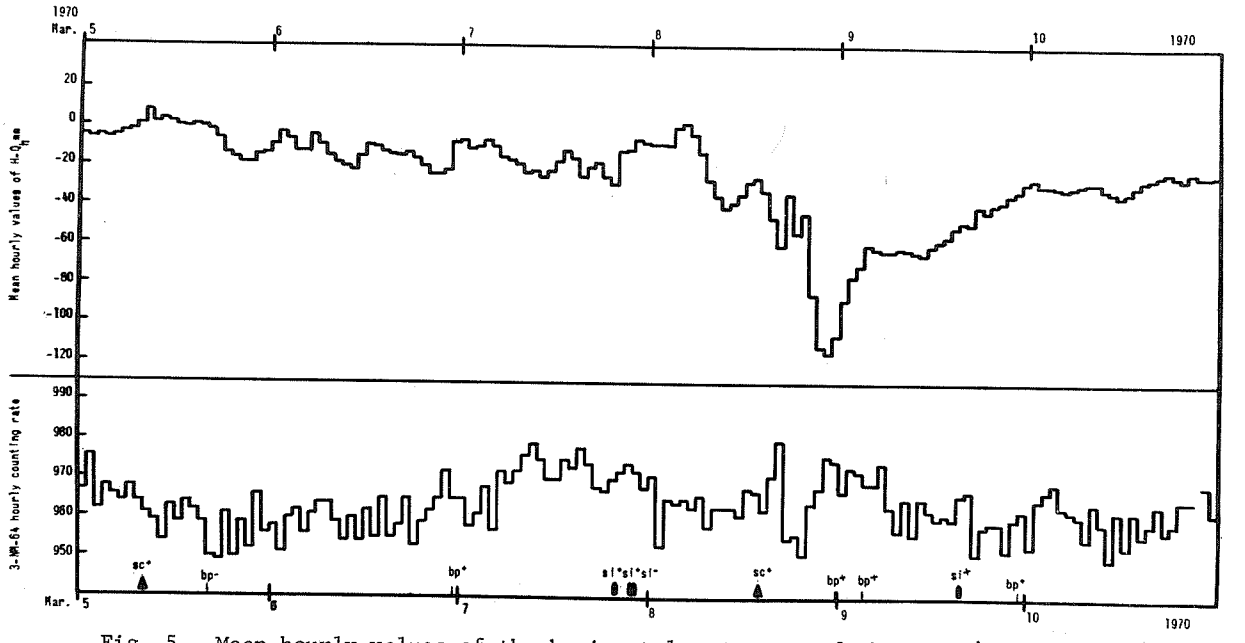

Fig. 5. Mean hourly values of the horizontal component of the earth's magnetic field with quiet day variation eliminated and of the neutron monitor 3-NM-64 counting rate from March 5 until March 10, 1970 with main magnetic incidents indicated.

The comparison of cosmic ray counting rate with magnetic disturbance indices

In Figure 6 a broad picture of daily cosmic ray counting rate and magnetic disturbance indices is taken from February 13, the beginning of a 27-day sunspot cycle, through March 12, the beginning of the next sunspot cycle, continuing to March 27, 1970.

Deep River 48-NM-64 results corrected to 74.7 cm Hg are used as a standard of comparison with Hermanus 3-NM-results, corrected to 1015 millibars.

The geographic coordinates of Deep River, Canada are N46°06' W77°30'.

Kp, the geomagnetic planetary index is used as a standard of comparison with K for Hermanus.

The conclusion to be drawn is that there was a Forbush decrease on March 5 which continued until March 6. The recovery on March 7 was interrupted near the end of the day by various si which resembled sc and another Forbush decrease occurred on March 8, 1970. The rate of recovery was slow, about a week.

Whether the maximum magnetic activity precedes or follows the minimum cosmic ray activity by two days cannot be decided in this storm as there were two sc within three days of one another. See Sandström [1965].

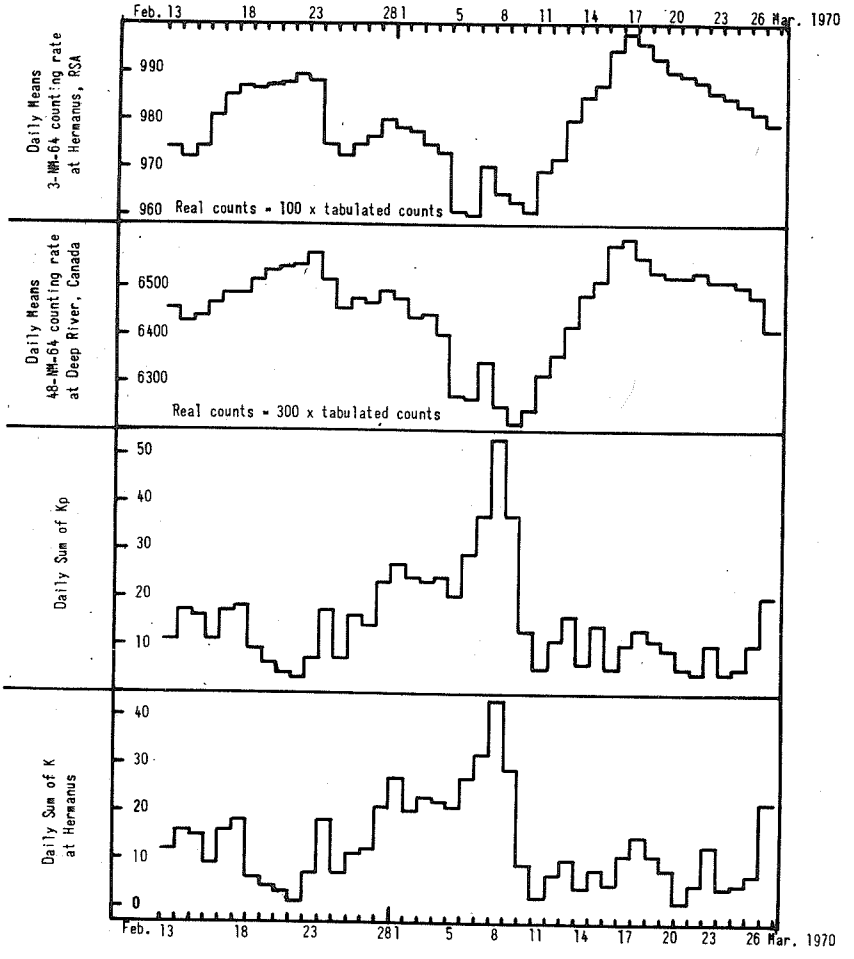

Fig. 6. Comparison of mean daily cosmic ray counting rate with geomagnetic activity indices
Kp = geomagnetic planetary indices
K = magnetic disturbance index at Hermanus

Solar phenomena

There was no recorded solar flare.

There was a minimum of solar flux (adjusted to 1 A.U.) of frequency 8800 MHz on March 5 and maxima for the month of March 1970 of frequency 2800 MHz and 2695 MHz on March 1 and March 8, and frequency 1415 MHz on March 8 and 606 MHz on March 8 (and March 13), Solar-Geophysical Data [April 1970].

This information is stated as one wavelength of Solar Flux gave a decrease on March 5 and four wavelengths gave increases on March 8, which were the days of the sc and Forbush decreases.

There was a solar eclipse on March 7 whose phases were:

	Time	Latitude	Longitude
Beginning	15 04.9	-11° 41'	+ 134° 32'
	16 05.2	- 2 00	+148 42
Central eclipse at local apparent noon	18 03.8	+25 32	+88 11
	19 11.5	+55 01	+22 36
End	20 11.9	+45 24	+35 31

The end of the solar eclipse almost coincided with the beginning of the magnetic substorm on March 7.

Acknowledgements

Thanks are given to other members of the Magnetic Observatory, Hermanus, staff who assisted with advice or carrying out practical details in preparing this report: Mr. A. M. van Wijk, S. Williams, D. Rossouw and Miss S. Brand.

REFERENCES

BARTELS, J. and S. CHAPMAN 1940 Geomagnetism, Vol. II, second edition 1951, 545-605.

BLACKMAN, R. B. and J. W. TUKEY 1958 The measurement of power spectra, vii.

DIEMINGER, W., J. P. SCHÖDEL, G. SCHMIDT and G. K. HARTMANN 1970 Recording gravity waves by means of geostationary beacon satellites, J. Atmos. Terr. Physics, 32, 1615.

SANDSTRÖM, A. E. 1965 Cosmic Ray Physics.

"Magnetic Storm of March 8, 1970 at Onagawa Magnetic Observatory, Tohoku University"

by

T. Saito
Geophysical Institute
Tohoku University
Sendai, Japan

The following two figures were supplied by Dr. Saito. They are part of a paper in press, "Some Geomagnetic Characteristics of the Large Magnetic Storm on March 8, 1970" by T. Saito, T. Sakurai and A. Morioka, Report of Ionosphere and Space Research in Japan, 25, No. 1, 1971. The HISSA equipment is described in another paper in press, "High Speed Spectrum Analyzer (HISSA) for Geomagnetic Pulsation Study" by T. Saito and M. Kuwashima, Proceedings of the Third IASY Symposium, Institute of Space and Aeronautical Science, University of Tokyo, 1971.

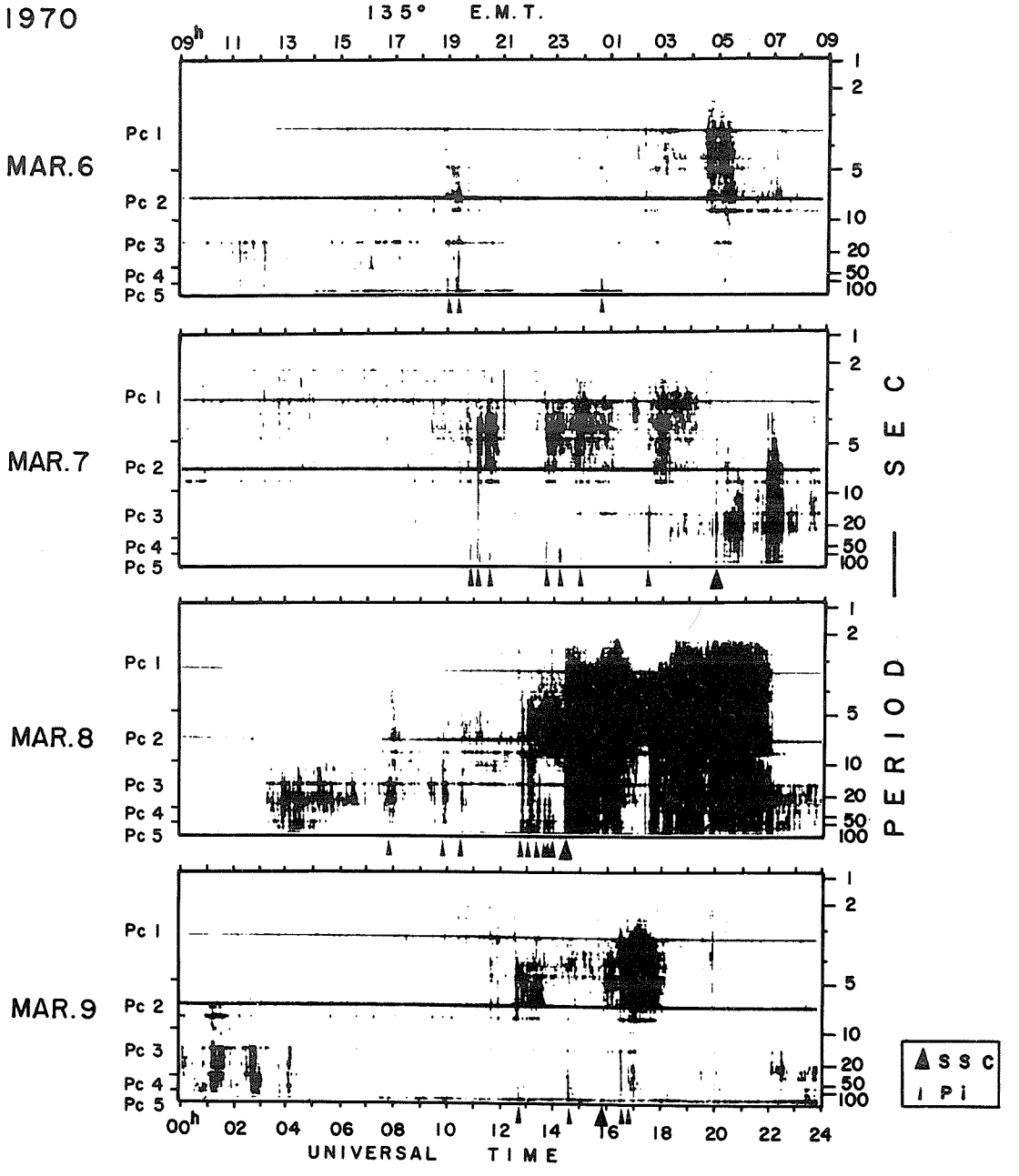

Fig. 1. Dynamic spectra (hissagrams) for March 6-9 obtained by HISSA. One hissagram sheet covering all frequencies Pc1 through Pc5 is obtained within 12 seconds.

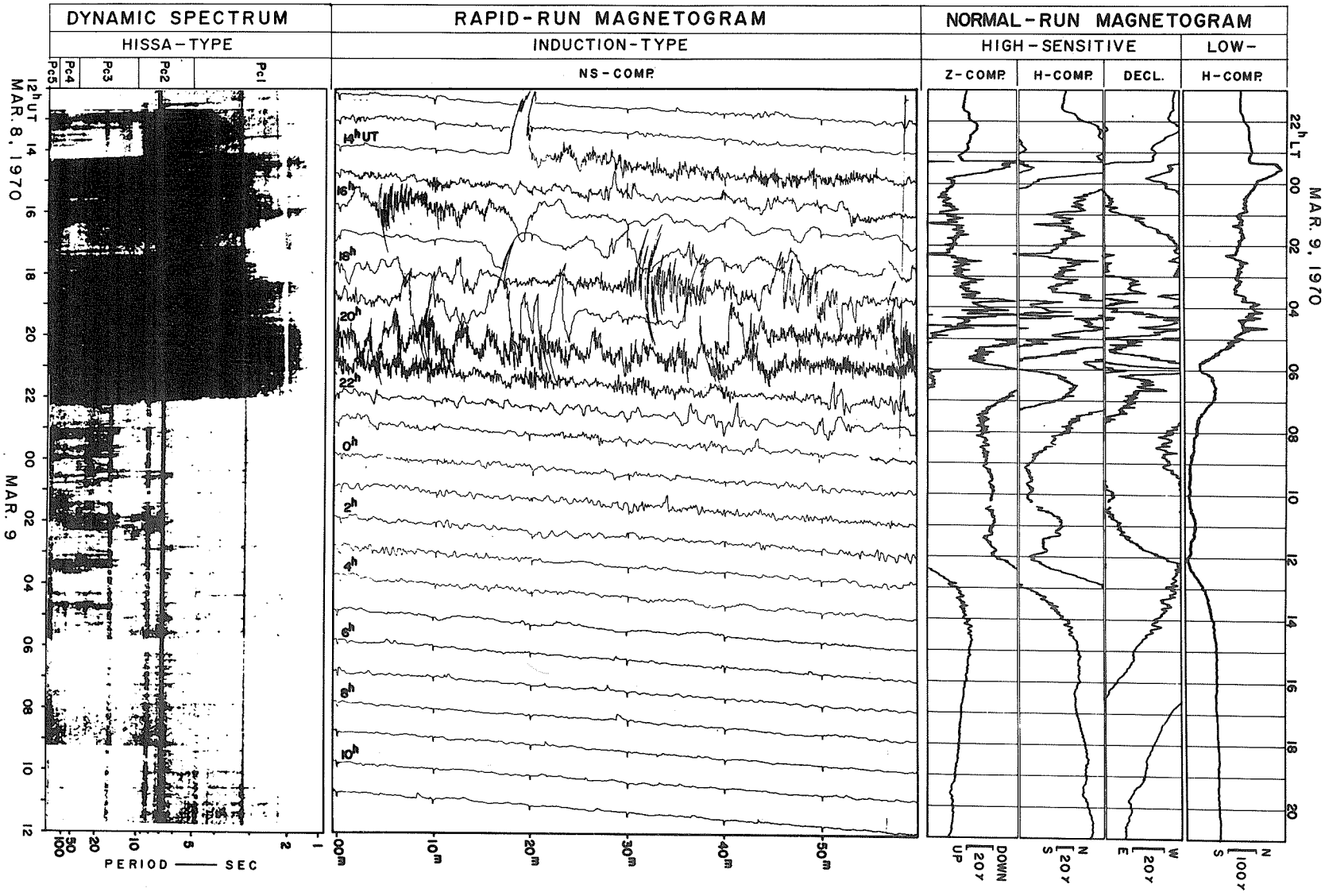

Fig. 2. The large March 8 magnetic storm recorded at the Onagawa Magnetic Observatory, Tohoku University, Japan.
(Top) Normal-run low- and high-sensitive magnetograms.
(Middle) Rapid-run induction magnetogram registered by a pen-writing helicoidal recorder.
(Bottom) Wide-range dynamic spectrum of geomagnetic pulsations.
ULF signals recorded on a magnetic tape was analyzed by a newly-designed high speed spectrum analyzer (HISSA).

"On the Sudden Commencement Magnetic Storm of March 8/9, 1970 at Ibadan"

by

Ebun Oni
Department of Physics
University of Ibadan

Figure 1 shows the Sudden Commencement Storm of March 8/9 1970. The SC occurs at 1418 UT. It has a short rise time of about 3 minutes. The magnitudes of SC (H, D, Z) are 65γ , 4.2 minutes and 20γ respectively. The period of the initial phase is short, about 20 minutes, while the periods of the main phase and recovery phase are 6 hours 40 minutes each. The record shows one rapid decay rate which means that the plasma is located lower down in the magnetosphere. The magnitude of the main phase is about 134γ. The rise time of 3 minutes for the SC is within a range of 3-6 minutes found by the author for most of the SC records observed during the first half of the IASY 1968/69. A paper on this analysis has been sent for publication elsewhere.

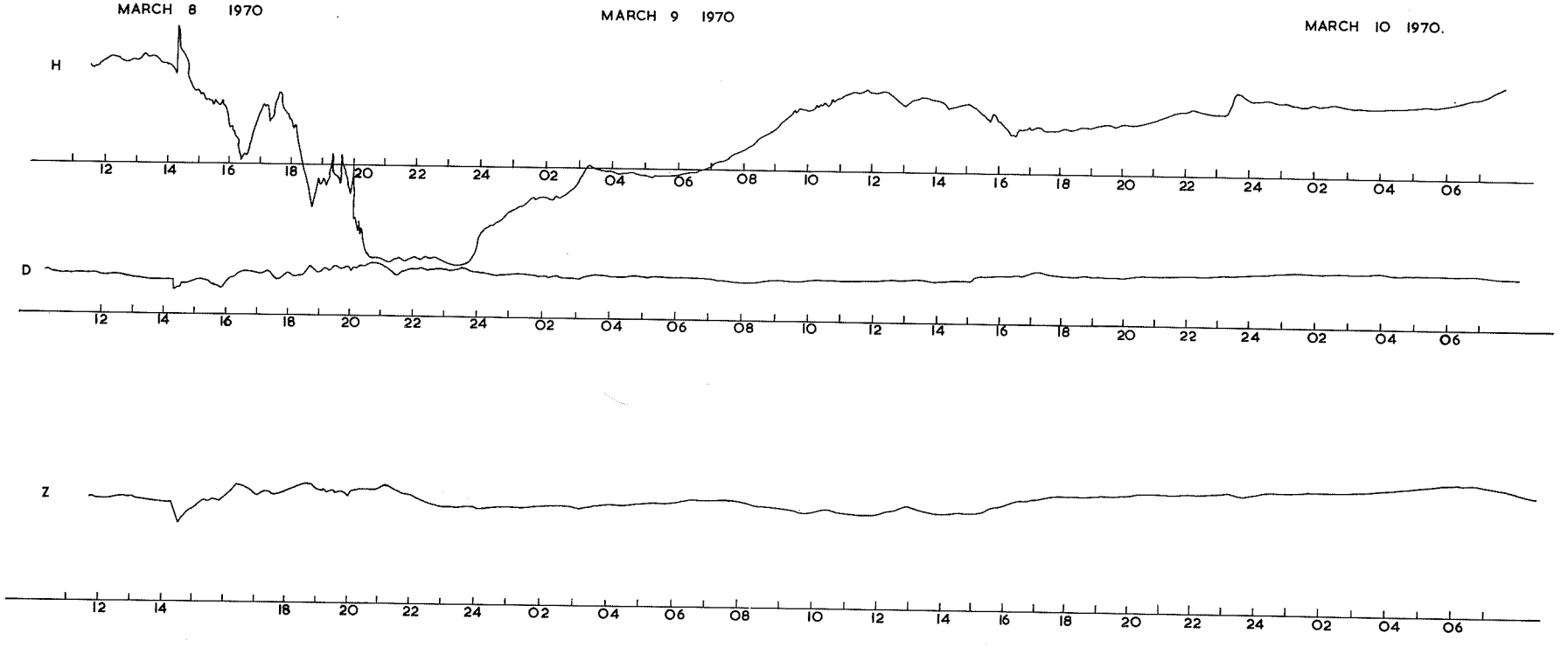

Fig. 1. H, D and Z components as observed at Ibadan March 8-10, 1970.

"Effect of the Equatorial Electrojet on the Sudden Commencement (sc) of the March 8, 1970 Storm"

by

O. Fambitakoye
O.R.S.T.O.M. - Services Scientifiques Centraux
70-74, Route d'Aulnay, 93 - Bondy, France

Distribution of Stations

A chain of stations recording normal variations of the earth's magnetic field have operated, since the beginning of 1968, in Africa in the neighborhood of the magnetic equator.

The beginning of this experiment was a concerted study of geomagnetism and equatorial aeronomy between the following French organizations: O.R.S.T.O.M. (Overseas Office of Scientific and Technical Research), I.P.G. (Institute of Physics of the World) and G.R.I. (Ionospheric Research Group). This experiment consisted of covering the region under the influence of the electrojet by five Askania variometers. Two stations, Largeau, north of this region, and Bangui, south of this region, serve as reference points. The map of Figure 1 indicates the geographic positions of the experiment, and Table 1 gives the geographic coordinates of the stations occupied.

Table 1

Stations Occupied During the Experiment

Station		Latitude	Longitude	Equipment
La	Largeau *	N17°56'	E19°06'	LACOUR
BO	Bol *	N13°28'	E14°43'	ASKANIA
Kn	Koundoul *	N11°58'	E15°09'	"
Mo	Mogroum	N11°07'	E15°25'	"
Bn	Bongor *	N10°17'	E15°23'	"
Ml	Miltou	N10°14'	E17°27'	"
Ga	Gayam	N09°19'	E17°54'	"
Pa	Pastor *	N09°12'	E18°21'	"
Kt	Kotongoro	N08°36'	E18°37'	"
Bc	Bouca *	N06°30'	E18°17'	"
Ba	Bangui *	N04°26'	E18°34'	LACOUR

The longitude band of interest is centered approximately on the 17°E meridian. The magnetic dip equator cuts this meridian at latitude N10°. The stations Miltou and Bongor, therefore, occupy the central position of the zone under the influence of the electrojet. The stations marked by an asterisk on Table 1, operating at the time of the storm, are the object of this note. It thus seems interesting to determine the diurnal amplification of the electrojet of the sc on the horizontal component.

Study of the sc

The storm began March 8, 1970 at 1418 UT (local time = UT + 1 hour 8 minutes).

The sudden commencement is an sc⁻ (ssc*) type. The duration is about two minutes.

The amplitude measurements have been made for the H-component. They have been placed as a function of station latitude on Figure 2(a) which shows a very clear amplification in the zone of the electrojet. The zero for latitude is taken as the equator of zero declination (N10° geographic).

For comparison, traced in Figure 2(b) are the amplitude values of an si at night (March 7 at 2004 UT, being 2112 in local time).

Finally to appreciate the effect of the electrojet, we have determined the value of the ratio of amplitudes of the sc at Bongor (100γ) and at Largeau and Bangui (55γ at the two stations); Largeau and Bangui are supposed to be outside the influence of the electrojet. This value is 1.8.

[Translated from the French text by one of the compilers.]

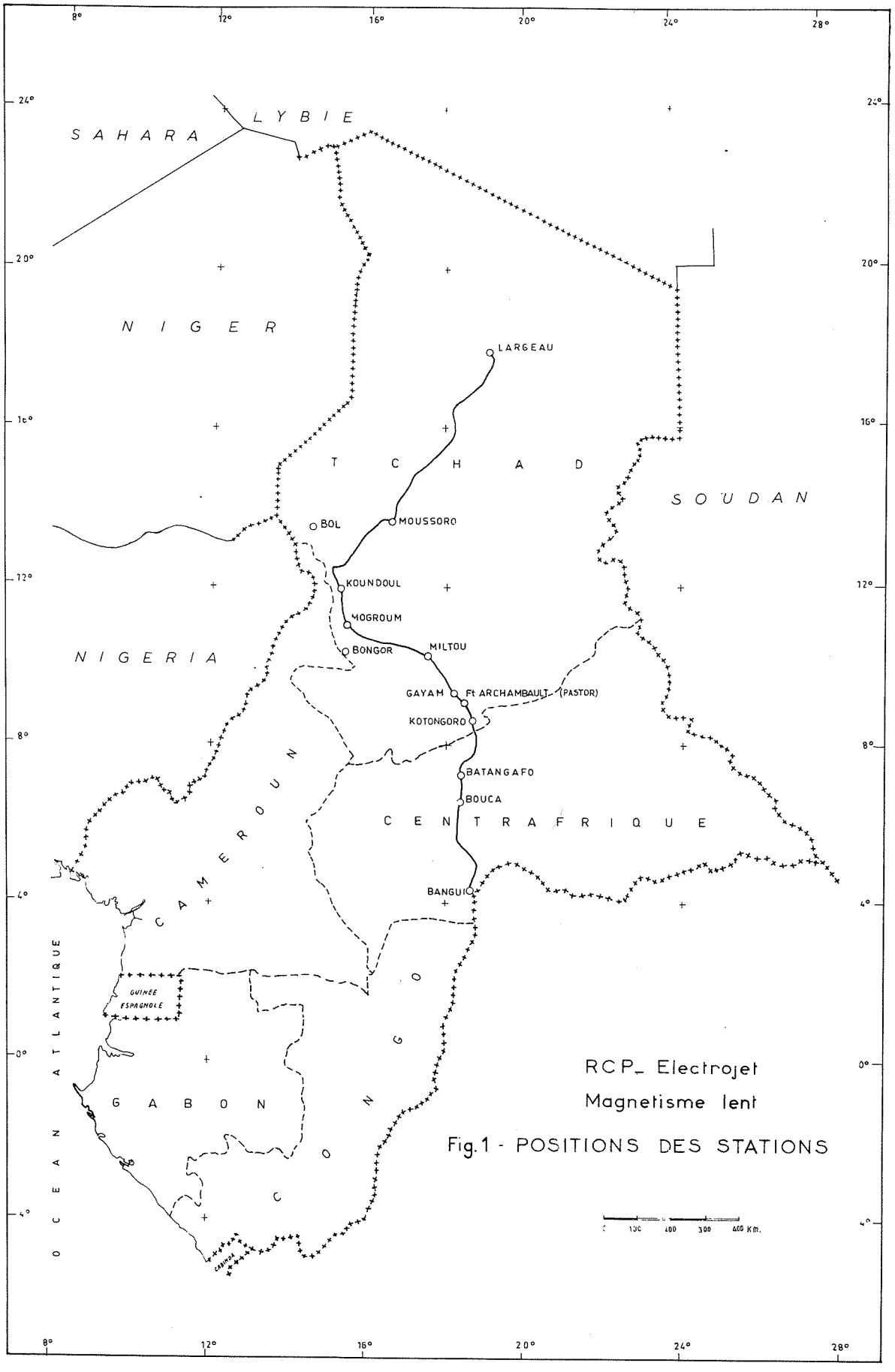

Fig. 1. Positions of the stations.

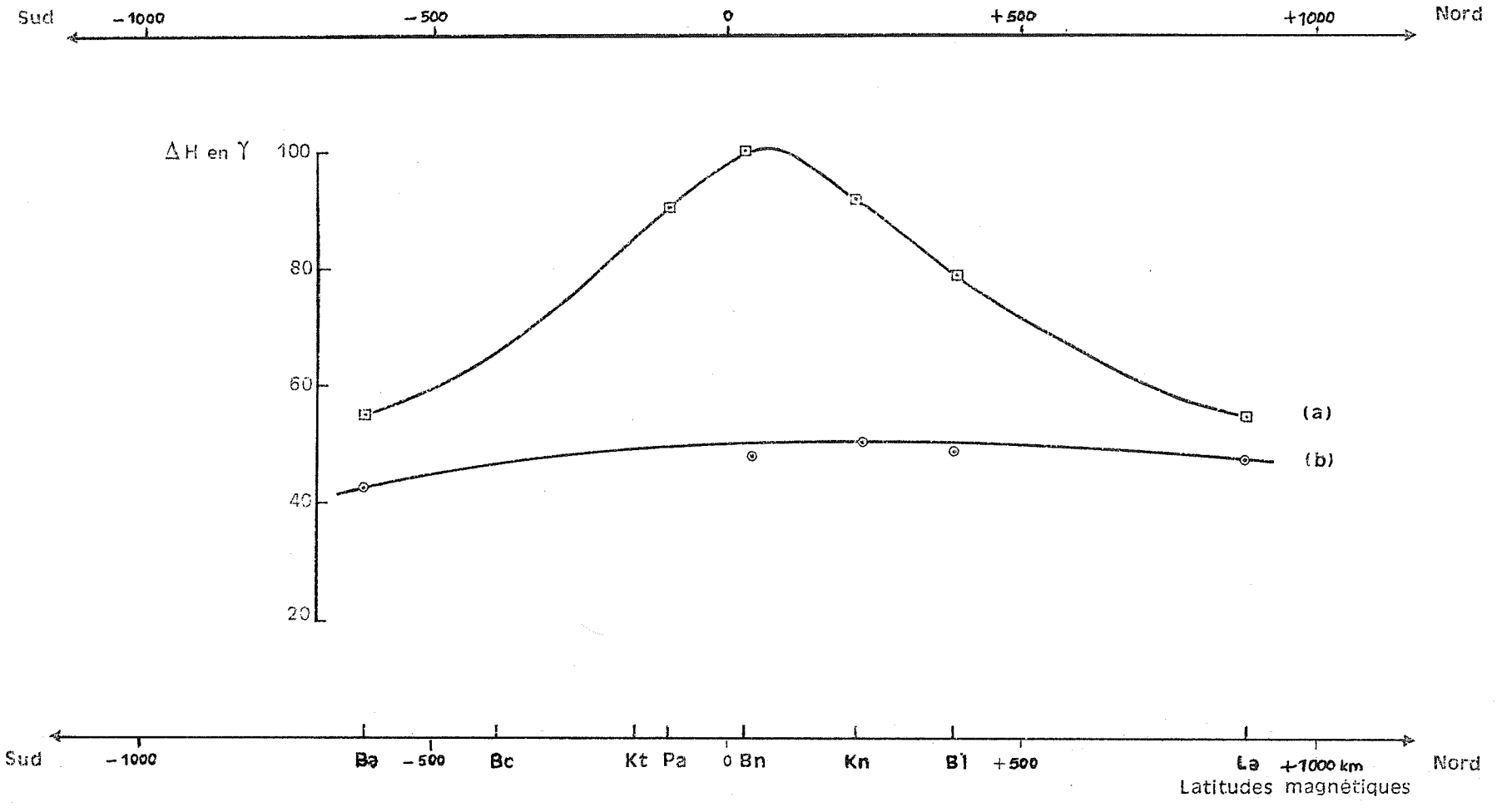

Fig. 2. Amplitude variation of sc of March 8, 1970 as a function of latitude.

"Magnetic Storm of March 8, 1970 near Magnetic Equator in Africa (Tchad and Ethiopia)"

by

J. Roquet
Institut de Physique du Globe
Universite de Paris

During the period we are considering (March 6-10, 1970) rapid run geomagnetic recordings (chart speed 6 mm/minute) (ULF: 1/5 to 1/200 Hz) were made in H and D at Addis-Ababa (Ethiopia) and Pastor (near Ft. Archambault, Tchad). These stations are located 60 and 105 km, respectively, to the south of the magnetic equator. Recordings of geomagnetic variations (chart speed 30 mm/minute) in the frequency band, 3 to 1/10 Hz, were made simultaneously at Pastor.

The geographic coordinates of the two stations are N9°02' E38°46' for Addis-Ababa and N9°12' E18°21' for Pastor. The Addis-Ababa station operates continuously under the Geophysical Observatory. The Pastor station, a temporary one, has been established for the study of rapid geomagnetic variations in correlation with the equatorial electrojet, a study made cooperatively by the Institut de Physique du Globe de Paris, Office de la Recherche Scientifique et Technique d'Outre-Mer and Centre National de la Recherche Scientifique (France).

From the magnetic point of view, the period March 6 to 10 has been marked principally by the storm of March 8; however, two phenomena preceding the storm are of note:

March 6

A series of pi 2, in H and D, with following characteristics occurred: three pi 2 of quality A, with sudden commencement (2208-2225, 2251-2256 and 2302-2312 UT), a pi 2 of quality C, with sudden commencement (2242-2249 UT) and a pi 2 of quality B (2316 UT March 6 to 0012 UT March 7). Pulsations of pi 1 type with periods $T \geq 10$ seconds accompanied these pi 2.

March 7

A first abrupt oscillation, in H and D, at 2004 UT has been followed by mean magnetic disturbance of the pi 1 type. Immediately after a second abrupt oscillation, which occurred at 2158 UT, a train of 7 oscillations appeared, very clear in H, less clear and of weaker amplitude in D (Figure 1). These oscillations have periods of 3 to 6 minutes, of the order of those of pc5. In H they were followed by oscillations of analogous periods, but less marked and of smaller amplitude. The sensitivity of the recording equipment for rapid geomagnetic variations is not known with precision for periods this large. From normal magnetograms at Pastor (Askania variometers - these magnetograms were put at our disposal by O. Fambitakoye) the peak-to-peak amplitude of the oscillations would have reached a maximum greater than 15γ in H and of the order of 6γ in D; in H the oscillations were superposed on large movements of longer duration, consequently their amplitude cannot be determined easily. Some pi 1 whose dominant periods range from 15 to 25 seconds, accompany the oscillations.

We give for comparison (Figure 2) the corresponding recording made at Garchy (France).

We recall that the pc5 registered at middle latitudes (for example at Chambon-la-Foret and Garcy in France) are rarely observed at equatorial latitudes (Addis-Ababa and Pastor in Africa), even for neighboring longitudes.

March 8 Storm

After a weak disturbance (irregular movements, pc3 and pc4) in the morning and at the beginning of the afternoon of March 8, a ssc has been recorded a little before 1418 UT ($14^h17^m45^s \pm 15$ seconds for our recordings).

It is remarkable that the disturbance due to the storm has ceased abruptly around 21 hours March 8. It was followed by pc3 then on the 9th by a mixture of pc3 and pc4.

Another characteristic fact in H and D is the succession of a dozen of these very abruptly, in the course of the storm between 1540 and 2010 UT. The microstructure of the storm in H and D between its sc and 21 hours UT comprises outside of large irregular movements, pi 1 whose dominant periods are spread out between 7 and 15 seconds from the sc to about 1630 UT, then between 10 and 25 seconds up to 2100 UT.

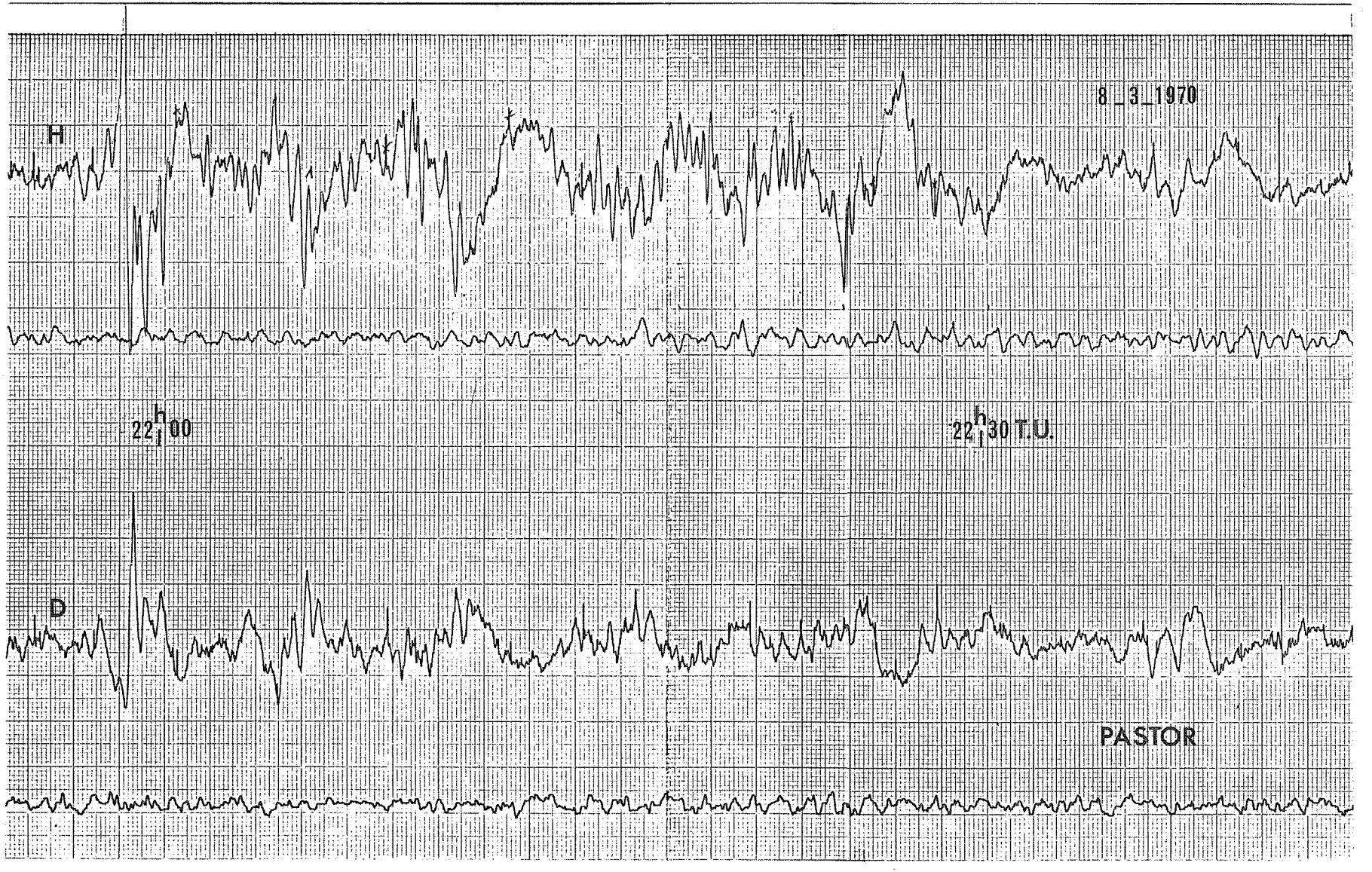

Fig. 1. Magnetogram at Pastor March 8, 1970.

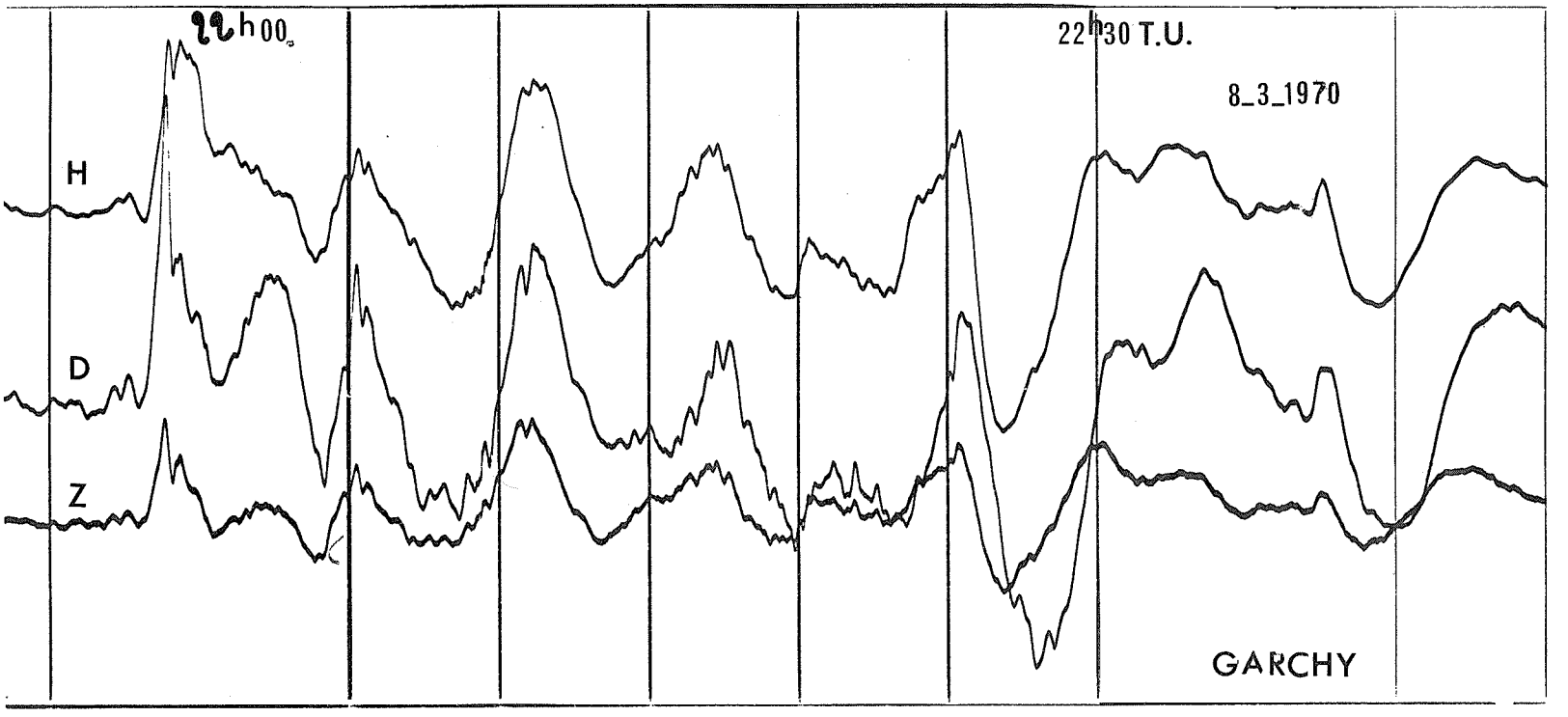

Fig. 2. The frequency response of the equipment is not the same at Garchy and at Pastor. In particular, at Pastor the sensitivity ought to be able to be reduced for periods greater than 1 minute, in order to calculate the amplification by the electrojet. The sense of the deviations corresponding to $\Delta H > 0$ are opposite at the two stations.

In conclusion, the storm of March 8 does not exhibit an exceptional character at the equator in the domain of rapid geomagnetic variations. On the contrary, the appearance even at low latitude on March 7 of a series of oscillations of long periods, similar to pc5, constitutes a fact which merits attention.

We thank Father Gouin, Director of the Geophysical Observatory, Addis-Ababa, for providing us with records of his station.

[Translated from the French by one of the compilers.]

"Explanation of the Origin of Geomagnetic Activity About the Time of the Storm of 8 March 1970 Based on the New Ideas of the Immediate Effects of Coronal Plasma"

by

Bohumila Bednářová-Nováková
Geophysical Institute
Czechoslovakia Academy of Sciences, Prague

As indicated in the title, this interpretation is based on the concept that the disturbances of the geomagnetic field are mediated directly by the coronal plasma [Bednářová-Nováková, 1966; Bednářová-Nováková and Halenka, 1969]. If a coronal formation is pointing towards the Earth, a geomagnetic disturbance or storm is generated. If no formation is pointing towards the Earth, a period of geomagnetic calm follows. These circumstances may be assessed indirectly by means of the observations of chromospheric activity [Bednářová-Nováková, 1961]. This is a procedure similar to that used in preparing forecasts of geomagnetic activity [Bednářová-Nováková, 1968].

In order to be able to point out the causes of the generation of storms, it is necessary to take into account the periods of geomagnetic calm as well. Only the concepts which are capable of explaining both alternatives are correct. The storm of 8 March 1970 offers a good opportunity for this purpose because the geomagnetic activity was very low for two rotations preceding it (see Figure 1). In the subsequent rotation intermediate activity prevailed, and a short decrease of geomagnetic activity, which was followed immediately by the storm, corresponded to the storm considered.

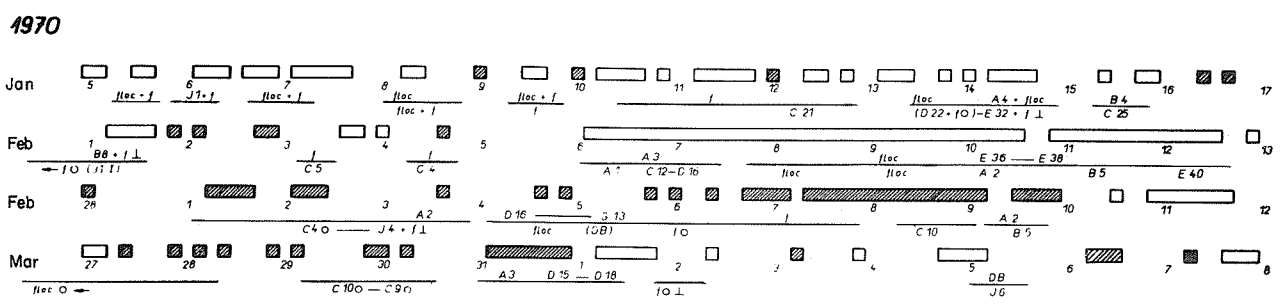

Fig. 1. Diagram of the retrospective interval at the time of the storm of March 8, 1970 (The investigation concerns rotations 1866, 1867, 1868 and 1869). The shaded areas indicate intervals with Kp max ≥ 4o, the white rectangles indicate intervals with Kp min ≤1o. The empty areas indicate average geomagnetic activity with Kp max <4o. For each rotation the passages of certain important regions of the Sun with spots, filaments and flocculae are shown.

As no observations of our own are available for this period, I used Freiburg solar maps and microfilms from the Photographic Atlas of the Sun, Rome. They were used to produce Figure 1 for which the magnetic characteristics from Göttingen were also used.

An analysis of the investigated interval was then made for several subsequent rotations. In the course of rotation 1866 between January 5 and 15, 1970, nearly all local solar fields were non-centrical, so that geomagnetic calm and short, small disturbances could have occurred after CMP in the shape of a minimum corona in a quite narrow profile. But the disturbance of January 16 was a result of the generation of a central coronal formation.

In the course of the subsequent rotation 1867, between February 1 and 12, geomagnetic calm prevailed on the whole, with the exception of small disturbances as on February 1 and 2, which followed the CMP of an unstable filament of January 31 and following the CMP of a meridional filament on February 1. These facts are evidence of the formation of a radial coronal flow above the center of the solar disk. The disturbance of February 3 and 4 was rather due to the CMP of the peak of a minimum corona above the center of the disk which corresponds to the CMP of the gap between the field around the spot group C5 to the N and the southern fields in a narrow profile (C5 and J1). This was followed by geomagnetic calm lasting up to February 12 as a result of the simultaneous and non-central CMP of a series of fields to the N and S.

During rotation 1868 the storm period between February 28 and March 10 with two sudden commencements on March 5 and 8 had the following causes: The disturbance of February 28 which had already begun by the end of February 27 was the result of the CMP of the belt of the minimum corona which, together with a meridional filament, was in the gap between north E28 and south G9. The geomagnetic activity of March 1 to 4 was the result of a central flow above a local field with C7 - J4. The vanishing of the meridional filament in the southern hemisphere and of a group of spots A2 with a filament in its field in the northern hemisphere is connected with the sudden commencement of March 5. The next disturbed interval can be explained as due to the CMP of an unstable flocculae field. On March 6 this was followed by the CMP of a long filament from the north, indicating a connection between the northern and southern hemispheres, and subsequently a group of spots C10 with a filament passed through the center. In both cases the field was unstable. The partial vanishing of the filament can be seen well by comparing the two photographs of 0650 UT, March 6 and 0812 UT, March 7 from the Photographic Atlas of the Sun No. 30, Rome (Rot 1558). This situation may be used to explain the sudden commencement of the geomagnetic storm of 1418 UT, March 8. The decrease in activity on March 11 is due to the simultaneous CMP of non-central local fields to the N and S. In these cases even if some coronal formations were generated above the active centers, they could not affect the Earth.

Under the assumption that no substantial changes occurred after the CMP of the western limb (February 28 - March 1), one could expect from the photographs made during the total eclipse of the Sun on March 7, 1970 at 1735 UT by the French expedition (L'Institut d'Astrophysique, M. Laffineur, S. Koutchmy) smaller disturbances to occur. They materialized on March 2 and 3 (Ap = 16 and 15). After the CMP of the eastern limb one would rather have expected geomagnetic calm, and this was actually the case on March 14 and 15 (Ap = 3 and 7).

Rot. 1869: An unstable floccular field, which vanished on March 27, appeared between the 25 and 26. A large filament at a higher heliographic latitude also vanished. The ssc followed subsequently on March 27. The CMP of the group of spots C10 on March 29-30 was followed by a magnetic storm on March 31. Immediately afterwards, on April 1, a decrease of geomagnetic activity could be observed after the CMP of A9 to the north. Until April 5 the geomagnetic activity was characterized by lower Kp-indices. Kp max only reached 5o after the CMP of J6 penetrating to the center of the disk on April 6. Therefore, all the disturbances between March 25 and April 7 were due to the formation of a coronal stream above the center of the disk.

As regards the storm of March 8, complete geomagnetic calm preceded it during the two foregoing rotations, and a short interval of geomagnetic calm followed in the subsequent rotation, on April 5; this was followed immediately by a storm on April 6. This was connected with the passage of a field, at first stable, later unstable, in a region of spots. Whereas the longer calm intervals in the two preceding rotations were due to the passage on non-central fields. In the latter case no coronal formation was pointing towards the Earth.

REFERENCES

BEDNÁŘOVÁ-NOVÁKOVÁ, B.	1961	Connection between Geomagnetic Storms in IGY and IGC and Occurrence of Some Kinds of Filaments, Studia Geoph. et Geod., 5, 138.
BEDNÁŘOVÁ-NOVÁKOVÁ, B.	1966	Solar Indicators of the Origin of Geomagnetic Storms, Travaux de l Inst. Geoph. de l Acad. Tchecosl. des Sci. No. 256, Geofysikalni sbornik, 477.
BEDNÁŘOVÁ-NOVÁKOVÁ, B.	1968	New Method of Forecasting Geomagnetic Activity Using Features of the Solar Corona, Nature, 220, No. 5164, 250.
BEDNÁŘOVÁ-NOVÁKOVÁ, B. and J. HALENKA	1969	A Universal Interpretation of the Generation of Geomagnetic Storms Using Features of the Solar Corona, Planet. Space Sci., 17, 1039.

"Geomagnetic Storm of March 8, 1970 and the Relevant Geomagnetic Activity"

by

Jaroslav Halenka
Geophysical Institute
Czechoslovakia Academy of Sciences, Prague

The analysis of Göttingen 27-day diagrams of Kp indices indicates that the geomagnetically disturbed interval of March 5 to 10, 1970, was due to a certain interval of heliographic longitudes, causing isolated geomagnetic disturbances in the course of many solar rotations. From this point of view the storms of March 23, May 14, September 27, 1969, and May 27 and August 16, 1970, are suspicious. All had ssc's beginning during an interval of ±1 day around the 24th day of the geomagnetic rotations on which the maximum of the disturbed interval of March 5 - 10, 1970 occurred.

The occurrence of three-hour intervals with Kp of at least 4o or over 5o were investigated in geomagnetic rotations 1853 - 1875, i.e. between January 4, 1969 to September 16, 1970. The intervals were summed up in columns corresponding to the 1st to 27th day of the rotations, and the sequence of sums was smoothed by three-day gliding averages with a view to an acceptable glide of ±1 day. The sequence of gliding averages with its median is given in the first and

Smoothed Number of Cases	Days in Geomagnetic Rotations Nr. 1853 - 1875																				SSC							Median
	1	2	3	4	5	6	7	8	9	10	11	12	13	14	15	16	17	18	19	20	21	22	23	24	25	26	27	
Kp ≥ 4o	20	12+	15	14-	12+	13	10+	11	8+	9	15+	22+	26+	21+	15	11+	11	13	15	13-	14+	16-	27-	28-	28-	23	20+	15
	20	12+	15	14-	12+	13	10+	11	8+	9	15+	22+	26+	21+	15	11+	11	13	15	12+	13	12	21-	21	23+	21+	20+	14-
																					storm values eliminated							
Kp > 5o	6	3+	2+	4-	3+	4-	2+	2+	1-	1+	5+	7-	9+	6	6-	2+	2-	1	3-	3-	3	4	12	15-	16-	11-	10-	4-
	6	3+	2+	4-	3+	4-	2+	2+	1-	1+	5+	7-	9+	6	6-	2+	2-	1	3-	3-	3-	3-	9	11	13	10-	10-	3+
																					storm values eliminated							
Kp < 1- Kp < 1o	3	3	3	4-	4+	5	5	5-	7-	7-	5+	2	2-	1+	1+	1-	2+	4-	5+	6+	7	6+	4+	4-	4-	4+	4-	4-

Table 1

second part of Table 1, the values differing by more than 25% or 50% from the median have been offset by one or two lines, respectively, from the basic line in the corresponding direction. Instead of expressing the thirds numerically, the symbols + or - were used following the corresponding lower or higher total value. Table 1 also shows the day of the beginning and of the maximum of the storm of March 8, 1970, and vertical lines divide the columns with the disturbed interval of March 5 to 10, 1970.

Clearly, there exist two marked periods of disturbance with abnormal occurrences of disturbed three-hour Kp intervals around the 13th and 24th - 25th days of the rotation. Of the two the larger is the second period which corresponds to the time of the disturbed period at the time of the storm of March 8, 1970. The nature of the sequence will not change substantially even if the values corresponding to the interval of March 5 - 10 are omitted; the second maximum remains the larger for Kp over 5o.

The distribution of marked decreases of geomagnetic activity, defined as a period of at least four subsequent values of Kp below 1- or (individually) below 1o, was treated analogously and given in the third part of Table 1. Two maxima, again exist, shifted into the interval of the onset of disturbed periods, but not into the intervals between them, which one might expect in the case of a random distribution of geomagnetic activity. A similar effect can frequently be observed in individual cases as a marked decrease of activity immediately preceding a geomagnetic storm.

The occurrence frequency of ssc's in the investigated period is too small to be able to yield clear-cut results under an analogous treatment.

"The Properties of Geomagnetic Pulsations at the Time of the Magnetic Storm of March 8th, 1970"

by

Karel Prikner and Jaroslav Stŕeštík
Geophysical Institute
Czechoslovak Academy of Sciences
Prague, Czechoslovakia

A Brief Description of the Magnetic Storm

The storm was recorded by a Mating-Wiesenberg instrument (ε_H = 4.45 γ/mm) at the observatory of Pruhonice (λ = 14° 32.8' E, ϕ = 49° 58.4' N). The storm, which began on March 8th at 1417 UT, was preceded by an sfe event at 0804 UT on March 5th and by disturbances of the nature of a weak storm with a gradual beginning throughout the whole of March 7th. Prior to the sharp ssc at 1417 UT on March 8th the field was comparatively calm. In the subsequent storm one could observe a transitive phase with pulsation activity, a main phase with a decrease in the H-component to minimum, and a recovery phase of the field. During the active phase the H-component of the field did not decrease below the normal on the average, and the Z-component displayed an increase. During this period microstructure was abundant. The H-component attained its second maximum following the ssc at 1920 UT; subsequently the main phase of the storm began to develop. The intensities of the H- and Z-components decreased and reached their minima simultaneously after 2100 UT. The activity of the microvariations decreased. Periods of 6 - 10 s prevailed in the active phase, and periods of 1 - 5 s (not pearls) began to predominate at the end of the main phase after 2000 UT. The microstructure grew weak after 2100 UT. The recovery phase began at 2230 UT on March 8th. The intensity of the H-component was permanently below normal to which it gradually returned. The recovery phase lasted for 3 - 4 days, and an increased activity of pc3 pulsations could be observed in it. A substantial part of the disturbance is shown in Figure 1; the values of all the components of the field throughout the storm are summarized in Table 1.

Pc3 Pulsations

The pc3 pulsations, being the most characteristic pulsations of the geomagnetic latitude considered, occurred throughout the whole of the storm as well as immediately before and after it. For analysis groups of these pulsations lasting for 8 min were selected at approximately hourly intervals during the period of their occurrence between March 5th and 16th, 1970. On the whole 96 groups were treated. The pulsations were recorded at the observatory of Budkov (λ = 14°01' E, ϕ = 49°04' N) by a core induction variometer with a scale value of the order of 0.1 γ/mm and a recording speed of 15 mm/min. A period vs. time (T-t) graph was obtained by measuring and plotting the pulsation periods observed. Besides, the average diurnal amplitudes of the pulsations were measured to yield an amplitude vs. time ($\bar{A}$-t) graph. Both the graphs are shown in Figure 2.

The pulsation frequencies observed on March 5th through to 16th indicate a close connection between the variations of the pc3 frequency response and the phases of the magnetic storm. The pulsation periods displayed the effect of a smaller disturbance in the magnetic field in the course of March 7th by increasing the scatter in the values of the periods observed ($\bar{T} \approx 21 - 31$ s). The scatter was very small during the period immediately preceding the storm, and the mean period was smaller ($\bar{T} \approx 24$ s). In the course of storm phase with pulsation activity the microstructure was so abundant, in particular as regards periods of less than 10 s, that it prevented the identification and simple measurement of the pc3 pulsations. They could again be investigated during the recovery phase of the field on March 9th. In this storm with a marked field expansion a clear and continuous increase of the pc3 pulsation periods could be observed during the first two days of the recovery phase, on March 9th and 10th (maximum value $\bar{T} \approx 39 - 41$ s). The record of March 11th was not available but its absence does not disrupt the results. The increase in period prevails until March 12th, and this agrees with our earlier observations [Prikner, 1968a]. On March 13th the mean values of the pulsation period decreased abruptly to values of $\bar{T} \approx 29 - 30$ s where it remained during the subsequent days, at least until March 16th. The values of the periods were still larger than prior to the storm.

The measurements of the average diurnal amplitudes of pc3 pulsation in the X-component showed that the amplitudes decreased continuously from 0.5 to 0.25γ during March 5th to 7th. On March 8th the amplitudes again increased to 0.5γ. The average amplitudes rapidly increased to 1.1γ at the time of the recovery phase. This increase also lasted throughout March 10th. In the subsequent days the amplitudes returned to within the limits of the standard, 0.3 - 0.5γ, as they were prior to the storm. As regards the Y-component the amplitudes of the pc3 pulsations were below 0.2γ before the storm, they increase to 0.3 - 0.4γ on March 9th and 10th, and beginning with March 12th they went back again to below 0.2γ. Therefore, the N-S direction prevailed in the oscillations of the pc3 pulsations, and this did not change in the course of the magnetic storm.

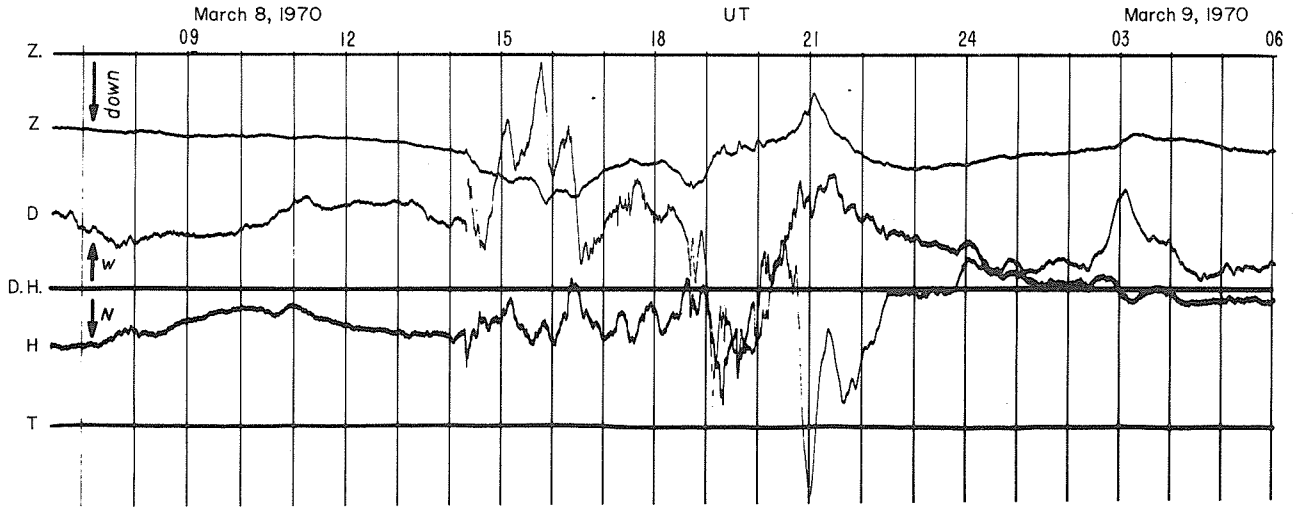

Fig. 1. Reproduced record of the Mating-Wiesenberg instrument (Pruhonice) for March 8-9, 1970.

Table 1

Values of the intensity of the magnetic field during the magnetic storm.

	pre-storm 1415 UT	maximum (+)	minimum 2105 UT	recovery phase 0600 9th		ssc	max in storm
H	19660γ	19768γ	19393γ	19604γ	ΔH	+62.3γ	375γ
Z	43380γ	43477γ	43268γ	43375γ	ΔZ	-7.35γ	209γ
D	0°38.4'W	---	---	0°30.8'W	ΔD	2.55'E 11.72'W	84.2'

(+) 1920 UT in H, 1552 UT in Z component

Interpretation

As regards the phenomena observed in the frequency response a similar interpretation to that of Rosser [1964] offers itself. A radial displacement of the limits of the radiation belts is assumed with a development of drift streams of particles at the end of the magnetic storm. With abating of the external disturbance factors (impingement of the stream of solar plasma) the current systems in the magnetosphere, in the regions where the plasma is trapped in radiation zones, have the possibility of developing in full. These currents simultaneously cause the decrease of the overall intensity of the field at the Earth's surface, and an increase of the field intensity at the magnetosphere boundary. As a result of the perturbing of the hydrostatic equilibrium of the pressures of the Earth's magnetic field and of the solar-wind plasma at the boundary of the magnetosphere, the latter is displaced further away from the Earth's surface. In accordance with previous conclusions [Prikner, 1968b] one may then consider the changes in the properties of the resonator in which the pc3 pulsations are generated. These processes will then be in direct relation to the changes of the frequency response of the pulsations in the course of the magnetic storm investigated.

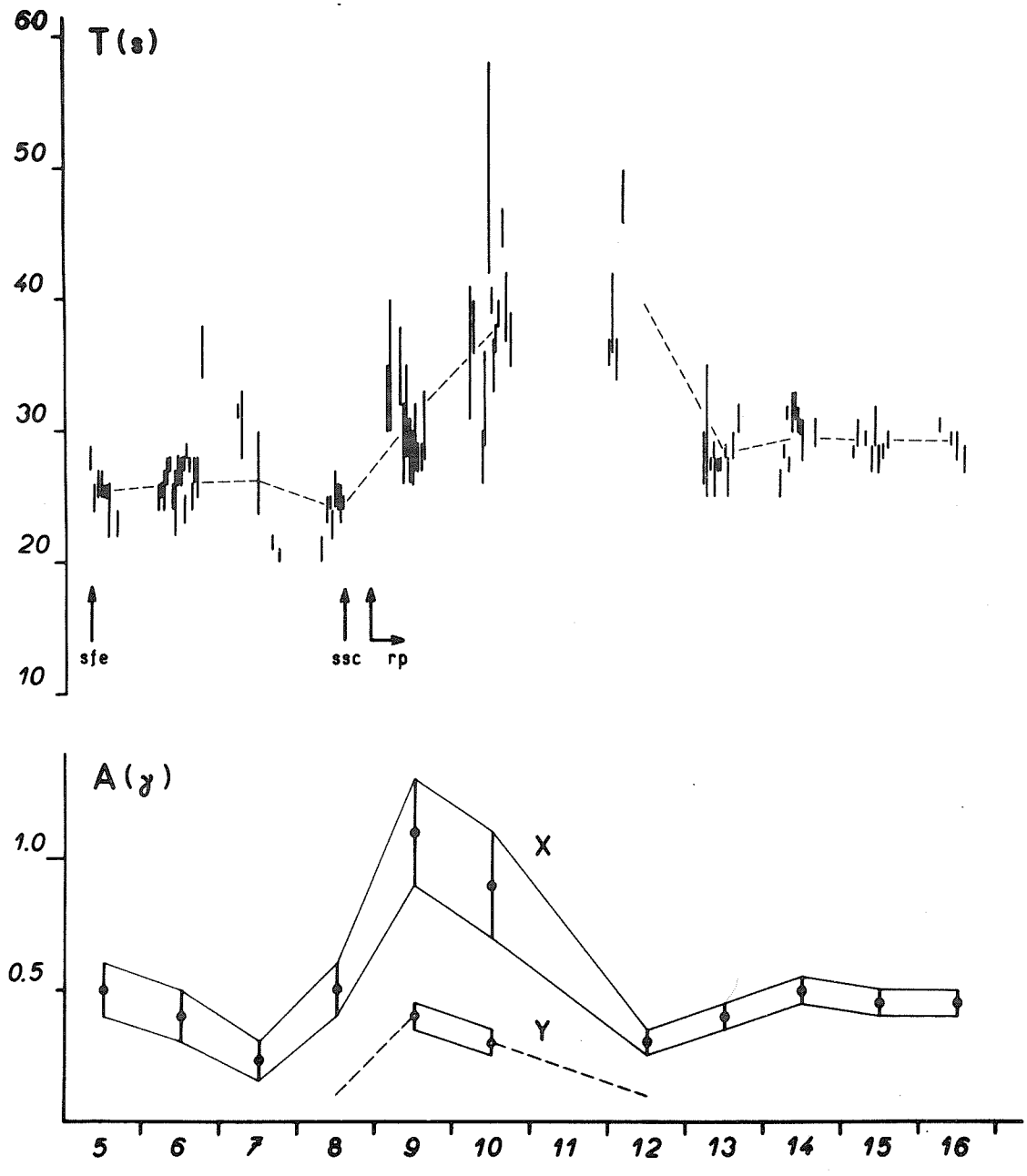

Fig. 2. Top: Periods of pc3 pulsation during the magnetic storm. The vertical lines indicate the interval of periods for a given group of pulsations. The dashed line shows the variation of mean diurnal periods. rp = recovery phase. Bottom: Variation of average diurnal amplitudes of pc3 pulsations in the X-component (black circles) and the Y-component (white circles). The vertical lines indicate the interval. The horizontal axis gives the days in March 1970.

REFERENCES

PRIKNER, K. 1968a — Pc Pulsations with Periods between 5 and 40 s (Ipc) during Geomagnetic Storms, Travaux de l'Inst. Geophys. Acad. Tchecosl. Sci., No. 280, Geofysikalni sbornik 1967, Academia, Praha

PRIKNER, K. 1968b — Resonance of a Plane HM-Wave in the Lower Magnetosphere and Pc Pulsations with Periods of 5 to 40 Seconds Occurring during Geomagnetic Storms, Studia Geoph. et Geod., 12, 224

ROSSER, W.G.V. 1964 — The Van Allen Radiation Zones, Contemporary Physics, 5, 198

"Some Geomagnetic Micropulsation Observations in Canada during the Period March 6-10, 1970"

by

R. J. Stening, J. C. Gupta and G. Jansen van Beek
Earth Physics Branch
Energy, Mines and Resources, Ottawa, Canada

Introduction

During the period March 6-10, 1970, geomagnetic micropulsations were recorded at a large number of Canadian stations. This period was of special interest because a world-wide magnetic storm occurred a few hours after the total eclipse of March 7. While many of these stations were operated primarily for the purpose of investigating effects related to the eclipse, they also provided an opportunity to compare micropulsations at widely separated locations during a time of intense magnetic activity.

The bulk of the observations in this report were obtained at the four stations listed in Table 1. The equipment has been described by Gupta et al., [1971]. The records at Ottawa and Meanook were being taken at maximum sensitivity during most of the period and so frequently were unreadable. Yet it was thought worth while to note some relative amplitude of micropulsations during this time of intense activity. In particular we examine amplitudes during the period of most intense activity when Kp reached a value of 9. Also a number of Pi's occurring in the March 6-10, 1970 interval are catalogued.

Table 1

Station	Geographic		Geomagnetic		Maximum sensitivity used (γ /mm)	
	Lat.	Long.	Lat.	Long.	H or X	D or Y
Ottawa	45.4°N	75.6°W	57.0°N	8.5°W	0.19	0.19
Meanook	54.6°N	113.3°W	61.9°N	59.3°W	0.55	0.50
Baker Lake	64.3°N	96.0°W	73.9°N	45.2°W	0.88	0.83
Resolute Bay	74.7°N	94.9°W	83.1°N	72.3°W	0.69	0.94

General Micropulsation Activity

A period of intense micropulsation activity commenced with the s.s.c. at 1418 UT on 8 March and ceased at ~2100 at all stations. The records were too disturbed and often overlapping during this time but some of the largest oscillations were selected in different period ranges and their amplitudes were measured (see Table 2).

Table 2

	8-12 sec	20-30 sec	60-120 sec
Ottawa	5γ	38γ	93γ
Meanook	5γ	21γ	>100γ
Baker Lake	2.6γ	9γ	24γ
Resolute Bay	10γ	15γ	104γ

Most striking are the comparatively low amplitudes at Baker Lake in all period ranges. The high amplitudes at Ottawa, particularly in the 20-30 second range indicate a southward shift of the site of maximum Pc3 amplitude. In the polar cap (Resolute Bay) the 8-12 second pulsations have their largest amplitude and the Pc4 amplitudes are also high.

Some typical micropulsation maximum amplitudes were measured for the hours before the s.s.c. and these are shown in Table 3 for purposes of comparison:

Table 3

Date	Time UT	Type	Ottawa	Meanook	Baker Lake	Resolute Bay
March 7	0800-1200	Pc3	1.7γ	8.3γ	1.9γ	0.8γ
		Pc4	3.6γ	14.0γ	6.8γ	1.4γ
	1500-1800	Pc3	0.8γ	5.5γ	1.7γ	2.1γ
		Pc4	1.2γ	7.5γ	7.2γ	4.7γ
March 8	0200-0400	Pc4	1.1γ	7.3γ	3.4γ	5.4γ

The first set of results (08-12 UT, March 7) are typical of the average latitude variation of amplitude. Meanook has the maximum amplitude for all the measurements but Baker Lake already has smaller amplitudes than Resolute Bay some hours before the s.s.c.

Pi Micropulsation Activity

In Table 4 some of the Pi events are listed which occurred at four Canadian observatories during the period March 6-10, 1970. It was not possible to isolate any Pi events occurring during the very disturbed period between the s.s.c. at 0418 UT on March 8 and 2100 UT on that day.

Table 4 Amplitudes and Periods of First Cycle of Pi Events

Date	UT	LMT (90°W)	Kp	Ottawa	Meanook	Baker Lake	Resolute Bay
March 6	0745	0145	3	1.7γ	12.0γ	2.1γ	--
				96sec	108sec	82sec	--
	0815	0215	3	2.0γ	25.9γ	2.9γ	3.5γ
				68sec	92sec	72sec	68sec
	1410	0810	2	1.8γ	6.8γ	--	--
				60sec	76sec	--	--
	1725	1125	3+	4.0γ	14.8γ	2.9γ	--
				120sec	80sec	69sec	--
	1741	1141	3+	1.5γ	19.2γ	4.6γ	5.7γ
				100sec	72sec	60sec	144sec
	1809	1209	4	3.3γ	14.6γ	0.9γ	0.7γ
				120sec	72sec	36sec	44sec
	1850	1250	4	2.8γ	13.5γ	1.7γ	0.9γ
				132sec	88sec	68sec	48sec
	1902	1302	4	3.1γ	14.1γ	1.7γ	2.2γ
				116sec	92sec	40sec	80sec
	2326	1726	6-	4.9γ	12.1γ	0.7γ	1.9γ
				76sec	66sec	42sec	80sec
	2335	1735	6-	9.9γ	23.6γ	1.1γ	--
				84sec	92sec	--	--
March 7	0207	2007	5+	6.9γ	6.5γ	--	--
				116sec	108sec	--	--
	0213	2013	5+	4.0γ	15.9γ	1.7γ	2.4γ
				48sec	68sec	40sec	40sec
	0242	2042	5+	9.5γ	4.1γ	64.9γ	7.5γ
				64sec	--	100sec	104sec
	0245	2045	5+	15.0γ	9.4γ	65.4γ	11.7γ
				124sec	70sec	60sec	148sec
	0750	0150	3	--	46.4γ	2.8γ	1.1γ
				--	72sec	80sec	--
	1820	1220	6-	11.1γ	6.0γ	--	--
				100sec	72sec	--	--
	1849	1249	6-	5.2γ	21.9γ	2.5γ	6.9γ
				88sec	72sec	30sec	42sec
	2003	1403	6-	>55.0γ	70.2γ	56.9γ	21.6γ
				64sec	100sec	100sec	48sec
	2337	1737	6-	3.6γ	45.2γ	2.5γ	7.3γ
				120sec	96sec	92sec	60sec
March 8	0330	2130	5	0.6γ	4.1γ	16.3γ	9.3γ
				44sec	134sec	68sec	104sec
	0403	2203	5	1.3γ	20.9γ	18.0γ	4.6γ
				84sec	136sec	80sec	76sec
March 9	1548	0948	6	27.7γ	>82.0γ	26.1γ	11.8γ
				100sec	132sec	128sec	56sec

Out of 22 events listed, 17 have their maximum amplitude at Meanook. And these occur at times exhibiting a variety of different Kp values. Twice the maximum falls at Ottawa and on both these occasions the Pi is not detectable at the two highest latitude stations. On three occasions the maximum amplitude is at Baker Lake and these are all during local night-time. On seven occasions the amplitude at Resolute Bay was found to exceed the amplitude at Baker Lake.

The Pi at 2003 UT on March 7 is notable for its high amplitude at all stations and particularly for its clear characteristic form at Resolute Bay. Usually Pi pulsations at Resolute Bay do not have the damped oscillations form even when this is present at lower latitude stations at the same time. The 2003 UT Pi accompanied a large SI which could be seen on all normal magnetograms in Canada.

The difference in period of the first cycle of the Pi at the four stations is erratic. Rarely is the same period found at all four stations. Sometimes the period is higher at the higher latitudes and sometimes at the lower latitudes. It is noticeable, however, that periods at two or three stations are often simple multiples of each other. At Meanook, sometimes the period of the H-component was twice the period of the D-component.

In summary it can be seen that there is no consistent behaviour of Pi amplitudes or periods which can be extracted from this data. The lack of clear systematic changes with the different Kp values is especially remarkable.

Pc5 Event March 6, 2100-2400 UT

	Geomagnetic		Maximum			
Station	Lat.	Long.	ΔH	ΔD	ΔZ	Period
Meanook	61.9	300.7	--	4.9γ	--	5 min.
The Pas	63.25	316.05	--	17γ	8γ	5 min.
Thompson	65.44	319.26	--	60γ	70γ	5.7 min.
Lynn Lake	66.04	314.38	30γ	55γ	36γ	5 min.
Great Whale River	66.8	347.2	41.4γ	56γ	98.5γ	5 min.
Fort Churchill	68.8	322.5	<5γ (doubtful same phenomenon)			1.5 min.

The small latitudunal extent of the event is characteristic of a "giant micropulsation" Pg. The event was not observed at Winnipeg (59.46°) and its presence is doubtful at Fort Churchill. Thus the latitudinal extent is less than 9°. The longitudinal extent is greater, more than 47°.

At Thompson and Great Whale River, where the amplitude is large, the Z component is the largest of the three components.

Acknowledgments

The authors are grateful to the members of the Geomagnetism Division who have assisted with technical help. They express sincere thanks to Drs. E. R. Niblett and P. H. Serson for helpful discussions. One (RJS) acknowledges a Postdoctorate Fellowship from the National Research Council of Canada.

REFERENCES

GUPTA, J. C., R. J. STENING and G. JANSEN van BEEK 1971 A study of micropulsations in the Pc3,4 period range at four Canadian observatories, J. Geophys. Res. (in press).

15. INTERPLANETARY MAGNETIC FIELD

"The Distant Interplanetary Magnetic Field Measured by Pioneer 8 during the Period March 1 to 15, 1970"

by

B. Bavassano - F. Mariani
Laboratorio Plasma nello Spazio
Consiglio Nazionale delle Ricerche
Istituto di Fisica dell'Universita
Roma - Italia
and
N. F. Ness
NASA - Goddard Space Flight Center
Greenbelt, Maryland-USA

In the time interval from March 1 to 15, 1970 the Pioneer 8 space probe was on its heliocentric orbit East of the Sun-Earth line at an angular distance of about 50 degrees: the geometry of the orbit is shown in Figure 1.

The average time interval between each field value is about 7 seconds. Each vector component is the average of four consecutive measurements computed on board the spacecraft by a special computer, the Time-Average Unit. The time coverage was about 17 hours per day; for the days March 9 and 10 no data are available at the present time; however about 50% of these data will be available in the near future.

Hourly averages of the field elements are shown in Figure 2. More details are shown in Figures 3 and 4: the main feature of the measurement is the high level of the field initiated between 1930 UT on March 4 and 0230 UT on March 5 and lasting more than one full day until approximately 1700 UT on March 6. A steep discontinuity in the field magnitude is also observed at 0937 UT on March 5.

The definitions of the values plotted are as follows:

$\overline{F}$, the average field computed by the averages $\overline{x}$, $\overline{y}$, $\overline{z}$ of the field components

$\overline{\overline{F}}$, the average field magnitude computed by the individual field magnitudes. According to their definitions $\overline{\overline{F}}$ is always greater or equal to $\overline{F}$

θ and ϕ, i.e. the inclination (+ north, - south) and the azimuth of the field vector on the ecliptic plane (0° towards Sun, 90° east and 180° away from Sun).

Also the variances are given, according to the following definition

$$D = \left\{ \frac{1}{n} \sum_{i=1}^{n} \left[(x_i - \overline{x})^2 + (y_i - \overline{y})^2 + (z_i - \overline{z})^2 \right] \right\}^{\frac{1}{2}}$$

where x_i, y_i, z_i are individual values of the three field components.

D 1, the same as D computed on hourly averages

D 2, the hourly average of the 30 sec. variance D

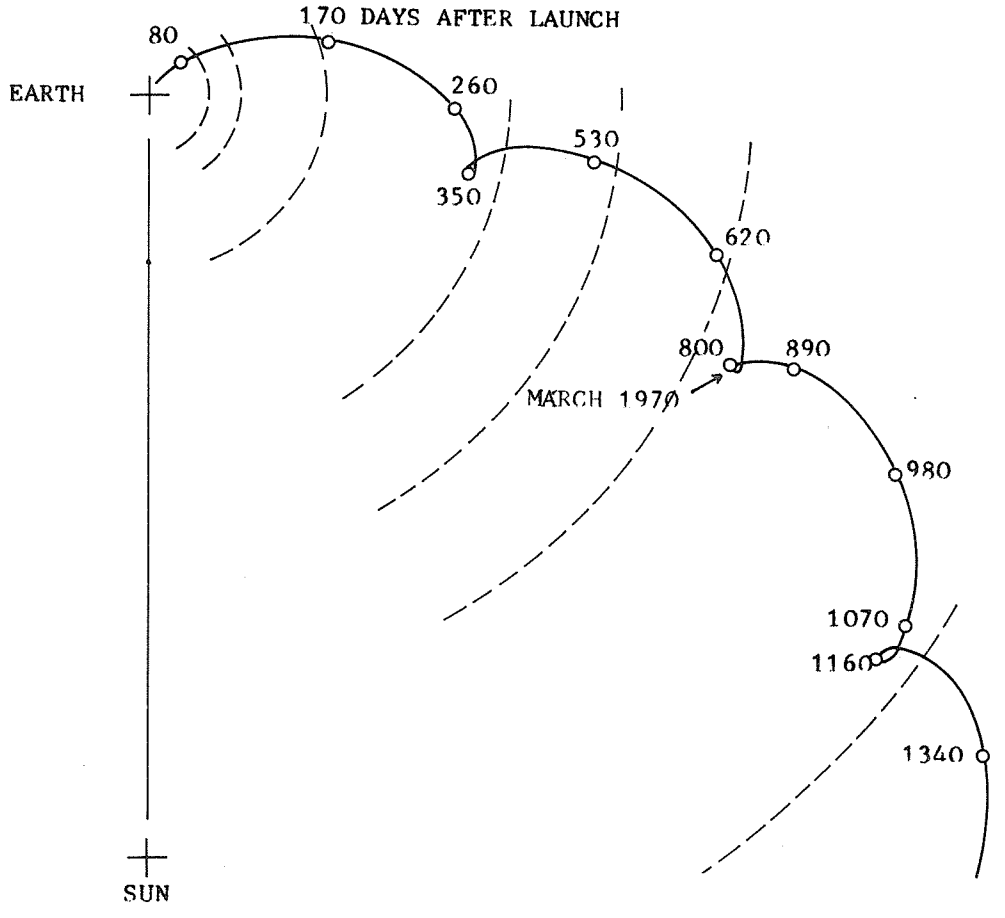

Figure 1. The trajectory of Pioneer 8 on the ecliptic plane, referred to the Sun-Earth line.

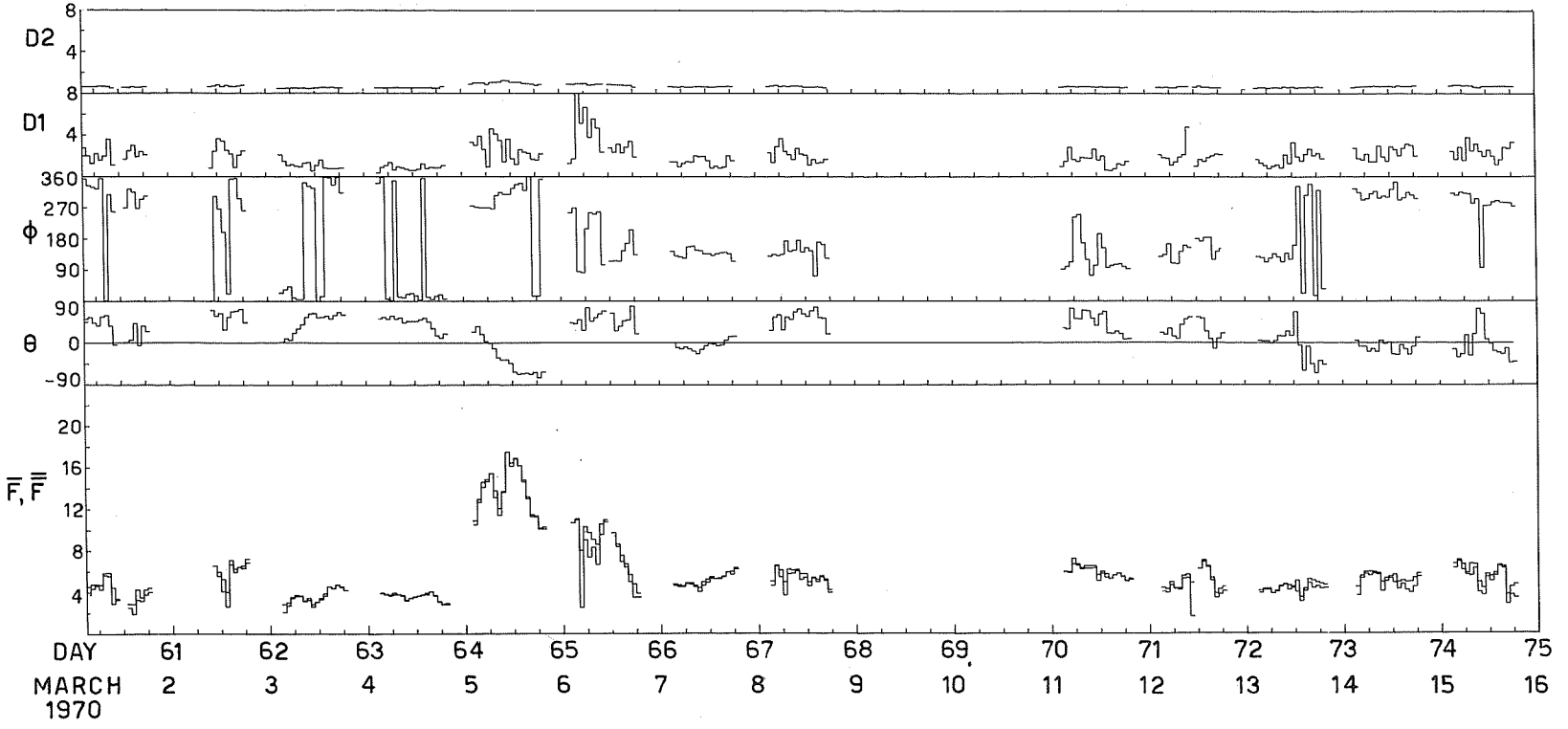

Figure 2. Hourly average field magnitude ($\bar{F}$, $\bar{\bar{F}}$), orientation (θ, ϕ) and variances D 1 and D 2. Magnitude and variances are in gammas; angles in degrees. The time is given as day of year (1st of January = day 1) and calendar day.

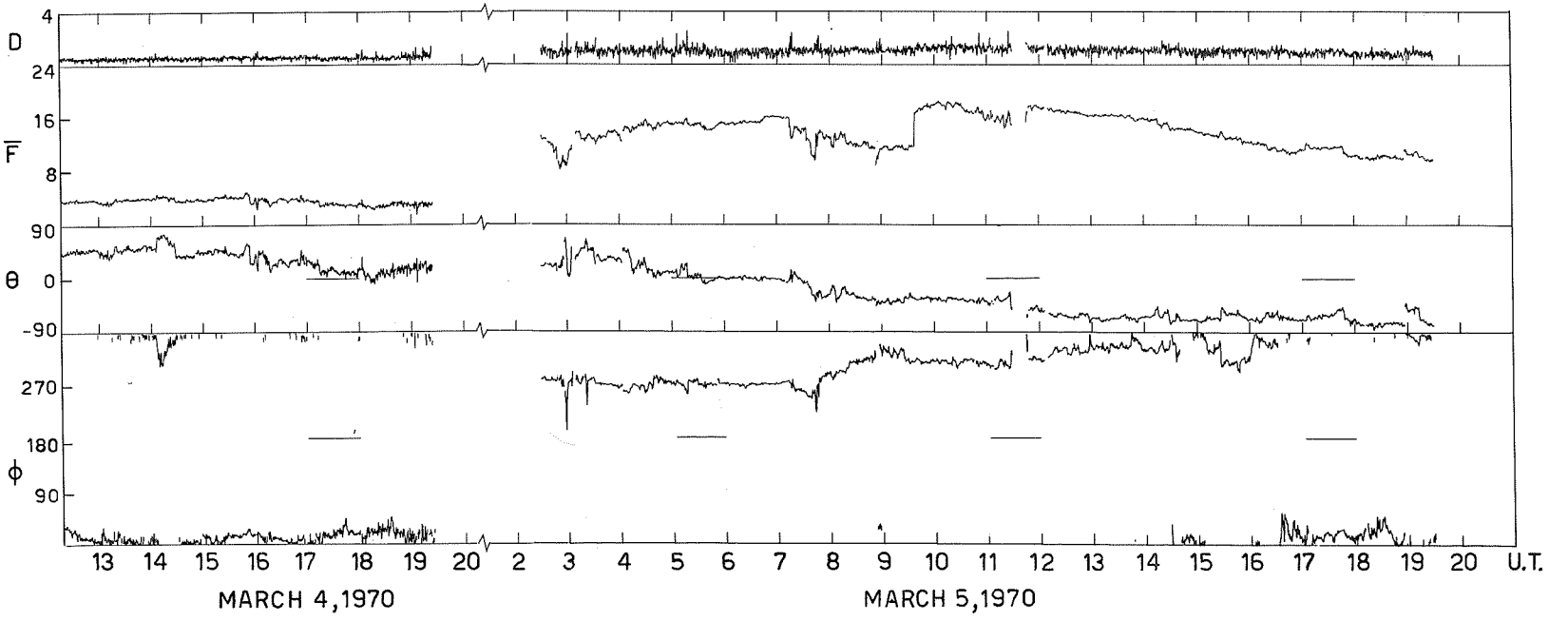

Figure 3. Thirty-sec average field magnitude ($\bar{F}$), orientation (θ, ϕ) and variance D. The time is given in hours. The gap in the data between 2000 UT March 4 and 0200 UT March 5 has to be noticed.

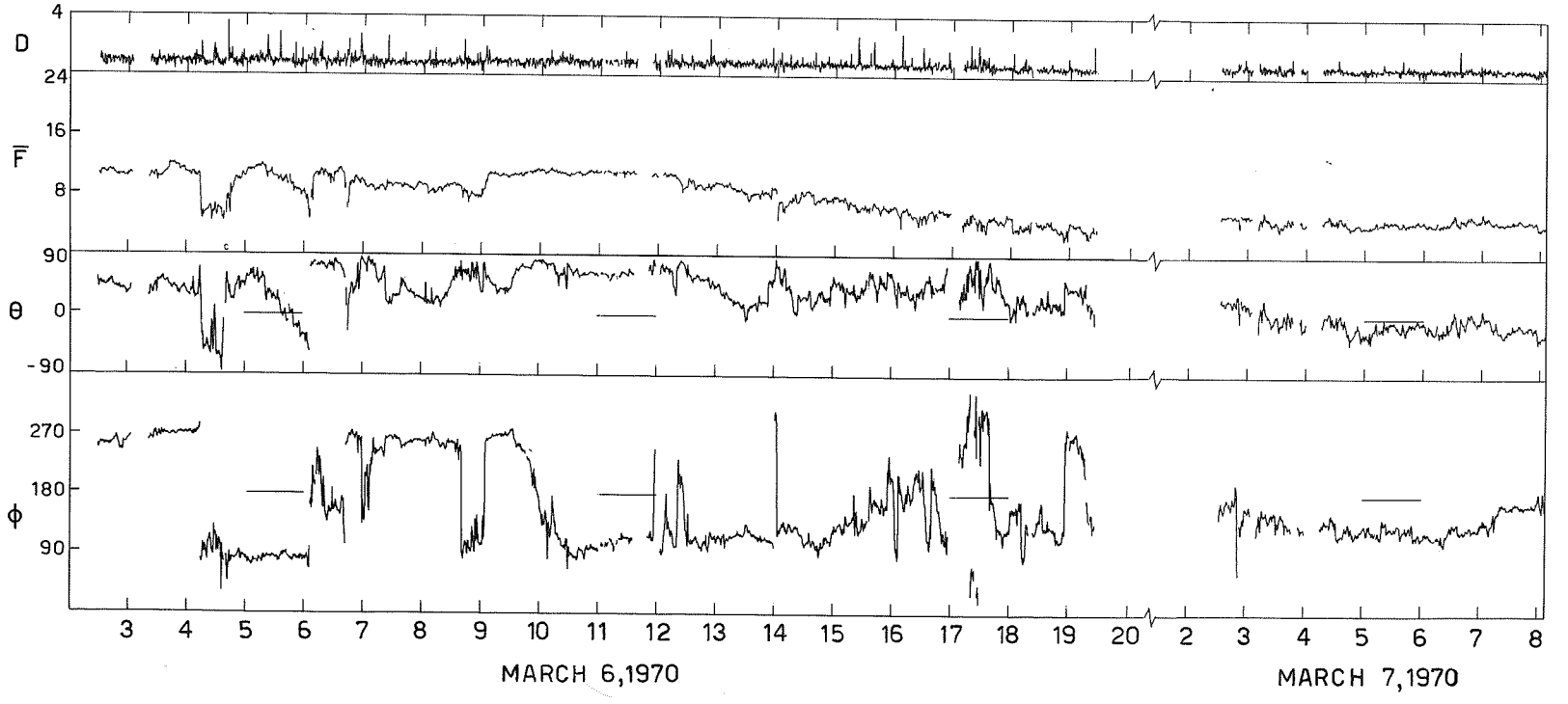

Figure 4. Thirty-sec average field magnitude ($\bar{F}$), orientation (θ, ϕ) and variance D for March 6 and 7,. The time is given in hours.

APPENDIX. ECLIPSE.

"Mauna Loa Coronagraph Observations Around the 7 March 1970 Eclipse"

by

Richard T. Hansen, Shirley F. Hansen and Charles J. Garcia

A paper with the above title has been published in Solar Physics, 15, 387, 1970. Synoptic K-coronagraph observations made at Mauna Loa, Hawaii, are used to identify the locations of seven principal coronal features at the time of the eclipse.

"Comparison of Prediction with Observation of Coronal Structure at the March 7, 1970 Solar Eclipse"

by

Sheldon M. Smith
NASA-Ames Research Center

and

Kenneth H. Schatten
NASA-Goddard Space Flight Center

This is a summary of papers recently published in Nature (see References).

The structure of the corona predicted by Kenneth Schatten [1970] for the March 7, 1970 eclipse was compared in an article in Nature with the structure photographed by Sheldon Smith and Leonard Weinstein [1970]. The major points of agreement and disagreement were tabulated and a modification of the technique for calculation of coronal magnetic fields above active regions was suggested. In summary, the predominantly open structure of the predicted corona was considered to be in agreement on a large scale basis with the maximum corona observed. The largest single structure apparent at the eclipse was accurately forecast. Detailed agreement of intermediate size features is less certain.

The photograph of the corona shown in Figure 1 is the result of a superposition of four negatives exposed at different times during the eclipse which causes the lunar limb to appear multiple in the west and northeast. Otherwise, the techniques used to produce Figure 1 are the same as described elsewhere [Smith and Schatten, 1970] [Smith, Henderson and Torrey, 1967]. Figure 2 indicates the structure of the corona predicted [Schatten, 1970] to appear at the March 7 eclipse. The reader is referred to the original article [Smith and Schatten, 1970] for a quantitative tabulation of the heliographic position angles of the predicted and observed coronal structures.

REFERENCES

SCHATTEN, K. H. 1970 Preliminary Comparison of Predicted and Observed Structure of the Solar Corona at the Eclipse of March 7, 1970, Nature, 226, 251.

SMITH, S. M. and K. H. SCHATTEN 1970 Preliminary Comparison of Predicted and Observed Structure of the Solar Corona at the Eclipse of March 7, 1970, Nature, 226, 1130

SMITH, S. M., M. E. HENDERSON and R. A. TORREY 1967 NASA TN D-4012.

A70-16l0-5-5

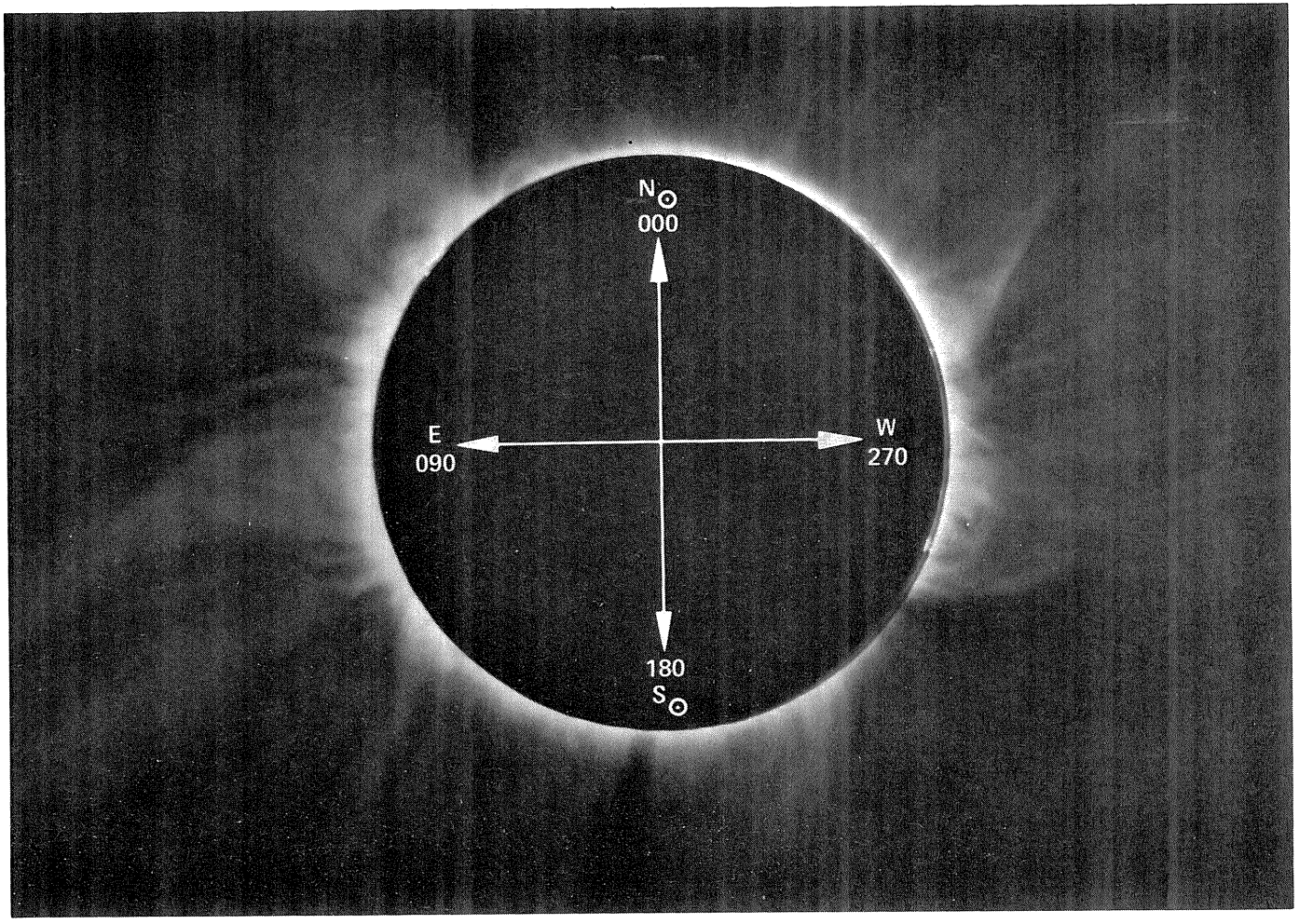

Fig. 1. The solar corona at 1841:59 UT on March 7, 1970. A radial transmission filter was employed to reduce the steep gradient of coronal brightness on this 2 s exposure. The Fluor-O-Dodge printer was also used to increase latitude in the reproduction process. A double reflection exists at the east edge.

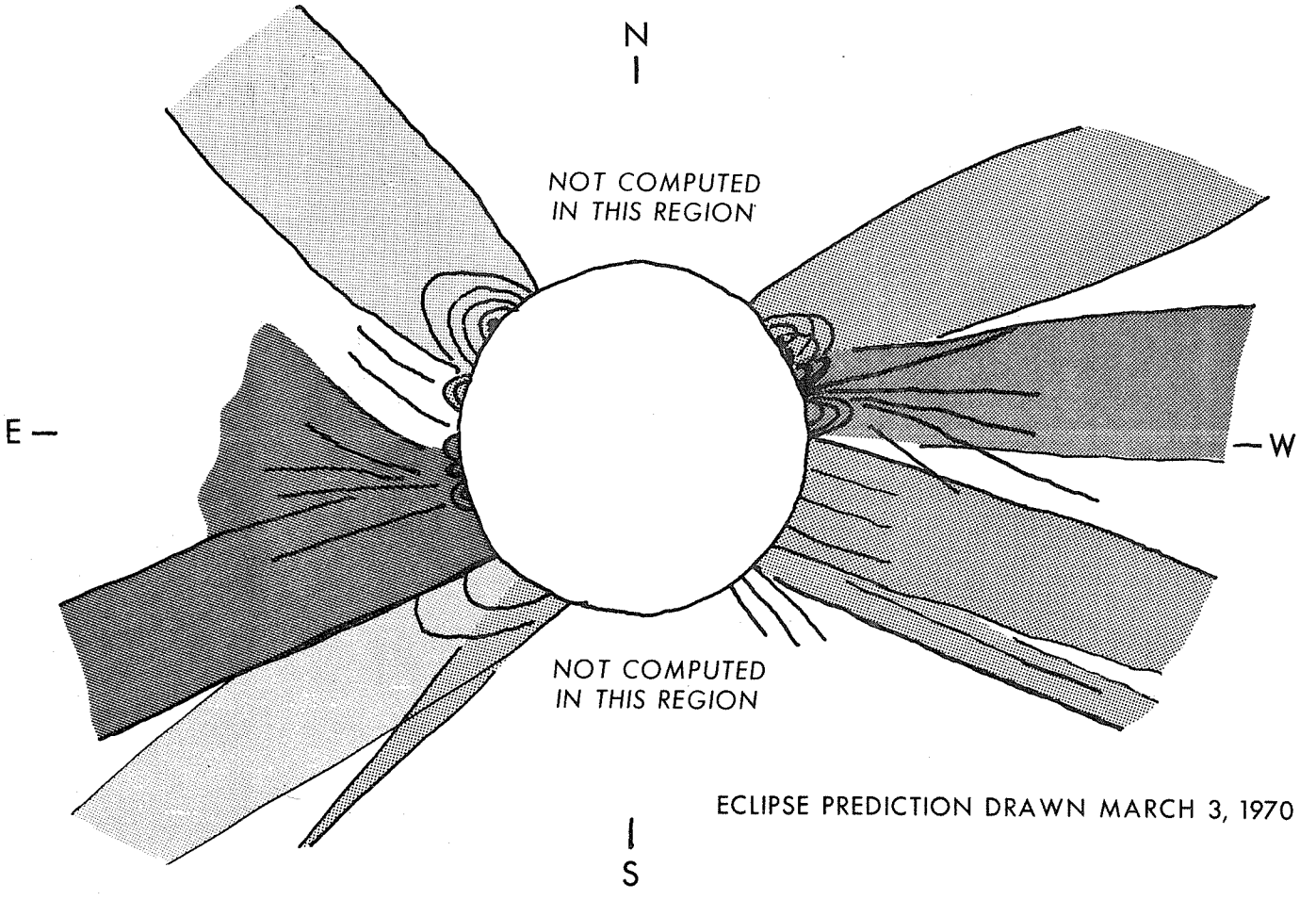

Fig. 2. The structure of the solar corona predicted for March 7, 1970.

"Observation of March 7, 1970 Solar Eclipse from OSO-5 in Far UV"

by

R. Parker and W. A. Rense
Laboratory for Atmospheric and Space Physics
University of Colorado
Boulder, Colorado 80302

Introduction

The solar eclipse of March 7, 1970, was observed by instruments in OSO-5 as a partial eclipse. First contact occurred between 1608 and 1609 UT; last contact, just after 1634 UT; and maximum phase at about 1626 UT. At the latter time, 87.84% of the area of the solar disk was covered by the moon. This report concerns data obtained during the eclipse with the University of Colorado calibrated ultraviolet spectrophotometer mounted in the wheel of OSO-5. The instrument utilizes a grating set at grazing incidence for dispersing the solar UV radiation. Radiation from the entire solar disk in three spectral bands is monitored by Bendix resistance strip photomultipliers; the spectral ranges are 280 - 370 Å (channel 1), 465 - 630 Å (channel 2) and 760 - 1030 Å (channel 3). The intensities of the three channels are measured once every two seconds, the period of the rotating wheel. The spectrophotometer data consist of photon flux counts over 30 milliseconds for each wheel rotation, for each channel, and can be converted into relative intensities. The instrument was turned on at the beginning of the eclipse, and data were obtained until shortly after maximum obscuration of the sun by the moon. Noise is present in the data, especially for channels 1 and 2, and the computed intensities at the beginning of the eclipse are affected by turn-on transients in photomultiplier behavior. Except in regions of obvious noise, the relative intensities are accurate to about 2% in any channel.

Intensity changes during the eclipse

The solid line curves of Figure 1 show for each channel, respectively, the variation of relative intensity as a function of time during the eclipse. The dashed curves outline the hypothetical intensity variations if the sun's visible disk were uniformly bright in the three spectral ranges (proportional to area of visible solar disk exposed). Most of the irregularities in the curves are attributed to noise. These effects are greater in channels 1 and 2. However, there are two time intervals (shown by arrow pairs in the figures) during which the intensity drops at a rate greater than that which the areal rate would indicate. For channels 1 and 2 these occur at times between 1618:30 and 1618:56 UT, and 1622:03 and 1623:00 UT, respectively, the times being the same for each channel. The second of these is duplicated in channel 3, but the first appears to be of longer duration in that channel.

Around the time of maximum obscuration of the moon, channels 1 and 2 are clearly brighter than would be the case were the emissions uniform over the sun's visible disk, as is shown by the fact that the areal curve falls well below the observed curve in each case. On the other hand, for channel 3, there is fair agreement between the observed curve and the areal curve in this region.

Discussion of results

For channels 1 and 2 (Figure 1), the deviations of the general features of the observed curves from the areal curves may be explained if one assumes limb-brightening in the emissions corresponding, respectively, to the two wavelength bands. Limb brightening for some of these wavelengths has been previously observed [see, for example page 33, Report to COSPAR, Thirteenth Meeting, Leningrad, USSR, May, 1970].

A rough quantitative estimate of the limb-brightening was made by fitting to the observed data a curve having the following equation:

$$I_\ell L + I_A A = I_o$$

Here I_ℓ represents the limb-brightening contribution, I_A the areal brightness contribution, L the perimeter of the solar disk exposed at any time, and A the area of the solar disc exposed at that time. The quantity, I_o, is the expected observed intensity. I_ℓ and I_A are taken to be constants (uniform distribution of both peripheral and areal brightness). For convenience, the uniform intensity source of limb-brightening was assumed to be located in a very narrow band around the circumference of the solar disk. The constant I_ℓ and I_A were obtained for each channel, respectively, by normalizing the equation to two points of each of the observed eclipse intensity curves. The equation was then used to predict the intensity changes during the eclipse as a function of time. The results for several times are shown by the small crosses on the curves of channel 1 and channel 2 in Figure 1. For channel 3 the value of I_ℓ is essentially zero, so that no limb-brightening is required, within the errors of observation, to explain the measured intensity variation.

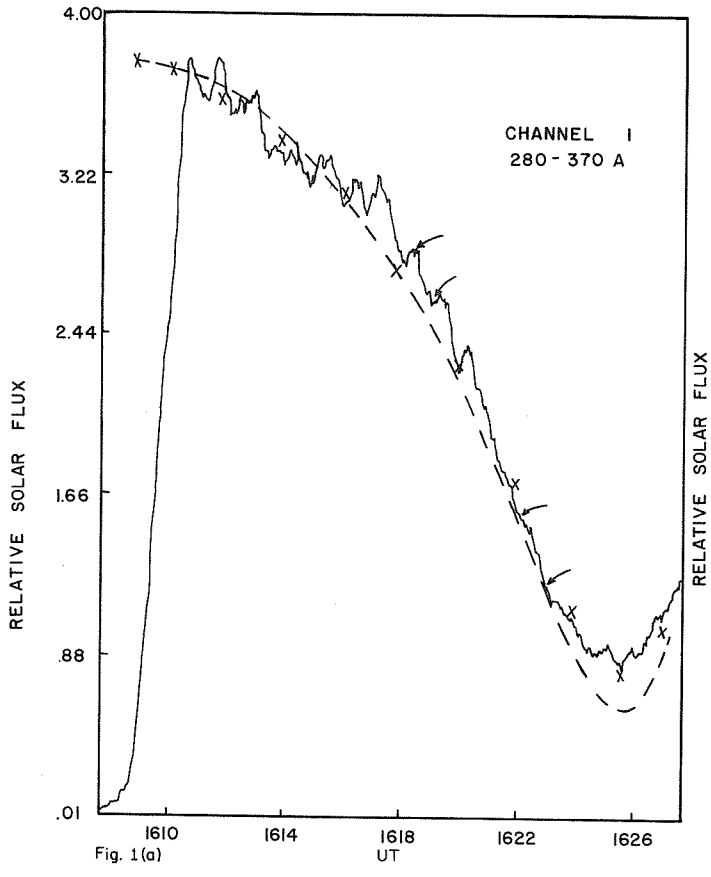

Fig. 1(a)

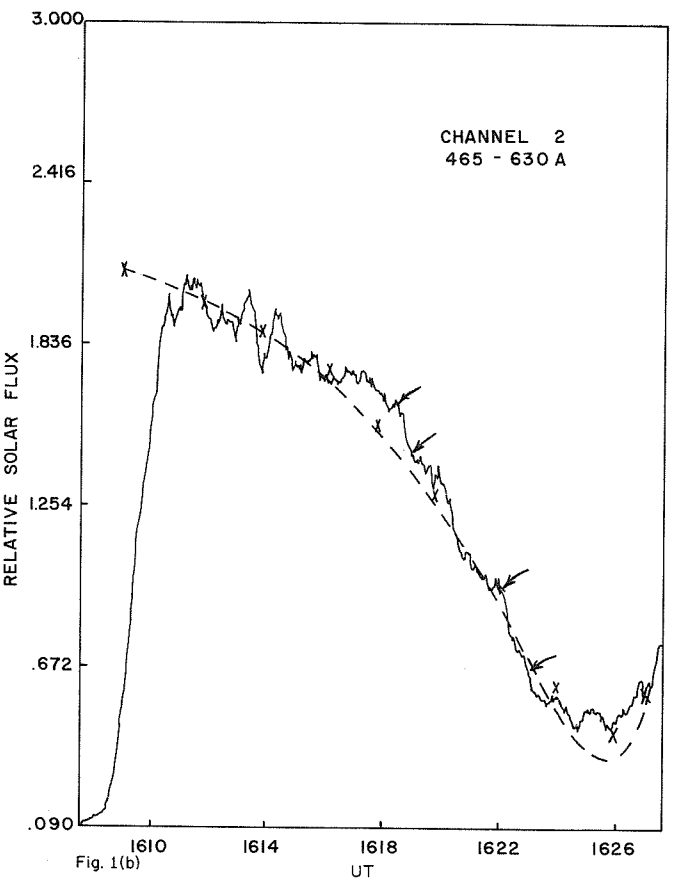

Fig. 1(b)

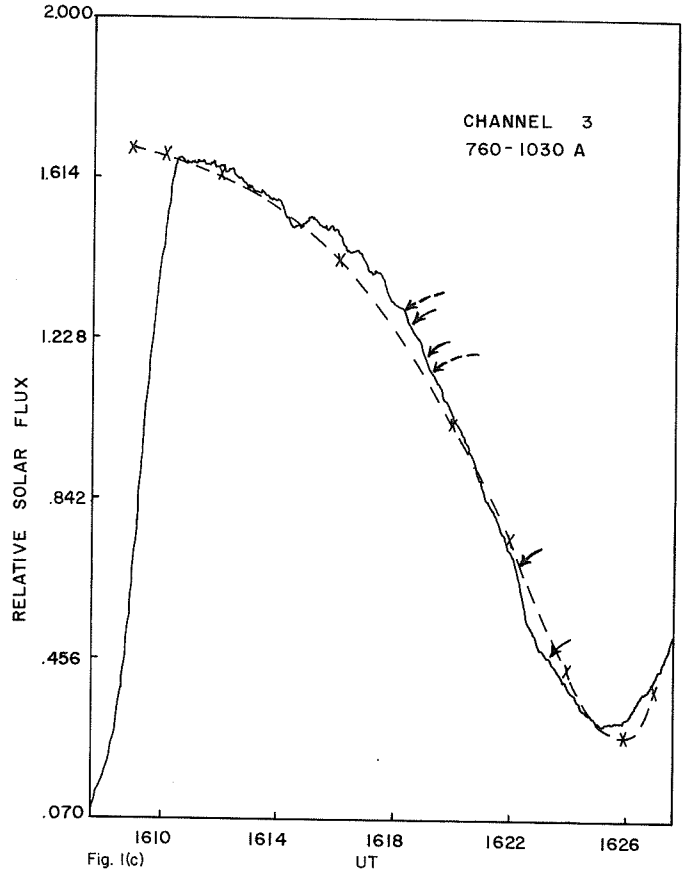

Fig. 1(c)

Fig. 1 Curves of relative intensity as a function of time for each euv channel during the March 7 partial solar eclipse as viewed from OSO-5. The arrows mark times during which active areas were covered by the lunar disk. The dashed curves are predicted variations if the solar disk were uniformly bright in the three euv bands. The crosses mark the predicted variations for channels 1 and 2 if limb brightening is assumed present.

For channel 1, the ratio $I_{\ell}L_{o}/(I_{A}A_{o} + I_{\ell}L_{o})$ is 0.15, and for channel 2, 0.12. These values are approximate measures of limb-brightening of the sun for the net radiation emitted in the wavelength range corresponding to each of the two channels, respectively.

An estimate can be made of the contribution of the active areas of the disk to the total brightness of the sun for the wavelength ranges of the three channels. The upper left hand photograph in Figure 2 shows the appearance of the solar disk in H alpha light on the day of the eclipse. The other three photographs simulate the progression of the eclipse as viewed from the satellite; they correspond to the approximate times, 1618:30, 1619 and 1622 UT, respectively.

Referring to the arrow pairs on the curves of Figure 1, which mark abrupt declines in intensity, and comparing these time intervals with the solar disk images of Figure 2, one can conclude that the intensity drops are the result of active areas being occulted by the moon. The decline on all three channels from 1618:30 to 1618:56 UT, corresponds to the covering by the lunar disk of McMath regions numbered 10618 and 10614. Since these regions were essentially all covered simultaneously, the effects of individual active regions cannot be distinguished on the curves. The decline in total solar intensity for the spectral regions for this interval is 3.3% on channel 1, 5.3% on channel 2 and 2.6% on channel 3, after allowance is made for quiet region contribution. Since the active regions as measured by calcium plage areas are at the most 1.3% of the total area of the solar disk, they are considerably brighter than the surrounding regions, at least by factors of 3, 4 and 2, respectively, for the three channel bands.

A similar analysis of the intensity drops from 1622:03 to 1623:00 UT indicates that the percentages of decline for radiation from all the active regions involved (McMath regions numbered 10607, 10617 and 10619) are 2.3, 5.6 and 3.3, respectively, for the three channel bands. Here the active regions are brighter than the surrounding regions, by, at least, factors of about 2, 4 and 2, respectively, for the three channels (the calcium plage areas are 1.6% that of the solar disk).

Since the sun's activity at the time of the eclipse was fairly typical of the solar maximum, the above data indicate that the total contribution by active areas to the intensity of solar radiation in the entire u.v. range 280 - 1030 Å is about 7% during solar maximum.

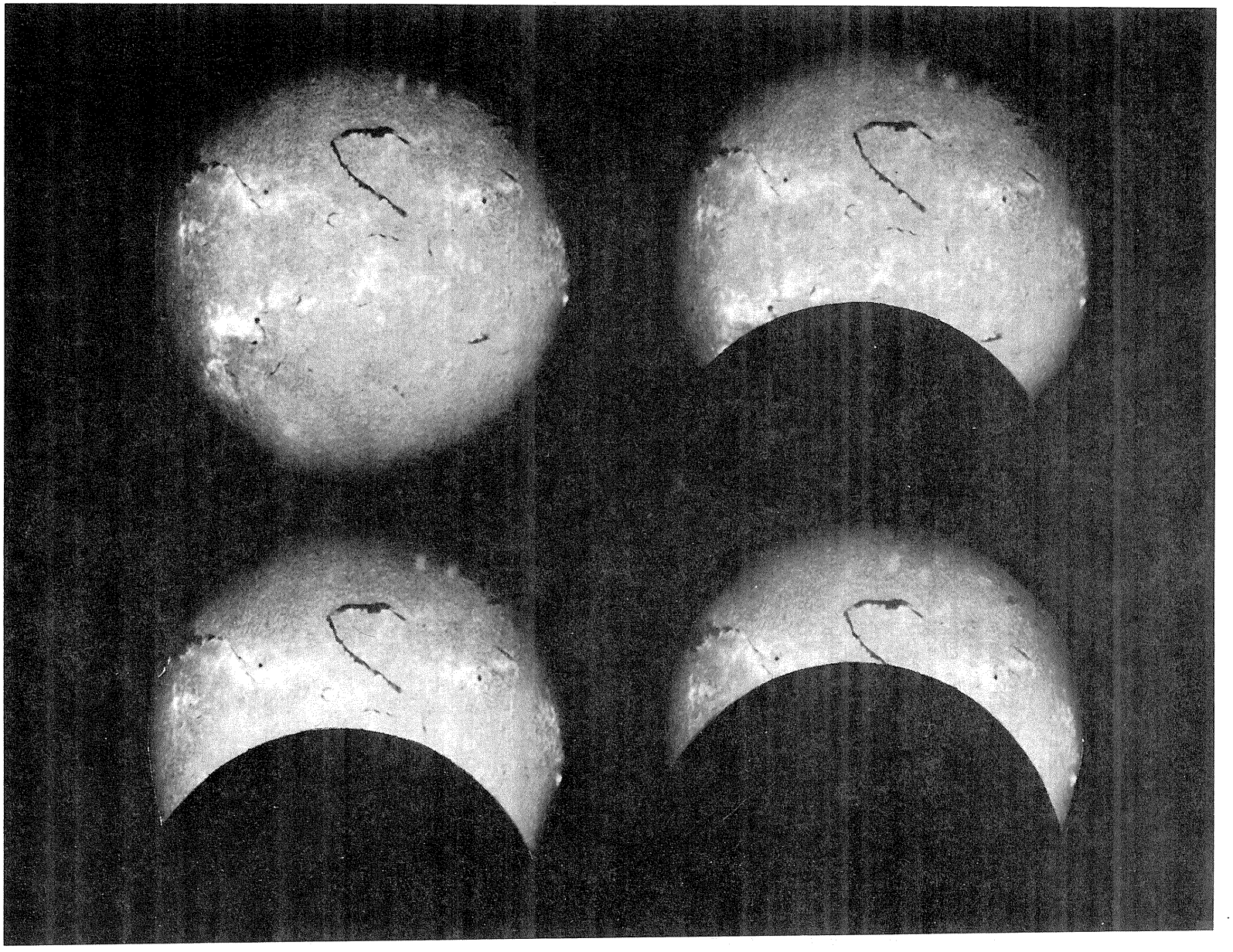

Fig. 2. The photograph on the upper left is the solar disk in H-α light on the day of the eclipse. The other photographs simulate the progress of the eclipse as viewed from the satellite. The photograph was provided by the Space Environment Services Center of the Space Environment Laboratory of NOAA.

"Large Fluxes of 1 kev Atomic Hydrogen at 800 km"

by

R. L. Wax, W. R. Simpson and W. Bernstein
TRW Systems Group
One Space Park
Redondo Beach, California 90278

This is a summary of the full paper published in the Journal of Geophysical Research.

Energetic (1 kev) neutral hydrogen fluxes in the range 10^9 - 10^{10} cm^{-2} sec^{-1} appear to have been detected during a rocket flight performed 7 March 1970 at 1847 UT as part of the Solar Eclipse Rocket Program at Wallops Island, Virginia. The payload was launched on a Javelin Rocket to an altitude of 840 km; at this altitude the attenuation of such energetic fluxes which might penetrate the atmosphere from the interplanetary medium would be about 1%. Although the rocket entered a region of only 80% totality, solar ultraviolet and other sources of background counts made no significant contribution to the observed atomic hydrogen and proton fluxes.

The average flux of energetic hydrogen atoms was 5×10^9 atoms cm^{-2} sec^{-1} str^{-1} kev^{-1} at 1 kev. The spectrum was exponential with an e-folding energy of $\sim$600 ev. The simultaneously measured total proton flux was 10^6 cm^{-2} sec^{-1} str^{-1} with an e-folding energy of 900 ev.

The observed atomic flux was not isotropic; the counting rates increased by a factor of 5-10 during part of the azimuthal scan. The sun appeared in the instrument field of view very near to the boundary of this region of increased counting rate. It is therefore unlikely, although possible, that the source of the energetic neutral flux was the sun.

Some eighteen hours after this flight, the largest geomagnetic storm of this solar cycle occurred. Since the measured atomic flux and its energy density are approximately a factor of 10^2 greater than those of the undisturbed solar wind, it is possible that this flux may be involved in the production of this particular storm.

REFERENCE

WAX, R. L., W. R. SIMPSON and W. BERNSTEIN 1970 Large fluxes at 1-kev atomic hydrogen at 800 km, J. Geophys. Res., 35, 6390-6393.

"Preliminary Results from a Meteorological Rocket Experiment During the Solar Eclipse of March 7, 1970"

by

Robert M. Henry
Principal Experimenter
Langley Research Center, NASA

Roderick S. Quiroz
Co-Experimenter
National Meteorological Center, NOAA

It is clear from evidence of previous experiments that large and important changes in the ionosphere occur during a solar eclipse. Changes in the neutral region of the stratosphere and mesosphere are not so clearly established. Large increases in total ozone amount deduced from ground observations are at variance with theoretical changes, and an earlier rocket experiment [Ballard et al., 1969] conducted at Tartagal, Argentina (23°S, 64°W) during the November 12, 1966 eclipse showed temperature decreases much larger than would be expected theoretically. These earlier data are open to some question because of the relatively large random errors of rocketsonde instruments at that time because of the difficult nature of operations at the temporary remote site and because corrections for aerodynamic heating, radiation, and other errors were not applied to these data.

In order to better define the eclipse related changes in the neutral atmosphere a series of ARCAS meteorological rockets was fired from the NASA Wallops Station before, during, and after the March 7, 1970 solar eclipse. Because of conflicts with the many other eclipse experiments at the Wallops Station, it was not possible to schedule all of the most desirable launch times, but the eight launches scheduled give good temporal coverage, and, with the addition of data from the pitot tube experiment, should provide a clear picture of changes in the stratosphere and mesosphere. All of the rockets were launched at the scheduled times, with excellent trajectories, radar trackings, and telemetry for all but one rocket. The telemetry signal of the final, post-eclipse-day rocket was unsatisfactory and a back-up launch was required.

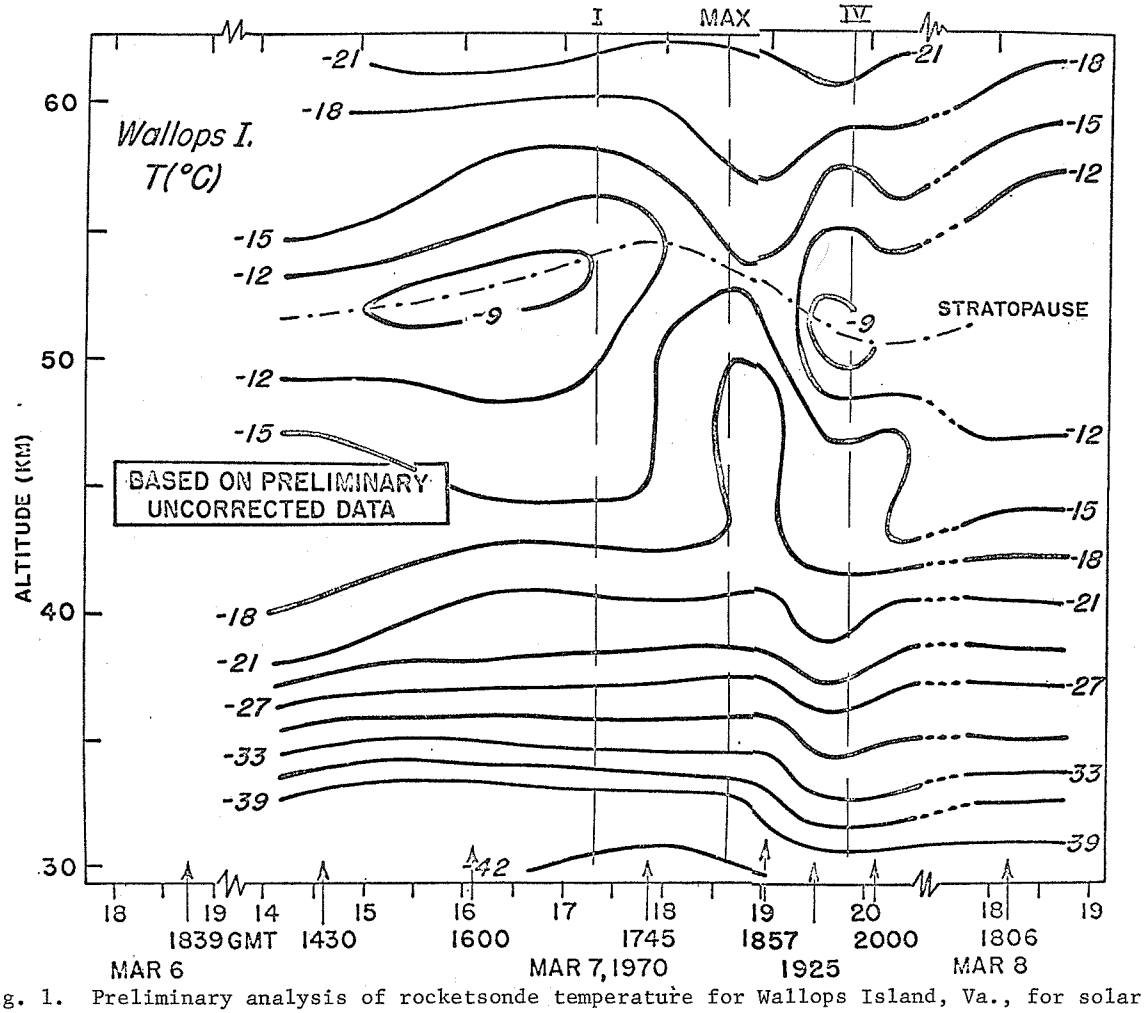

Fig. 1. Preliminary analysis of rocketsonde temperature for Wallops Island, Va., for solar eclipse of March 7, 1970. Arrows indicate the approximate time that the sensors were at the 50 km level.

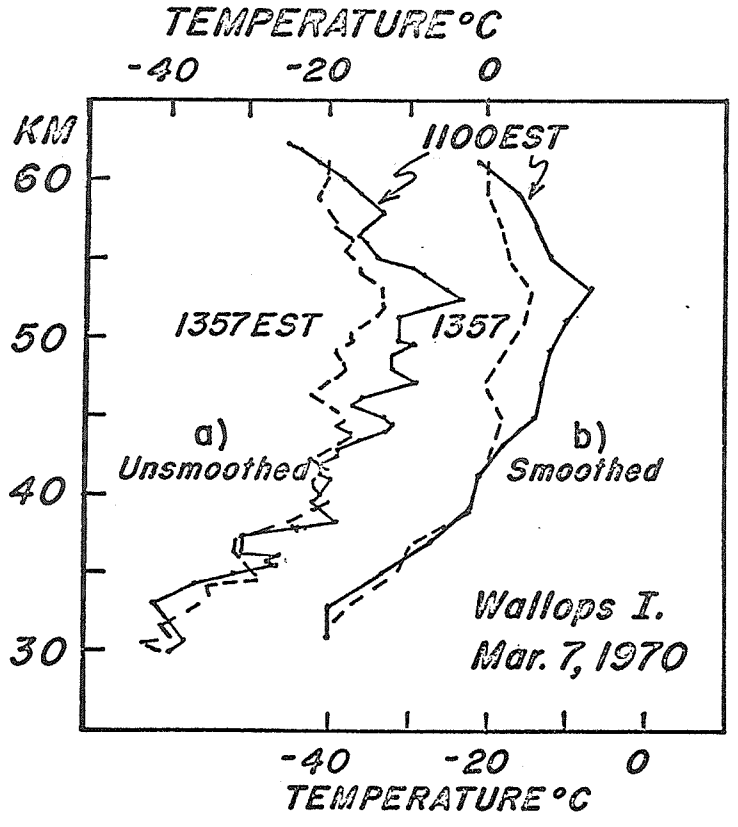

Fig. 2. Unsmoothed (a) and smoothed (b) temperature profiles before (1100 EST) and during (1357 EST) March 7, 1970 solar eclipse. Based on preliminary uncorrected data.

All of the temperature data will be corrected for aerodynamic heating, radiation and other errors using the procedures described by Lacey and Staffanson [1970]. However, these corrections, as well as the wind computations require use of the processed radar tapes, and all of these tapes have not yet been received from Wallops Station. Therefore, the present preliminary analysis is based on uncorrected temperature data. The analysis is shown in the form of a time-height cross-section in Figure 1 and in the form of temperature-altitude plots in Figure 2. In Figure 2 (b), a smoothing in the form of an overlapping running has been applied.

The salient features of this preliminary analysis are (1) a perturbation of the temperature field essentially contained within the period of the eclipse, and mainly within the 40-60 km layer; (2) maximum amplitudes of 5-7°C at 45-55 km with minimum temperatures indicated a few minutes after totality; (3) rapid warming just before the end of the eclipse.

Final conclusions must await not only the refinement and correction of the present data, but also comparison with other results, especially the pitot tube measurement and ozone measurements at Wallops Island, and other eclipse meteorological measurements at Eglin AFB, Florida, and in Mexico. A more complete discussion of this preliminary analysis was published in Nature, 226, 1970.

REFERENCES

BALLARD, H.N., R. VALENZUELA, M. IZQUIERDO, J. W. RANDAHWA, R. MORLA, J. F. BETTLE	1969	Solar Eclipse: Temperature, Wind, and Ozone in the Stratosphere, J. Geophys. Res., 74, 711.
LACY, W. W. and F. L. STAFFANSON	1970	A Data Reduction Program for a Rocketsonde Temperature Sensor, NASA Cr-66895.

"Travelling Ionospheric Disturbances Observed Near the Time of the Solar Eclipse of March 7, 1970"

by

G. M. Lerfald and R. B. Jurgens
National Oceanic and Atmospheric Administration
Environmental Research Laboratories
Boulder, Colorado 80302

and

J. Vesecky and D. Kanellakos
Stanford Research Institute
Menlo Park, California 94025

Chimonas and Hines [1970] and Chimonas [1970] have predicted the likelihood that the shadow of a solar eclipse moving at supersonic velocity can generate gravity waves of a magnitude which should be detectable by ground-based and/or ionospheric measuring techniques at considerable distances from the center of the eclipse path. Chimonas and Hines [1970] pointed out that the March 7, 1970 solar eclipse would provide a favorable opportunity for making measurements to detect the effects of such eclipse-generated gravity waves. This paper reports preliminary results from ionospheric measurements conducted during a 6½-hour period centered on the eclipse occurrence.

Two techniques were used; one employed transmission of very short pulses centered at a frequency of 18 MHz and the other the transmission of a cw signal which was linearly swept from 5 to 30 MHz at a 1 MHz/sec rate (CHIRP signal). The transmitters were located at Palo Alto, California and the receiving equipment at Boulder, Colorado. At this range (1500 km) the propagation during daytime is usually via one-hop E and F modes. The CHIRP ionosonde data, recorded on magnetic tape, were processed in the conventional way to obtain ionograms on 35 mm film, and later the data were reprocessed and recorded on a 16 mm framing camera. The latter film, when projected as a movie, showed evidence of interesting systematic changes in the ionogram traces with time. The 35 mm filmed ionograms were scaled in detail by use of an electromechanical scaler which recorded digital data on magnetic tape as each ionogram was traced by a manual pointer. These data were then processed by a large digital computer and the output plotted by a CRT plotter. Figure 1 shows a plot of the CHIRP ionosonde data, where signal delay is plotted versus time at one MHz frequency intervals.

The short-pulse experiments were performed using transmitters, described by Kanellakos [1969], which can radiate pulses of submicrosecond duration at HF with peak powers of several megawatts. At the receiving end, broad bandwidth receivers (0.5 and 1 MHz) were used and the coherent IF output was recorded by photographing a triggered oscilloscope trace. Time was maintained to within a few microseconds at the sending and receiving stations, so total signal propagation time and changes in the latter could be determined to within a few microseconds.

Figure 2 shows the variation of the starting times of the received pulses relative to time of transmission of the pulses (note the arbitrary shift in time reference) during the period 1654-2316 UT on March 7, 1970.

Another parameter measured from the recorded pulses is the duration of individual pulses. Figure 3 shows a time series plot of the pulse durations in microseconds for the same time period as that of Figure 2.

The data presented in the above figures exhibit a number of interesting features. Figures 1 and 2 show several fluctuations in signal delay, with average period about 40 minutes, which look like those expected from travelling ionospheric disturbances. There is good general agreement between the pulse delay variations of Figure 2 and the group delay changes at 18 MHz shown in Figure 1. The group delays on Figure 1 show a leading phase for the perturbations at the higher frequencies with respect to the lower frequencies (dashed lines connect approximate peaks). This is consistent with theoretical expectations and experimental data for travelling disturbances [See, e. g., Georges, 1967].

Figure 3 shows several peaks in the pulse length parameter. These coincide with times when the pulse start time is trending toward a maximum delay and may be indicative of multipath conditions which are most likely to occur when the reflection region is from the trough portion of a travelling disturbance. At such times, rays which leave the transmitter at azimuth angles slightly off the great circle path to the receiver, may be refracted sufficiently to cause focussing and/also pulse lengthening. Nonsymmetry of the pulse length peaks with the corresponding peaks in times of pulse starts is qualitatively consistent with tilts in the wave front of a travelling disturbance.

The principal objective of the experiment was to look for and study travelling disturbances which may have been generated by the moving eclipse shadow. The occurrence of a rather large

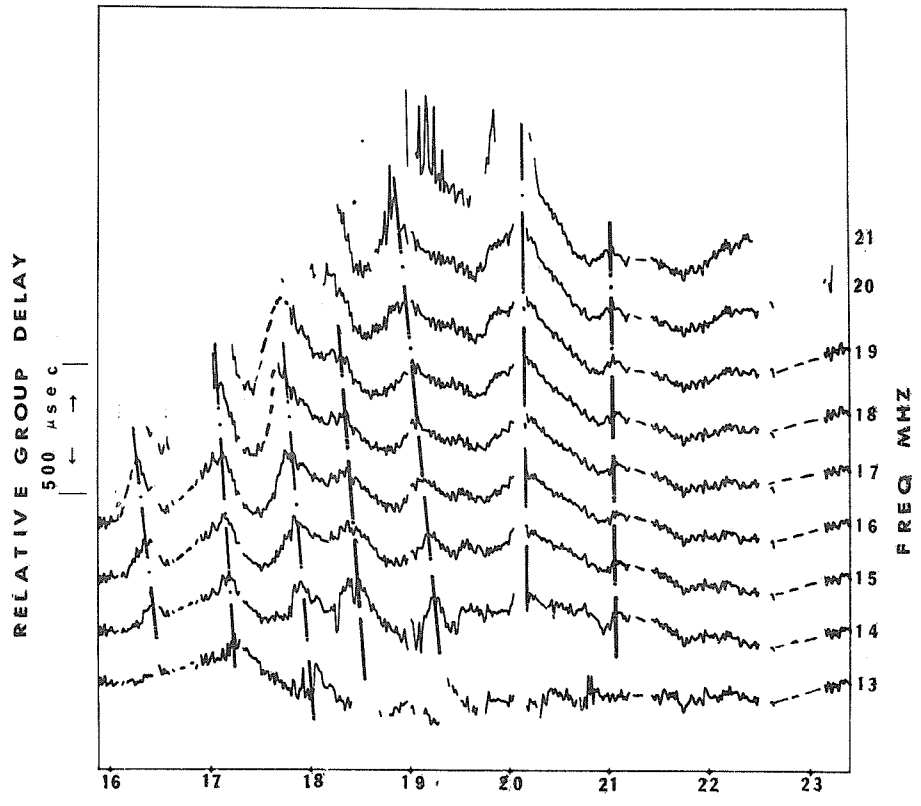

March 7, 1970 1553-2323 UT

Fig. 1. Group time delay vs. time curves derived from oblique CHIRP ionosonde data at several transmission frequencies. The path was from Palo Alto, California to Boulder, Colorado. Dotted lines indicate interpolations filling in gaps in the data. Traces have been shifted vertically to avoid overlap.

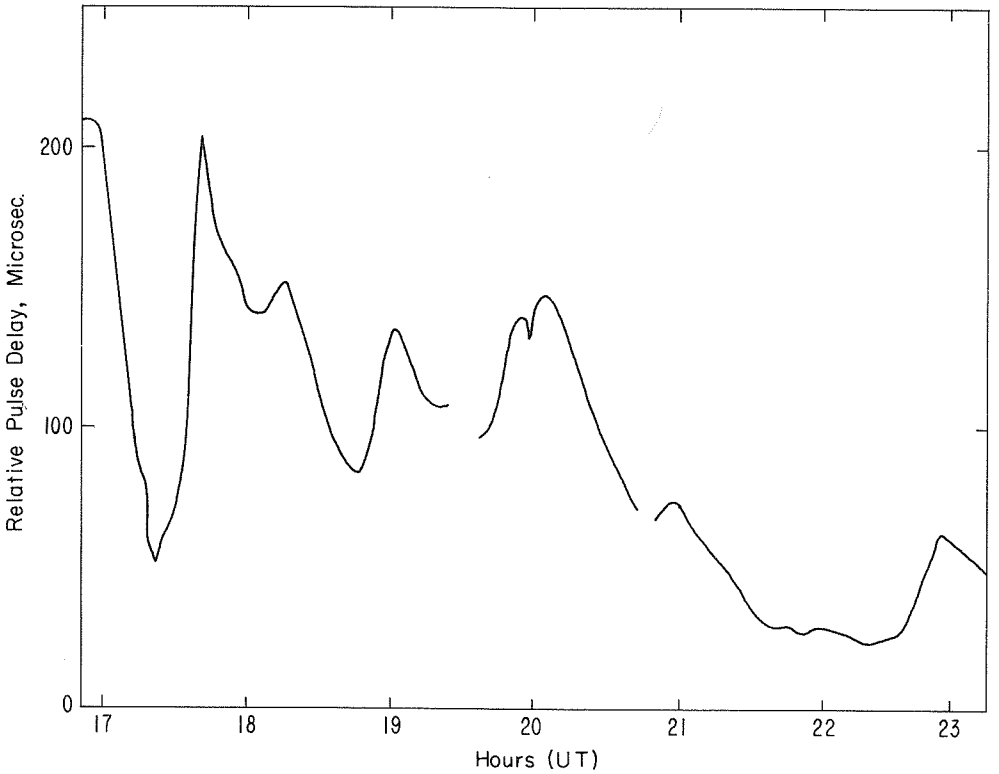

Fig. 2. Plot of pulse delay changes versus time during occurrence of ionospheric travelling disturbances.

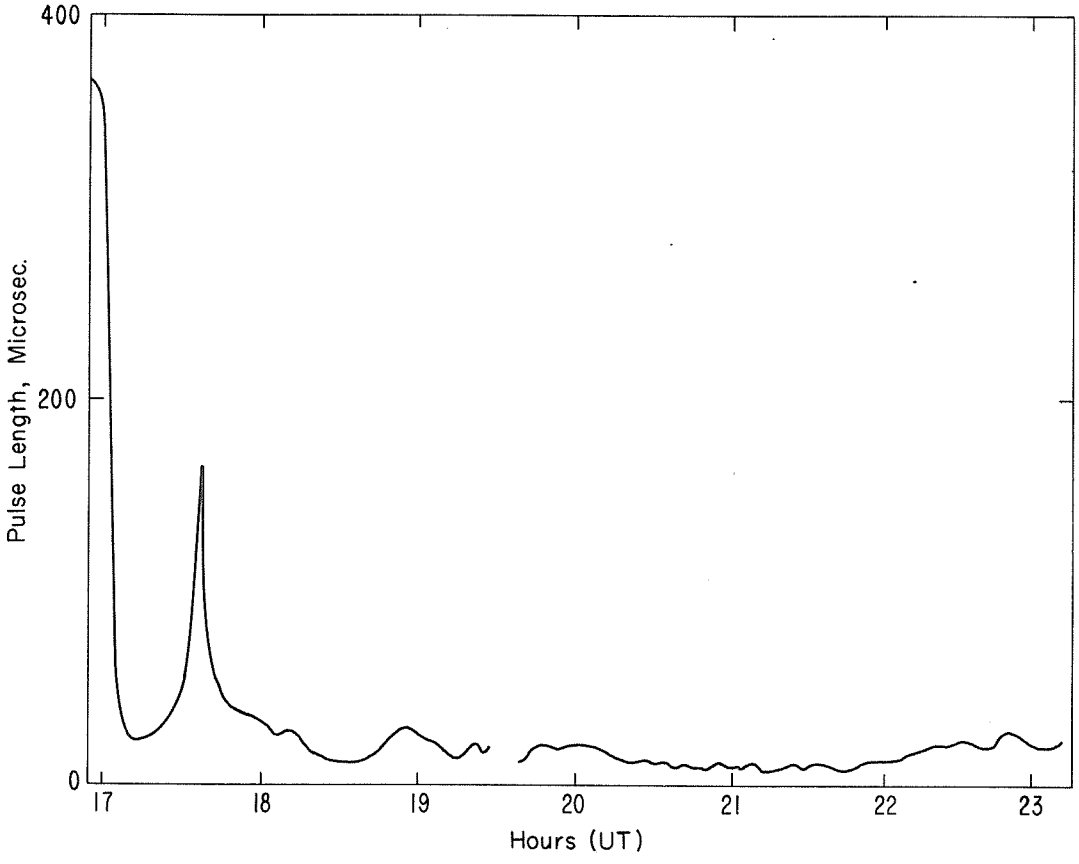

Fig. 3. Plot of pulse length versus time for the same time period as Figure 2.

solar flare at 1603 hrs. UT and the high level of geomagnetic activity which characterized this period serve to complicate the analysis. It is hoped that other data will become available which, coupled with the above, will be capable of determining the direction of travel of the apparent travelling disturbances. If some, or all, of these appeared to travel from south to north, it is likely that the eclipse could have generated the disturbances. If, on the other hand, they all travelled from north to south, it is likely that they were mainifestations of the geomagnetic storm in progress at the time.

REFERENCES

CHIMONAS, G. and C. O. HINES	1970	Atmospheric gravity waves induced by a solar eclipse, J. Geophys. Res., 75, 875.
CHIMONAS, G.	1970	Internal gravity-wave motions induced in the earth's atmosphere by a solar eclipse, J. Geophys. Res., 75, 5545-5551.
GEORGES, T. M.	1967, October	Ionospheric effects of atmospheric waves, ESSA Tech. Rept. IER 57-ITSA 54.
KANELLAKOS, D. P.	1969, May	Oblique HF experiments over the Palo Alto-to-Boulder path, Stanford Res. Inst. Final Rept. on Contr. E22-144-68(N).

"Ionospheric Effects from Gravity Waves upon Total Electron Content during the Eclipse 7 March 1970"

by

P. R. Arendt
U. S. Army Electronics Command
Fort Monmouth, New Jersey

A bow wave front of internal gravity waves produced by supersonic movement of the moon's shadow has been predicted for solar eclipses [Chimonas and Hines, 1970]. It is assumed that related pressure disturbances create travelling ionosphere disturbances, TID's, which could be observed when they produce variations of the total electron content measured along a slant path toward a synchronous satellite. Such variations of the total electron content were measured at Fort Monmouth, Diana Test Site (N 40.185° W 74.056°) by means of polarization data from ATS-3 signals on 137.35 MHz. The measuring and data evaluating system is fully mechanized. The slant path toward the satellite crossed the path of totality. The content data refer to a subsatellite point at N 37.9° W 75.2°. The geomagnetic field factor for conversion of polarization data to electron content values was estimated with 0.58583 gauss for the subsatellite point. This factor was assumed to be constant during observations. We have abstained from modifying this factor in order to meet obvious changes during the eclipse of the electron density vs. altitude profile because no experimental method is on hand for measuring, in real time, the shape factor, that is, the diurnal change of the geomagnetic field factor. We consider this uncertainty not to be a serious defect because the electron content variations were measured against a running average over 27 minutes. It is very unlikely that a substantial variation of the shape factor or of the geomagnetic factor will occur during such relatively short intervals. The ambiguity of the polarization data was solved by reference to the lowest polarization values before sunrise (on March 8). At that time the resultant polarization must be smaller than 360 degrees for a frequency in the 137 MHz range. The effect from the satellite's spin was eliminated by continuously averaging over 28 or 35 data points taken within 4 or 5 seconds. Those averages were obtained every 3 minutes during the period from 08 to 24 hours EST on the eclipse day.

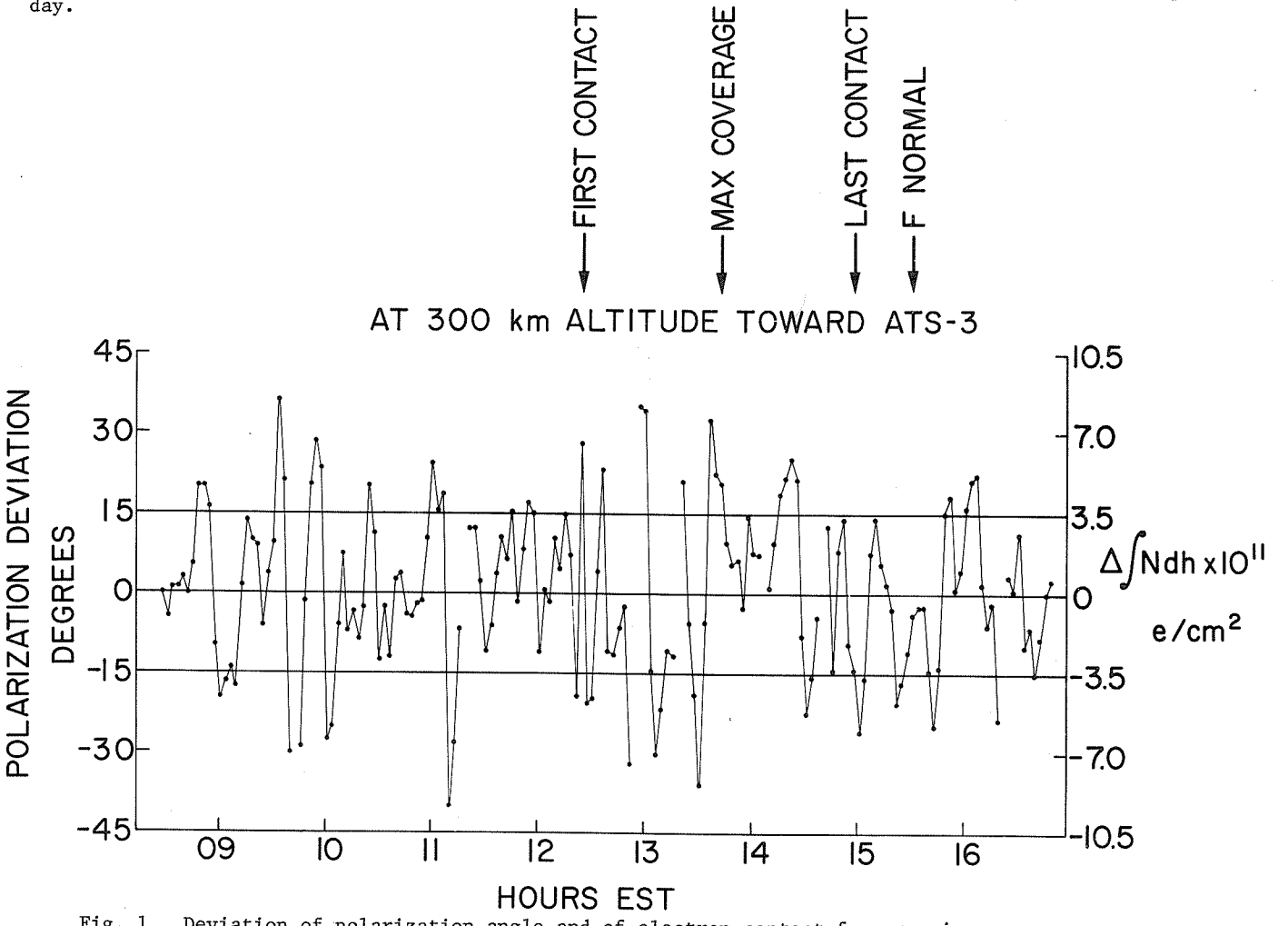

Fig. 1. Deviation of polarization angle and of electron content from running average reflecting the period of anticipated gravity waves.

A careful investigation of the statistical error of our measurement has been performed [Arendt, in press]. The readout precision of a single datum is $\pm$ one-half degree. The statistical error is $\pm$ 5.5 degrees for 99.73% of all data point averages (each taken over 3 minutes). For 50% of the averages the error is $\pm$ 1.2 degrees.

The search for the anticipated undulatory variation of the electron content was performed by a smoothing procedure, that is, taking a running average over 9 data points. This running average (over 27 minutes) was compared with the actual data at the center of the interval. The obtained differences were plotted against time (see Figure 1). The maximum statistical error for these differences is twice the error for each data point. Thus, we have a maximum possible error for all data in Figure 1 of $\pm$ 11.0 degrees and for 50% of the differences an error of $\pm$ 2.4 degrees. The related content values are 2.6×10^{11} e/cm^2 and 5.7×10^{10} e/cm^2 respectively. The variations recorded in Figure 1 are beyond these limits.

An attempt has been made to read the average wave period from the deviations in Figure 1. For this purpose only the peaks above and below the levels of $\pm$ 15 degrees were accounted for. A guess was made whether the interval between peaks was ½ or 1 or 2 periods. An average was found of about 18 min. per period with an uncertainty of $\pm$ 3 min. as introduced by the spacing of the original data averages.

On the EST time scale, the global start of the eclipse was at 11:00 hours. Thus, electron content variations before that time cannot be related to the eclipse. Variations like those midmorning variations prior to 11:30 EST (in Figure 1) are often observed with ATS signals at our test site. We leave it open here which effects are causing these observations. For the eclipse effects, we consider the time after 12:30 EST and note that the midmorning variation has faded out by 12 noon EST.

From satellite S-66 BEC observation of orbit 23690, we have estimated [Arendt, in press] the wavelength of the observed undulations. This passage crossed the totality path shortly after center of totality had passed. The observed content variations must have shown the beginning of the wake of the predicted bow wave [Chimonas and Hines]. The wavelength was found from observed minima of the electron content; it is estimated to be about 320 km. From this distance the velocity of the undulatory motion is calculated to be about 296 m/sec for a wave period of 18 minutes.

REFERENCES

CHIMONAS, G. and C. O. HINES	1970	Atmospheric Gravity Waves Induced by a Solar Eclipse, J. Geophys. Res., 75, 875.
ARENDT, P. R.	(In Print)	USAECOM Tech. Report

"Reaction of Ionospheric Regions to Solar Eclipse of March 7, 1970"

by

P. R. Arendt, F. Gorman, Jr., and H. Soicher
Institute for Exploratory Research
U. S. Army Electronics Command
Fort Monmouth, New Jersey 07703

Polarization measurements of ATS-3 beacon signals (137.35 MHz) were made at Fort Monmouth, N. J. (N40.185° W74.056°). The changes of corresponding electron content data (Fig. 1) were related to eclipse coverage at a 350 km subionospheric point (N37.9° W75.2°), near where bottomside soundings (kindly provided by courtesy of R. S. Gray) were taken by ESSA (now NOAA) at Wallops Island (N37.4° W75.5°) in support of the eclipse observations.

It is difficult to compare data of the eclipse day with similar data from days just before or just after the eclipse since magnetic storm activity lasted throughout the entire period. For example, our amplitude scintillation index measurements of the ATS-3 signals show extremely large values between March 5 and March 10, 1970. However, this scintillation activity was relatively small during the exact time interval when our eclipse observations were made. We abstain, therefore, from comparing data for the eclipse period with that from the previous or next days which may have been disturbed. We consider that our eclipse observations are related to the time period directly after local noontime, i.e., when the buildup of the ionospheric regions had already taken place. Thus, the reactions of the ionosphere to the eclipse phenomenon are not mixed with the strong slope of either increasing (midmorning) or decreasing (afternoon) electron density. These facts would have to be accounted for if a solar eclipse were observed during early morning [Szendrei and McElhinney, 1956] or late afternoon hours local time.

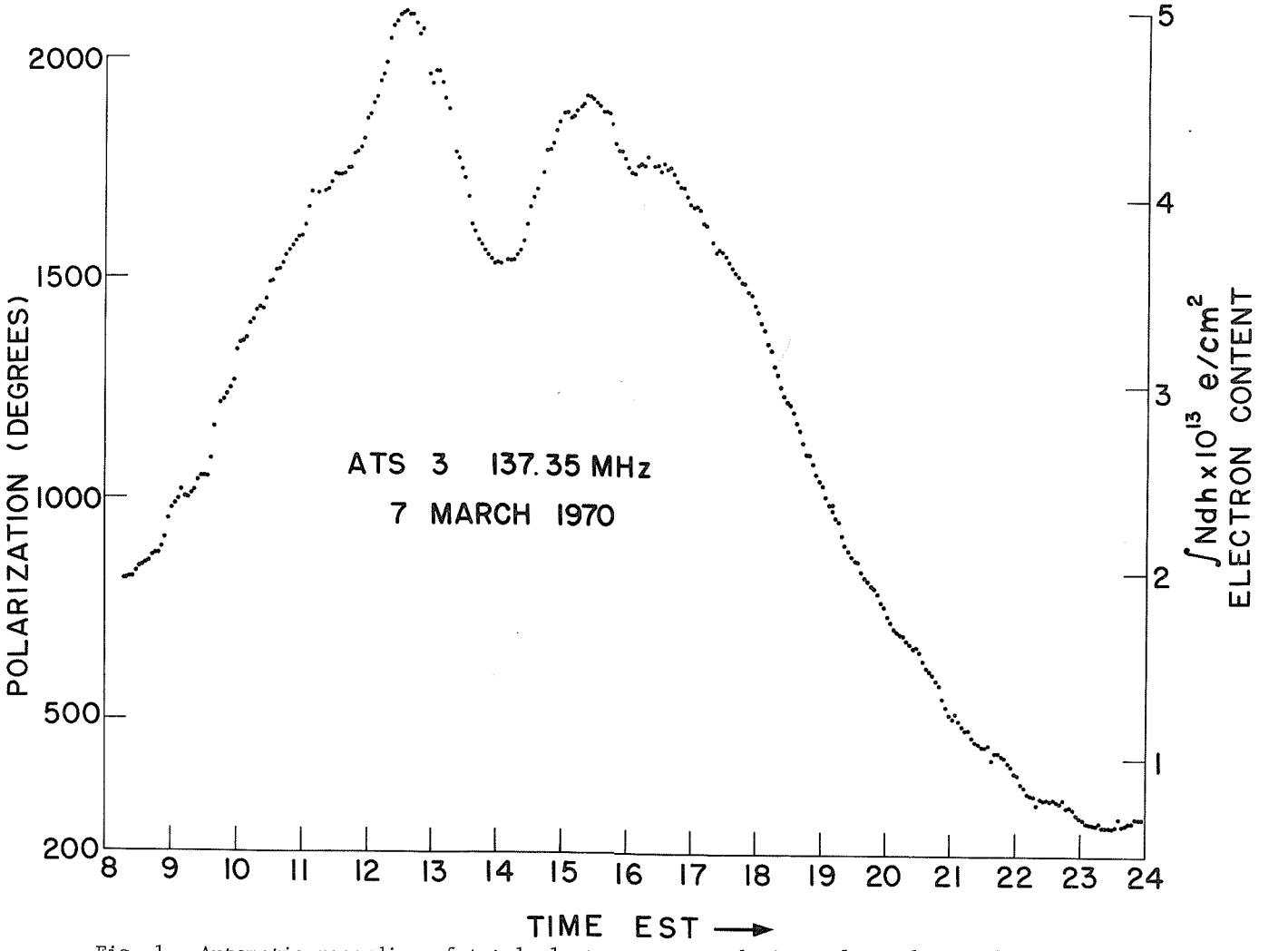

Fig. 1. Automatic recording of total electron content during solar eclipse of March 7, 1970. Data are printed every 3 minutes; the computer discarded data received during occasional hunting performance of the automatic system.

We ascribe the first ionospheric reaction to the eclipse to the first turning point in Fig. 1. The strongest reaction is ascribed as usual to the observed minimum; recovery is ascribed to the second turning point of the curve in Fig. 1. The E- and F-region reactions read from the Wallops Island ionograms follow a similar schedule: turning points before and after a minimum. We believe that for our eclipse observations the correlation of first turning point to first ionospheric reaction, and correlation of second turning points to ionospheric recovery is less misleading than correlation to data from days which were heavily disturbed.

We compared the times when turning points and minima occurred with the times when first contact, maximum coverage, and last contact would have been observed visually at the points of observation. Data of total electron content and of F-max were related to a 300-km altitude at the mentioned subionospheric point. The F-max data from Wallops Island were shifted in time by 2 minutes to compensate for the distance between the two locations. The E-region data have been related to 100-km altitude at the Wallops Island location. We thus arrived at the schedule presented in Table 1 where all times are given in EST. A similar table for time delays at maximum coverage has been given by Rawer and Suchy [1967].

A decrease in total electron content was found to precede the decrease in F-region maximum plasma frequency by about 5 minutes. These first reactions occurred 13 minutes and 17 minutes, respectively, after first visual contact as seen from the ionospheric position. The delay of 13±3 minutes for first reaction of the total content is shorter than the value of 40 minutes noted by Flaherty et al. [1970] for a subionospheric point more southerly and closer to the path of totality than our reference location. At maximum coverage, polarization of the ATS-3 signal had decreased to only 90% of its maximum decrease. The minimum electron content was delayed by 24 minutes with respect to visual maximum coverage; other authors [Flaherty et al., 1970; Almeida and Da Rosa, 1970; Bienstock et al., 1970] observed delays during this eclipse of between 20 and 39 minutes. Our minimum electron content values preceded minimum F-max values by about 12 minutes; however, this figure is rather uncertain (see Table 1) due to broad minima.

Table 1
IONOSPHERIC RESPONSE TO SOLAR ECLIPSE
(all times in EST)

	1st Turning or 1st Visual Contact	Min. Ionization or Max. Coverage	Ret. to Normal or Last Contact	
At 300 km				
Visual	12:25	13:42	14:55	
$\int$Ndh	12:38±3	14:06±3	15:26±3	
F_{max}	12:43±4	14:18±6	15:30±15	Interpolated to ATS-3 Point
At 100 km				
Visual	12:22	13:40	14:53	
E_{max}	12:12±1	13:40±1	14:45+8	At Wallops Island

The return to normalcy was observed for the total electron content after a delay of 31 minutes and for F-max, after a delay of 35 minutes relative to last visual contact; again, the F-region data are uncertain. The already cited observations of Flaherty et al. [1970] give a delay of 43 minutes for total content recovery.

Total content reaction preceding relative F-max observations is understandable when the known quick reaction of the E-region is accounted for. These quick reactions accelerate the total content reaction relative to the F-max reactions.

The reactions of the E-region were as follows (see Table 1): First reaction was about 10 minutes earlier than first visual contact; maximum reaction (E at minimum) coincided clearly with maximum coverage; and recovery was close to last contact or later within the tolerance limit. This latter tolerance value is rather large because some ionograms are missing due to a change in the sequence of ionograms at Wallops Island.

Literature citations [Rawer, 1956] as early as 1954 mention the advance reaction of the E-region relative to first contact. For a review of observations from 1932 to 1952, see Ratcliffe [1956]

citing coincidence, delay, or advance reactions. An Appleton observation from 1927 cited in recent literature [Bienstock et al., 1970] refers to a 4-minute delay between E-region minimum and maximum coverage. Our readout of the Wallops Island ionograms have been checked very carefully, but the data do not confirm the statement from 1927. We are in agreement with Rawer [1956] and Becker [1956] regarding the advance reaction of the E-region. It may be noted that Becker's data also refer to an eclipse observation close to local noontime.

A simple explanation of the advance reaction of the E-region does not appear to be possible. Zones of specific solar activity may play an important role, as may local events in the outer corona of the sun. Finally, horizontal electron drifts may have to be considered as excited by electron density gradients created by the shadow of the eclipse. This shadow produces a void of electrons (mainly due to recombinations in the E-region) at positions close to a point of observation where first contact has not yet been reached. Thus, there exists a temporary steep gradient which causes the number density in the observed part of the E-region to diminish just prior to the time of first contact. This horizontal gradient is large before first contact; it becomes smaller and smaller with increasing coverage. Horizontal drifts across magnetic lines of force may take place mainly at E-region altitudes due to the high collision frequency there. But similar motions are inhibited by the magnetic field at F-region altitudes, where the mean free path for electrons is considerably larger. Further, atmospheric motions like these created by internal gravity waves [Chimonas and Hines, 1970] must be considered. A synoptic description of the phenomenon could be given if fast E-region reaction (within a tolerance of ± 3 minutes) could be assumed throughout, and if effective corona zones could be assumed to extend so far out that even 10 minutes before first visual contact some shielding diminishes irradiation in the E-region. In this respect observations are of importance which indicate effective solar diameters larger than the optical diameter and a non-symmetric (i.e., elliptical) distribution [Ryle, 1956] of the solar disk's brightness. This concept may explain why different E-region reaction times are reported [Ratcliffe, 1956] for various eclipses; the shadow may approach the solar limb from directions where the effective diameter is either large (equatorial regions) or small (polar regions). It is very likely, however, that all the effects mentioned play a more or less important role in the observed phenomenon.

REFERENCES

ALMEIDA, O. G. and A. V. DA ROSA 1970 Observations of ionospheric electron content during the March 7, 1970 solar eclipse, Nature, 226, 1115-1116.

BECKER, W. 1956 The ionosphere above Lindau during the solar eclipse on 30 June 1954, Solar Eclipses and the Ionosphere, Ed. W.J.G. Beynon and G. M. Brown, Pergamon Press, 36-39.

BIENSTOCK, B. J., R. T. MARRIOUT, D. E. ST. JOHN, R. M. THOREN, and S. V. VENKATESWARAN 1970 Changes in the electron content of the ionosphere, Nature, 226, 1111-1112.

BOMKE, H. A., H. A. BLAKE, A. K. HARRIS, and D. J. SHEPPARD 1970 An investigation of solar sources of E-layer ionization by means of eclipse effects, Spring Meeting, U.S. National Committee of URSI.

CHIMONAS, G. and C. O. HINES 1970 Atmospheric gravity waves induced by a solar eclipse, J. Geophys. Res., 75, 875.

FLAHERTY, B. J., H. R. CHO, K. C. YEH 1970 Response of the F-region ionosphere to a solar eclipse, Nature, 226, 1121-1123.

RATCLIFFE, J. A. 1956 A survey of solar eclipses and the ionosphere, Solar Eclipses and the Ionosphere, Ed. W.J.G. Beynon and G. M. Brown, Pergamon Press, 1-13.

RAWER, K. 1956 Discussion remark, Solar Eclipses and the Ionosphere, Ed. W.J.G. Beynon and G. M. Brown, Pergamon Press 219.

RAWER, K. and K. SUCHY 1967 Radio observations of the ionosphere, Encyclopedia of Physics, Springer, Berlin, 49/2, 378.

RYLE, M. 1956 Radio investigations of the structure of the solar corona, Solar Eclipses and the Ionosphere, Ed. W.J.G. Beynon and G. M. Brown, Pergamon Press, 246-252.

SZENDREI, M. E. and M. W. MC ELHINNEY 1956 The Behaviour of the E 1 layer during the solar eclipse of 25 December 1954, Solar Eclipses and the Ionosphere, Ed. W.J.G. Beynon and G. M. Brown, Pergamon Press, 74-80.

"VLF Phase Changes Produced by the Total Solar Eclipse of 7 March 1970"

by

S. Ananthakrishnan and A. M. Mendes
Centro de Radio Astronomia e Astrofisica
Universidade Mackenzie, Sao Paulo, Brazil

Very low frequency (VLF) transmissions from three locations (Omega, Haiku 10.2 kHz; NLK, Seattle, Washington 18.6 kHz and NAA, Cutler, Maine 17.8 kHz) were received at Umuarama Radio Observatory, Campos do Jordao, Sao Paulo, Brazil, during the total solar eclipse of 7 March 1970 by two receiving stations controlled by a Rubidium Oscillator. The phase outputs have widths of 0-100 μsec (±1 μsec) and 0-10 μsec (±0.1 μsec) and the recording time constants are 50 sec, both in phase and amplitude. The propagation paths are 12,900 km and 7,900 km long, respectively. The simplified geometry of the propagation paths is shown in Figure 1. Phase and amplitude changes on the three frequencies are shown in Figure 2. Maximum phase retardation on NAA and NLK were 3.8 μsec and 3.6 μsec. The eclipse affected the Haiku - Sao Paulo path during the sunrise period and was in addition affected by an SID which occurred 35 minutes after first contact. It is, therefore, difficult to measure the magnitude of the phase retardation. Phase advances from night to day on normal days are usually of the order of 120 μs on Haiku, 75 μs on NLK and 57 μs on NAA. Percentage of eclipse to diurnal changes on the three paths were 3%, 5% and 7%, respectively. A comparison of these results with the oblique incidence VLF phase observations of Hildebrand [1969] in Southern Brazil during the total solar eclipse of November 12, 1966, showed that the two sets of results were similar. Hildebrand's observations show a phase retardation of about 6 μsec at 31.25 kHz falling to 1.0 μsec at 15.6 kHz and again rising to 4.0 μsec at 9.37 kHz. At a frequency of 8.75 kHz, the observed retardation was 3.0 μsec which is comparable with the 3.8 μsec and 3.6 μsec observed at 17.8 kHz and 18.6 kHz in the present case.

By making use of the tabulated full wave solutions of Wait and Spies [1964] and the percentage of path affected; changes in the conductivity in the affected portion of the path were calculated. The calculations were made, assuming that only the first order mode was dominant. The percentage of the path affected in each case was calculated graphically as follows: The time difference between the commencement of the phase change and first contact was noted. This was 24 minutes in the case of NLK and Haiku and 28 minutes for NAA. A circle was then drawn with radius equal to the minimum distance from the position of the eclipse trajectory at that instant to the propagation path. The length of path affected in each case is given in Table I. Since the eclipse trajectory crossed the Haiku - SP path at sunrise, only the portion of the path which was sunlit at the time the phase retardation commenced has been considered. The value of 3.2 mm quoted in Table I is the lower limit, since the portion of sunlit, path increases as the eclipse progresses. Table II gives the values of β and h_o, the conductivity gradient and reference height for the new profiles in the portion of the path affected by the eclipse.

Table I

Station	Total path	Affected	Percentage
NAA	7,900 km	2,400 km	29%
NLK	10,900 km	1,900 km	17%
Haiku	12,900 km	3,200 km	31%

Table II

Station	Path Affected	v/c	β km^{-1}	h_o
NAA	2,400 km	0.9989	0.28	75 km
NLK	1,900 km	0.9988	0.32	73 km

Table III

Station	Deeks 60%	Deeks 100%	Observed
NAA	4.6 μs	6.0 μs	3.8 μs
NLK	3.5 μs	5.1 μs	3.6 μs

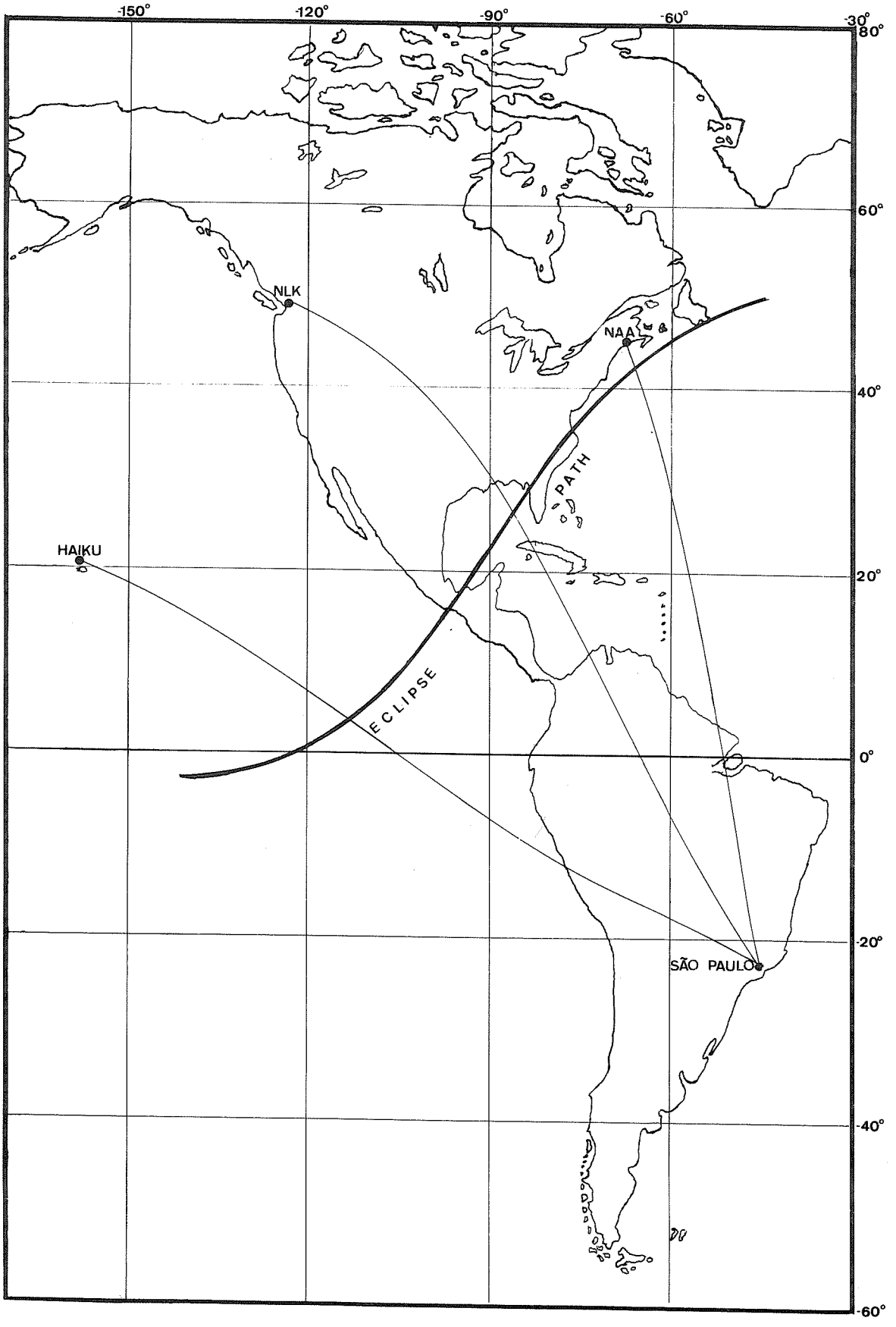

Fig. 1. The geometry of the propagation paths from transmitters Haiku, NLK and NAA received at Sao Paulo and the path of totality of the March 1970 eclipse.

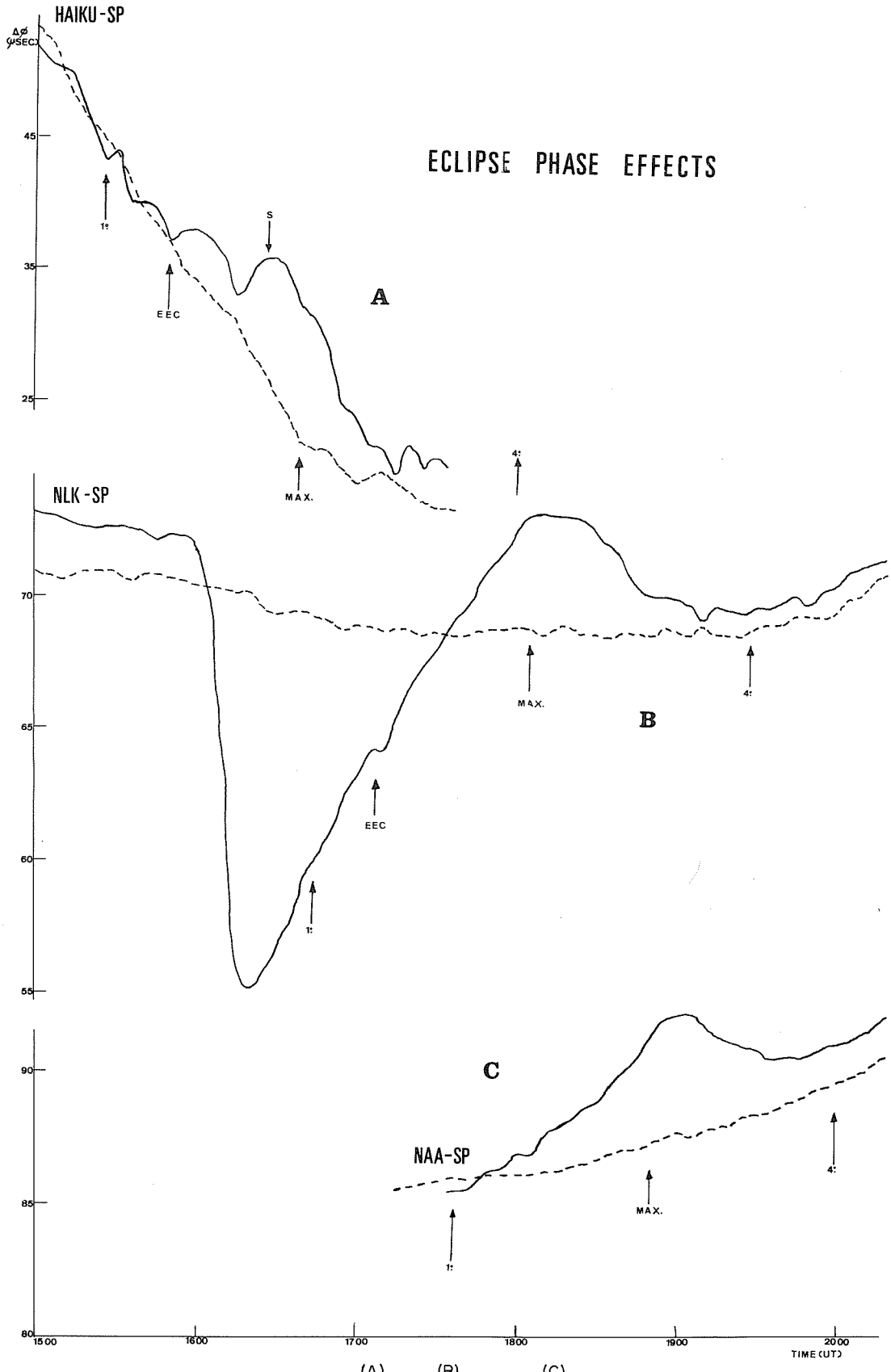

Fig. 2. Phase retardations on Haiku(A), NLK(B) and NAA(C) produced by the eclipse. Phase records on average normal (dashed line) are also shown.

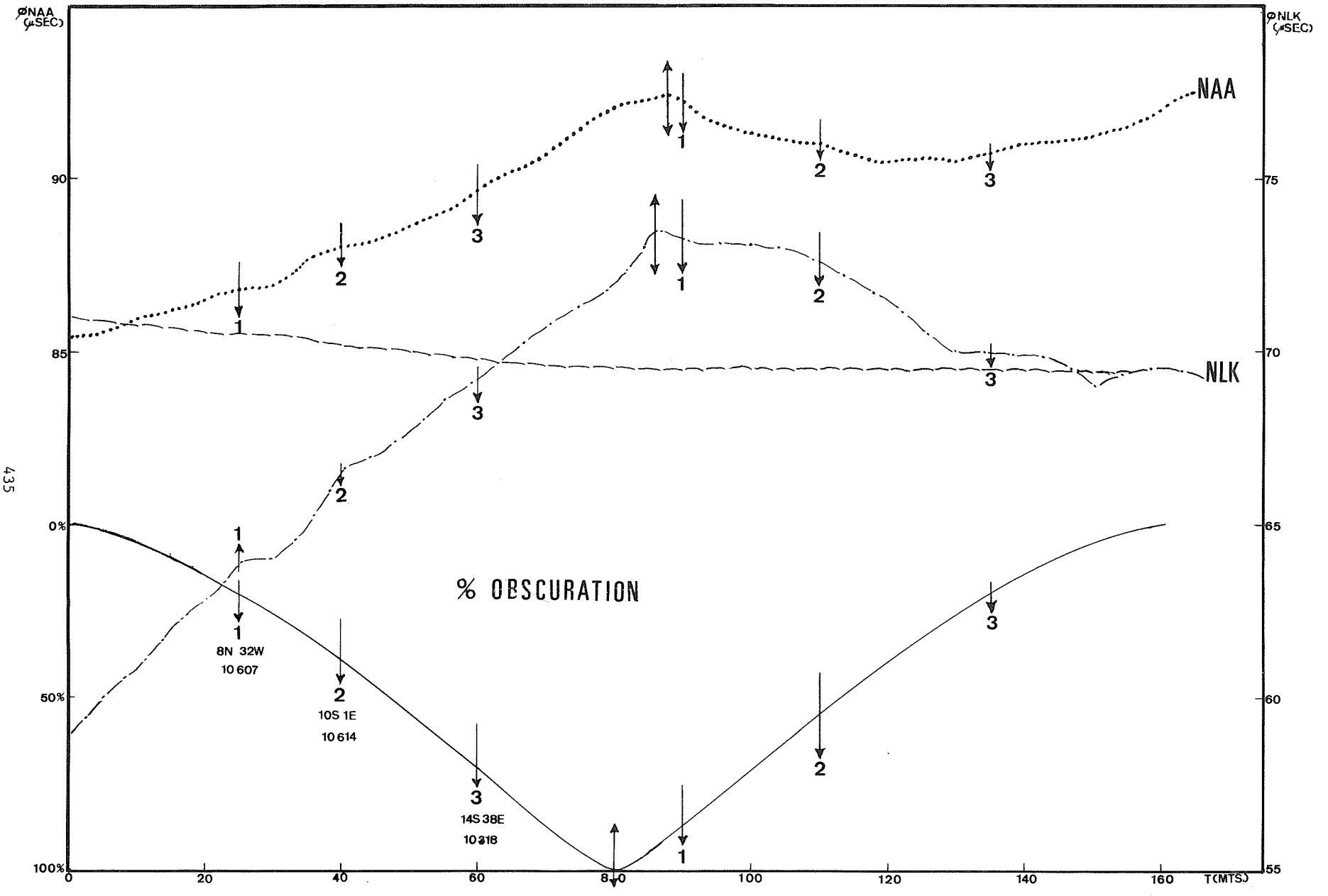

Fig. 3. Phase changes on NLK and NAA and the percentage obscuration of the sun's disk by the moon. Note the effects on the phase records as active regions 1, 2 and 3 successively covered and uncovered.

Deeks [1966] has used a general interpretation of VLF eclipse observations to construct electron density profiles. The theoretical phase variations expected from these profiles have been calculated using the full wave solutions of Wait and Spies. Table III gives the results of these calculations for NAA and NLK. No calculations were made for the Haiku-SP path, in view of the mixing up of the flare and eclipse effects. It should also be mentioned that no attempt was made to discriminate between the portions of path lying within the penumbral and umbral portions of the eclipse. Table III gives the results of these calculations.

As mentioned earlier, an SID which occurred at 1605 UT affected the phase and amplitude of both Haiku and NLK. The plage responsible for this SID had coordinates 14S 38E. Figure 3 shows a plot of the phase changes on NAA and NLK with time. Also shown is the percentage obscuration of the sun's disk by the moon. The arrows labelled 1, 2 and 3 correspond to the eclipsing and uncovering of active regions whose respective coordinates are also given. There is a time difference of 6 minutes and 8 minutes, respectively, between 100% obscuration and the phase maximum on NLK and NAA, respectively. It is also interesting to note that there are two distinct kinks on the phase curve corresponding to the eclipsing of regions 1 and 2. There is a noticeable effect present during the uncovering period also, as can be readily inferred from Figure 3.

Acknowledgements

It is a pleasure to thank Professor P. Kaufmann, E. Scalise, Jr. and R. E. Schaal for helpful suggestions. We also wish to thank Roberto Hanada and Berginia Maria Totti for assistance in the scaling of the VLF data, and part of the eclipse calculations. This work forms part of a program of research supported by the U. S. Army Element Defense Research Office Latin America, Grant No. DA-ARO-49-092-65-G77, Fundacao de Amparo a Pesquisa do Estado de Sao Paulo (FAPESP) and Conselho Nacional de Pesquisas (CNPq). One of us (S.A.) wishes to thank the Brazilian National Research Council and Mackenzie University for financial assistance during his stay here.

REFERENCES

DEEKS, D. G. 1966 D-Region Electron Distributions in Middle Latitudes Deduced from the Reflexion of Long Radio Waves, Proc. Roy. Soc., 291, 413.

HILDEBRAND, V. E. 1969 VLF Measurements of Time Lag During an Eclipse and Solar X-ray Bursts, Record of the Third Aeronomy Conference Report No. 32, Edited by C. F. Sechrist, Jr., Univ. of Illinois, 434.

WAIT, J. R. and K. P. SPIES 1964 Characteristics of the Earth-Ionosphere Waveguide for VLF Radio Waves, N.B.S. Tech. Note 300.

"LF Observations during a Solar Eclipse and Suggested Particle Precipitation Between March 6 and 14, 1970"

by

R. H. Doherty
U.S. Department of Commerce
Office of Telecommunications
Institute for Telecommunication Sciences
Boulder, Colorado 80302

The phase and amplitude changes on low frequency pulse signals are presented for a solar eclipse in March 1970 and for one in July 1963. Differences between the two sets of observations are tentatively attributed to seasonal changes in the ionospheric D region. During the period associated with the March 1970 eclipse, a solar proton event and an associated PCA occurred. The nighttime LF pulse observations showed rapid phase and amplitude disturbances, which have been tentatively interpreted as particle precipitation events. The disturbances first appeared on the more northerly latitude paths and several nights later appeared on the lower latitude paths.

Background

Solar Eclipse Measurements

Phase and amplitude observations of one-hop, ionospherically reflected LF pulse signals have been obtained for the period 1-14 March 1970 for the following propagation paths:

Nantucket, Massachusetts; Jupiter Inlet, Florida
(both directions, NT→JP, JP→NT)

Dana, Indiana; Jupiter Inlet, Florida
(both directions, DN→JP, JP→DN)

Dana, Indiana to Bermuda (DN→BR)

Dana, Indiana to Cape Race, Newfoundland (DN→CP)

Cape Race, Newfoundland to Nantucket, Massachusetts (CP→NT)

Cape Race, Newfoundland; Sandur, Iceland
(both directions, CP→SA, SA→CP)

Jupiter, Florida to Boulder, Colorado (JP→BO)

Nantucket, Massachusetts to Boulder, Colorado (NT→BO)

Cape Fear, North Carolina to Boulder, Colorado (CF→BO)

Phase and amplitude changes observed on all of these paths during this period constitute the basis for the discussions in this paper.

In July 1963, the path of a solar eclipse swept across the Aleutian Islands of Alaska and subsequently across Canada. Low frequency (100 kHz) pulse transmissions of the U.S. Coast Guard Alaskan Loran-C chain were observed in the one-hop sky-wave propagation mode for several paths of near solar eclipse totality. In addition, the three paths to Boulder, listed above, were partially eclipsed. Two of the paths in the Aleutian Islands where data were obtained were the following:

Sitkinak to Port Clarence (SK→PC, totally eclipsed)

Attu Island - Sitkinak
(both directions TT→SK, SK→TT 94 percent eclipsed)

See Figure 1 for a comparison of the paths observed in 1963 and those observed in 1970.

Nighttime Disturbances

For these low frequency pulse signals the daytime height of reflection is near 70 km and the nighttime height near 90 km. Over the 1830-km path between Nantucket, Massachusetts, and Jupiter Inlet, Florida, with a midpoint at 34°15'N, 75°28'W geographic, or 45°40'N, 352°20'E geomagnetic coordinates, rapid simultaneous phase and amplitude fluctuations are frequently observed at night.

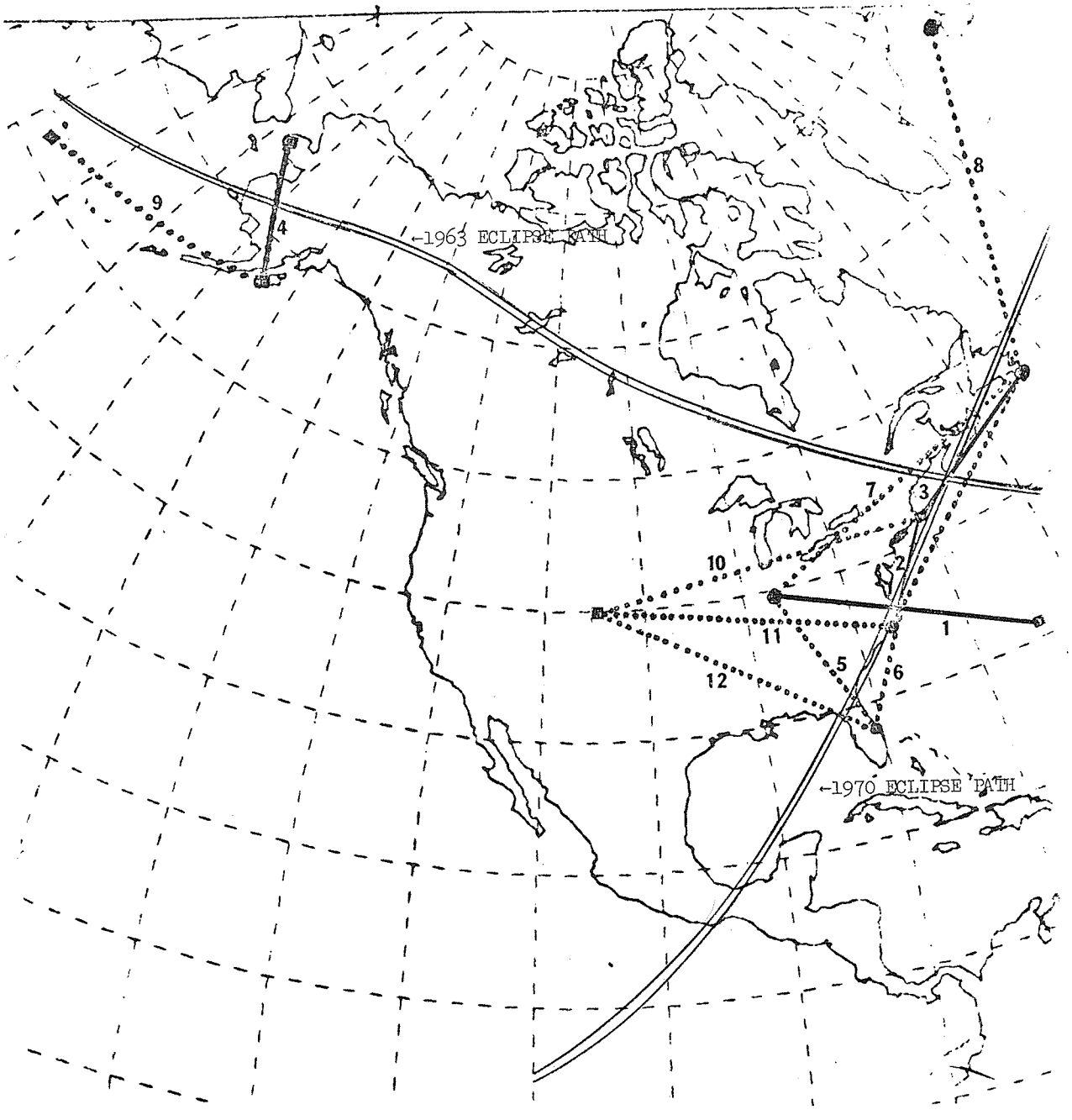

PATHS TOTALLY ECLIPSED _____ PATHS PARTIALLY ECLIPSED .....

1. DA → BR	1970		5. JP → DN	1970	94%	9. TT → SK	1963	94%	
2. CF → NT	1970		6. NT → JP	1970	96%	10. NT → BO	1963	74%	1970 63%
3. CP → NT	1970		7. CP → DN	1970	89%	11. CF → BO	1963	58%	1970 65%
4. SK → PC	1963		8. CP → SA	1970	84%	12. JP → BO	1963	46%	1970 72%

Fig. 1. Eclipse positions and paths monitored in 1963 and 1970.

Statistically these events occur more frequently near the equinox, seasonally; and near dawn, diurnally. They seem to occur more frequently on the path indicated above than they do on higher latitude paths situated at quite different geomagnetic longitudes, and they have not been observed on paths at geomagnetic latitudes below 30°N. A possible explanation for the greater sensitivity on the path mentioned above could be the fact that the midpoint of this path lies slightly west of the conjugate to the South Atlantic anomaly. Westward drifting protons suffering pitch angle diffusion in the South Atlantic anomaly might precipitate into this region.

Detailed correlation of both phase and amplitude as seen at both ends of reciprocal propagation paths tend to rule out gradients, offpath reflections, or instrumentation as causes for producing these events. Investigations in which several different propagation paths were used suggest that these effects may be quite localized, but that paths with similar geomagnetic latitudes may be similarly affected even when they are separated by more than 100° in geomagnetic longitude. Nearly simultaneous events have been observed on paths widely separated in longitude but at similar geomagnetic latitudes at times when comparable paths at different geomagnetic latitudes were extremely quiet. Figure 2 illustrates a highly disturbed night in October 1969. The detailed structure as seen at opposite ends of the same propagation path is highly correlated. The records for a normal quiet night would show fluctuations of no more than 2 or 3° and 1 or 2 dB in amplitude during a comparable 3-1/2 hour period. This phenomenon is more thoroughly covered by Doherty [1971].

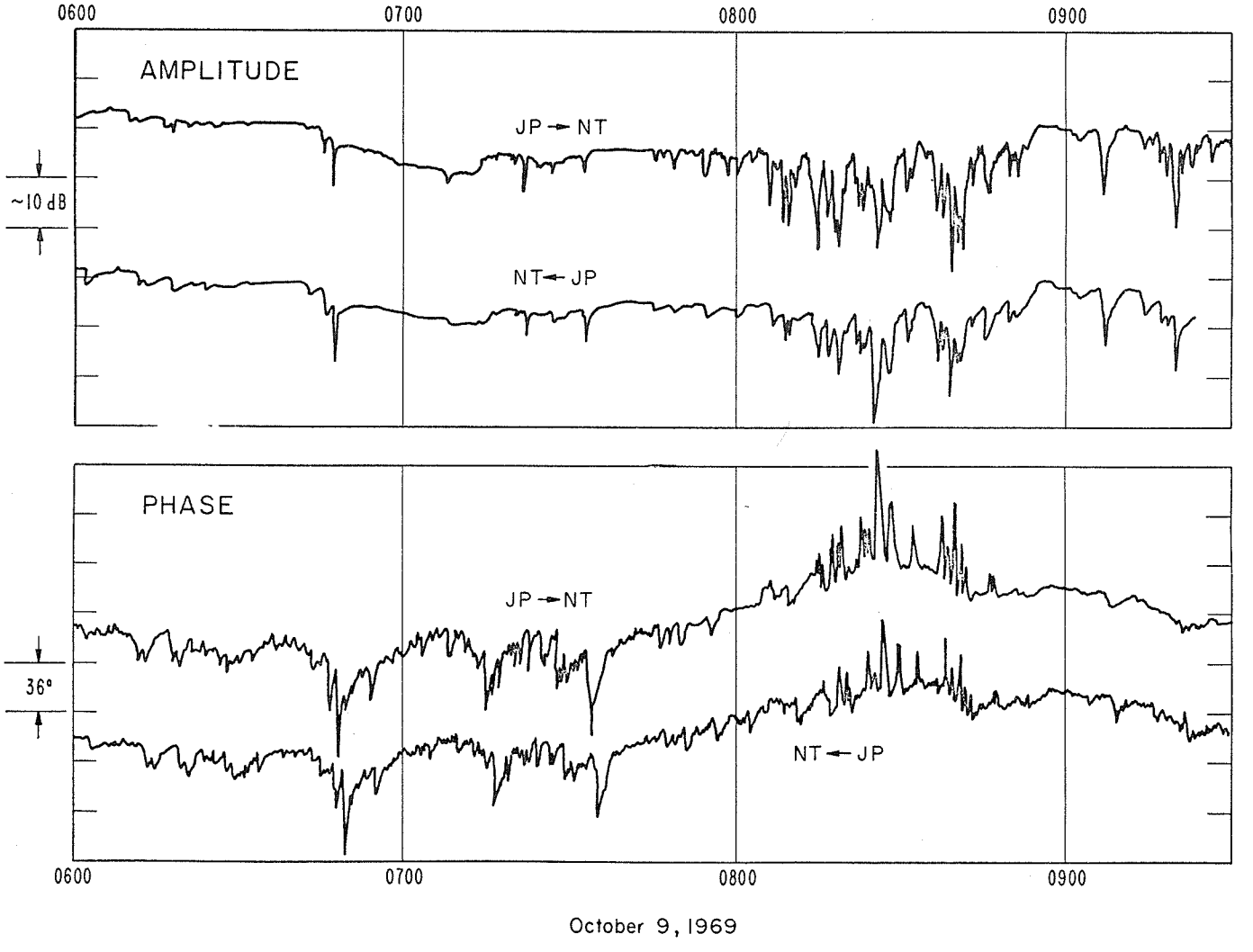

Fig. 2. A disturbed night as seen at opposite ends of a propagation path.

Results of the Solar Eclipses

During the March 1970 solar eclipse, LF pulse observations were made over several paths of eclipse totality or near totality in the U.S. The path midpoints ranged from 34° to 56°N latitude, and the path lengths ranged from 1000 to 3000 km. The effects observed during this eclipse were rather rapid phase retardations near the eclipse totality, with the maximum apparent height of reflection occurring 5 min after totality; a rather small amplitude change was observed, with the maximum signal level occurring slightly before the eclipse totality. It should be pointed out that on March 7, 1970 a solar flare occurred less than 1 hour before the eclipse started. This flare appreciably affected all the LF skywave signals, and they had not returned to normal conditions by the time the solar eclipse began. The flare effects may partly account for the amplitude maximum occurring before the time of maximum obscuration, but a complete explanation of this phenomenon is not easy. Figure 3 presents the phase and Figure 4 the amplitude for several of the totally or near totally eclipsed paths on March 7, 1970. The results observed for this eclipse were similar on all of the observation paths, but were considerably dissimilar from the results observed for the July 1963 eclipse. Figure 5 shows the comparison between the 1963 and 1970 observations for paths of totality or near totality (1970 path is from Dana to Bermuda).

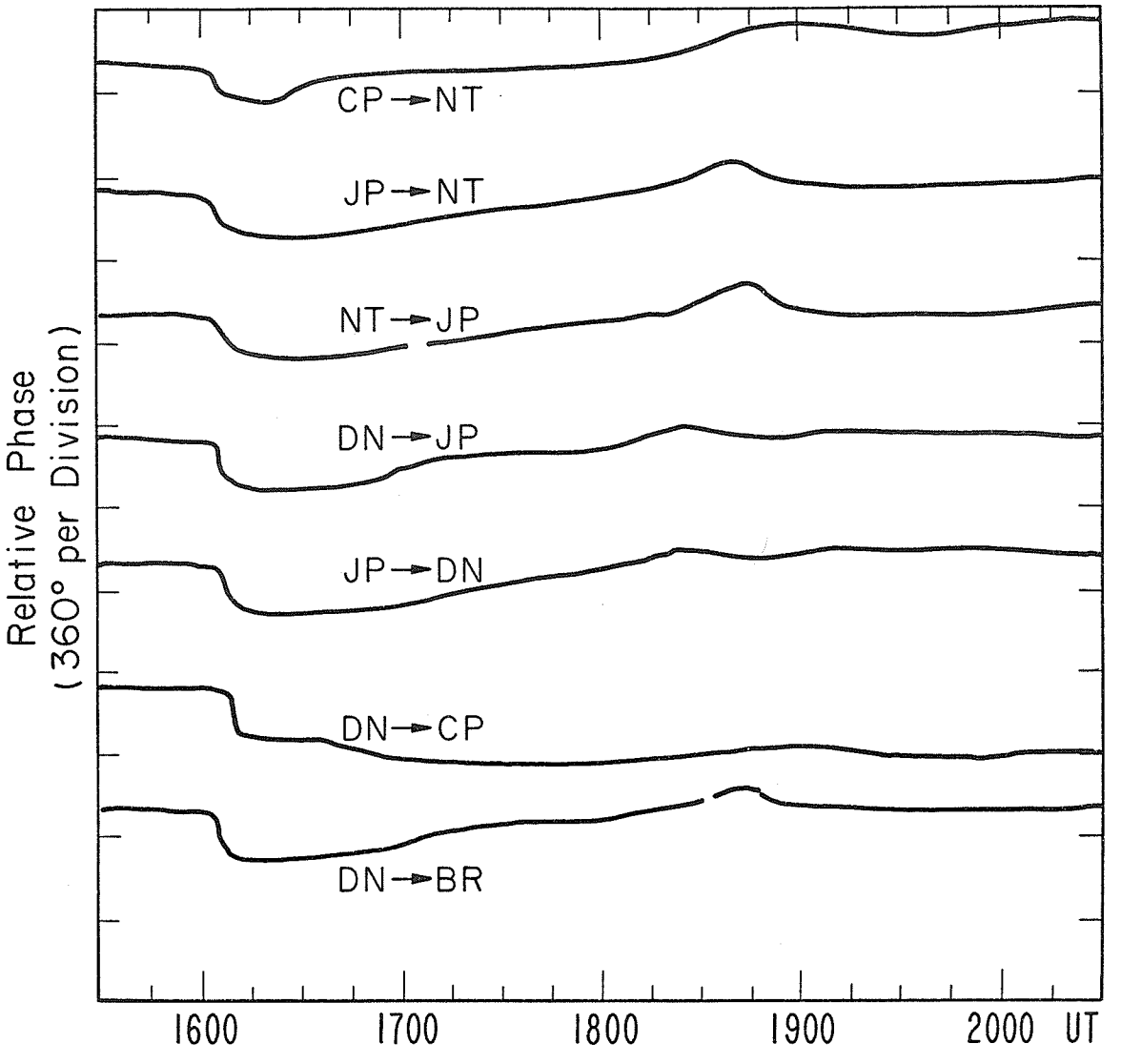

Fig. 3. Phase measurements for several eclipse paths in 1970.

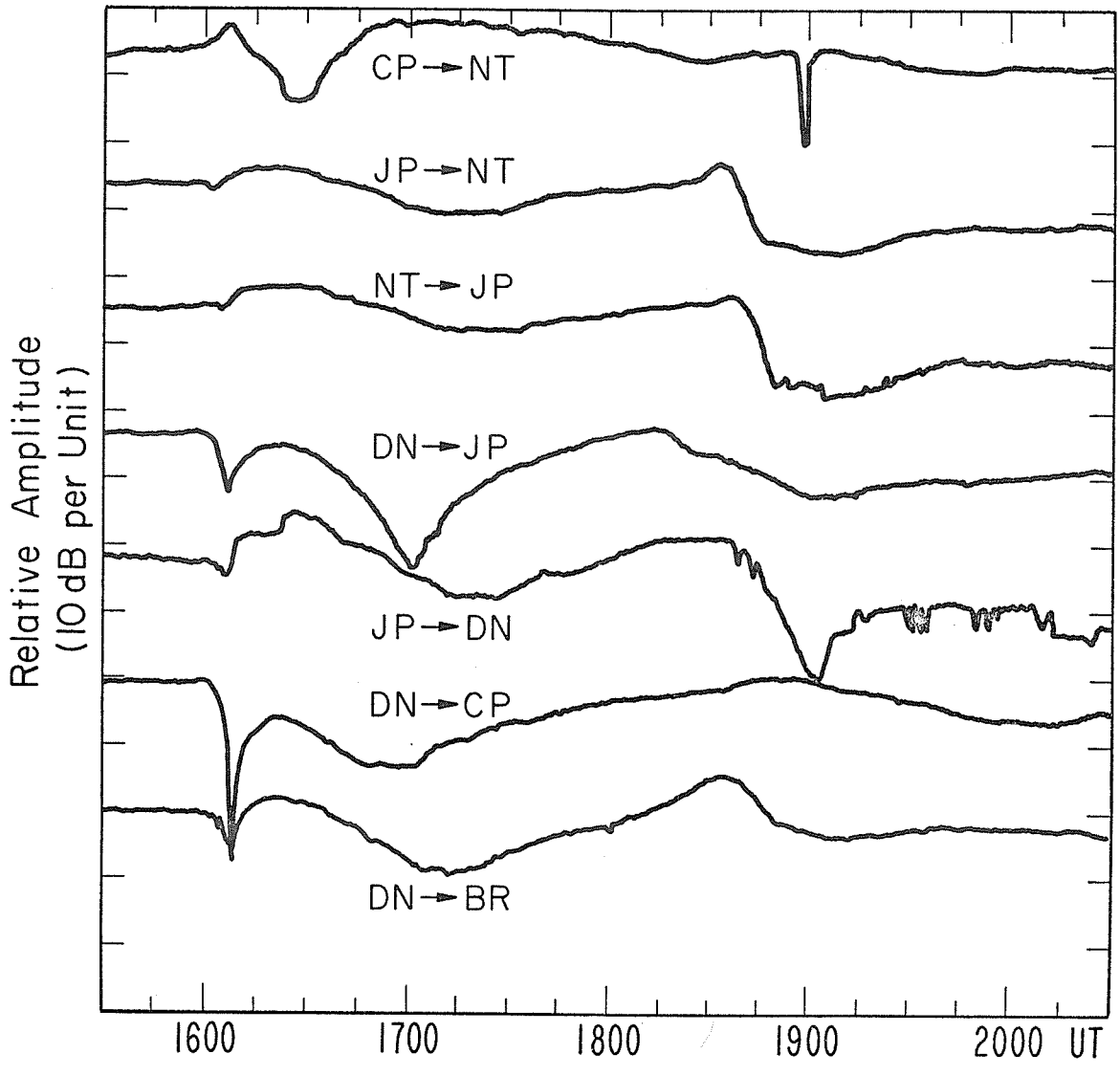

Fig. 4. Amplitude measurements for several eclipse paths in 1970.

The 1963 eclipse results have been described by Doherty [1968, 1970], but a brief review is presented here. The retardation of the phase of the ionospheric signal from Attu to Sitkinak was nearly proportional to the increasing solar obscuration, indicating a maximum apparent reflection height near maximum obscuration. Following the maximum obscuration, the phase advanced with an overshoot following the end of the eclipse (see Figure 5). This pattern was shown to be similar to a theoretically calculated change in ozone densities at heights above approximately 65 km. The amplitude of the LF pulse signal over the totally obscured path from Sitkinak to Pt. Clarence increased rapidly near the eclipse totality and reached a maximum value 4 min. after the time of totality. These changes were shown to be similar to calculated changes in the atomic oxygen density for heights below about 65 km. except for the 4-min. delay, which was attributed to an ionic reaction time constant that would exceed 4 min. if the [O] $<10^8$ atoms/cm^3 during the eclipse.

Figure 6 shows the comparison of data observed over the partially obscured path between Cape Fear, North Carolina, and Boulder, Colorado, for both the 1963 and 1970 eclipses. Although the observations for the 1970 eclipse occur during the recovery phase of the solar flare, it is apparent that the effects of the partial eclipse on this path must be far less in 1970 than they were in 1963. This is true even though the path was slightly more obscured in 1970 than in 1963 (65 percent as opposed to 58 percent). The greater effect of the eclipse on the propagation paths in 1963 than in 1970 can be seen on all of the partially eclipsed paths.

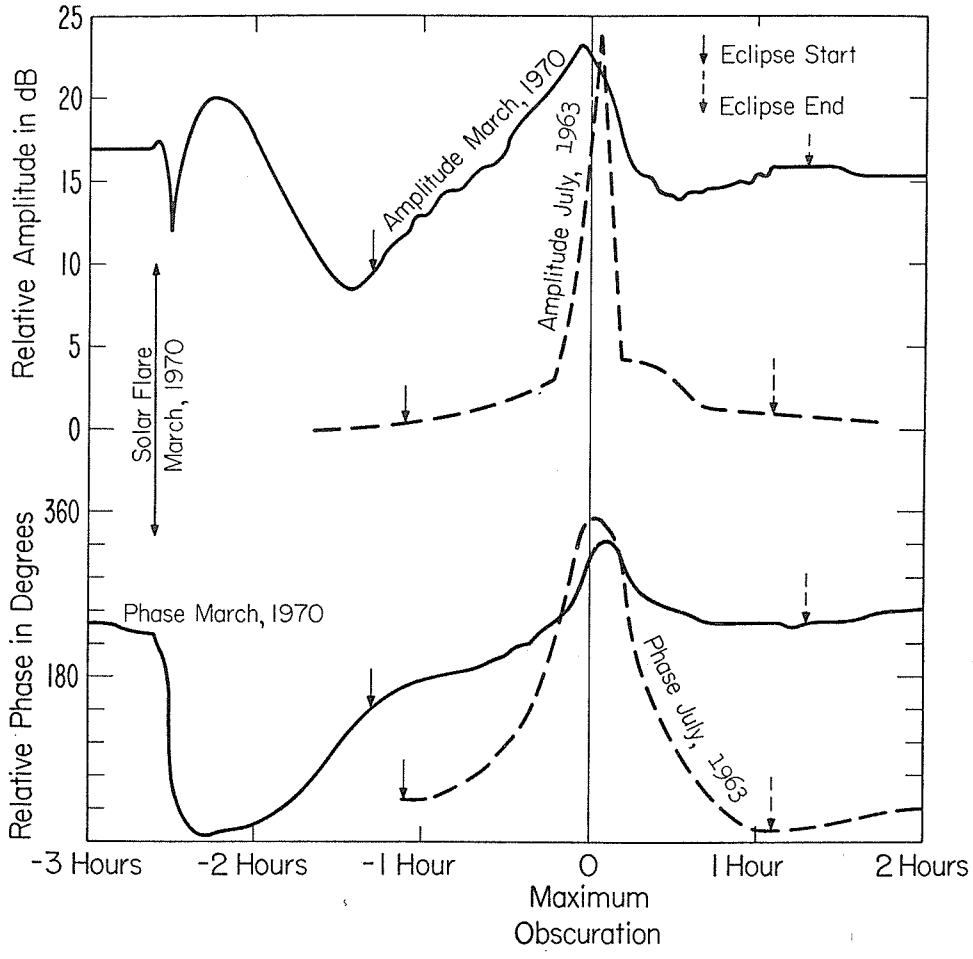

Fig. 5. Comparison of paths of eclipse totality in 1963 and 1970.

Suggested Particle Precipitation Related to the March 6th PCA

On March 6, 1970, a solar proton event and a resulting PCA were observed. On the night following the solar eclipse, nighttime disturbances were observed on the paths from Cape Race, Newfoundland, to Nantucket (midpoint at 55°43'N, 8°57'E geomagnetic), Nantucket to Boulder, Colorado (midpoint at 52°49'N, 358°49'E geomagnetic), and Attu Island, Alaska, to Pt. Clarence, Alaska (midpoint at 54°2'N, 234°41'E geomagnetic). Figure 7 shows large and rapid amplitude variations on the signals received at Nantucket from Cape Race, at Attu Island from Pt. Clarence, at Pt. Clarence from Attu Island, and at Boulder received from Nantucket, respectively, from the top trace to the bottom trace. The activity also occurred on these paths for two nights following the one shown. On all three of these nights, paths at lower latitudes showed no activity at all; on March 12, 1970, activity began on the lower latitude paths. Figure 8 shows a comparison for the lower latitude paths. The top three traces show the phase fluctuations seen at Nantucket from Jupiter, at Jupiter from Nantucket, and at Bermuda from Dana, Indiana, respectively. The bottom three traces show the amplitude variations for these same three paths in the same order. The path from Dana to Bermuda is 2196 km long, which is somewhat longer than from Nantucket to Jupiter, and generally the events observed at Bermuda were considerably smaller than those on the Nantucket-Jupiter path.

On the night of March 14, activity was noted on most of the propagation paths monitored. Although this was not as active a night as the 12th or 13th on most of the paths, there was one particularly large event that occurred at 0329 UT that could be identified on several of the paths monitored. Figure 9 shows the results of this event observed on the different paths. The event produced the largest effect on the path from Nantucket to Boulder, and no effect was observable on the path from Cape Race to Nantucket. The effect observed on the Nantucket to Jupiter path was very small, but that observed on the Dana to Bermuda path was relatively large. The longitudes of the midpoints of the Nantucket-Jupiter and Dana to Bermuda paths are identical; the midpoint of the Dana to Bermuda path is only 2° farther north than the other path. The results suggest that the effect cuts off rather abruptly at a certain latitude. Since no effect was seen on the Cape Race to Nantucket path, this suggests a

cutoff on the longitude also. This particular event appeared to cover a range of at least 20° in latitude and at least 10° in longitude. This event was different in this respect from the more frequently observed events in that they seem to be quite localized in area of coverage; however, this event was of short duration, which helped isolate it as a discrete event on the different paths.

These comparisons are significant because of the close correlations of the particular events as seen on signals for paths monitoring different parts of the ionosphere. The close correlations would appear to rule out such things as gravity waves, gradients, blobs, or irregularities in the ionosphere as causes of the events. Probably the only known phenomenon that could produce such close correlations at widely separated locations would be a particle precipitation event, where the same 'dumping' mechanism affects all the paths involved.

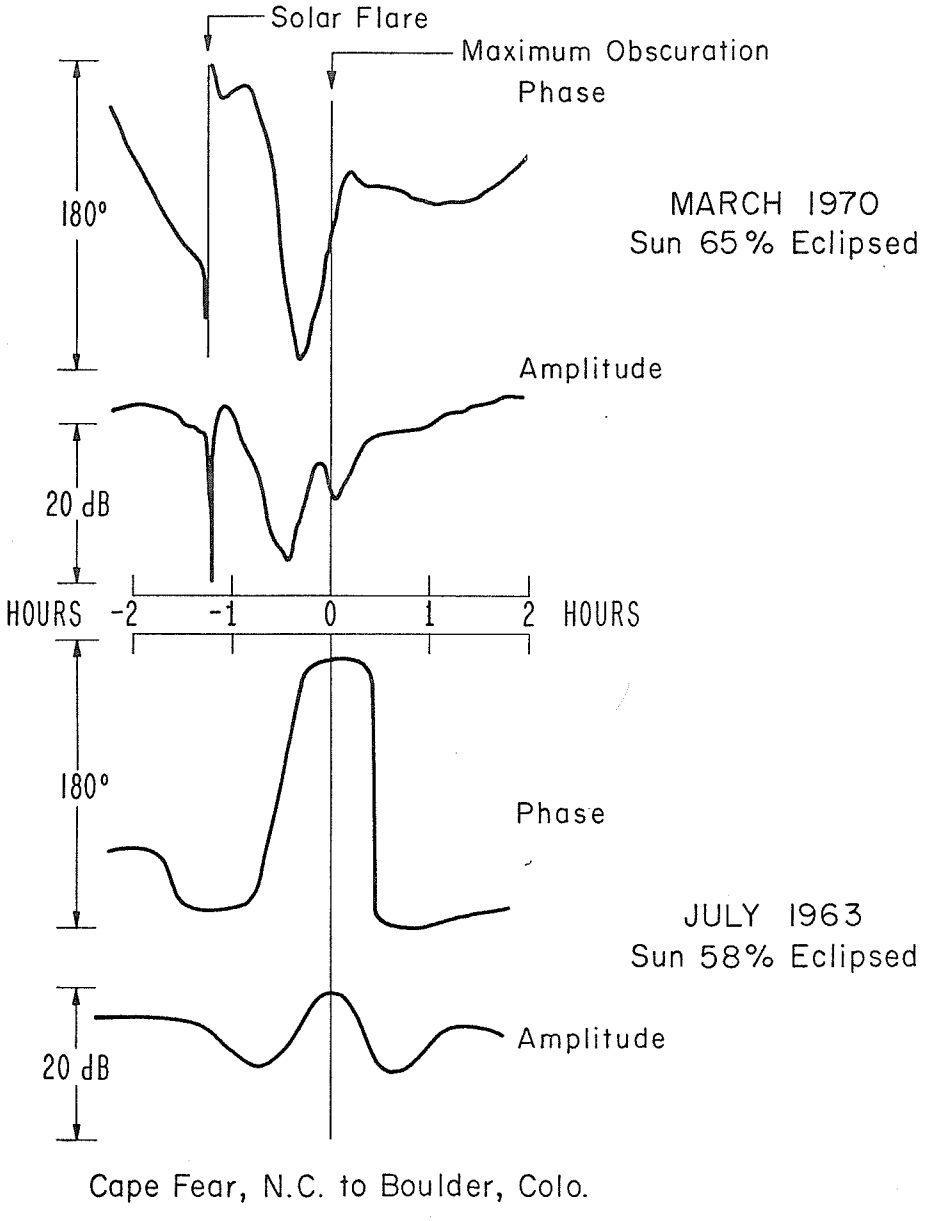

Fig. 6. Comparison of the partial eclipse measurements between Cape Fear, North Carolina, and Boulder, Colorado, for 1963 and 1970.

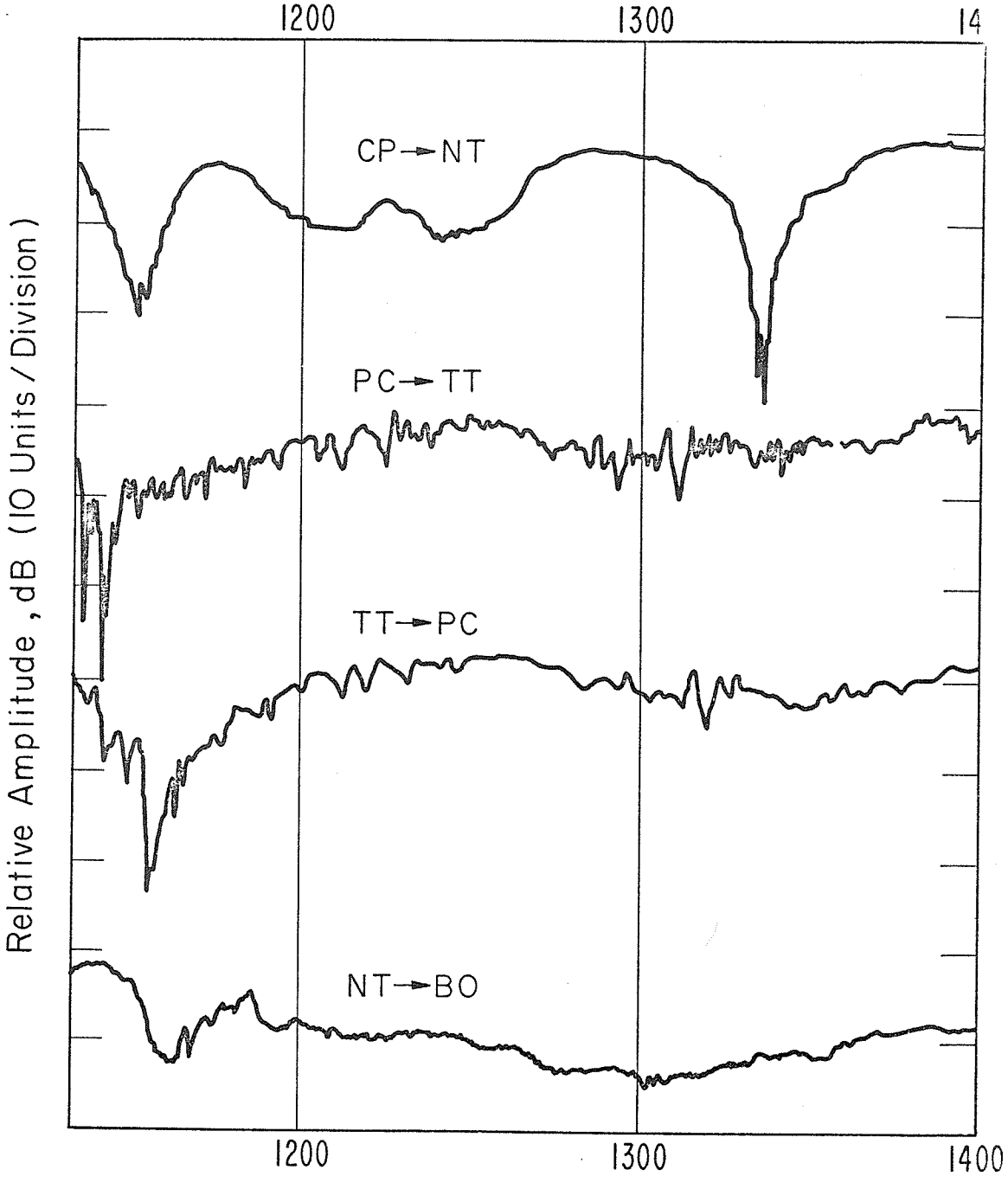

Fig. 7. Disturbances observed on higher latitude paths on the night of March 8, 1970.

Conclusions

Aside from the problems produced by the solar flare preceding the eclipse, it is interesting from an ionospheric standpoint that the eclipse-produced effects were so different in March 1970 and July 1963. These differences might be attributed to different times in the solar cycle, different locations or path lengths for the measurements, or different seasons of the year. Since in both cases the eclipse occurred near local noon, different times of day should not be a factor. Routine LF skywave observations suggest that the propagation does not change appreciably with the solar cycle except from an increase in flare-produced effects observed during solar maximum. The measurements in March 1970 covered several latitudes and several path lengths; if latitude or path length were a factor, the results from this eclipse should therefore have changed from path to path. Also the

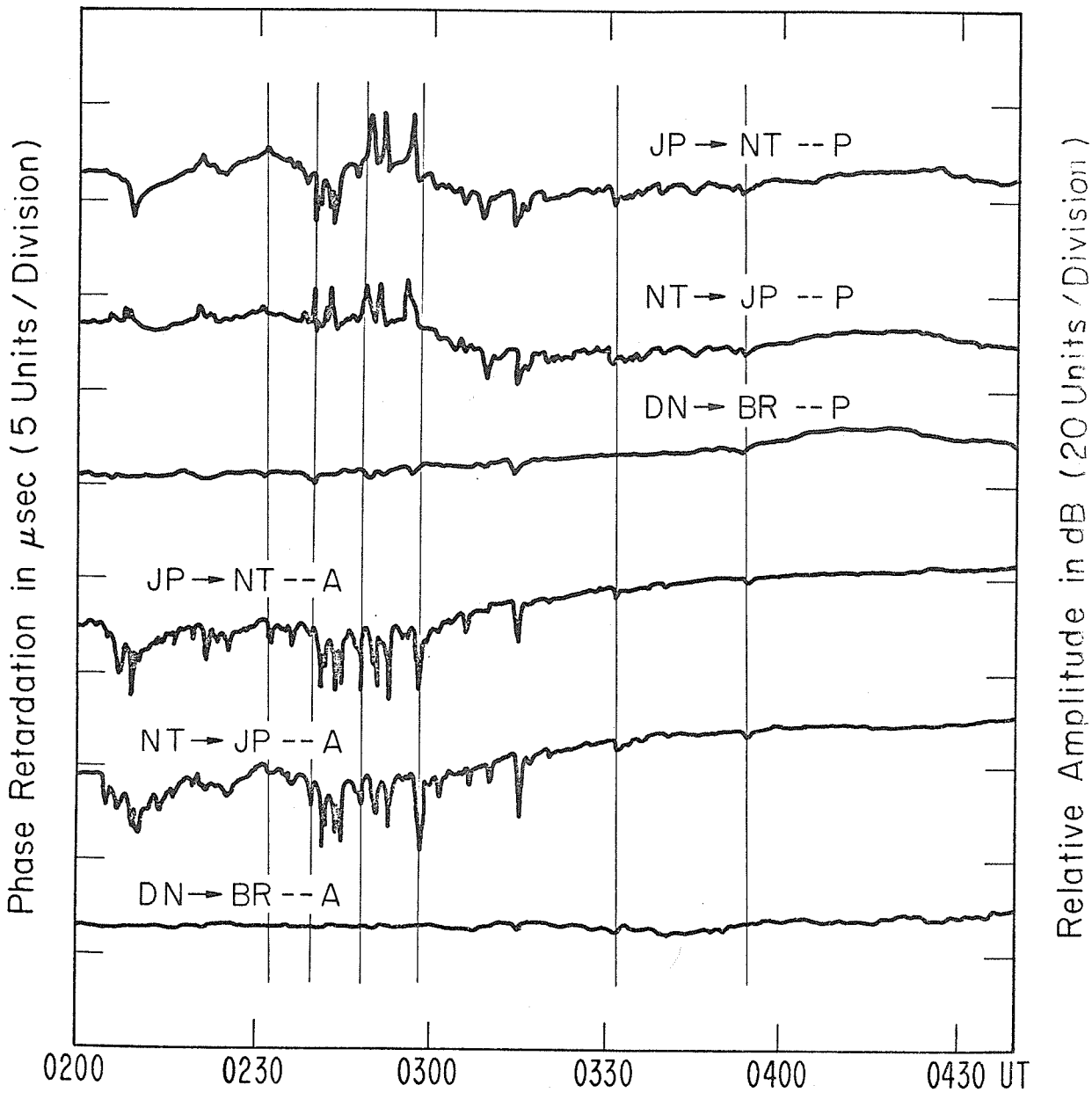

Fig. 8. Disturbances observed on lower latitude paths on the night of March 13, 1970.

comparison shown in Figure 6 indicates that the eclipse effects were different between July 1963 and March 1970 even on the same propagation path.

Seasonal propagation changes do occur; they are similar in the United States and the Aleutian Islands of Alaska. They produce a lower reflection height and greater ionospheric absorption in July than in March. A lower reflection height and greater signal absorption could relate to increased electron densities associated with increased atomic oxygen production and concentrations during summer months. This relation could exist from associative detachment of electrons from O_2^- by atomic oxygen [LeLevier and Branscomb 1968]. The daytime atomic oxygen density profile would be expected to be lower in height in the summer than in March because more solar energy is available in the summer. Therefore, the five-min delay between the eclipse maximum and the phase peak observed in March could have been caused by the same mechanism that produced the four-min delay in the amplitude peak in the July measurements. If the apparent height of reflection in March is determined by the atomic oxygen density profile, few electrons would be produced by associative detachment by atomic oxygen at heights below this reflection height because of rapidly decreasing

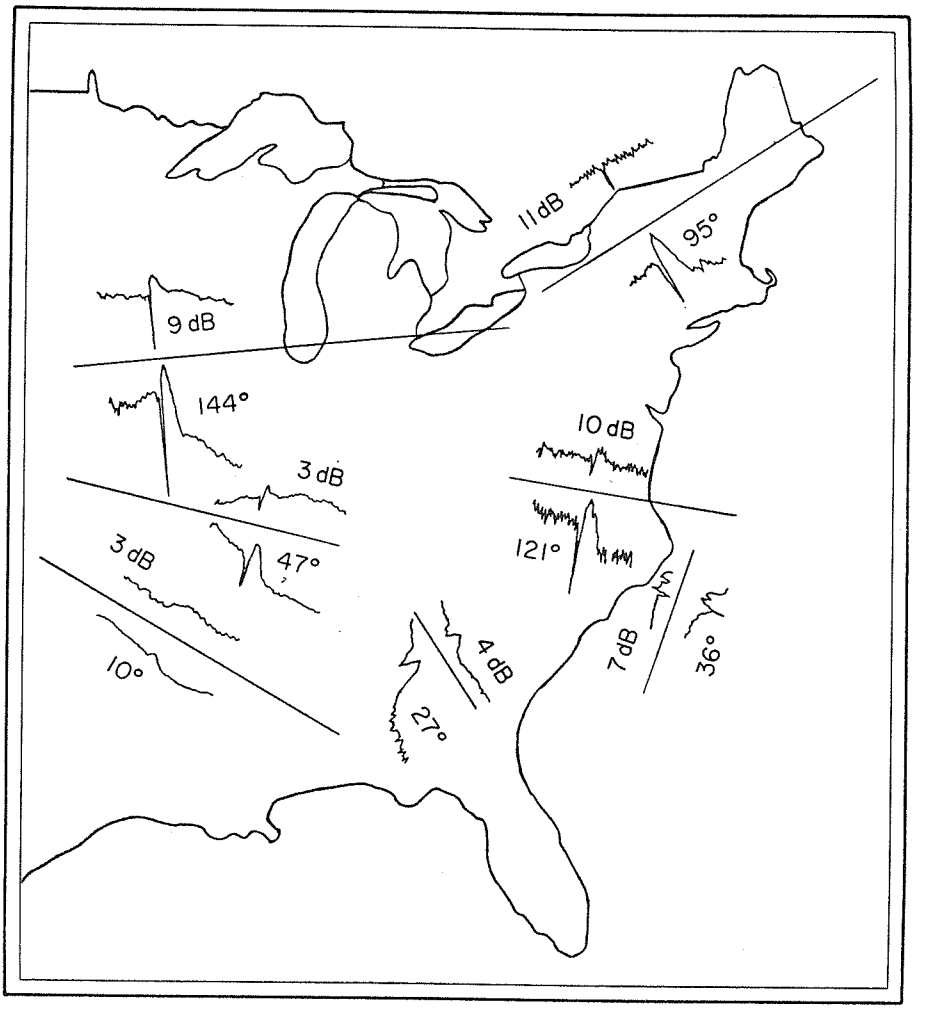

Fig. 9. Disturbances observed simultaneously on many paths at 0329 on March 14, 1970.

atomic oxygen densities. Large amplitude changes, such as those observed in July, would not be expected to correlate with changes in the atomic oxygen density in this case.

It has not been possible to show a direct one-to-one relation between other geophysical phenomena and the occurrence of the LF nighttime disturbances. There is a strong tendency for the occurrence of these events to follow solar disturbances that produce proton fluxes capable of causing PCA events. This may be more related to large magnetic disturbances associated with proton events, than the proton fluxes per se.

Ionospheric propagation at this frequency is very sensitive to relatively small changes in electron densities in the D region. Oblique paths covering distances up to the geometrical optical horizon are influenced by a minimum ionospheric area affecting the reflection. Oblique paths that extend well beyond this distance into the diffraction region are influenced by much larger areas in the ionosphere, as are long range VLF cw transmission paths. The nighttime events described above become less pronounced as the path length is increased, suggesting that they are quite localized and that the integrating effect of longer paths tend to mask the effects. Particle fluxes capable of producing electrons in the 10 to 100 $e/cm^3 sec$ range near 80 km at night would be expected to produce variations such as those measured. These LF pulse measurements over oblique paths may prove to be an excellent method for detecting leakage or dumping of charged particles from the radiation belts into the lower ionosphere.

Acknowledgements

The author wishes to acknowledge both logistic and monetary support for all of the above measurements to Headquarters U.S. Coast Guard (EEE4/63). Without their excellent cooperation and support very few of the measurements would have been possible. The author also wishes to acknowledge the loan of two Loran-C receivers by A.G.M.C. Newark Air Force Station from 1 to 15 March 1970.

REFERENCES

DOHERTY, R. H. 1968 J. Geophys. Res., 73, 2429

DOHERTY, R. H. 1970 J. Atmos. Terrest. Phys., 32, 1519

DOHERTY, R. H. 1971 Radio Science, To be published

LELEVIER, R. E. and L. M. BRANSCOMB 1968 J. Geophys. Res., 73, 58

"Radio Observations during March 7-8, 1970 at the University of Michigan"

by

Newbern Smith *
Department of Electrical Engineering
The University of Michigan

The ionosonde was operated at its temporary location at Willow Run, Michigan, N42°14' W83°31' from 6 March 1700 EST (2200 UT) to 8 March 1800 EST (2300 UT), at which time an equipment failure occurred. The temporary antenna was a long horizontal folded dipole with a resistor at the feed point to prevent overload at resonant frequencies. This antenna did not have good radiation characteristics between 6 and 8 MHz, or over 13 MHz; consequently, received echoes were occasionally below the noise, especially at night.

The operation of the sounder was resumed on 12 March and continued until 28 March. Thus, it was possible to obtain a median curve for March to compare with the eclipse day and the data during the geomagnetic disturbance on March 6-8.

During the eclipse day, March 7, data were taken from 1225 to 1459 EST at five minute intervals, and half-hourly at other times. The eclipse period was about 1230 to 1440 EST, with the middle about 1330. As noted on the field-strength recordings, there was a solar flare shortly after 1100 EST on 7 March. This showed up as a loss of the E and F1 traces at 1120 and 1149 EST, but did not erase the foF2.

The f-plots for 7-8 March are given in Figure 1. Also shown are the March foF2 and foE medians; the F1 cusps were not usually sufficiently developed to obtain significant median values.

The f-plot for the eclipse day, March 7, (Figure 2) shows significant eclipse effects. During the eclipse a well-developed F1 cusp appeared, splitting into several stratifications during the maximum phase of the eclipse. Compared with the small F1 inflections before and after the eclipse, the foF1 at the maximum phase were 0.7 to 0.85 of normal.

In the case of the E region, the minimum foE occurred at 1350 EST and was about 0.765 of the monthly median value. Considering that the degree of the eclipse at Detroit was 0.778, that Willow Run is about 35 miles west of Detroit, and that the maximum degree of the eclipse at 100 km altitude was less than at the ground, the degree of the E-layer eclipse was estimated to be about 0.73. The corresponding fraction of the solar disk left uneclipsed is 0.34. If foE is proportional to the fourth root of the solar flux, and the solar flux is taken as proportional to the uneclipsed area of the solar disk, one would expect the minimum foE to be $\sqrt[4]{.34}$ of normal, which is consistent with the observed fraction 0.765 of the median value. It should be noted, however, that the foE before and after the eclipse was slightly lower than the median; using this as a reference, the foE decrease was to 0.785 of normal.

The bay in the foF2 covers the same time span as those in the foF1 and foE. It strongly suggests a real F2 effect, although the variation is no greater than is sometimes observed under normal or somewhat disturbed ionospheric conditions. It is of interest to recall that during one of the early ionospheric eclipses observed, in February 1935 by Gilliland et al. [1936] a similar F2 effect was seen, whereas in one or more summertime eclipses no F2 effect was noticed.

Generally, the F2 plots show the presence of disturbance, as evidenced by the persistent spread-F and depressed night foF, accompanied by high h'F. The dramatic disappearance of F2 echoes at 1000 EST on March 8, followed by a short period of high electron density from 1350 to 1550 EST and then nearly or completely unstructured reflections from the F region, indicates the existence of severely disturbed conditions.

Lake Angelus Riometer Record

The 18 MHz riometer trace for March 7 and 8, obtained at the McMath-Hulbert Observatory, was examined to see if any eclipse effects were seen (See Figure 1). No such effects were obvious, but large fluctuations were observed starting at 0800 EST March 8. The absorption increased greatly after 1330 EST, causing complete loss of signal between 1400 and 1450 EST. This suggests possible polar cap event observed at the latitude of Detroit, about 53° geomagnetic.

Field-Strength Records

The field strength of WWV (10 MHz) at Fort Collins, Colorado, is recorded on a strip chart at the McMath-Hulbert Observatory, Lake Angelus, Michigan, as a part of their solar patrol work. The record chart is not calibrated, but the system for receiving and recording is conventional and is known to produce an approximately logarithmic scale over a dynamic range of 30 to 40 dB.

* currently Guest Worker at Institute for Telecommunication Sciences, Boulder, Colorado.

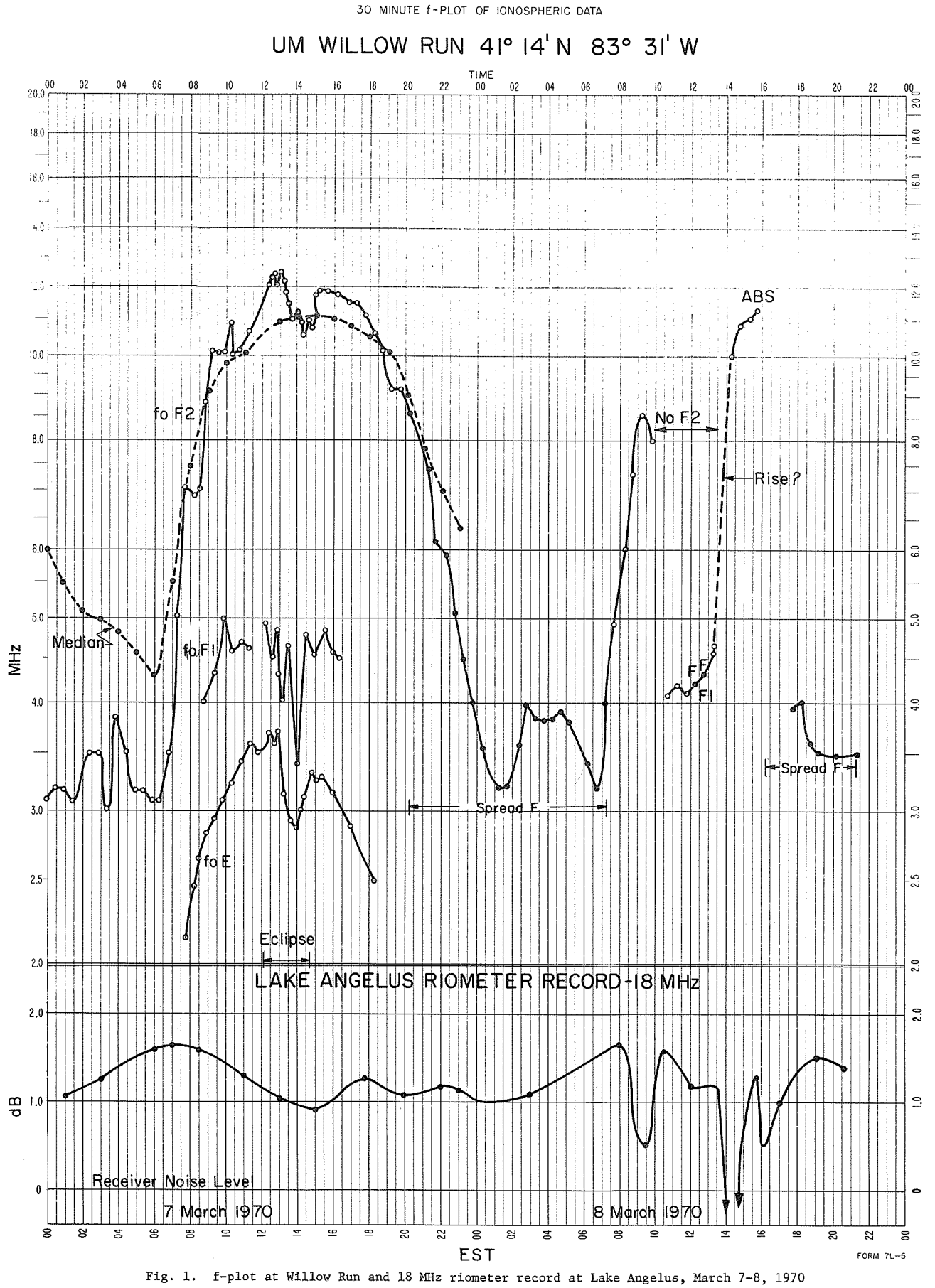

Fig. 1. f-plot at Willow Run and 18 MHz riometer record at Lake Angelus, March 7-8, 1970

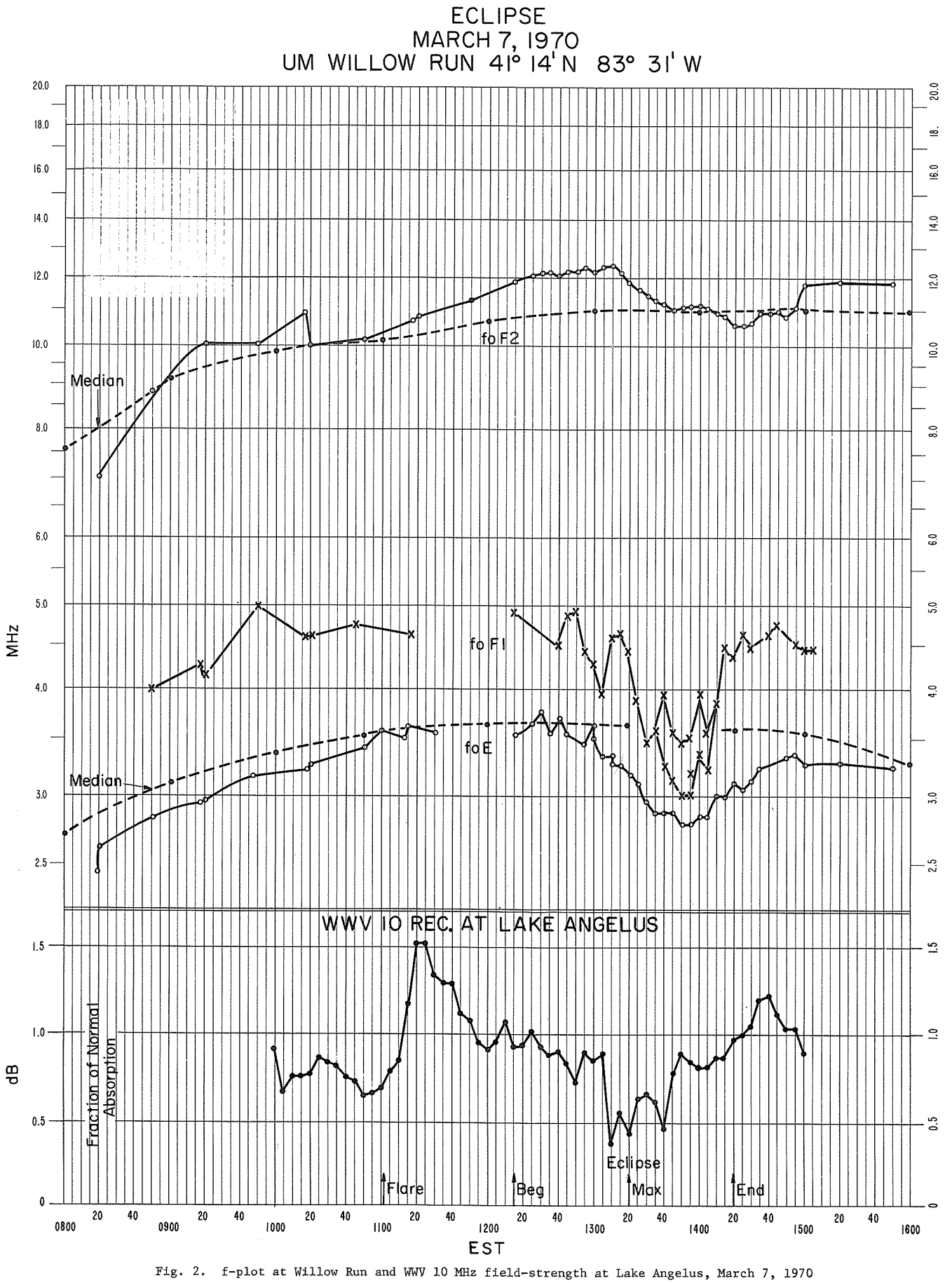

Fig. 2. f-plot at Willow Run and WWV 10 MHz field-strength at Lake Angelus, March 7, 1970

The recordings were scaled in arbitrary linear units for March 7, 1970, the day of the eclipse, and also for March 6, which appeared to be a normal day; the quantity scaled was the 5 minute median value, for each 5 minutes of the day from 1000 EST to 1500 EST.

The highest 5-minute mean field strengths at night were taken to represent zero absorption. The absorption was then calculated for the above periods as the difference between the scaled values and the zero-absorption value. To normalize the absorption the differences on March 7 were divided by the March 6 differences. These quotients then represent the percentages of the normal decibel absorption for the day of March 7; Figure 3 gives a graphical plot of the values.

The solar flare beginning at 1106 EST is associated with a rise in absorption to 1.5 normal, in what appears to be a slow-SWF. During the eclipse there is a 40 minute period of significantly less-than-normal absorption, reaching a minimum of about 0.4 to 0.5.

Considering the degree of eclipse to be 0.47 at Denver, 0.715 at Chicago and 0.78 at Detroit, we can estimate the corresponding fractions of maximum solar flux as 0.65, 0.36, and 0.28 for the middle of the eclipse, making the questionable assumption that the flux is uniform over the solar disk. On this assumption, the average flux over the Denver-Detroit path is 0.43 normal at the middle of the eclipse. This suggests that the decibel absorption is proportional to the solar flux, or ionizing radiation, which is not inconsistent with the conventional processes in the D region.

Relative Phase Path Measurements

Recordings were made of the relative phase path length between Fort Collins, Colorado (WWVB, 60 kHz) and the High Altitude Research Laboratory of the University of Michigan at Ann Arbor, Michigan, using a strip chart recorder. The recorder was not well calibrated as to the drift rate, so that there was some lack of precision in determining a reference phase; the reference was obtained by examining the night recordings for days that seemed to be undisturbed. It is believed to be a reasonable one within a microsecond or two.

The recordings were made in terms of the relative delay time in microseconds. The days of March 9 and 10 appeared to be relatively undisturbed, the data for March 10 were used to represent a "normal day".

Figure 4 gives the relative path delay in microseconds, compared to the assumed nighttime reference described above, for the days of March 7 and 8 (disturbed days, shown by solid lines) and the "normal day" (shown by dashed lines).

No particular eclipse effect is obvious on the March 7 record. It is obvious, however, that the traces for at least 0600 March 7 to 1800 March 8, EST, are markedly different from the normal. No particular interpretation is given at this time. It may be noted, however, that if a simple geometrical model is used for the propagation path, the incremental phase delay in microseconds happens to be about equal to the incremental reflection height in km.

REFERENCE

KIRBY, S. S., T. R. GILLILAND and E. B. JUDSON 1936 Ionospheric studies during the partial solar eclipse of February 3, 1935, NBS J. of Res., 16, 213-225

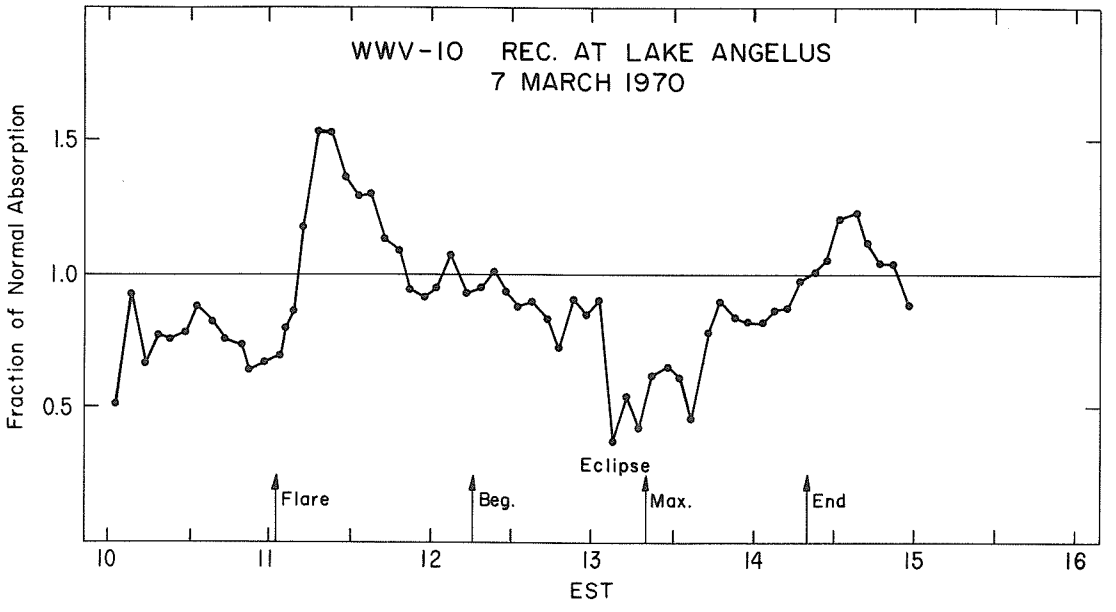

Fig. 3. Field-strength of WWV 10 MHz at Lake Angelus, March 7, 1970

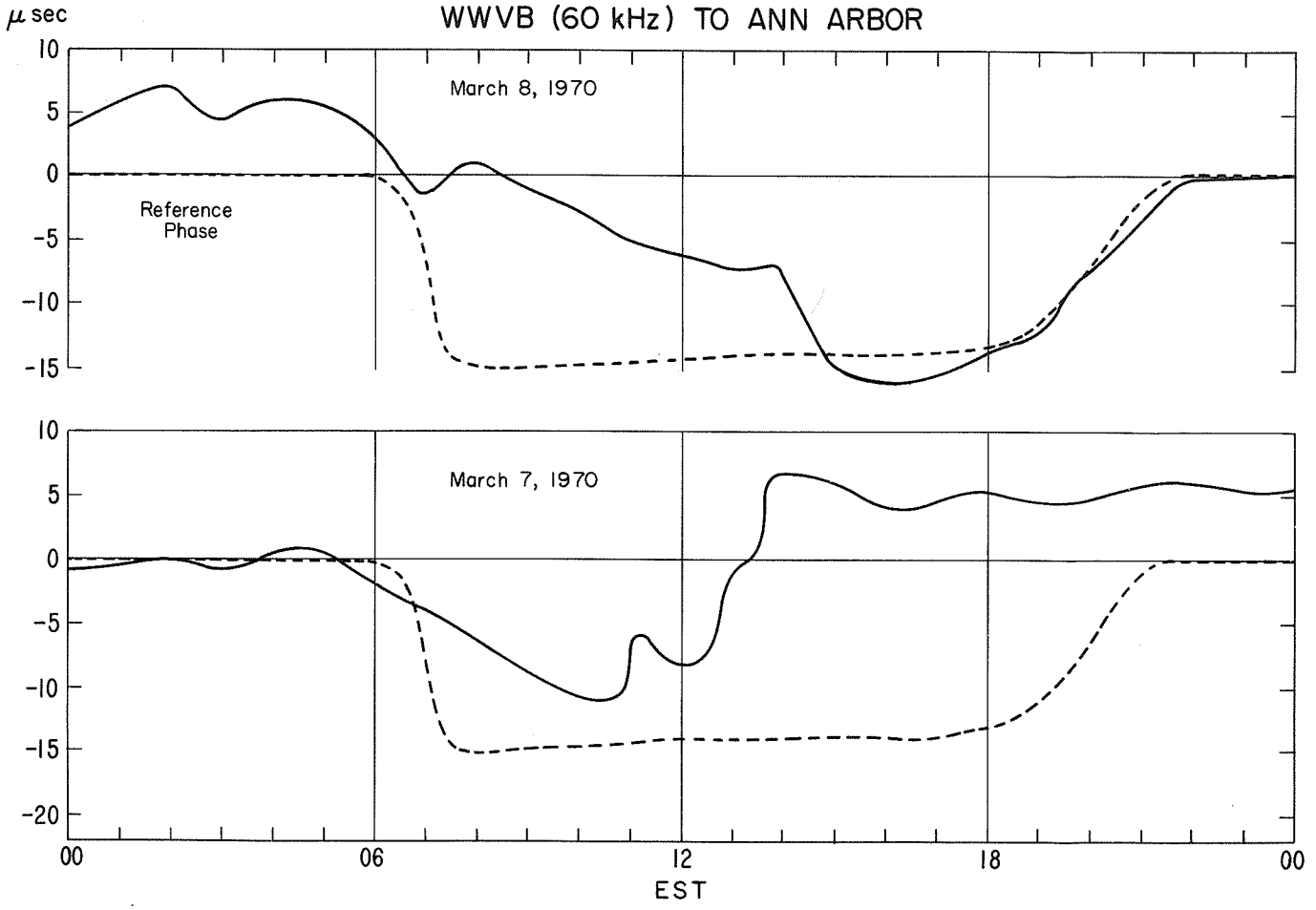

Fig. 4. Relative path delay of WWVB 60 kHz recorded at Ann Arbor March 7-8, 1970

"Normal Magnetic and Micropulsation Observations in Canada During the March 7, 1970 Solar Eclipse"

by

R. J. Stening, J. C. Gupta, G. Jansen van Beek
Earth Physics Branch
Energy Mines and Resources, Ottawa, Canada

Introduction

To study the effect of the eclipse on geomagnetic variations, four stations situated on a line approximately at right angles to the path of totality were specially equipped with geomagnetic variographs (Table 1).

Table 1

Stations Used in Eclipse Study

Station	Geographic Lat.	Geographic Long.	Geomagnetic Lat.	Geomagnetic Long.	Slow Run Speed of Chart	Slow Run Sensitivity	Rapid Run Speed of Chart	Rapid Run Sensitivity	Percent* Obscuration at Maximum Eclipse
St. John's	47.6N	52.7W	58.7N	21.4E	2"/hr	2.0γ/mm	1"/min	0.197γ/mm	99.06
Dartmouth	41.7N	63.6W	56.3N	6.9E	2"/hr	1.95γ/mm	2"/min	0.197γ/mm	100.0
Fredericton	45.9N	66.7W	57.6N	3.0E	2"/hr	1.0γ/mm	2"/min	0.197γ/mm	91.78
Ottawa	45.4N	75.5W	57.0N	351.5E	2"/hr	2.0γ/mm	1"/min	0.197γ/mm	77.45

* Kindly calculated at 3 minute intervals by Communications Research Centre, Shirley Bay, Ottawa.

The geomagnetic sensor used at the four stations was a saturable core transistorized fluxgate of the type described by Serson [1957]. The rapid run recorders were protected from large long period disturbances by a band pass filter with a gain of unity in the period range 3-10 seconds and a gain of 0.5 at periods of 0.7 and 800 seconds.

Effect of Eclipse on Long Period Magnetic Variations

Observations at four stations were used to study the eclipse effect on ionospheric electric currents (Table 1). The three-component variations at these stations during the eclipse period are shown in Figure 1. It is clear that considerable disturbance is present and that measurements of ΔH or ΔX from some baseline value are unlikely to reveal any eclipse effect. The Kp value during the eclipse was 6-. However, an attempt was made to isolate an eclipse effect by cross-correlating changes at the station with total eclipse (Dartmouth) with the other stations. This method was used by Boyd [1966]. He performed cross-correlations for only two intervals, one of five hours during the eclipse and one of three hours after. In the present study a series of half-hour intervals were used. These correlations are shown in Figure 2. The dip seen in the Dartmouth-Ottawa correlation at 1900-1930 (Figure 2a) is the result expected from an eclipse effect but there are too many other variations present to make this convincing. The low and negative D,Y correlation values probably indicate local structure in the disturbance. The large variations in the correlation make this method of little value and the result of Boyd may be fortuitous.

An examination of the Dartmouth record shows that, during the eclipse, the X variation has smaller short period fluctuations than it has at the other stations. A series of these deviations were selected so that each deviation was identifiable at each of the four stations and their amplitudes were measured. The ratio of the amplitude at Dartmouth to the amplitudes at the other stations outside the path of totality are plotted in Figure 3. Here an eclipse effect can be clearly seen. Fredericton, being closest to Dartmouth, has the smallest effect (largest ratio). St. John's is almost totally eclipsed 9 minutes after the eclipse maximum at Dartmouth and this probably accounts for the sharp rise in the Dartmouth/St. John's ratio after 1900 h.

The fourth contact of the eclipse at Dartmouth is at 2003 UT and coincides with an SI which, at the four stations considered here, has greatest amplitude at Ottawa and then decreases to the smallest amplitude at St. John's.

The small deviations showing the eclipse effect probably represent rather more localized currents than those found during eclipses at low latitudes [Kato, 1960]. The small spatial extent of the eclipse effect is also remarkable. The distance from Dartmouth to Fredericton is only 175km.

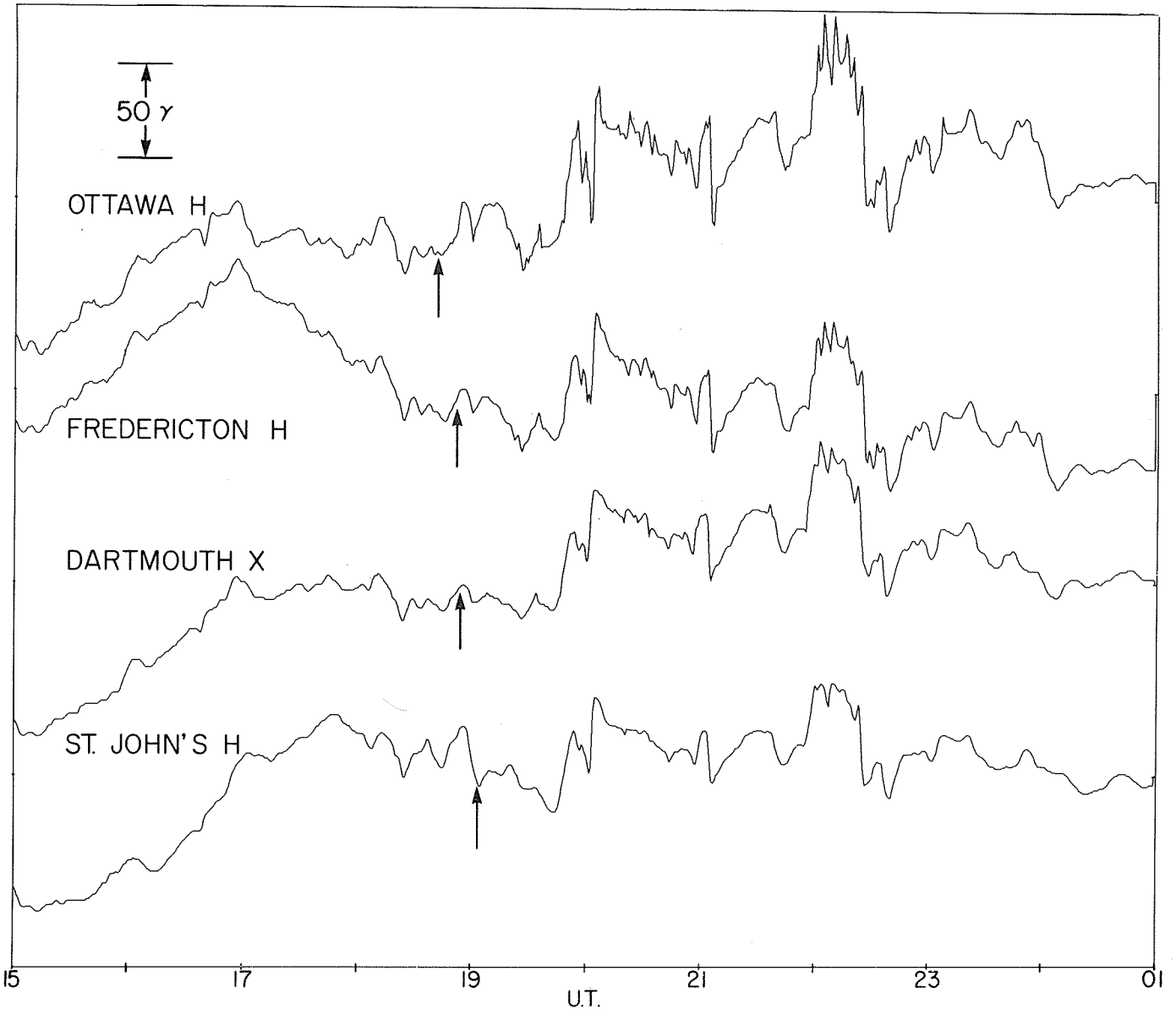

Fig. 1a. Magnetic variations during the eclipse period of March 7, 1970. (These are reconstructed plots from one minute digitized values.) Arrows indicate the time of maximum eclipse.

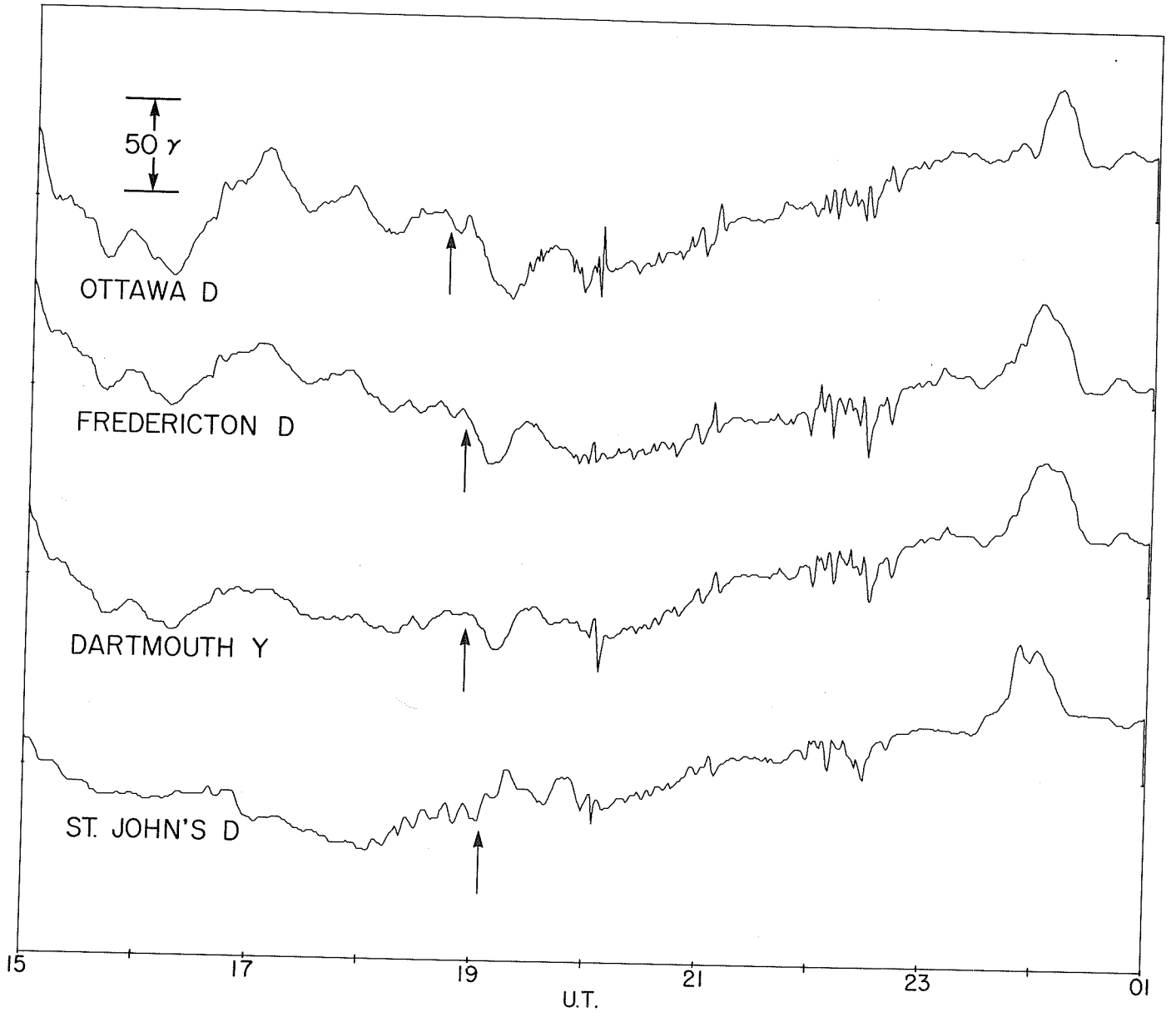

Fig. 1b. Magnetic variations during the eclipse period of March 7, 1970. (These are reconstructed plots from one minute digitized values.) Arrows indicate the time of maximum eclipse.

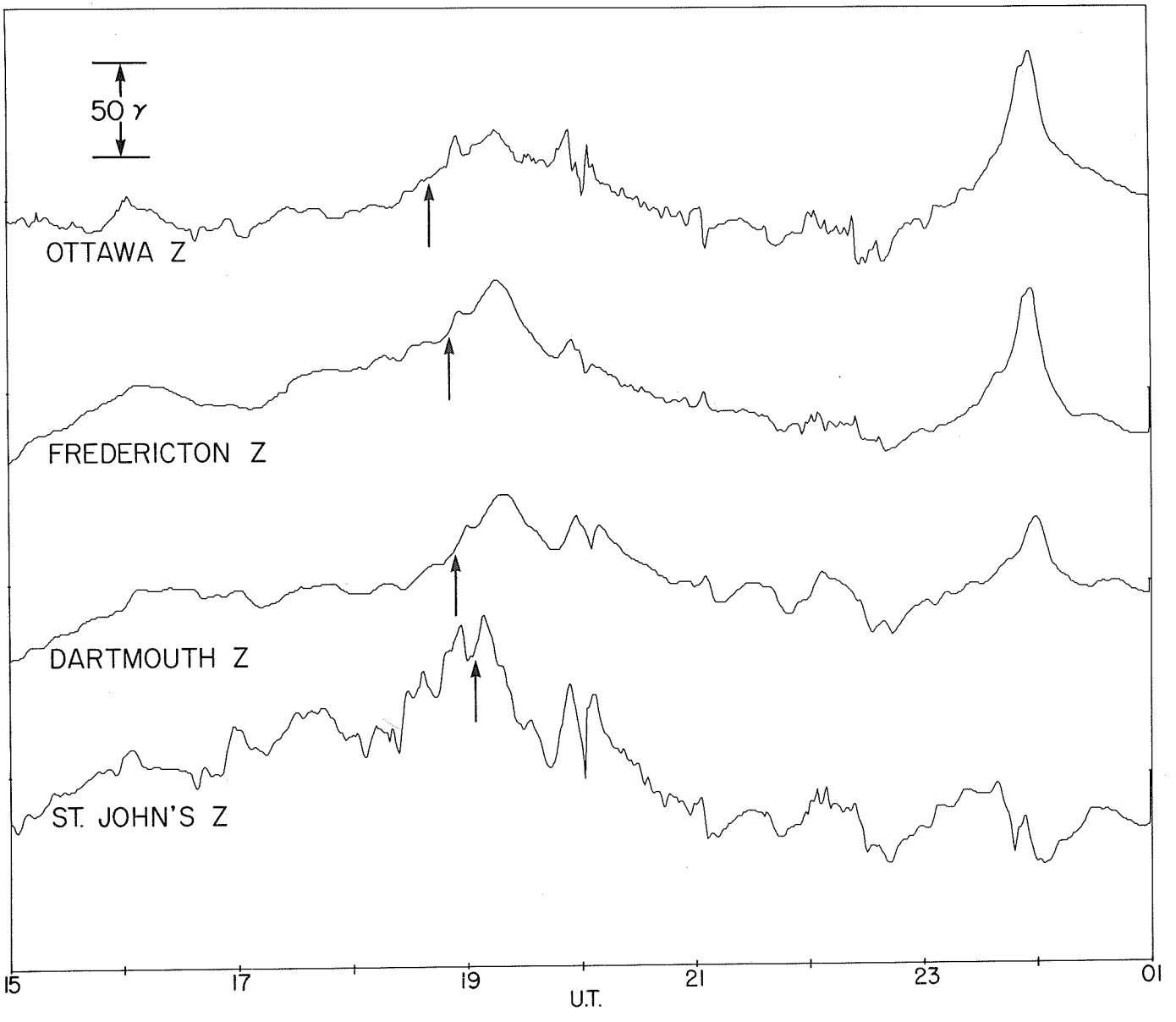

Fig. 1c. Magnetic variations during the eclipse period of March 7, 1970. (These are reconstructed plots from one minute digitized values.) Arrows indicate the time of maximum eclipse.

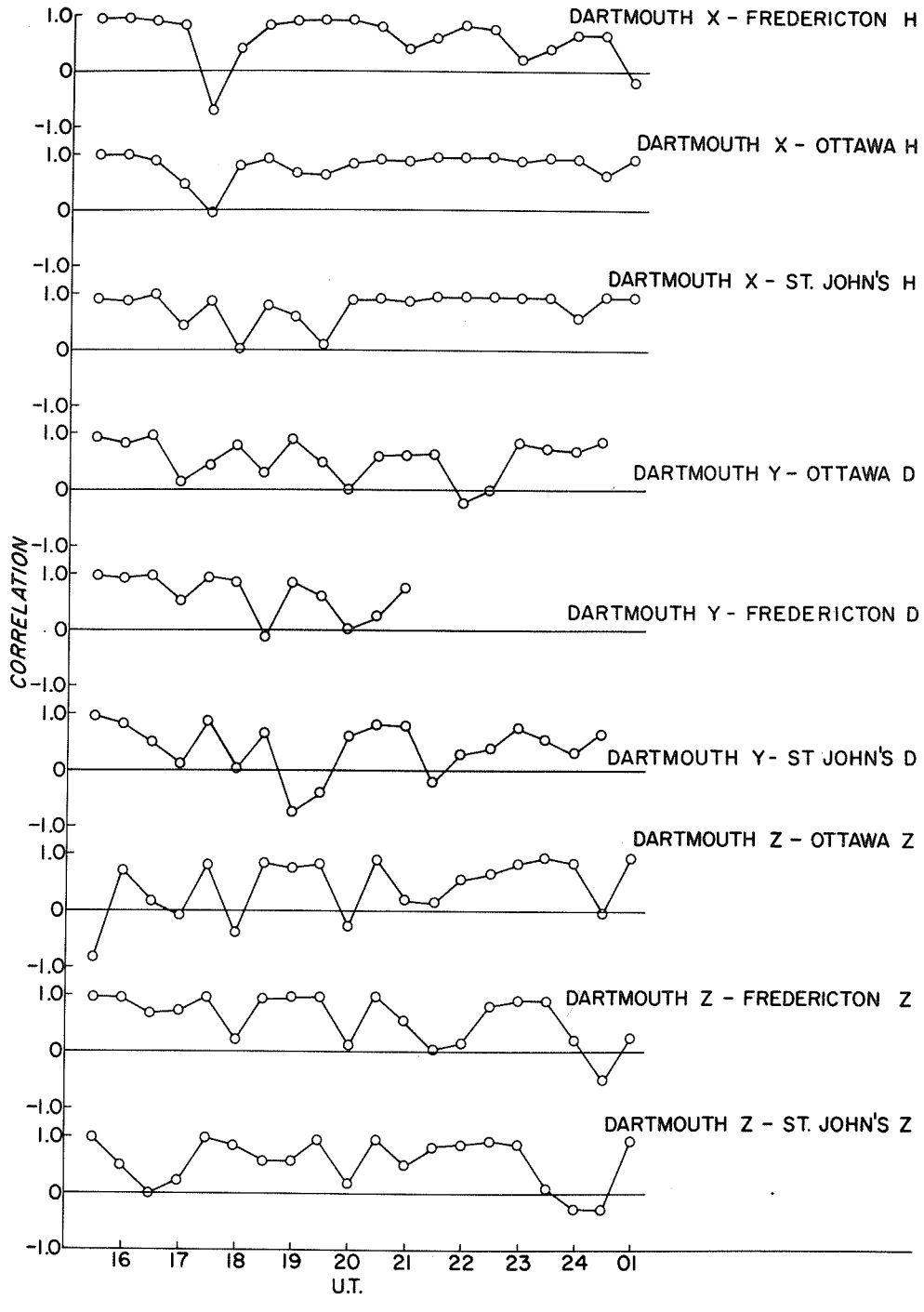

Fig. 2. Changes of cross-correlation coefficients of magnetic variations at non-eclipsed stations with variation at Dartmouth (a) H or X, (b) D or Y, (c) Z. A slight error in digitizing the Fredericton D record made results after 2000 inaccurate for that station.

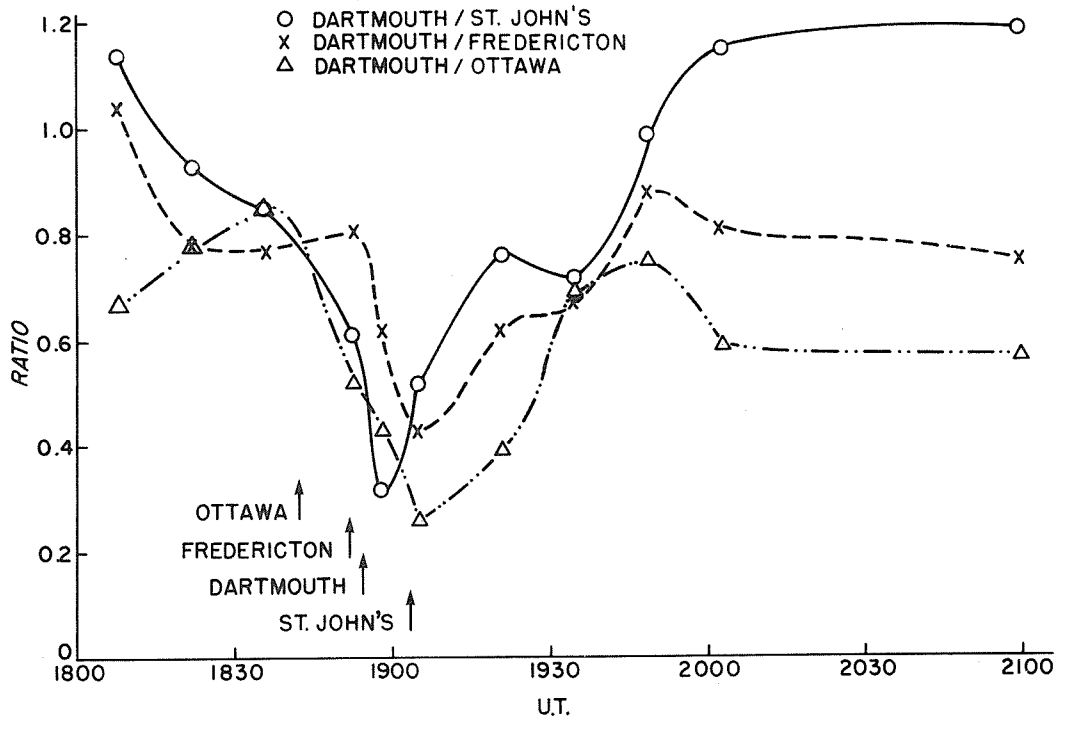

Fig. 3. Ratio of amplitudes of selected variations in the magnetic record at Dartmouth to the amplitudes of the same variations at non-eclipsed stations. Arrows indicate the time of maximum eclipse.

A similar treatment of the D,Y components was not made because it was found impossible to identify sufficient similar variations at the different stations. The Z variation represents effects from currents some distance from the observing station and not from those overhead.

A similar study to this was made on the July 20, 1963 eclipse by Roy [1964]. The eclipsed station was Disraeli, Quebec (N45.9° W71.3°) and the Kp value was 3+ at the time of the eclipse. The negative result reported by Roy was probably due to the lower sensitivity and lower time resolution of the records he used.

Eclipse Effect on Geomagnetic Micropulsations

The effects of eclipses on micropulsations are rather elusive. Kato and Watanabe [1957] summarize some of the observations and note in particular a decrease in micropulsation amplitude during the eclipse. Figure 4a shows the variation in Pc2,3,4 amplitude during the March 7, 1970 eclipse and there is no clear change in amplitude. The sporadic occurrence of micropulsations really prevented the observation of any clear effect. In Figure 4b the variation of Pc5 amplitude is shown. While there is a decrease in amplitude at Dartmouth and Fredericton near the eclipse maximum, there are too many other variations present to attribute this decrease to the eclipse. (The dashed lines in the Dartmouth result indicate that Pc5 was absent during this interval).

Another eclipse effect is described by Kato [1965]. He found that the direction of the principal axis of the horizontal polarization vector diagram changed during the eclipse (20 July, 1963, at Northway, Alaska). A search for a similar effect was made in the Dartmouth records of the March 7, 1970, eclipse. While no clear change in the direction of the polarization axis was found similar to that seen by Kato, there was a tendency for the phase difference between the two horizontal components to change during the eclipse. The variation of this phase difference during the eclipse is plotted in Figure 5. A large change is seen at Dartmouth at the time of eclipse maximum. This change is also noticeable at Fredericton and St. John's. However, at St. John's the change is simultaneous with that at Dartmouth and not with the time of maximum eclipse at St. John's. It should be mentioned that many of these phase measurements were difficult to perform as the micropulsations frequently lacked a clear sinusoidal form. At Dartmouth the X-component usually had a lower amplitude than the Y-component. A similar change in the phase difference can be inferred from Kato's results. However, it seems necessary to perform further analysis to show that this effect does not also occur at times other than during an eclipse.

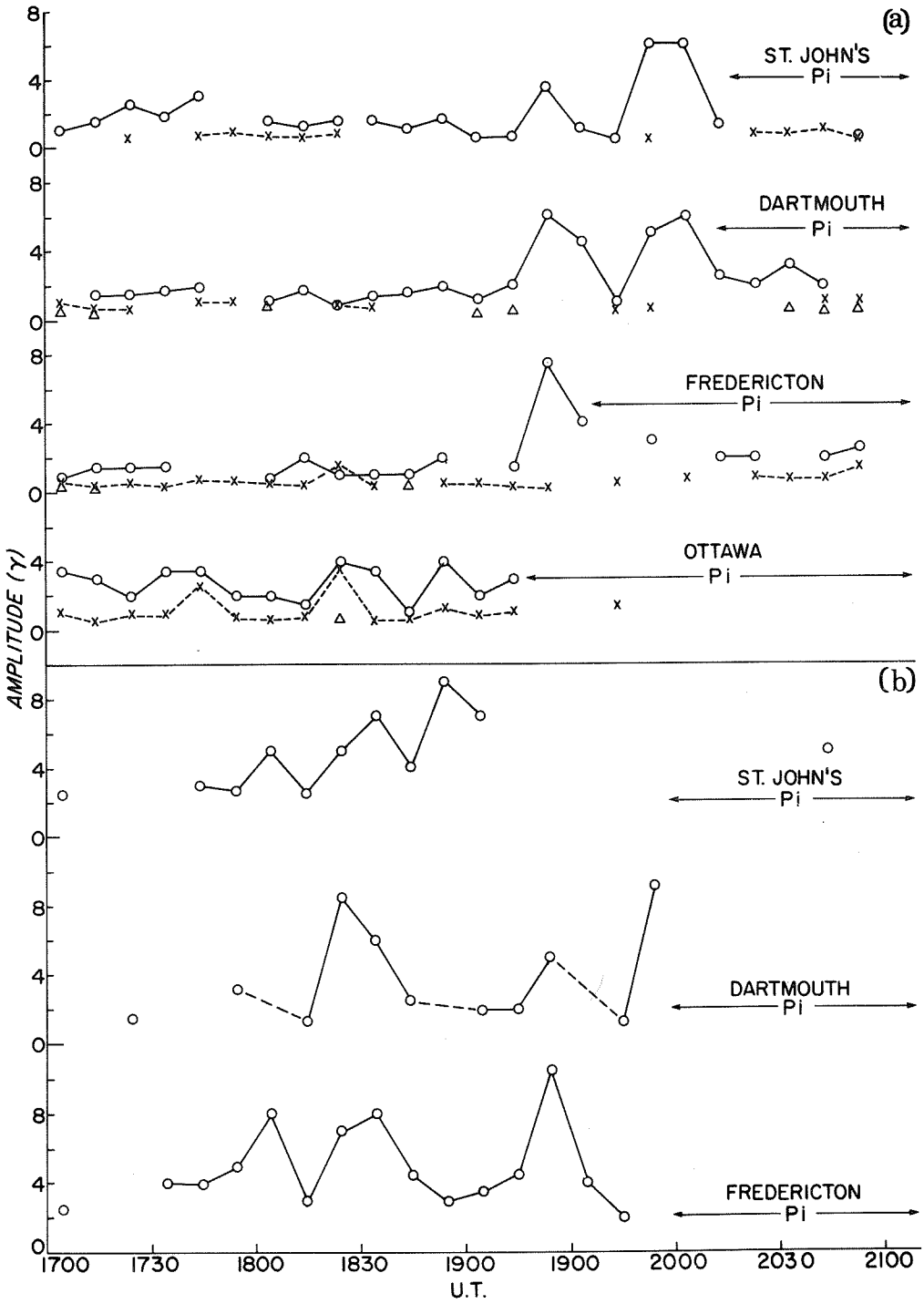

Fig. 4. Amplitudes of geomagnetic micropulsations during the eclipse period (a) Pc2,3,4, (b) Pc5.

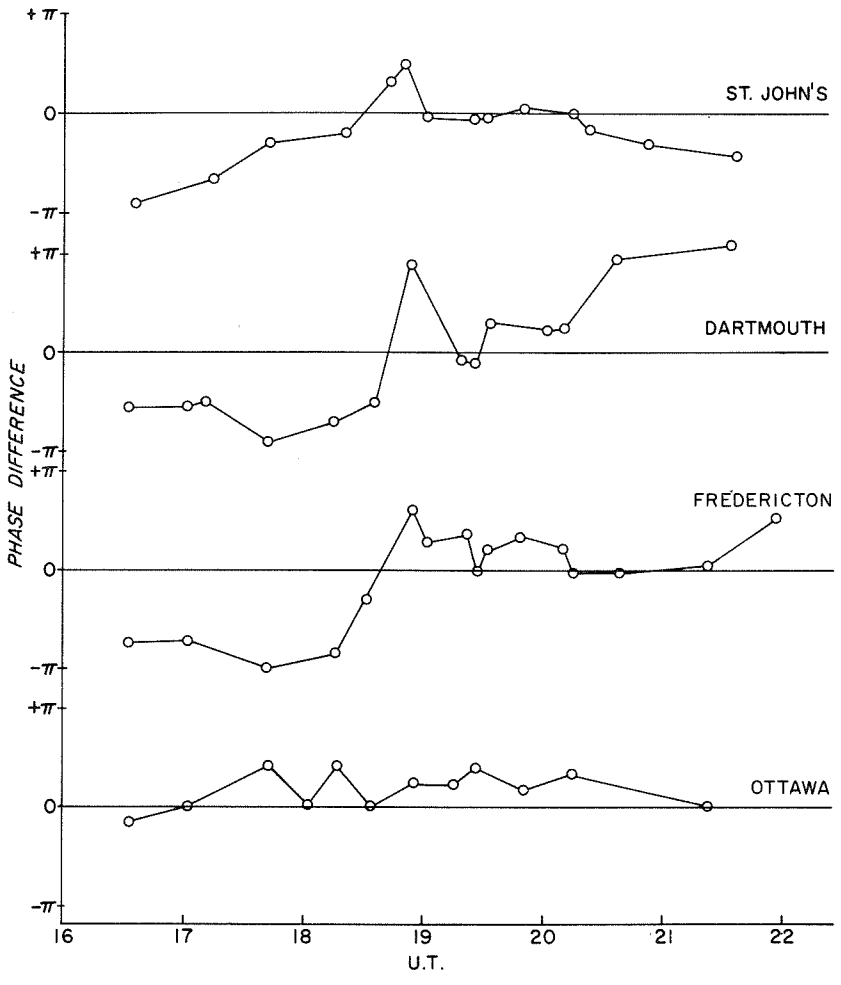

Fig. 5. Phase difference between the two horizontal magnetic components of Pc3,4 micropulsations during the eclipse period.

Acknowledgements

The authors are grateful to Dr. S. Srivastava and his staff at the Bedford Institute of Oceanography for running the Dartmouth station and to other members of the Geomagnetism Division, in particular Mr. G. Massie, for technical assistance. They express sincere thanks to Drs. E. R. Niblett and P. H. Serson for helpful discussions. One (RJS) acknowledges a Postdoctorate Fellowship from the National Research Council of Canada.

REFERENCES

BOYD, G. M. 1966 Solar eclipse magnetic observations and Pc1 geomagnetic micropulsations. Earth and Planet. Sci. Letters, 1, 333-334.

KATO, Y. 1960 The effect on the geomagnetic field of the solar eclipse of October 12, 1958. Sci. Rept. Tohoku Univ. Fifth Ser., 12, 1-10.

KATO, Y. 1965 The effect on the geomagnetic micropulsation of the solar eclipse of 20 July, 1963. Sci. Rept. Tohoku Univ. Fifth Ser., 16, 49-62.

KATO, Y. and T. WATANABE 1957 A survey of observational knowledge of the geomagnetic pulsation. Sci. Rept. Tohoku Univ. Fifth Ser., 8, 157-185.

ROY, J. L. 1964 Magnetic observations in Eastern Canada during the eclipse of July 20, 1963. Can. J. Phys., 42, 831-832.

ACKNOWLEDGEMENTS

This Report would not have been possible without the many contributions from the worldwide scientific community.

ALPHABETICAL INDEX

AUTHOR INDEX

USCOMM-NOAA-ASHEVILLE-4-23-71--1100

Upper Atmosphere Geophysics Report UAG-1
"IQSY Night Airglow Data" by L. L. Smith, F. E. Roach and J. M. McKennan of Aeronomy Laboratory, ESSA Research Laboratories, July 1968, single copy price $1.75. [Catalog No. C52.16/2:1]

Upper Atmosphere Geophysics Report UAG-2
"A Reevaluation of Solar Flares, 1964-1966" by Helen W. Dodson and E. Ruth Hedeman of McMath-Hulbert Observatory, The University of Michigan, August 1968, single copy price 30 cents. [Catalog No. C52.16/2:2]

Upper Atmosphere Geophysics Report UAG-3
"Observations of Jupiter's Sporadic Radio Emission in the Range 7.6-41 MHz, 6 July 1966 through 8 September 1968" by James W. Warwick and George A. Dulk, Department of Astro-Geophysics, University of Colorado, October 1968, single copy price 30 cents. [Catalog No. C52.16/2:3]

Upper Atmosphere Geophysics Report UAG-4
"Abbreviated Calendar Record 1966-1967" by J. Virginia Lincoln, Hope I. Leighton and Dorothy K. Kropp of Aeronomy and Space Data Center, Space Disturbances Laboratory, ESSA Research Laboratories, January 1969, single copy price $1.25. [Catalog No. C52.16/2:4]

Upper Atmosphere Geophysics Report UAG-5
"Data on Solar Event of May 23, 1967 and its Geophysical Effects" compiled by J. Virginia Lincoln, World Data Center A, Upper Atmosphere Geophysics, ESSA, February 1969, single copy price 65 cents. [Catalog No. C52.16/2:5]

Upper Atmosphere Geophysics Report UAG-6
"International Geophysical Calendars 1957-1969" by A. H. Shapley and J. Virginia Lincoln, ESSA Research Laboratories, March 1969, single copy price 30 cents. [Catalog No. C52.16/2:6]

Upper Atmosphere Geophysics Report UAG-7
"Observations of the Solar Electron Corona: February 1964 - January 1968" by Richard T. Hansen, High Altitude Observatory, Boulder, Colorado and Kamuela, Hawaii, October 1969, single copy price 15 cents. [Catalog No. C52.16/2:7]

Upper Atmosphere Geophysics Report UAG-8, Parts 1 and 2
"Data on Solar-Geophysical Activity October 24 - November 6, 1968" compiled by J. Virginia Lincoln, World Data Center A, Upper Atmosphere Geophysics, ESSA, March 1970, single copy price $1.75. Part 1 [Catalog No. C52.16/2:8/1], Part 2 [Catalog No. C52.16/2:8/2]

Upper Atmosphere Geophysics Report UAG-9
"Data on Cosmic Ray Event of November 18, 1968 and Associated Phenomena" compiled by J. Virginia Lincoln, World Data Center A, Upper Atmosphere Geophysics, ESSA, April 1970, single copy price 55 cents. [Catalog No. C52.16/2:9]

Upper Atmosphere Geophysics Report UAG-10
"Atlas of Ionograms" edited by A. H. Shapley, ESSA Research Laboratories, May 1970, single copy price $1.50. [Catalog No. C52.16/2:10]

Upper Atmosphere Geophysics Report UAG-11
"Catalogue of Data on Solar-Terrestrial Physics", compiled by J. Virginia Lincoln and H. Patricia Smith, World Data Center A, Upper Atmosphere Geophysics, ESSA, June 1970, single copy price $1.50. [Catalog No. C52.16/2:11]